

# University of St Andrews



Full metadata for this thesis is available in  
St Andrews Research Repository  
at:

<http://research-repository.st-andrews.ac.uk/>

This thesis is protected by original copyright

A STUDY OF REACTIONS OF THE  
NITROPRUSSIDE ION WITH SOME  
FUNCTIONAL GROUPS OF CLINICAL  
SIGNIFICANCE

being a Thesis  
presented by  
ADRIANNE CALSY HARRISON, B.Sc.,  
to the  
UNIVERSITY OF ST. ANDREWS  
in application for  
THE DEGREE OF DOCTOR OF PHILOSOPHY

St. Andrews

October, 1987



Th  
A764

*To my husband and parents*

DECLARATIONS

I was admitted to the Faculty of Science of the University of St. Andrews under Ordinance General No.12 on the 1st October, 1984, and as a candidate for the degree of Ph.D. in November, 1985.

Signed .....

Date .....

I hereby certify that the candidate has fulfilled the conditions of the Resolution and Regulations appropriate to the Degree of Ph.D.

Supervisor .....  
.....

Date ..... 14 October 1987 .....

I, Adrienne Calsy Harrison, hereby certify that this thesis has been composed by myself, that it is a record of my own work, and that it has not been accepted in partial or complete fulfilment of any other degree or professional qualification.

Signed .....

Date .....

## ACKNOWLEDGEMENTS

I would like to thank Dr. A. R. Butler, my supervisor, and Dr. C. Glidewell, who has also advised me in the research for this thesis, for their sustained interest and encouragement.

I am indebted to Professor Wyatt and Professor Cole-Hamilton for the use of the facilities in the department, and to the technical staff, in particular, Mrs. M. Smith, Mrs. S. Smith, and Mr. C. Smith. I am thankful for the assistance of Dr. P. Sørensen, Dr. J. Reglinski, Dr. I. Hunter and Mr. J. Hunt, for the reasons indicated in appropriate sections of the text. A significant portion of this thesis represents collaboration with Ian Johnson to whom I owe many thanks. I am appreciative of the guidance of Derek Higgins in the use of the computing facilities for molecular modelling studies.

I am indebted to Mrs. Pay for typing this thesis. Finally, I am very grateful for the provision of an Elizabeth Soutar Award during the period of this research.

---

## ABSTRACT

The work described in this thesis represents an attempt to understand further the mode of action and metabolism of the hypotensive agent sodium nitroprusside ( $\text{Na}_2[\text{Fe}^{\text{II}}(\text{CN})_5\text{NO}]$ ). The nitrosyl and cyanide ligands have been implicated in, respectively, the activity and toxicity of sodium nitroprusside and a brief review of the relevant literature is given in Chapter 1. Investigations of some *in vitro* reactions of the nitroprusside ion (NP), to better assess its *in vivo* reactions, are reported with particular interest in the integrity of the pentacyanoferrate moiety and reactions that result in nitrosation or release of NO.

Most carbanions react with NP to form an oxime (Chapter 3), with the exceptions of the carbanions of pentane-2,4-dione and 3-methylpentane-2,4-dione for which an unusual mechanism involving metal to ligand charge transfer is proposed (Chapter 4). Consideration of the nmr spectra of some carbanions and oximes (Chapter 2) and the reactions of iron(II) with oximes (Chapter 5) contributes to the elucidation of this mechanism.

A mechanism for the reactions of NP with a wide range of thiols, involving reduction of NP and slow release of NO, is proposed in Chapter 6. Although the primary product of NP reduction is  $[\text{Fe}(\text{CN})_4\text{NO}]^-$  there has been no evidence of unbound cyanide, attributed to rapid ligand rearrangement yielding hexacyanoferrate(II). The same mechanism is consistent with the reactions of NP with the active site thiols

of the enzymes papain and glyceraldehyde-3-phosphate dehydrogenase and the intracellular thiol glutathione of intact erythrocytes (Chapter 7). There is evidence (Chapter 8) of rapid reduction of NP and NO release upon reaction with the haem-containing enzymes catalase and lactoperoxidase, models for the enzyme guanylate cyclase through which NP and related agents are thought to effect hypotension.

C O N T E N T S

## CHAPTER 1 INTRODUCTION

1.1	Properties of sodium nitroprusside	1
1.2	Metabolism of nitroprusside and standard analytical procedure for quantification of free cyanide	3
1.3	Hypotensive action of nitroprusside	4
1.4	The role of the nitrosyl ligand of nitroprusside	6
	References	9

## CHAPTER 2 A DISCUSSION OF THE NMR DATA FOR SOME CARBON ACIDS AND OXIMES

2.1	Introduction	14
2.2	Results and Discussion	15
2.2.1	Pentane-2,4-dione (Hacac)	15
2.2.2	3-Hydroxyiminopentane-2,4-dione (Hinaa)	15
2.2.3	3-Methylpentane-2,4-dione (MHacac)	17
2.2.4	3-Methyl-3-nitrosopentane-2,4-dione	18
2.3	Experimental	19
	References	22

## CHAPTER 3 THE REACTION OF THE NITROPRUSSIDE ION WITH ETHYL CYANOACETATE IN ALKALINE SOLUTION

3.1	Introduction	24
3.2	Results and Discussion	26
3.2.1	Attempted isolation of the adduct of nitroprusside and ethyl cyanoacetate	26
3.2.2	Isolation of the oxime of ethyl cyanoacetate	26
3.2.3	Identification of the inorganic products of reaction	27

3.2.4	Kinetic studies	31
3.2.4.1	Determination of the $pK_a$ of ethyl cyanoacetate	32
3.2.4.2	Rate of adduct formation	32
3.2.4.3	Rate of adduct decomposition	34
3.3	Conclusions	34
3.4	Experimental	36
	References	42

## CHAPTER 4 THE REACTION OF THE NITROPRUSSIDE ION WITH PENTANE-2,4-DIONE (HACAC) IN ALKALINE SOLUTION

4.1	Introduction	44
4.2	Results	46
4.2.1	Attempted isolation of isonitroso- acetylacetone (Hinaa)	46
4.2.2	Formation of tris(pentane-2,4-dionato- -0,0) iron(III) ( $Fe(acac)_3$ )	46
4.2.3	Adduct isolation and characterisation	48
4.2.3.1	Infra-red spectroscopy of reaction solutions	49
4.2.3.2	Rate of adduct formation	50
4.2.3.3	Spectrophotometric studies of reaction solution	51
4.2.4	Attempted detection of free cyanide or hydrogen cyanide in reaction solutions	53
4.2.5	Isolation of NO	55
4.2.6	Determination of the inorganic products of reaction	55
4.2.7	Determination of the organic products of reaction	58
4.2.8	Reactions of acetylacetone with other cyanoferrate complexes	62

4.2.9	Reaction of nitroprusside with 3-methylpentane-2,4-dione in alkaline solution	63
4.2.10	Reactions of nitroprusside with other 1,3-diketones	66
4.3	Discussion	68
4.4	Experimental	76
	References	83

## CHAPTER 5 COMPLEXATION OF IRON(II) WITH 3-HYDROXYIMINOPENTANE-2,4-DIONE (HINAA)

5.1	Introduction	85
5.2	Results and Discussion	87
5.2.1	Characterisation of the iron(II) inaa <sup>-</sup> complex	87
5.2.2	Kinetic studies of the formation of Fe(inaa) <sub>3</sub>	88
5.2.3	Attempted studies of related reactions	90
5.3	Experimental	91
	References	93

## CHAPTER 6 THE REACTION OF THE NITROPRUSSIDE ION WITH HYDROGEN SULPHIDE AND METHYL SULPHIDE IONS, GLUTATHIONE, CYSTEINE AND RELATED THIOLS IN ALKALINE SOLUTION

6.1	Introduction	95
	Identification of the primary product of nitroprusside reduction	98
6.2	Results	100
6.2.1	Reactions of nitroprusside with hydrogen sulphide and methyl sulphide ions	100
A	Adduct formation from nitroprusside and equimolar hydrogen sulphide or methyl sulphide ions	100

B	Intermediate species of the reaction of nitroprusside with equimolar hydrogen sulphide or methyl sulphide ions	100
C	Products of the reaction of nitroprusside with equimolar hydrogen sulphide or methyl sulphide ions	101
6.2.2	Reactions of nitroprusside with an <b>excess</b> of hydrogen sulphide or methyl sulphide ions	101
6.2.3	Reaction of nitroprusside with cysteine, penicillamine and related thiols	104
A	Consideration of the $pK_a$ values for N-acetylcysteine, N-acetyl- $\beta$ -methylcysteine, N-acetylpenicillamine and glutathione	106
B	Reactions of nitroprusside with several thiols including N-acetylcysteine and N-acetylpenicillamine in the <b>presence</b> of air	108
C	Reactions of nitroprusside with several thiols including N-acetylcysteine and N-acetyl-penicillamine in the <b>absence</b> of air	113
6.3	Discussion	117
6.4	Concluding remarks	127
6.5	Experimental	129
	References	137

## CHAPTER 7 THE REACTION OF THE NITROPRUSSIDE ION WITH INTACT ERYTHROCYTES AND THE ENZYMES PAPAIN AND GLYCER-ALDEHYDE-3-PHOSPHATE DEHYDROGENASE

7.1	Introduction	140
7.2	Results	146
7.2.1	Spin-echo proton nmr of nitroprusside incubated with intact erythrocytes	146
7.2.2	Transport of nitroprusside across erythrocyte membranes	148

7.2.3	Kinetic studies of the inhibition of the catalytic activity of papain by nitroprusside	148
7.2.4	Molecular modelling of nitroprusside and papain	150
7.2.5	Kinetic studies of the inhibition of the catalytic activity of GAPDH by nitroprusside	150
7.2.6	Molecular modelling of nitroprusside and GAPDH	151
7.2.7	Epr and carbon-13 nmr studies of the reaction of nitroprusside with GAPDH	152
7.3	Discussion	153
7.4	Experimental	157
	References	163

## CHAPTER 8 THE REACTIONS OF THE NITROPRUSSIDE ION WITH THE HAEM ENZYMES CATALASE AND LACTOPEROXIDASE

8.1	Introduction	167
8.2	Results	170
8.2.1	Inhibition of lactoperoxidase activity	170
8.2.2	Visible spectra of lactoperoxidase and cyanoferrate complexes	171
8.2.3	Attempted inhibition of catalase activity	171
8.2.4	Visible spectra of catalase and cyanoferrate complexes	171
8.2.5	Epr spectra of catalase and nitroprusside	171
8.2.6	Carbon-13 nmr of catalase and nitroprusside	172
8.3	Discussion	173
8.4	Experimental	177
	References	180

**APPENDIX 1**

Publications

182

**APPENDIX 2**

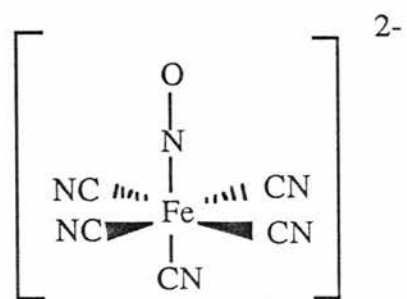
Photographs

183

CHAPTER ONE

INTRODUCTION

The nitroprusside ion



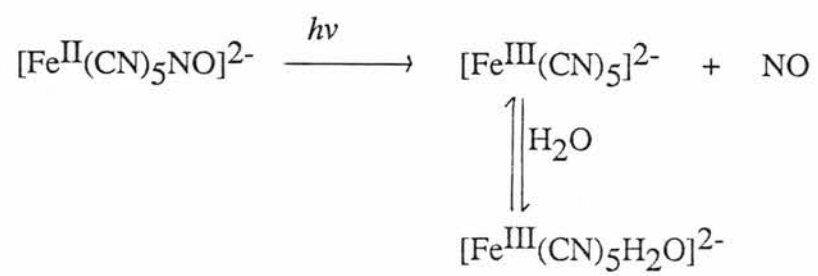
Sodium nitroprusside (SNP,  $\text{Na}_2[\text{Fe}^{\text{II}}(\text{CN})_5\text{NO}]^{\dagger}$ ) is well known<sup>1-4</sup> in the medical field as an effective and sensitive agent for reducing blood pressure, particularly during surgeries. Although the hypotensive action of sodium nitroprusside has been known<sup>5</sup> for nearly a century its metabolic products and mode of action are sources of considerable controversy. Nevertheless, infusion of the nitroprusside ion  $[\text{Fe}^{\text{II}}(\text{CN})_5\text{NO}]^{2-}$ , NP) into the bloodstream remains a beneficial means of reducing and controlling blood pressure. Consideration of the work to date is important to understanding further the *in vivo* reactions of NP by characterisation of some *in vitro* reactions with physiologically relevant functional groups.

### 1.1 PROPERTIES OF SODIUM NITROPRUSSIDE

First prepared by Playfair<sup>6</sup> in 1849, sodium nitroprusside is a diamagnetic iron(II) complex, of  $C_{4v}$  symmetry.<sup>7</sup> There has been some uncertainty as to the charge on the nitrosyl ligand ( $\text{NO}^{\cdot}$  or  $\text{NO}^+$ ) and the oxidation state of iron ( $\text{Fe}^{3+}$  or  $\text{Fe}^{2+}$ ) but the charge distribution has been calculated<sup>8</sup> and is formally  $\text{Fe}^{2+}$  and  $\text{NO}^+$ . Several physical properties of SNP distinguish it from other pentacyanoferrate(II) complexes; the cyanide stretch is in the (infra-red) region usually associated<sup>9</sup> with cyanide coordinated to iron(III) and the carbon-13 chemical shift<sup>10</sup> of the nitroprusside ion NP is approximately 40 p.p.m. upfield of other iron(II) cyanide complexes.<sup>10,11</sup>

<sup>†</sup> Sodium nitroprusside is available as the dihydrate  $\text{Na}_2[\text{Fe}^{\text{II}}(\text{CN})_5\text{NO}].2\text{H}_2\text{O}$

**Scheme 1 :** Photolytic decomposition of nitroprusside



The formation constants of iron(II) cyanide complexes are exceptionally high ( $\beta_6$  is  $10^{36}$  for hexacyanoferrate(II)<sup>12</sup>), representing insignificant dissociation of the complex to its component ligands. In addition to the thermodynamic stability described by the formation constant, a complex can be described as either kinetically inert or labile to ligand substitution. As a low spin  $d^6$  complex, NP is kinetically inert to substitution in equilibrium conditions; neutral aqueous solutions of NP are stable for long periods if stored in the absence of light.<sup>13-16</sup>

In alkaline solution NP reacts with hydroxide to form nitropentacyanoferrate(II),  $[\text{Fe}(\text{CN})_5\text{NO}_2]^{4-}$ , in equilibrium with aquapentacyanoferrate(II),  $[\text{Fe}(\text{CN})_5\text{H}_2\text{O}]^{3-}$ , which is subject to polymerisation or ionisation in solution. Reactions of NP normally involve attack at the nitrosyl ligand and retention of the  $[\text{Fe}(\text{CN})_5]^{3-}$  moiety.

The formation constants of iron(III) cyanide complexes are also quite high, but  $d^5$  iron(III) complexes are kinetically labile; the cyanide ligands of hexacyanoferrate(III), for instance, are subject to ligand substitution.

In solution, NP is exceptionally photosensitive and the primary products of photolysis are nitric oxide (NO) and  $[\text{Fe}^{\text{III}}(\text{CN})_5\text{H}_2\text{O}]^{2-}$  (Scheme 1).<sup>17,18</sup> This reaction arises from the excitation of electrons to antibonding orbitals, thereby promoting bond weakening and breaking. It has also been shown<sup>16</sup> that hexacyanoferrate(II), which will be revealed as a significant product of the reaction of NP with some nucleophiles, is photolabile. To guard against photolysis, solid SNP and all solutions containing NP or its reaction products

were kept in the dark and wrapped in foil during the experimental work described in succeeding chapters.

## 1.2 METABOLISM OF THE NITROPRUSSIDE ION

The extreme toxicity of the cyanide ion arises from ready binding to the essential enzyme cytochrome oxidase, vital to cellular respiration<sup>3</sup> and a pertinent medical concern is the metabolic fate of NP, more specifically the cyanide ligands, when infused as a dilute solution into the blood stream. The hypotensive activity of NP is characterised by its rapid and short-lived action, without apparent side effects, but there are many reports in the medical literature<sup>1,3,4,19-24</sup> of the release of free cyanide ions. From a chemical viewpoint, release of cyanide from nitroprusside in physiological conditions is not consistent with either its high formation constant or degree of kinetic inertness, but the complexity of biological reactions must not be disregarded.

### Analytical procedure for quantification of free cyanide

The 'carrier-gas' technique<sup>21</sup> has been, in most cases of reported cyanide release from NP, the standard method for measuring the amount of cyanide in biological samples. In this method the sample is acidified and nitrogen is bubbled through the sample to flush out any cyanide present as HCN. The effluent gas is trapped in an alkaline solution, regenerating cyanide ion which can then be assayed spectrophotometrically in isolation from the rest of the sample.

It has been suggested<sup>13,14,25-27</sup> that reports of cyanide release from nitroprusside upon infusion are not consistent with the large formation constants of NP and other

cyanoferrate complexes but are a result of the inappropriate analytical procedures for free cyanide. The carrier-gas technique is subject to false readings for free cyanide if kinetically labile cyanoferrate complexes are present in the sample to be analysed. Aquapentacyanoferrate(III), as an example of a kinetically labile complex, is of high thermodynamic stability but is subject to ligand substitution. In the extreme, non-equilibrium conditions of the carrier-gas technique the cyanide ligands of this complex in exchange with water are protonated by added acid and expelled as volatile HCN, an entropy-driven process.

There are several possible sources of kinetically labile cyanoferrate complexes from NP incubated with biological materials. The photodecomposition of NP to aquapentacyanoferrate(III) and NO has been described and it is possible that the metabolic products of NP are iron(III) complexes.

With the use of carbon-13 nmr, a non-destructive and non-invasive technique, Butler *et al*<sup>25</sup> did not detect release of <sup>13</sup>CN upon incubation of 90% carbon-13 labelled nitroprusside in blood.

### 1.3 HYPOTENSIVE ACTION OF NITROPRUSSIDE

Despite reports of cyanide release from NP, the use of NP to lower blood pressure during surgery is widespread.<sup>1-5</sup> Controlled hypotension in surgery is desirable for several reasons; bleeding obscuring the field of operation and blood loss are minimised when blood pressure is low.<sup>5</sup> The advantages of NP compared to other hypotensive agents are instantaneous onset of action, sensitivity of the response to

dose facilitating precise and prolonged control of blood pressure, and no apparent side effects.<sup>2</sup> Almost immediately after stopping infusion of NP, blood pressure is restored to its original level, not 'overshooting' to a higher level as with many other hypotensive agents.<sup>13</sup>

The rapid, short-lived action and high potency of NP<sup>5</sup> infused into the bloodstream indicate that the reaction of NP responsible for hypotension is fast and specific. There is general agreement<sup>28-32</sup> that NP, in common with sodium nitrite, nitric oxide (NO), N-methyl-N'-nitro-N-nitrosoguanidine (MNNG), nitroglycerine (GTN) and amyl nitrite, affects hypotension through activation of the enzyme guanylate cyclase [GTP pyrophosphate (cyclising), EC 4.6.1.2]. Guanylate cyclase has been identified in nearly all mammalian tissues and catalyses the conversion of guanosine triphosphate (GTP) to guanosine 3':5'-monophosphate (cyclic GMP).<sup>33</sup> Cyclic GMP is involved in the regulation of myocardial contractability, and the hypotensive action of NP, along with other compounds containing or releasing NO, has been associated with increased cyclic GMP formation.<sup>28,32,34,35</sup>

It has been demonstrated<sup>32,33</sup> that guanylate cyclase activity is regulated not by hormonal agents but by the redox state of the enzyme, an unusual enzyme mechanism. Crude preparations of guanylate cyclase are sensitive to a variety of redox active agents<sup>29,30,36-47</sup> but recent work<sup>28,48,49</sup> with highly purified preparations identifies several possible reacting centres. Guanylate cyclase has been purified to homogeneity in either haem-deficient or haem-containing forms<sup>48-52</sup> and the degree of activation by NO containing and

releasing compounds has been found to vary with haem content.<sup>44,50,52-54</sup> The redox states of enzyme thiol groups are apparently important to activation as well<sup>29,39,40,55-57</sup> but it is not yet clear how enzyme thiol and/or haem groups modulate activation by nitroprusside and related compounds.

#### 1.4 THE ROLE OF THE NITROSYL LIGAND OF NP

The hypotensive activity of NP has been attributed to the nitrosyl ligand since early this century and the similarities of guanylate cyclase activation by NO, NP, and other NO containing or releasing agents indicate that the nitroprusside ion functions as an extremely effective and specific transporter of NO. Flitney and Kennovan<sup>58</sup> report that twitch contractions of frog ventricular trabeculae are not affected by NP when the experiments are conducted in the complete absence of light. However, they demonstrated that the intensity of the twitch contraction correlates with the extent of illumination of the preparation during NP administration; the active product of NP photodegradation is thought to be NO.

Further evidence for the importance of NO to NP induced hypotension arises from the lack of dependence of NP activity on the presence of vascular endothelial cells; some related vasoactive substances have no effect on smooth muscle cell preparations scraped free of these cells.<sup>59</sup> Endothelial cells release vasoactive substances in response to mechanical force and various neurohumoral mediators, and one of the most potent of these substances is referred to as endothelium-derived relaxing factor (EDRF).<sup>60</sup> EDRF stimulates

vascular muscle guanylate cyclase and the endothelium-dependent hypotensive action of acetylcholine has been attributed to a concomitant increase in the level of cyclic GMP. The actions of EDRF and nitric oxide-containing hypotensive agents on vascular smooth muscle are similar and recent work has conclusively identified EDRF as NO.<sup>61</sup>

There are several significant conclusions drawn from the literature that have influenced the investigations reported in this thesis. It seems certain that NP and related agents lower blood pressure by activation of the enzyme guanylate cyclase. NO is fundamental to the activation of guanylate cyclase but the reaction(s) through which NO is released from NP and related agents have not been identified. The onset of hypotension upon NP infusion is effectively instantaneous suggesting that the reaction of NP with target functional groups is rapid.

The products of the reactions of the nitroprusside ion with a variety of nucleophiles have been the subject of chemical investigation<sup>9,62-68</sup> and Cambi, Scagliarini and colleagues in particular described the reactions of NP with a wide range of compounds at the beginning of this century. With the advent of modern spectroscopic techniques it has been possible to describe more fully the reaction schemes they postulated and it is the reactions of NP with physiologically occurring functional groups that lead to release of NO or rapid nitrosation that are of interest here.

The release of NO following reaction of NP and amines has been shown to be slow<sup>63,65</sup> compared to the hypotensive

action of NP. The reactions of NP with carbanions<sup>62</sup> and a wide range of thiols including thiol-containing enzymes and the intracellular thiol glutathione of intact erythrocytes are much more rapid and will be discussed below. Additionally, as the presence of a prosthetic haem has been implicated in guanylate cyclase activation, the reactions of NP with two readily available haem-containing enzymes will be considered.

## REFERENCES

1. W. P. Arnold, D. E. Longnecker, and R. M. Epstein, *Anesthesiology*, 1984, **61**, 254.
2. V. A. W. Kreye in "Pharmacology of Antihypertensive Agents" (A. Scriabine, Ed.), Ravens Press, 1980, New York, 373-396.
3. A. D. Ivankovich, D. J. Miletich, and J. H. Tinker, *Int. Anesthesiol. Clin.*, 1978, **16**, 1.
4. J. H. Tinker and J. D. Michenfelder, *Anesthesiology*, 1976, **45**, 340.
5. V. A. W. Kreye and F. Gross in "Antihypertensive Agents" (F. Gross, Ed.), Springer-Verlag, Berlin, Heidelberg, 1977, 418-430.
6. L. Playfair, *Proc. Roy. Soc. (London)*, 1849, **5**, 846.
7. P. T. Manoharan and W. C. Hamilton, *Inorg. Chem.*, 1963, **2**, 1043.
8. P. T. Manoharan and H. B. Gray, *J. Am. Chem. Soc.*, 1965, **87**, 3340.
9. J. H. Swinhart, *Coord. Chem. Rev.*, 1967, **2**, 385 and references therein.
10. A. R. Butler, C. Glidewell, A. R. Hyde, and J. McGinnis, *Inorg. Chem.*, 1985, **24**, 2931.
11. B. A. Narayan and P. T. Manoharan, *J. Inorg. Nucl. Chem.*, 1978, **40**, 1993.
12. G. D. Watt, J. J. Christensen, and R. M. Izatt, *Inorg. Chem.*, 1965, **4**, 220.

13. W. I. K. Bisset, M. G. Burdon, A. R. Butler, C. Glidewell, and J. Reglinski, *J. Chem. Res. (M)*, 1981, 3501.
14. W. I. K. Bisset, A. R. Butler, C. Glidewell and J. Reglinski, *Brit. J. Anaesth.*, 1981, **53**, 1015.
15. C. J. Vesey and G. A. Batistoni, *J. Clin. Pharm.*, 1977, **2**, 105.
16. A. G. MacDiarmid and N. F. Hall, *J. Am. Chem. Soc.*, 1954, **76**, 4222.
17. S. K. Wolfe and J. H. Swinhart, *Inorg. Chem.*, 1975, **14**, 1049.
18. G. Stochel, R. Van Eldik, and Z. Stasicka, *Inorg. Chem.*, 1986, **25**, 3663.
19. V. Schulz, R. Gross, T. Pasch, J. Busse, and G. Loeschcke, *Klin. Wochenschr.*, 1982, **60**, 1393.
20. J. R. Krapez, C. J. Vesey, L. Adams, and P. V. Cole, *Brit. J. Anaesth.*, 1981, **53**, 793.
21. F. L. Rodkey and H. A. Collison, *Clin. Chem.*, 1977, **23**, 1969.
22. C. J. Vesey, V. Cole, and P. J. Simpson, *Brit. J. Anaesth.*, 1976, **48**, 651.
23. R. P. Smith and H. Kruszyna, *J. Pharmacol. Exp. Ther.*, 1974, **191**, 557.
24. N. R. Fahmy, *Anesthesiology*, 1981, **54**, 305.
25. A. R. Butler, C. Glidewell, J. McGinnis, and W. I. K. Bisset, *Clin. Chem.*, 1987, **33**, 490.
26. W. I. K. Bisset, A. R. Butler, and C. Glidewell, *Brit. J. Anaesth.*, 1984, **56**, 311.
27. A. R. Butler, C. Glidewell, and W. I. K. Bisset, *Brit. J. Anaesth.*, 1982, **54** (July correspondence).

28. F. Murad, J. A. Lewicki, H. J. Brandwein, C. K. Mittal, and S. A. Waldman in "Advances in Cyclic Nucleotide Research" (J. E. Dumont, P. Greengard, and G. A. Robinson, Eds.), Ravens Press, New York, 1981, Vol. XIV, 229-239.
29. H. Schröder, E. Noack, and R. Müller, *J. Mol. Cell. Cardiol.*, 1985, **17**, 931.
30. L. J. Ignarro, H. Lipton, J. C. Edwards, W. H. Baricos, A. L. Hyman, P. J. Kadowitz, and C. A. Gruetter, *J. Pharm. Exp. Therap.*, 1981, **218**, 739.
31. W. P. Arnold, C. K. Mittal, S. Katsuki, and F. Murad, *Proc. Natl. Acad. Sci. USA*, 1977, **74**, 3203.
32. J. M. Braughler, C. K. Mittal, and F. Murad, *Proc. Natl. Acad. Sci. USA*, 1979, **76**, 219.
33. N. D. Goldbert and M. K. Haddox, *Ann. Rev. Biochem.*, 1977, **46**, 823.
34. K. Laustiola, P. Vuorinen, H. Vapaatalo, and T. Metsa-Ketela, *Eur. J. Pharm.*, 1983, **91**, 301.
35. R. M. Rapoport, M. D. Draznin, and F. Murad, *Proc. Natl. Acad. Sci. USA*, 1982, **79**, 6470.
36. J. M. Braughler, *Biochem. Pharm.*, 1983, **32**, 811.
37. J. M. Braughler, *Biochem. Pharm.*, 1982, **31**, 3847.
38. J. M. Braughler, *Biochem. Pharm.*, 1982, **31**, 1239.
39. H. J. Brandwein, J. A. Lewicki, and F. Murad, *J. Biol. Chem.*, 1981, **256**, 2958.
40. L. J. Ignarro, P. J. Kadowitz, and W. H. Baricos, *Arch. Biochem. Biophys.*, 1981, **208**, 75.
41. E. H. Ohlstein, B. K. Barry, D. Y. Gruetter, and L. J. Ignarro, *FEBS Lett.*, 1979, **102**, 316.

42. J. M. Braughler, C. K. Mittal, and F. Murad, *J. Biol. Chem.*, 1979, **254**, 12450.
43. J. M. Braughler, C. K. Mittal, and F. Murad, *Proc. Natl. Acad. Sci. USA*, 1979, **76**, 219.
44. P. A. Craven and F. R. DeRubertis, *J. Biol. Chem.*, 1978, **253**, 8433.
45. F. R. DeRubertis and P. A. Craven, *J. Biol. Chem.*, 1977, **252**, 5804.
46. H. Kimura, C. K. Mittal, and F. Murad, *J. Biol. Chem.*, 1975, **250**, 8016.
47. P. Needleman and E. M. Johnson, *J. Pharm. Exp. Therap.*, 1973, **184**, 709.
48. R. Gerzer, E. Böhme, F. Hofmann, and G. Schultz, *FEBS Lett.*, 1981, **132**, 71.
49. R. Gerzer, F. Hofmann, and G. Schultz, *Eur. J. Biochem.*, 1981, **116**, 479.
50. L. J. Ignarro, J. B. Adams, P. M. Horowitz, and K. S. Wood, *J. Biol. Chem.*, 1986, **261**, 4997.
51. P. A. Craven and F. R. DeRubertis, *Biochim. Biophys. Acta*, 1983, **745**, 310.
52. L. G. Ignarro, J. N. Degnan, W. H. Baricos, P. J. Kadowitz, and M. S. Wolin, *Biochim. Biophys. Acta*, 1982, **718**, 49.
53. E. H. Ohlstein, K. S. Wood, and L. J. Ignarro, *Arch. Biochem. Biophys.*, 1982, **218**, 187.
54. J. C. Edwards, B. K. Barry, D. Y. Gruetter, E. H. Ohlstein, W. H. Baricos, and L. J. Ignarro, *Biochem. Pharm.*, 1981, **30**, 2531.
55. J. D. Horowitz, E. M. Antman, B. H. Lorell, W. H. Barry, and T. W. Smith, *Circulation*, 1983, **68**, 1247.

56. L. J. Ignarro, B. K. Barry, D. Y. Gruetter, E. H. Ohlstein, C. A. Gruetter, P. J. Kadowitz, and W. H. Baricos, *Biochim. Biophys. Acta*, 1981, **673**, 394.
57. L. J. Ignarro and C. A. Gruetter, *Biochim. Biophys. Acta*, 1980, **631**, 221.
58. F. W. Flitney and G. Kennovan, *Proceedings of the Physiol. Soc.*, Dundee Meeting, 1986, **C.18**, 41P
59. Y. Shirasaki and C. Su, *Eur. J. Pharm.*, 1985, **114**, 93.
60. P. M. Vanhoutte, *Nature*, 1987, **327**, 459.
61. R. M. J. Palmer, A. G. Ferrige, and S. Moncada, *Nature*, 1987, **327**, 524.
62. A. R. Butler, C. Glidewell, V. Chaipanich, and J. McGinnis, *J. Chem. Soc., Perkin Trans. II*, 1986, 7.
63. A. R. Butler, C. Glidewell, J. Reglinski, and A. Waddon, *J. Chem. Res., Synop.*, 1984, **9**, 279.
64. J. Casodo, M. A. Lopez Quintela, M. Mosquera, M. F. Rodriguez Prieto, and J. Vasquez Tato, *Ber. Bunsen Ges. Phys. Chem.*, 1983, **87**, 1208; *Chem. Abstr.*, 1984, 100,63071c.
65. H. Maltz, M. A. Grant, and M. C. Navaroli, *J. Org. Chem.*, 1971, **36**, 363.
66. G. Scagliarini, *Atti V. Congr. Nazl. Chim. Pura Appl.*, Rome (1935), 1936, Pt.1, 546; *Chem. Abstr.*, 1937, 31,3407.
67. L. Cambi, A. Cagnasso, and T. Ricci, *Gazz. Chim. Ital.*, 1931, **61**, 3; *Chem. Abstr.*, 1931, 25,2383.
68. L. Cambi, *Atti Accad. Nazl. Lincei*, 1914, **23**, 812; *Chem. Abstr.*, 1915, **9**, 452.

## CHAPTER 2

A DISCUSSION OF THE NMR DATA

FOR SOME CARBON ACIDS AND OXIMES

## 2.1 INTRODUCTION

The reactions of the nitroprusside ion (NP) with the carbon acids pentane-2,4-dione and 3-methylpentane-2,4-dione in alkaline solution are discussed in Chapter 4 but nmr spectra of some of the compounds important to elucidation of the reaction mechanisms will be considered here. Unless otherwise specified, all spectra were recorded in  $D_2O$  and the chemical shifts are referenced to TMS.

Keto and enol isomers of acetylacetone (Hacac)

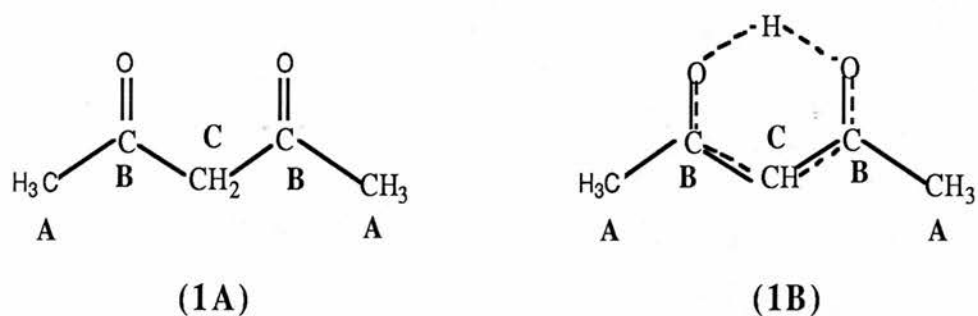


**Table 1 :** Carbon-13 nmr data for acetylacetone (Hacac)

<i>chemical shift/ppm</i>	<i>intensity</i>	<i>assignment</i>	<i>structure</i>
24.4	22	A	1B
30.8	100	A	1A
57.6	67	C	1A
101.3	17	C	1B
193.3	8	B	1B
208.6	42	B	1A

Acetylacetonate (acac-)

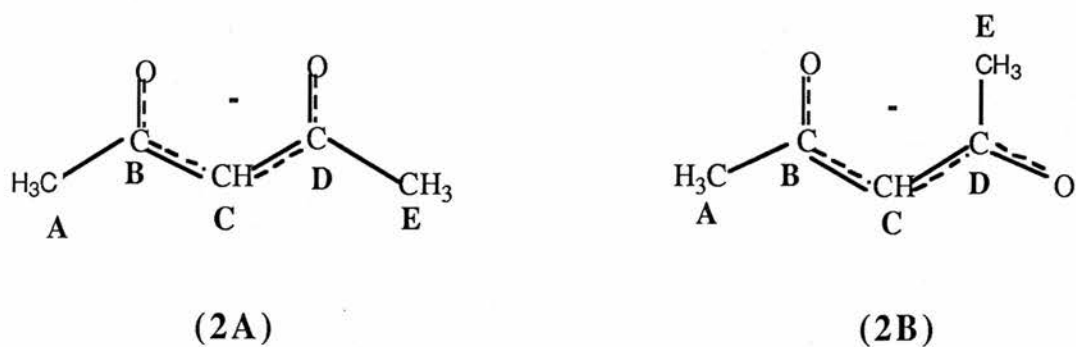


**Table 2 :** Carbon-13 nmr data for acetylacetonate (acac-)

<i>chemical shift/ppm</i>	<i>intensity</i>	<i>assignment</i>	<i>structure</i>
28.0	59	A	2B
102.0	42	C	2B
195.0	59	B	2B

## 2.2 RESULTS AND DISCUSSION

### 2.2.1 Pentane-2,4-dione (Hacac)

Pentane-2,4-dione, commonly referred to as acetylacetone (Hacac), is a carbon acid of low  $pK_a$  (8.87).<sup>1</sup> In solution, Hacac exists as an equilibrium mixture of the keto (1A) and enol (1B) isomers. Hacac can act as a bidentate ligand, coordinating through the oxygen atoms of the two carbonyl groups, to form complexes with many transition metals. Loss of a proton at the 3-position leads to aromatisation of the ligand.

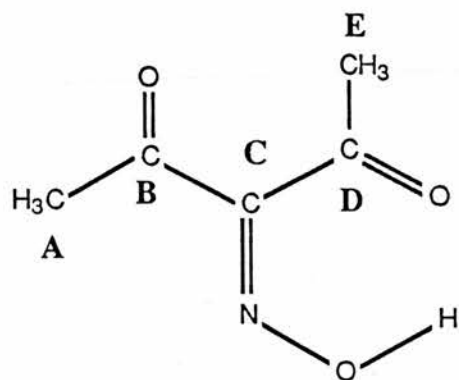
Data from the carbon-13 nmr spectra of Hacac in  $D_2O$  and in alkaline solution (e.g. acetylacetonate,  $acac^-$ ) are displayed in Tables 1 and 2.

### 2.2.2 3-Hydroxyiminopentane-2,4-dione (Hinaa)

The proton nmr spectrum of 3-hydroxyiminopentane-2,4-dione, referred to as isonitrosoacetylacetone (Hinaa), has been recorded by other workers,<sup>2,3</sup> but with a nitrogen-15 label the proton nmr spectrum (Table 3), as well as the carbon-13 (Table 4) and nitrogen-15 spectra of Hinaa reveal some interesting features.

From a proton nmr spectrum of Hinaa (reported<sup>2</sup> as  $\delta_H(CDCl_3)$ : 2.43 (s, 6H) ppm) it would seem that the two methyl groups are equivalent, but Patel and Halдар<sup>3</sup> have postulated the cyclic conformation (3) on the basis of a spectrum ( $\delta_H(CCl_4)$ : 2.7 (3 H, s), 3.2 (3 H, s) ppm) in which the two methyl groups are clearly not equivalent. In the present study there is further evidence for conformation (3) from the nitrogen-15

Isonitrosoacetylacetone (Hinaa)



(3)

Table 3: Proton nmr data for Hinaa

	<i>chemical shift/ppm</i>	<i>integral</i>
Hinaa in CDCl <sub>3</sub>	2.41	3H
	2.43	3H
	10.3	1H
<sup>15</sup> N labelled Hinaa in CDCl <sub>3</sub>	2.41 <sup>a</sup>	3H
	2.43	3H
	10.3	1H
<sup>15</sup> N labelled Hinaa in D <sub>2</sub> O	2.41	3H
	2.43 <sup>b</sup>	3H

a. doublet,  $^4J_{\text{NH}} = 0.6\text{Hz}$

b. incompletely resolved doublet

Table 4: Carbon -13 nmr data for isonitrosoacetylacetone (Hinaa)

	<i>chemical shift/ppm</i>	<i>intensity</i>	<i>assignment</i>	<i>structure</i>
Hinaa	25.3	73	A or E	3
	30.4	93	A or E	3
	156.5	27	C	3
	197.8	26	B	3
	203.8	26	D	3
<sup>15</sup> N labelled Hinaa	25.1	100	A or E	3
	30.2	73	A or E	3
	156.1	31	C	3
	198.0 <sup>a</sup>	21	B	3
	204.4	29	D	3

a. doublet,  $^2J_{\text{CN}} = 11.6\text{Hz}$

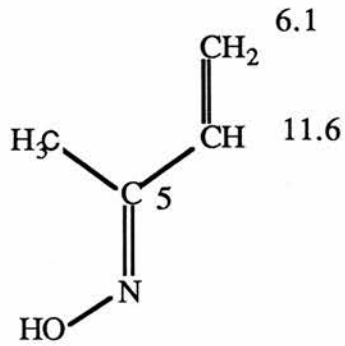
nmr spectrum of nitrogen-15 labelled Hinaa; a closely spaced quartet (14.62 ppm,  ${}^4J_{\text{NH}} = 0.6$  Hz) was recorded at high field. This splitting pattern must arise from coupling with one set of methyl protons, e.g. coupling over four bonds, which has only been resolved in the presence of a  $\pi$  system,<sup>4</sup> as found for (3). Additionally, in the proton nmr spectrum (Table 3) of nitrogen-15 labelled Hinaa, one of the methyl signals was split into a doublet. The coupling constant ( ${}^4J_{\text{NH}} = 0.6$  Hz, determined from the spectrum recorded in  $\text{CDCl}_3$ , of better resolution than the spectrum in  $\text{D}_2\text{O}$ ) is identical to the ( ${}^4J_{\text{NH}}$ ) coupling constant determined from the nitrogen-15 spectrum.

One carbonyl resonance of the carbon-13 nmr spectrum of nitrogen-15 labelled Hinaa was split into a doublet (Table 4). The assignment of this nitrogen to carbon coupling was made with consideration of the coupling constants<sup>5</sup> for the two isomers of methyl vinyl ketoxime (4A and 4B). The similarity of the  ${}^2J_{\text{CN}}$  value (11.6 Hz) for (4A) and the experimental coupling constant (11.4 Hz) indicates there is two-bond coupling of nitrogen-15 and Hinaa carbonyl B (3). Two-bond couplings to nitrogen are related to the orientation of the nitrogen lone pair and can be used to distinguish between isomers; coupling is large (and negative) to nuclei close in space to the lone pair but small (and positive) to those nuclei more distant.<sup>6</sup>

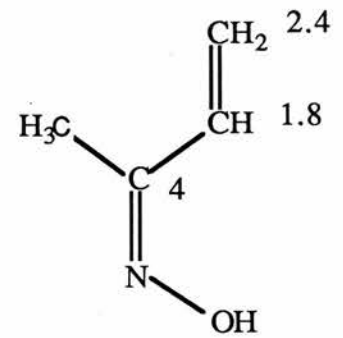
The  $\text{p}K_{\text{a}}$  of Hinaa is 7.4,<sup>7</sup> representing loss of the oxime hydroxyl proton. A number of tautomers can be drawn for this structure but from the carbon-13 nmr of Hinaa in alkaline

Two isomers of methyl vinyl ketoxime

(Numbers represent the absolute values (Hz) of  $J_{CN}$  coupling constants)

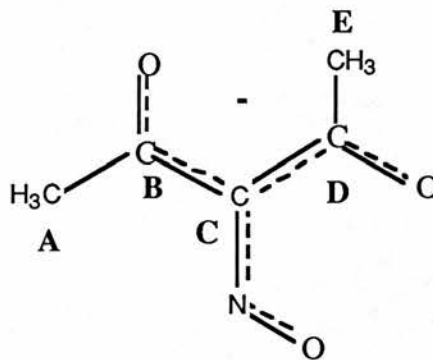


(4A)



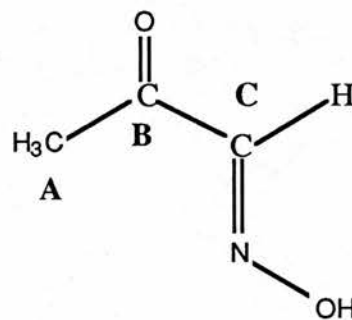
(4B)

Anion of isonitrosoacetylacetone (inaa-)



(5)

Isonitrosoacetone



(6)

**Table 5 :** Carbon-13 nmr data for Hinaa in alkaline solution (inaa-)

	<i>chemical shift/ppm</i>	<i>intensity</i>	<i>assignment</i>	<i>structure</i>
[HO <sup>-</sup> ] = 0.2 M [Hinaa] =1.0 M	25.3	73	E	3
	26.1	9	A or E	5
	30.4	100	A	3
	156.4	32	C	3
	197.7	31	B	3
	203.8	32	D	3
[HO <sup>-</sup> ] = 0.5 M [Hinaa] =1.0 M	22.6	293	A or E	5
	25.5	303	A or E	3
	26.2	77	A or E	5
	30.7	296	A or E	3
	70.4	18	C	5
	173.5	<18	D or B	5
	180.0	113	D or B	5
	198.7	95	B	3
	205.1	55	D	3
[HO <sup>-</sup> ] = 1.0 M [Hinaa] =1.0 M	22.6	100	A or E	5
	26.2	71	A or E	5
	70.3	26	C	5
	173.6	16	D or E	5
	179.7	50	D or E	5

**Table 6 :** Carbon -13 nmr of isonitrosoacetone (Ina) and acetate

<i>chemical shift/ppm</i>	<i>intensity</i>	<i>assignment</i>	<i>structure</i>
23.4	60	-	(acetate)
27.5	57	A	6
151.8	74	C	6
181.1	<20	-	(acetate)
203.0	<20	B	6

3-Methylpentane-2,4-dione (MHacac)

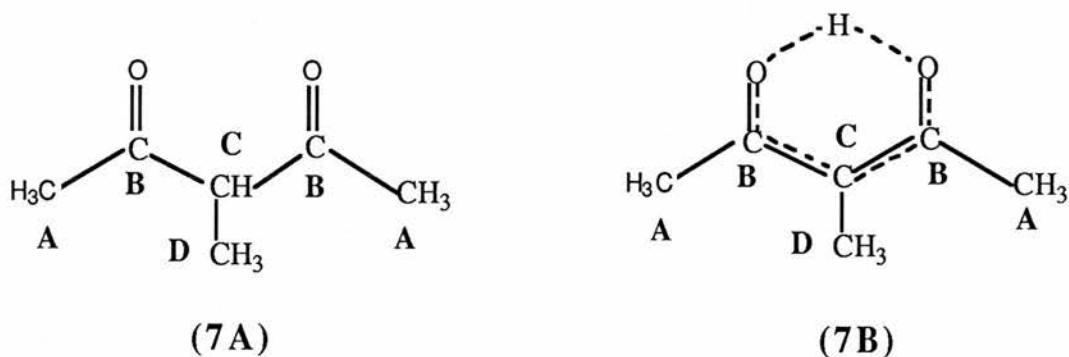


**Table 7 :** Carbon-13 nmr data for 3-methylpentane-2,4-dione (MHacac)

<i>chemical shift/ppm</i>	<i>intensity</i>	<i>assignment</i>	<i>structure</i>
12.5	47	D	7A
21.0	<15	D	7B
26.3	<15	A	7B
29.3	80	A	7A
61.1	49	C	7A
190.2	<15	B	7B
211.8	36	B	7A

3-Methylpentane-2,4-dione in alkaline solution (Macac-)

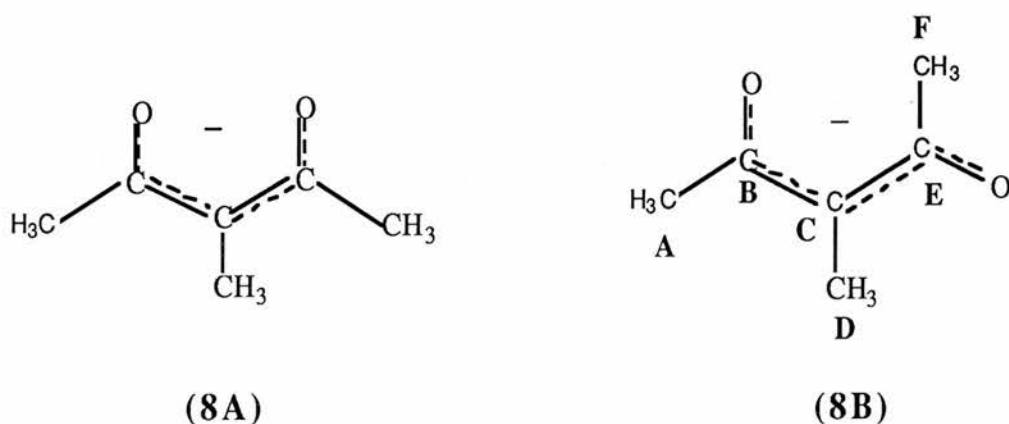


**Table 8 :** Carbon-13 nmr data for 3-methylpentane-2,4-dione in alkaline solution (Macac-)

<i>chemical shift/ppm</i>	<i>intensity</i>	<i>assignment</i>	<i>structure</i>
13.9	30	D	8B
19.4	30	A2 or F2	8B
27.1	26	A2 or F2	8B

solution (Table 5), the best representation of the oximate anion  $\text{inaa}^-$  is (5). Although interpretation of the carbon-13 nmr of acetate and isonitrosoacetone (Ina, (6)) was straightforward, the data given in Table 6 are important to consideration of the stability of Hinaa in alkaline solution. Cambi and colleagues<sup>8</sup> report that Ina and acetate arise from decomposition of the oxime Hinaa in alkaline solution. However, it is clear from comparison of the data in Tables 5 and 6 that in alkaline solution (5) is formed, which does *not* decompose to Ina and acetate. The significance of this result will be discussed in further detail in Chapter 4.

### 2.2.3 3-Methylpentane-2,4-dione (MHacac)

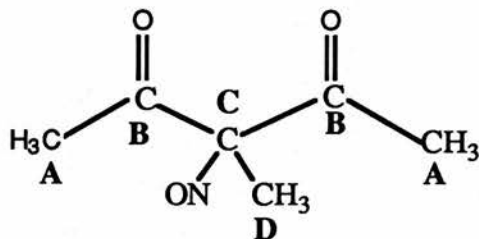
3-Methylpentane-2,4-dione ( $\text{pK}_a$  11.0)<sup>9</sup>, referred to as MHacac, exists as an equilibrium mixture of the (predominantly) keto (7A) and enol (7B) isomers in solution (Table 7). Like pentane-2,4-dione (Hacac), MHacac forms complexes with transition metals, as a bidentate ligand co-ordinated through the two carbonyl oxygens. Aromatisation of this ligand can be achieved through loss of the proton at the 3-position.

In the carbon-13 nmr spectrum of an alkaline solution of MHacac, only three (methyl) signals were resolved (Table 8). The appearance of three signals indicates that carbanion (8B) is formed; for the other tautomer (8A) it is expected that two of the three methyl groups will be equivalent.

### 2.2.4 3-Methyl-3-nitrosopentane-2,4-dione

It was not possible, due to its low solubility, to record

3-Methyl-3-nitrosopentane-2,4-dione



(9)

**Table 9** : Carbon-13 nmr data for 3-methyl-3-nitrosopentane-2,4-dione in CDCl<sub>3</sub>

<i>chemical shift/ppm</i>	<i>intensity</i>	<i>assignment</i>	<i>structure</i>
20.4	60	A	9
16.7	80	D	9

(Carbons B and C were not resolved in this spectrum)

a carbon-13 nmr spectrum of 3-methyl-3-nitrosopentane-2,4-dione (9) in water and the data for the carbon-13 nmr of (9) in  $\text{CDCl}_3$  are displayed in Table 9. By nitrosation<sup>9</sup> of MHacac (20 atom %  $^{13}\text{C}$  in the 3-methyl group), carbon-13 labelled (9) was prepared. It had been established in separate experiments that (9) decomposed rapidly in alkaline solution and the labelling experiment represented an attempt to record the products of decomposition. These products were not identified but there were three peaks, at 23.7, 14.9 and 7.5 ppm, in the carbon-13 nmr of carbon-13 labelled (9) in DMSO to which sodium hydroxide had been added.

## 2.3 EXPERIMENTAL

### Materials and instruments

Pentane-2,4-dione (Hacac) was redistilled prior to use. Sodium hydroxide solutions were prepared by dilution of concentrated volumetric solutions. Methyl iodide (63.4 atom %  $^{13}\text{C}$ ) and sodium nitrite (99 atom %  $^{15}\text{N}$ ) were obtained from MSD isotopes. All other materials were AnalaR where available.

Carbon-13 nmr spectra were recorded on a Varian CFT-20 instrument in the FT mode at room temperature, with a carbon resonance of 20 MHz in a field of 1.9 T. The number of scans was typically 15,000 with a pulse width of 7  $\mu$  seconds and no pulse delay. The sodium salt of 3-(trimethylsilyl)propanesulphonate was used as an internal reference but all chemical shifts quoted refer to TMS. The nitrogen-15 nmr spectrum was recorded on a Bruker WH-360 spectrometer at the S.E.R.C. Regional NMR Service, University of Edinburgh, in the FT mode at 25 °C. The nitrogen resonance was at 36.5 MHz in a field of 8.5 T and the reference was external  $\text{CH}_3^{15}\text{NO}_2$ . The number of scans was 64 with a 28  $\mu$  second pulse width and no pulse delay. Proton nmr spectra were recorded on a Bruker WP-80 instrument in the FT mode.

Data from the spectra tabulated in the results section are not repeated below.

### Methods

#### Preparation of 3-hydroxyiminopentane-2,4-dione (Hinaa)<sup>10</sup>

Sodium nitrite (17.5 g, 0.25 mol) in water (75 ml) was

added to acetylacetone (25.0 g, 0.25 mol) dissolved in dilute sulphuric acid (7%, 250 ml). After stirring for 20 minutes the solution was extracted with methylene chloride and the extracts were combined and dried ( $\text{MgSO}_4$ ). After evaporation of the solvent under reduced pressure white crystalline Hinaa (yield, 25.2 g, 70%) was collected and recrystallised from methylene chloride and 60/80 petroleum ether. M.p. 72 - 74 °C (lit.<sup>10</sup> 75 °C).

Nitrogen-15 labelled Hinaa (99 atom %  $^{15}\text{N}$ ) was prepared on a smaller scale, with similar results.

#### Preparation of isonitrosoacetone (Ina)<sup>11</sup>

An equimolar solution of acetone, nitroprusside and hydroxide was extracted exhaustively with methylene chloride shortly after mixing. The organic fractions were combined, dried ( $\text{MgSO}_4$ ) and the solvent was evaporated under reduced pressure. Ina was collected as white crystals and recrystallised from methylene chloride and 60/80 petroleum ether. M.p. 57 - 59 °C, mixed m.p. with an authentic sample 57 - 59 °C (lit.<sup>12</sup> 69°).

#### Preparation of 3-methylpentane-2,4-dione (MHacac)<sup>13</sup>

Methyl iodide (25 ml, 0.4 mol) was added to Hacac (33.4 ml, 0.33 mol) and anhydrous  $\text{K}_2\text{CO}_3$  (42.0 g, 0.30 mol) in dry acetone (37 ml) and the resulting mixture was refluxed for 24 hours. After cooling,  $\text{K}_2\text{CO}_3$  was removed by filtration and the solvent (of the filtrate) was evaporated under reduced pressure, leaving a yellow liquid. Upon distillation, colourless MHacac (yield 22.0 g, 60%) was collected. B.p.

78 - 80 °C / 13 mmHg.  $\delta_{\text{H}}(\text{CDCl}_3)$  1.40 (3 H, d), 2.20 (6 H, s), 3.75 (1 H, q) ppm.

Carbon-13 labelled MHacac (20 atom %  $^{13}\text{C}$  in the 3-methyl group) was prepared on a smaller scale using 20 atom %  $^{13}\text{C}$  methyl iodide, with similar results.

#### Preparation of 3-methyl-3-nitrosopentane-2,4-dione<sup>9</sup>

Sodium nitrite (2.76 g, 0.04 mol) was added to MHacac (4.56 g, 0.04 mol) in dilute sulphuric acid (2%, 200 ml). After stirring one hour in an ice bath, 3-methyl-3-nitrosopentane-2,4-dione (yield 2.51 g, 44%) precipitated as a fine white powder. M.p. 116 - 118 °C (lit.<sup>9</sup> 115 - 116 °C). Found: C, 49.81%; H, 6.34%; N, 9.50%. 3-Methyl-3-nitrosopentane-2,4-dione requires C, 50.35%; H, 6.34%; N, 9.78%.

Carbon-13 labelled 3-methyl-3-nitrosopentane-2,4-dione (20 atom %  $^{13}\text{C}$  in 3-methyl group) was prepared by nitrosation of carbon-13 labelled MHacac (20 atom %  $^{13}\text{C}$  in the 3-methyl group) on a smaller scale, with similar results.

## REFERENCES

1. J. P. Guthrie, *Can. J. Chem.*, 1979, **57**, 1177.
2. D. A. White, *J. Chem. Soc. A*, 1971, 233.
3. N. J. Patel and B. C. Halidar, *J. Inorg. Nucl. Chem.*, 1967, **29**, 1037.
4. G. C. Levy and R. L. Lichter, *Nitrogen-15 NMR Spectroscopy*, J. Wiley and Sons, Inc., New York, p.117, 1979.
5. R. L. Lichter, D. E. Dorman and R. Wasylshen, *J. Am. Chem. Soc.*, 1974, **96**, 930.
6. Reference 4, page 11.
7. J. D. Aubort, R. F. Hudson and R. C. Woodcock, *Tetr. Lett.*, 1973, **24**, 2229.
8. L. Cambi, *Atti Accad. Nazl. Lincei*, 1914, **23**, 812 (*Chem. Abstr.*, 1915, **9**, 452).
9. Yu E. Sklyar, R. P. Erstigneeva and N. A. Preobrazhenzkii, *Khim. Geterotsikl. Soedin.*, 1969, **70** (*Chem. Abstr.*, 1969, **70**, 114919g).
10. L. Wolff, *Annalen*, 1902, **325**, 129.
11. K. W. Loach and T. A. Turney, *J. Inorg. Nucl. Chem.*, 1961, **18**, 179.
12. P. Alderliesten, A. Almenningen and T. G. Strand, *Acta Chem. Scan. B*, 1975, **29**, 811.

13. A. W. Johnson, E. Markham, R. Price and K.B. Shaw,  
*J. Chem. Soc.*, 1958, 4257.

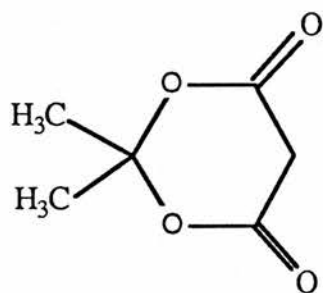
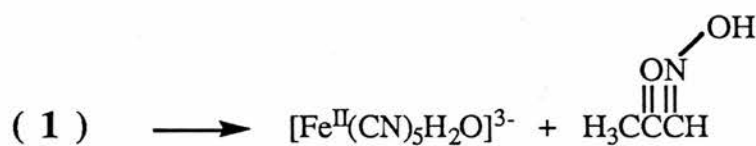
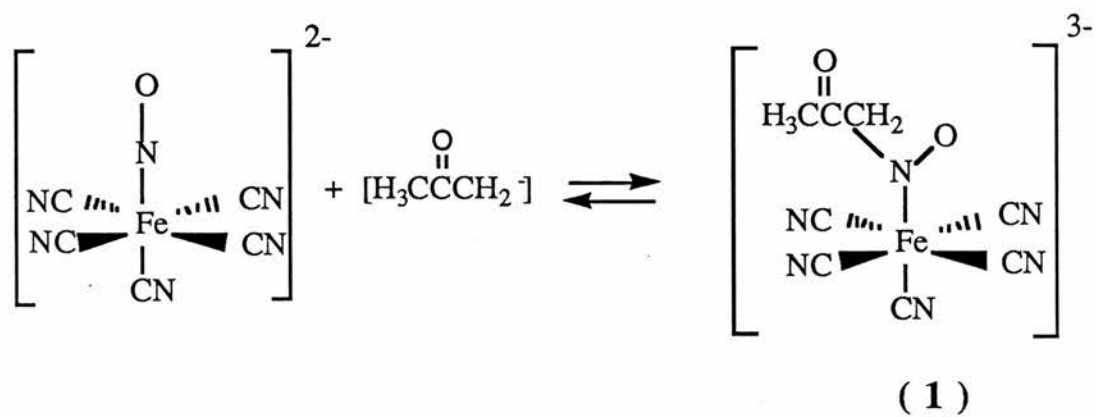
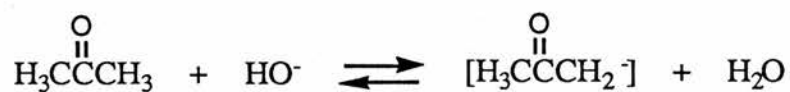
CHAPTER 3

THE REACTION OF THE NITROPRUSSIDE ION

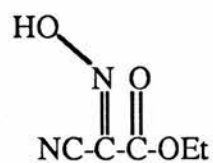
WITH ETHYL CYANOACETATE IN

ALKALINE SOLUTION

**Scheme 1 :** The reaction of nitroprusside with the carbanion of acetone



( 2 )



( 3 )

### 3.1 INTRODUCTION

The reaction of sodium nitroprusside (SNP,  $\text{Na}_2[\text{Fe}^{\text{II}}(\text{CN})_5\text{NO}]$ ) with carbon acids in alkaline solution is characterised by the rapid formation of a bright red species which for acetone<sup>1</sup> and several other carbon acids<sup>2</sup> has been shown to be an adduct of the type (1) illustrated in Scheme 1. The adducts are formed by nucleophilic attack of the carbanion at the nitrosyl ligand: SNP is a source of  $\text{NO}^+$  in alkaline solution.

The adducts of  $\text{NP}^*$  and carbon acids decompose rapidly in solution, marked by fading to yellow, and a number of kinetic studies of the rates of formation and decomposition of the adducts have been conducted.<sup>3-5</sup> The final products have always been assumed to be the oxime of the carbon acid and aquapentacyanoferrate(II) based on the isolation of the oxime in several preparative studies<sup>6,7</sup> although the inorganic products have never been unambiguously identified. As a continuation of investigations of reactions of sodium nitroprusside which might serve as models for its rapid and specific hypotensive action, the reactions of NP with several carbon acids of low  $\text{pK}_a$  were studied as a closer approximation to physiological conditions than previous studies with weak carbon acids requiring highly basic conditions which can contribute to side reactions.

There was no apparent reaction of NP with an alkaline solution of Meldrum's acid (2) a carbon acid of low  $\text{pK}_a$ , presumably due to the steric requirements and low

\* Nitroprusside ion

nucleophilicity of its carbanion.<sup>3</sup> The reaction of NP with acetylacetone was also considered (to be discussed in Chapter 4) but this reaction proved to be more complicated than previous workers<sup>8</sup> reported and although an adduct was formed neither the oxime of acetylacetone nor aquapentacyanoferrate(II) were identified. To confirm that the reaction of NP with acetylacetone was anomalous and that the assertions of previous workers<sup>1,4,5</sup> regarding the products of reactions of NP with other carbon acids were correct, the reaction of ethyl cyanoacetate and NP was chosen as a system from which the crystalline oxime<sup>9</sup> (ethyl isonitrosocyanacetate, (3)) could readily be isolated. The technique of isotopic dilution was utilised as a precise measure of oxime yield and, with use of 90% carbon-13 labelled SNP, it has been possible to identify the inorganic products by recording the carbon-13 nmr spectra of reaction solutions.

The  $pK_a$  of ethyl cyanoacetate was measured at the same ionic strength ( $I = 0.1$ ) as used for kinetic studies of adduct formation and found to be effectively the same as the  $pK_a$  determined at higher ionic strength ( $I = 1.0$ ).<sup>10</sup> Although the measured  $pK_a$  (11.47) is close to that used for malononitrile (11.4) in related studies<sup>3</sup> no second ionisation could be detected.

## 3.2 RESULTS AND DISCUSSION

### 3.2.1 Attempted isolation of the adduct of nitroprusside and ethyl cyanoacetate

The bright red colour ( $\lambda_{\text{max}}$  480 nm) immediately apparent upon addition of alkali to a solution of NP and ethyl cyanoacetate is characteristic of adducts of NP and other carbon acids. Subsequent reactions of the NP and ethyl cyanoacetate adduct are rapid as the red solution rapidly fades to yellow. Attempts to isolate this adduct from ice-cold alcoholic solution yielded hygroscopic brownish red powders that decomposed in air and did not analyse consistently. Although other nitroprusside and carbanion adducts have been isolated by this method, it was found that isolation of adducts of very short life was not possible by this method.<sup>3</sup> Considering evidence of the adduct isolated by a different method<sup>6</sup> and the transient but characteristic red colour of a solution of NP and ethyl cyanoacetate immediately after mixing, it seems reasonable to assume that an adduct of nitroprusside and ethyl cyanoacetate analogous to that of Scheme 1 is formed.

### 3.2.2 Isolation of the oxime of ethyl cyanoacetate

Sodium nitrite, a direct nitrosating agent, reacts readily with ethyl cyanoacetate in acidic solution to form ethyl isonitrosocyanoacetate, the oxime from ethyl cyanoacetate (3), which can be isolated in high yield by extraction with methylene chloride. From a solution of equimolar NP, ethyl cyanoacetate and sodium hydroxide it was possible to isolate the oxime of ethyl cyanoacetate in 23% yield by extraction of

the neutralised reaction solution with methylene chloride. As the low yield could be attributed either to side reactions or inefficient extraction (the reaction was conducted in alcoholic solution to enhance the low water solubility of ethyl cyanoacetate), the technique of isotopic dilution<sup>11</sup> was used as a means of accurately determining the yield of the oxime. Additionally, this technique can be employed with accuracy at low concentrations as used for the kinetic studies.

Carbon-14 labelled ethyl cyanoacetate was prepared by esterification of cyanoacetic acid with carbon-14 labelled ethanol. Unfortunately, due to the exceptional quenching of ethyl isonitrosocyanoacetate, the activities of the solutions containing the carbon-14 labelled oxime could not be determined directly and the yields calculated by indirect means ranged from 49% to 54%. The uncertainty in the oxime yield can be attributed to the imprecision of the quenching curve but despite this limitation it is obvious that the oxime of ethyl cyanoacetate is a major product of reaction of ethyl cyanoacetate with NP. Reasons for the less than quantitative yield of the oxime will be discussed later.

### 3.2.3 Identification of the inorganic products of reaction

Previous studies<sup>4,5</sup> of the reactions of NP with carbon acids in alkaline solution have utilised uv/visible spectroscopy for the identification of inorganic products as well as for kinetic studies; it is difficult to isolate cyanoferrate complexes from aqueous solutions. However, it is also difficult to identify unambiguously cyanoferrate

**Table 1** : Carbon-13 nmr spectra of 90% carbon-13 labelled NP and ethyl cyanoacetate in alkaline solution

**A.** NP (0.025M) + ethyl cyanoacetate (0.202M)

<i>chemical shift/ppm</i>	<i>intensity</i>	<i>assignment</i>
13.6	36	ethyl cyanoacetate
25.2	18	ethyl cyanoacetate
64.1	33	ethyl cyanoacetate
134.3	175	NP ( $^{13}\text{CN}_{\text{eq}}$ )

**B.** NP (0.022M) + ethyl cyanoacetate (0.177M) +  $\text{HO}^-$  (0.088M)  
after three hours

13.6	17	ethyl cyanoacetate
16.8	<17	ethanol <sup>a</sup>
24.8	<17	ethyl cyanoacetate
57.8	<17	ethanol <sup>a</sup>
64.1	17	ethyl cyanoacetate
134.4	24	NP ( $^{13}\text{CN}_{\text{eq}}$ )
175.4	175	$[\text{Fe}^{\text{II}}(\text{CN})_5\text{H}_2\text{O}]^{3-}$ ( $^{13}\text{CN}_{\text{eq}}$ ) <sup>b</sup>

**C.** NP (0.022M) + ethyl cyanoacetate (0.177M) +  $\text{HO}^-$  (0.088M)  
after three days under nitrogen atmosphere

134.4	24	NP ( $^{13}\text{CN}_{\text{eq}}$ )
175.4	160	$[\text{Fe}^{\text{II}}(\text{CN})_5\text{H}_2\text{O}]^{3-}$ ( $^{13}\text{CN}_{\text{eq}}$ ) <sup>b</sup>
~178.8	<17	$[\text{Fe}^{\text{II}}(\text{CN})_6]^{4-}$ <sup>c</sup>

**D.** NP (0.0163M) + ethyl cyanoacetate (0.0172 M) +  $\text{HO}^-$  (0.0133 M)  
after 10 minutes and 50 minutes

132.1 (multiplet)	>5	NP ( $^{13}\text{CN}_{\text{ax}}$ )
134.4 (doublet)	100	NP ( $^{13}\text{CN}_{\text{eq}}$ )
175.4 (doublet)	<2	$[\text{Fe}(\text{CN})_5\text{H}_2\text{O}]^{3-}$ ( $^{13}\text{CN}_{\text{eq}}$ ) <sup>b</sup>

a. Product of ethyl cyanoacetate hydrolysis, see text.

b. Or polymeric derivative.

c. From ligand rearrangement of  $[\text{Fe}(\text{CN})_5]^{3-}$ , see text.

complexes by this technique for while the adduct absorption maximum at 480 nm is a unique assignment, there is substantial overlap of the absorbance maxima of nitroprusside,<sup>2</sup>  $[\text{Fe}^{\text{II}}(\text{CN})_5\text{NO}_2]^{4-}$ ,<sup>4</sup>  $[\text{Fe}^{\text{II}}(\text{CN})_5\text{H}_2\text{O}]^{3-}$ ,<sup>12</sup>  $[\text{Fe}^{\text{III}}(\text{CN})_5\text{H}_2\text{O}]^{2-}$ ,<sup>13</sup> and  $[\text{Fe}_2(\text{CN})_{10}]^{6-}$ .<sup>13</sup>

Consequently, carbon-13 nmr is the only readily available technique for unambiguously determining the inorganic reaction products. However, in none of the carbon-13 nmr spectra of alkaline ethyl cyanoacetate and NP reaction solutions (Table 1, spectra A - D) was complete conversion of nitroprusside to aquapentacyanoferrate(II) apparent, on the basis of previously published chemical shifts of cyanoferrate complexes.<sup>14</sup> Before considering further these carbon-13 nmr spectra, there are several observations that are pertinent to assignment of the signals.

The cyanide ligands of SNP prepared from 90% enriched  $\text{Na}^{13}\text{CN}$  via hexacyanoferrate(II) are assumed to be statistically distributed; 59.0% of the ions are  $[\text{Fe}(^{13}\text{CN})_5\text{NO}]^{2-}$ , 26.2% are  $[\text{Fe}(^{13}\text{CN}_{\text{ax}})(^{12}\text{CN}_{\text{eq}})(^{13}\text{CN}_{\text{eq}})_3\text{NO}]^{2-}$  and 6.6% are  $[\text{Fe}(^{12}\text{CN}_{\text{ax}})(^{13}\text{CN}_{\text{eq}})_4\text{NO}]^{2-}$ .<sup>14</sup> The other isotopic species are not significantly abundant and the differences in chemical shifts between the three major species are negligible so that 90% carbon-13 labelled pentacyanoferrate(II) species are readily characterised by their distinctive carbon-13 nmr splitting pattern. Four equivalent equatorial  $^{13}\text{CN}$  ligands are split into a doublet (134.4 ppm) by coupling to the axial  $^{13}\text{CN}$  ligand, which is similarly split into a quintet (132.4 ppm). The quintets due to axial ligands were not resolved

in the spectra A - D of Table 1 and thus chemical shifts reported below refer to the equatorial cyanide ligands (doublets) alone unless otherwise indicated.

It has not been possible to isolate aquapentacyanoferrate(II),  $[\text{Fe}(\text{CN})_5\text{H}_2\text{O}]^{3-}$ ; in concentrated solutions the dimer  $[\text{Fe}_2(\text{CN})_{10}]^{6-}$  is formed.<sup>15</sup> The literature value for the carbon-13 nmr chemical shifts of aquapentacyanoferrate(II) ( $^{13}\text{CN}_{\text{eq}}$  172.8,  $^{13}\text{CN}_{\text{ax}}$  177.2 ppm) originates from the spectrum of an alkaline solution of 90% carbon-13 labelled NP; NP reacts with hydroxide to form nitropentacyanoferrate(II) ( $[\text{Fe}(\text{CN})_5\text{NO}_2]^{4-}$ ;  $^{13}\text{CN}_{\text{eq}}$  176.7,  $^{13}\text{CN}_{\text{ax}}$  174.4 ppm) which is in equilibrium with the aqua complex.<sup>14</sup>

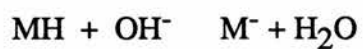
The signals at 175.4 ppm in spectra A - D of Table 1 could represent equatorial cyanide ligands, either aquapentacyanoferrate(II) or nitropentacyanoferrate(II); it is difficult to propose any other cyanoferrate complex that reasonably could be a major diamagnetic product of reaction. There was no apparent reaction of the oxime of ethyl cyanoacetate, or the products of ethyl cyanoacetate hydrolysis, cyanoacetic acid and ethanol, with nitroprusside or nitroprusside in alkaline solution [e.g. a mixture of aquapentacyanoferrate(II) and nitropentacyanoferrate(II)]. A degassed solution of sodium hydroxide added to a degassed (equimolar) solution of NP and ethyl cyanoacetate did not lead to observation of any EPR active species up to two hours after mixing.

Although the consistently observed peaks at 175.4 ppm can be assigned to nitropentacyanoferrate(II) on the basis of the similarity of that value with the literature value ( $^{13}\text{CN}_{\text{eq}}$

176.7 ppm) contrasted to the greater divergence from the literature value for aquapentacyanoferrate(II) ( $^{13}\text{C}_{\text{N}_{\text{eq}}}$  172.8 ppm), there are sound reasons for rejecting this argument. Variation in chemical shift with concentration and pH is expected, and for the case of aquapentacyanoferrate(II) it is expected that the complex itself will vary with these conditions. There is some controversy<sup>16-18</sup> in the literature as to the  $\text{pK}_{\text{a}}$  of aquapentacyanoferrate(II) (estimated values range from 7.6 to 17) and it is known that dimerisation and oxidation occur in more concentrated solutions. Aquapentacyanoferrate(II) and its anion or dimer will be collectively referred to as the aqua complex as it is not clear which species is present in these solutions.

If the signals at 175.4 ppm in spectra A - D (Table 1) represented nitropentacyanoferrate(II) then either of two trends would be expected; increase in the intensity of these signals due to continuing formation of nitropentacyanoferrate(II) or decrease in these signals and the appearance of another in accordance with solvation of nitropentacyanoferrate(II) to the aqua complex. However, there was no difference in spectra of the same sample recorded at ten and fifty minutes after mixing (Table 1, spectra D). Additionally, a reaction solution spectra recorded after three days (Table 1, spectrum C) was identical to a spectrum of the same sample recorded within three hours of mixing (Table 1, spectrum B), except for a small additional single peak at 178.8 ppm in the former which corresponded closely to a previously recorded value for hexacyanoferrate(II).<sup>19</sup> The aqua complex is in equilibrium

**Scheme 2 :** Equilibrium concentrations of hydroxide and the carbanion of ethyl cyanoacetate



$$[\text{MH}]_t = [\text{M}^-]_e + [\text{MH}]_e$$

$$[\text{HO}^-]_t = [\text{M}^-]_e + [\text{HO}^-]_e$$

$$K' = K_a/K_w = [\text{M}^-]_e/[\text{MH}]_e[\text{HO}^-]_e$$

$$[\text{M}^-]_e = K_a/K_w \{[\text{MH}]_e [\text{HO}^-]_e\}$$

$$[\text{M}^-]_e = K_a/K_w \{[\text{MH}]_t - [\text{M}^-]_e\} \{[\text{HO}^-]_t - [\text{M}^-]_e\}$$

(MH and  $\text{M}^-$  refer to ethyl cyanoacetate and its carbanion,  $[\ ]_t$  and  $[\ ]_e$  refer to total and equilibrium concentrations, respectively)

with  $[\text{Fe}(\text{CN})_5]^{3-}$  which, as it will be shown in Chapter 6, can undergo ligand rearrangement to form hexacyanoferrate(II).

Finally, the assignment of the signals at 175.4 ppm in Table 1 to nitropentacyanoferrate(II) is obviously inconsistent with the isolation of the oxime as a major product of reaction. The less than theoretical yield of the oxime as well as incomplete conversion of nitroprusside to the aqua complex, can be rationalised by the rapid hydrolysis of ethyl cyanoacetate in alkaline solutions, to be discussed in full later. The above evidence supports previous proposals<sup>1,4,5</sup> that the major inorganic product of reaction of NP and carbon acids in alkaline solution is the aqua complex.

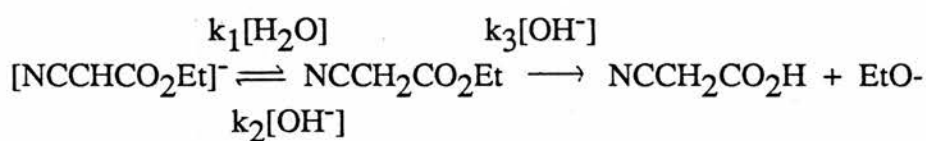
#### 3.2.4 Kinetic Studies

It has been established that for the reaction of carbon acids and SNP in alkaline solution the formation of the carbanion is not the rate-determining but a pre-equilibrium step.<sup>3</sup> It is therefore the equilibrium concentrations of hydroxide and the ethyl cyanoacetate carbanion that must be used to analyse the kinetic data. These concentrations can be calculated using the quadratic equation to solve the following equation knowing the total carbanion and hydroxide concentrations and the constants  $K_w$  and  $K_a$ . (Scheme 2)

$$[\text{M}^-]_e = (K_a/K_w) ([\text{MH}]_t - [\text{M}^-]_e) ([\text{HO}^-]_t - [\text{M}^-]_e)$$

(MH and  $\text{M}^-$  refer to ethyl cyanoacetate and its carbanion,  $[\ ]_t$  and  $[\ ]_e$  refer to total and equilibrium concentrations, respectively.

**Scheme 3 : Hydrolysis of ethyl cyanoacetate**



$M^-$

$MH$

products

$$(K = k_1/k_2, \quad K_a = K' \cdot K_w, \quad K_w = 10^{-14})$$

$$\frac{d[M^-]}{dt} = k_2[MH][\text{OH}^-] - k_1[\text{H}_2\text{O}][M^-]$$

$$= \frac{k_1[\text{H}_2\text{O}]k_3[\text{OH}^-]}{k_1[\text{H}_2\text{O}] + k_2[\text{OH}^-]} \cdot [M^-]$$

$$\frac{d[M^-]}{[M^-]} = \frac{k_1[\text{H}_2\text{O}]k_3[\text{OH}^-]}{k_1[\text{H}_2\text{O}] + k_2[\text{OH}^-]} dt = k_{\text{obs}}$$

$$\frac{1}{k_{\text{obs}}} = \frac{k_1}{k_1k_3[\text{OH}^-]} + \frac{k_2[\text{OH}^-]}{k_1k_3[\text{OH}^-]}$$

$$\frac{1}{k_{\text{obs}}} = \frac{1}{k_3 \cdot [\text{OH}^-]} + \frac{K'}{k_3}$$

### 3.2.4.1 Determination of the $pK_a$ of ethyl cyanoacetate

The literature  $pK_a$  of ethyl cyanoacetate, determined by Lienhard and Jencks<sup>10</sup> at an ionic strength of 1.0, is surprisingly low compared to the values for malononitrile (11.4) and diethyl malonate (13.3).<sup>3</sup> As the kinetic studies of the reaction of NP and ethyl cyanoacetate were conducted at an ionic strength of 0.1, it was worthwhile to determine the  $pK_a$  of ethyl cyanoacetate under these conditions.

Ethyl cyanoacetate rapidly hydrolyses in alkaline solution; this reaction precludes  $pK_a$  determination by standard methods but does not interfere with kinetic studies of NP and ethyl cyanoacetate adduct formation, discussed later. Use of the steady state approximation (Scheme 3)<sup>20</sup> leads to the following expression for the rate of disappearance of the absorbance at 260 nm corresponding to the carbanion of ethyl cyanoacetate.

$$\frac{1}{k_{\text{obs}}} = \frac{1}{k_3[\text{OH}^-]} + \frac{K'}{k_3}$$

From the values of the slope and intercept of a plot of  $1/k_{\text{obs}}$  against  $1/[\text{OH}^-]$  (Figure 1) the  $pK_a$  of ethyl cyanoacetate has been calculated to be 11.47.

### 3.2.4.2 Rate of Adduct Formation

The formation of the red colour attributed to the NP and ethyl cyanoacetate adduct could be monitored by stopped-flow spectrophotometry. Pseudo first-order conditions were maintained with a substantial excess of hydroxide and ethyl cyanoacetate; solutions of various hydroxide concentrations

**Figure 1** : Plot of  $1/k_{\text{obs}}$  vs.  $1/[\text{HO}^-]$  for the hydrolysis of ethyl cyanoacetate

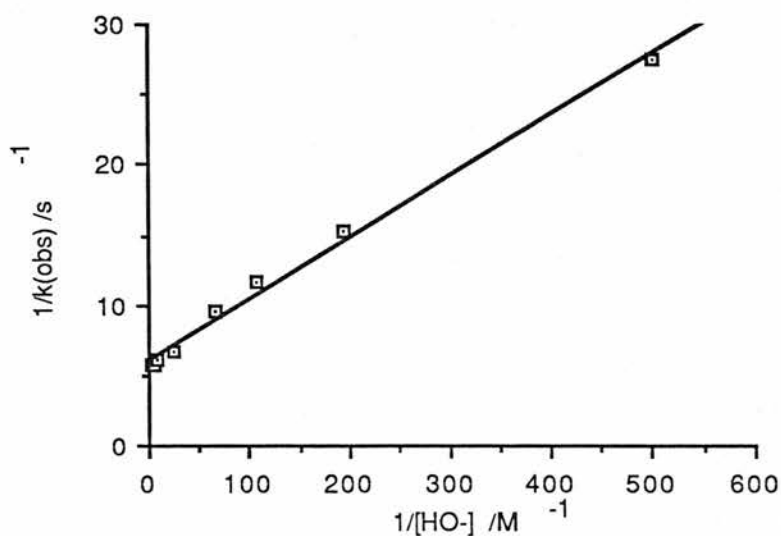


**Table 2** : Kinetic data for the hydrolysis of ethyl cyanoacetate<sup>a</sup> at 25° C

pH <sup>b</sup>	$1/[\text{HO}^-]/\text{M}$	$1/k_{\text{obs}} / \text{s}$	$10^2 k_{\text{obs}}^{\text{c}} / \text{s}^{-1}$
11.30	501	27.5	3.63
11.71	195	15.3	6.52
11.97	107	11.7	8.50
12.17	67	9.5	10.50
12.62	24	6.7	14.81
12.98	9.5	6.1	16.29
13.31	4.9	5.74	17.43
13.57	2.7	5.66	17.68

a. Initial concentration typically  $1.0 \times 10^{-3} \text{ M}$

b.  $I = 0.1 \text{ M}$

c. First-order rate constant were determined using the Kedzy - Swinbourne method for the rate of disappearance of the ethyl cyanoacetate carbanion at 260 nm. Correlation coefficients were always better than 0.999.

**Figure 2 :** Plot of  $k_{\text{obs}}$  vs.  $[M^-]$  for the reaction of nitroprusside with the carbanion of ethyl cyanoacetate

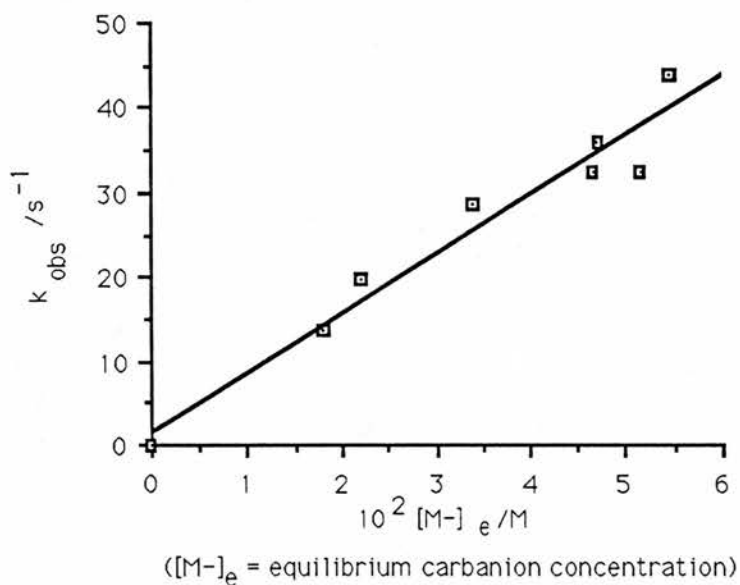


**Table 3 :** Kintetic data for the reaction of nitroprusside<sup>a</sup> with the carbanion of ethyl cyanoacetate<sup>b</sup> at 25° C

$10^2 [\text{HO}^-]_t$ <sup>c</sup> /M	$10^2 [\text{-HCCNCO}_2\text{Et}]_e$ <sup>d</sup> /M	$k_{\text{obs}}/\text{s}^{-1}$
2.00	1.80	$13.7 \pm 1.0$
2.50	2.22	$19.9 \pm 2.0$
4.00	3.40	$28.8 \pm 1.4$
5.00	4.66	$32.6 \pm 0.3$
6.25	4.71	$36.1 \pm 1.0$
7.50	5.15	$32.6 \pm 2.0$
9.00	5.45	$44.0 \pm 1.0$

- a. Initial concentration =  $1.875 \times 10^{-3}$  M
- b. Stoichiometric concentration =  $6.25 \times 10^{-2}$  M
- c. Stoichiometric hydroxide concentration
- c. Equilibrium carbanion concentration

were in one syringe, an aqueous solution of ethyl cyanoacetate and SNP in the other syringe. In this way, the concentrations of the ethyl cyanoacetate carbanion could be varied by changing the concentrations of the hydroxide solutions and with consideration of the  $pK_a$  of ethyl cyanoacetate, equilibrium carbanion and hydroxide concentrations could be calculated. Upon mixing, the absorbance at 480 nm increased rapidly but the onset of slower decay at this wavelength as the adduct hydrolysed limited the accuracy of the observed rate constants (Table 3).

There is a rectilinear relationship between the first order rate constant  $k_{obs}$  for the formation of the adduct and the equilibrium carbanion concentration  $[M^-]$  (Figure 2). This relationship suggests that the rate determining step is the reaction of NP with the ethyl cyanoacetate carbanion. Similarly, the rate determining step for the reaction of NP and ethyl malononitrile ( $pK_a$  12.8) was found to be the irreversible reaction of NP with the carbanion.<sup>3</sup> However, formation of the adduct of NP and malononitrile, a carbon acid of similar  $pK_a$  (11.4) proceeds by a different mechanism.<sup>3</sup> There is a rectilinear relationship not between the first order rate constant  $k_{obs}$  and the equilibrium concentration of the malononitrile carbanion but between  $k_{obs}$  and the product of the equilibrium hydroxide and carbanion concentrations attributed to a second ionisation. There are two explanations for the divergent reactivity of these two carbon acids with nitroprusside in alkaline solution. Malononitrile could more readily undergo a second ionisation.

**Table 4** : Kinetic data for the decomposition of the adduct obtained from nitroprusside<sup>a</sup> and the carbanion of ethyl cyanoacetate<sup>b</sup> at 25° C.

$10^2 [\text{HO}^-]_t^c / \text{M}$	1.0	2.0	4.0	6.3	8.8	15.0	18.8	25.0
$10^2 k_{\text{obs}} / \text{s}$	3.11	2.66	2.76	3.11	3.11	3.18	3.16	2.84

a. Initial concentration  $1.88 \times 10^{-3} \text{ M}$

b. Initial concentration  $6.25 \times 10^{-2} \text{ M}$

c. Stoichiometric concentration of hydroxide

Alternatively, although malononitrile is more of a normal acid (in the Eigen sense proton-transfer reactions are not generally rate determining) than ethyl cyanoacetate, this relationship does not necessarily apply to nucleophilicity and it is nucleophilicity not basicity that is important to reaction with NP. Some detailed observations of the acidities of cyanocarbons have recently been made by Kresge *et al*<sup>22</sup> which point to the latter explanation.

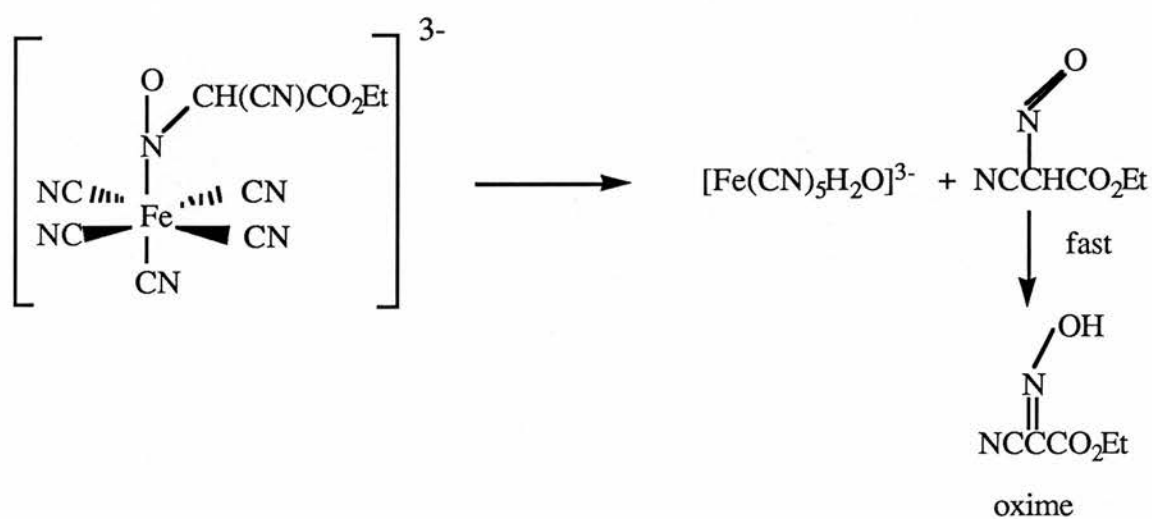
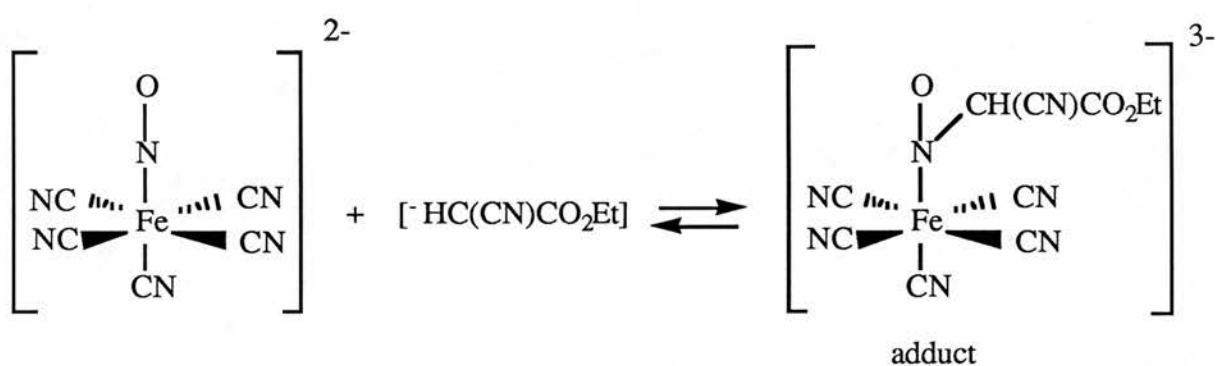
#### 3.2.4.3 Rate of adduct decomposition

The red colour attributed to the ethyl cyanoacetate and NP adduct fades rapidly to yellow and this fading reaction can be followed on a conventional spectrophotometer. As for the kinetic studies of the rate of adduct formation, solutions of sodium hydroxide of various concentrations were added to solutions of NP and ethyl cyanoacetate and the change in absorbance at 480 nm was monitored. The results are displayed in Table 4 and it is clear that the rate of decay of the adduct is independent of carbanion and hydroxide concentrations over a twenty five-fold range of initial hydroxide concentration.

### 3.3 CONCLUSIONS

From the above observations, a mechanism for the reaction of ethyl cyanoacetate with NP can be proposed (Scheme 4) that is consistent with the schemes of previous studies in which the oxime of the carbon acid and aquapentacyanoferrate(II) are the final products following formation of the adduct of

**Scheme 4 :** The reaction of nitroprusside with the carbanion of ethyl cyanoacetate



NP and the carbon acid. However, the concurrent reactions of both nitroprusside and ethyl cyanoacetate with hydroxide have been cause for some consideration.

Careful evaluation of the carbon-13 nmr spectra of reaction solutions initially containing ethyl cyanoacetate and 90% carbon-13 labelled NP (Table 1, spectra A - D) indicates that nitropentacyanoferrate(II) is not formed. The chemical shifts ( $^{13}\text{CN}_{\text{eq}}$  175.4 ppm) of signals characteristic of a pentacyanoferrate(II) complex deviate from the literature value recorded for aquapentacyanoferrate(II) ( $^{13}\text{CN}_{\text{eq}}$  172.8 ppm) but as this species is subject to dimerisation and ionisation, change in chemical shift with concentration and pH is expected. The product resulting from solvation of pentacyanoferrate(II) upon adduct decomposition is therefore referred to as the aqua complex.

The rates of hydrolysis of ethyl cyanoacetate in buffers of various pH used for determination of the  $\text{pK}_a$  indicate that this reaction does not interfere with the kinetic studies of the more rapid rate of adduct formation. However, hydrolysis of ethyl cyanoacetate is competitive with the decomposition of the adduct which explains the presence of unreacted NP in a spectrum with an initial five-fold excess of ethyl cyanoacetate and hydroxide fifty minutes after mixing (not shown but similar to spectra D of Table 1) as well as the less than theoretical yield of the oxime of ethyl cyanoacetate in preparative experiments. Kinetic studies demonstrating that adduct decomposition is independent of hydroxide and carbanion concentrations were not influenced

by this side reaction as there is no overlap of the spectra of the adduct ( $\lambda_{\text{max}}$  480 nm) and the ethyl cyanoacetate carbanion ( $\lambda_{\text{max}}$  260 nm).

The kinetic studies indicate that the rate determining step of adduct formation is the reaction of the ethyl cyanoacetate carbanion with NP; there is no evidence for second ionisation of ethyl cyanoacetate in contrast to the situation for the reaction of malononitrile with NP where there is a rectilinear relationship between  $k_{\text{obs}}$  and the product of the equilibrium concentrations of the carbanion and hydroxide. Therefore it is concluded that ethyl cyanoacetate, unlike malononitrile, does not act as a true cyanocarbon.

The use of carbon-13 nmr in conjunction with radioisotopic labelling and stopped-flow spectrophotometry has contributed to this study of NP as a nitrosating agent of the carbon acid ethyl cyanoacetate in alkaline solutions, the first system for which the mechanism as well as all final reaction products have been identified. Having demonstrated that the reaction of NP with carbon acids does occur in the manner suggested by previous workers it is possible to investigate the anomalous reactivity of acetylacetone with NP.

### 3.4 EXPERIMENTAL PROCEDURES

#### Materials and instruments

Ethyl cyanoacetate (Laboratory grade) was redistilled prior to use, and solutions were always made up and used on the same day. Sodium hydroxide solutions were prepared by dilution of concentrated volumetric solutions and, for kinetic

experiments, were made up and used on the same day. Carbon-14 labelled ethanol was obtained from Amersham International. Samples of  $\text{Na}_2[\text{Fe}^{\text{II}}(\text{}^{13}\text{CN})_5\text{NO}]\cdot 2\text{H}_2\text{O}$  were prepared by Dr. J. McGinnis, as previously reported.<sup>14</sup> All other reagents, with the exceptions of those prepared as described below, were of AnalaR grade where available.

Solid sodium nitroprusside was stored in a dark cupboard. All solutions containing nitroprusside were protected from light with a complete covering of aluminium foil during storage and use.

All carbon-13 nmr spectra (except spectra D, Table 1) were recorded at room temperature on a Varian CFT-20 instrument in the FT mode with a carbon resonance of 20 MHz in a field of 1.9 T. The number of scans was typically 8,000 with a pulse width of 7  $\mu$  seconds and no pulse delay. The sodium salt of 3-(trimethylsilyl)propane sulphonate was used as an internal reference but all chemical shifts quoted refer to tetramethylsilane (TMS).

Spectra D of Table 1 were recorded on a Bruker WH-360 spectrometer in the FT mode at 25 °C at the S.E.R.C. Regional NMR Service at the University of Edinburgh with a carbon resonance of 90.56 MHz in a field of 8.5 T. The number of scans was typically 100 with a pulse width of 4  $\mu$  seconds and a delay time of 0.33 seconds. The reference was external TMS.

The EPR experiment was conducted by Ian Johnson at the University of St. Andrews at room temperature in a quartz capillary using a Bruker ER 200D spectrometer. A degassed solution of NaOH was added to a degassed solution of NP and

ethyl cyanoacetate; concentrations were approximately 0.1 M.

Proton nmr experiments were conducted on a Bruker WP-80 instrument in the FT mode. Uv/visible spectra were recorded on a Pye-Unicam SP8-100 spectrophotometer, infra-red spectra were obtained as Nujol mulls on a Perkin Elmer 1420 spectrometer.

The rates of formation of the NP and carbanion adducts were determined by use of a Hi-Tech 3F-3L stopped-flow spectrophotometer and SF-40C control unit attached to a Data-Lab DL901 transient recorder and Farnell DIV12-14 oscilloscope; data acquisition and processing were conducted by an Apple II microcomputer using a Hi-Tech kinetic software package.

Radioactive counting was conducted on an EMI NE LSC-2 liquid scintillation counter. The solutions for counting were made up with a pseudocumene scintillation cocktail (NE265 from EMI).

## Methods

### Preparation of the oxime of ethyl cyanoacetate

A solution of sodium hydroxide (10 ml, 0.02 mol) was added to SNP (6.00 g, 0.02 mol) and ethyl cyanoacetate (2.28 g, 0.02 mol) in water (50 mls) and ethanol (10 mls) while stirring. The solution turned bright red but quickly faded to yellow and after 10 minutes was neutralised with dilute HCl. The reaction solution was extracted four times with methylene chloride and the organic fractions were combined and dried over  $MgSO_4$ . Upon evaporation of the solvent

the oxime of ethyl cyanoacetate was obtained as white needles (0.59 g, .0046 mol) in 23% yield. M.p. 128 - 130 °C, mixed melting point with a genuine sample (prepared from an acidic solution of sodium nitrite and ethyl cyanoacetate) 128 - 130 °C (lit.<sup>9</sup> 133 °C).  $\delta_{\text{H}}(\text{CDCl}_3)$  1.40 (3 H, t) and 4.45 (2 H, q),  $\delta_{\text{C}}(\text{acetone-d}_6)$  13.6, 64.0, 126.2 and 159.5 ppm.

#### Preparation of carbon-14 labelled ethyl cyanoacetate

Esterification of cyanoacetic acid (3.90 g, 0.047 mol) with carbon-14 labelled ethanol (50  $\mu\text{Ci}$ ) diluted with approximately 10 ml ethanol gave ethyl cyanoacetate in 26% yield (1.40 g,  $1.24 \times 10^{-2}$  mol). The activity of a solution (0.18 M) of this labelled ethyl cyanoacetate was measured to be 161.1  $\mu\text{Ci}/\text{mol}$ .

#### Radiation Experiments

The technique of isotopic dilution was used to determine the amount of radioactive oxime present in a large sample of inactive oxime added to the reaction solution as a carrier. Equal volumes of ethyl cyanoacetate, NP and hydroxide solutions (all 0.18 M) were reacted as for the preparation of the oxime detailed above, with the addition of an eleven-fold excess of inactive oxime as a carrier after 10 minutes when the red solution had faded to yellow. The direct measure of the activity of a small sample of the recovered oxime was not feasible as the oxime of ethyl cyanoacetate was established to be an exceptionally strong quenching agent in separate experiments. Ethyl cyanoacetate itself was judged not to quench the activity of ethanol significantly.

By measuring the 'quenched' activity of a known amount of active oxime the actual activity could be calculated from a quenching curve. The quenching curve, expressed in quantity of oxime and counting efficiency (percentage 'quenching'), was established by measuring the decrease in activity (quenching) after addition of a known amount of inactive oxime to a solution of ethanol of known activity. In this way, the 'quenched' activity associated with a known amount of active oxime could be correlated with the quenching curve and the activity of the oxime itself determined. The yields calculated from several repetitions of this method ranged from 49 - 54%

### Kinetic Studies

The rates of formation of the adduct of ethyl cyanoacetate and NP were measured at 25.0 °C and 480 nm by stopped-flow spectrophotometry. Ionic strength was maintained ( $I = 0.25$ ) with KCl. The concentrations of ethyl cyanoacetate (in one syringe also containing NP) and hydroxide (in the other syringe) were in excess to maintain pseudo first-order conditions and the carbanion concentration was varied by changing the concentration of the hydroxide solutions. The linear correlation plot (log absorbance against time), provided by the Hi-Tech kinetics software programme, established the linearity of the data for each run and thus the validity of the assumption of first-order kinetics for this system.

Conditions for recording the rate of decay of the adduct were identical except that this slower process was followed

on a conventional spectrophotometer. The observed rate constants were calculated using the Kedzy-Swinbourne method (correlation coefficients were better than 0.9990).

Each reported observed rate constant represents the average of at least six runs giving consistent results.

## REFERENCES

1. K. W. Loach and T. A. Turney, *J. Inorg. Nucl. Chem.*, 1961, **18**, 179.
2. J. H. Swinehart, *Coord. Chem. Rev.*, 1967, **2**, 385 and references therein.
3. A. R. Butler, C. Glidewell, V. Chaipanich and J. McGinnis, *J. Chem. Soc., Perkin I*, 1966, 7.
4. J. H. Swinehart and W. G. Schmidt, *Inorg. Chem.*, 1967, **6**, 232.
5. S. K. Wolfe and J. H. Swinehart, *Inorg. Chem.*, 1968, **7**, 1855.
6. L. Cambi, *Gazz. Chim. Ital.*, 1931, **61**, 3 (*Chem. Abstr.*, 1931, **25**, 2383).
7. L. Cambi, *Atti Acad. Nazl. Lincei*, 1912, **22**, 376 (*Chem. Abstr.*, 1913, **7**, 2551).
8. L. Cambi, *Atti Acad. Nazl. Lincei*, 1914, **23**, 812 (*Chem. Abstr.*, 1915, **9**, 752).
9. J. U. Nef, *Annalen*, 1894, **280**, 331.
10. G. E. Lienhard and W. P. Jencks, *J. Am. Chem. Soc.*, 1965, **87**, 3863.
11. R. A. Faires and G. G. J. Boswell, *Radioisotope Laboratory Techniques*, 4th ed., Butterworth & Co., London, 1981, pp. 257-259.

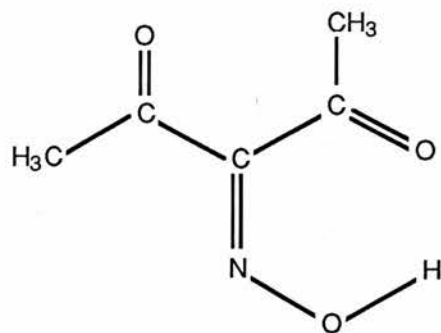
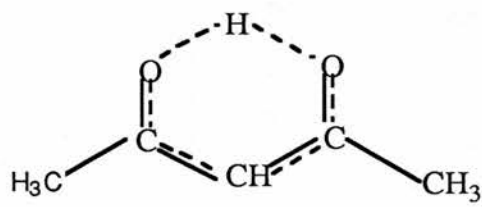
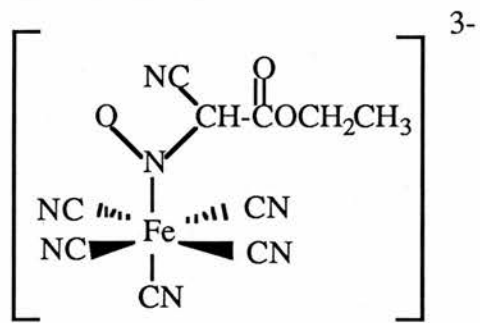
12. E. B. Borghi, M. A. Blesa, and P. J. Aymonino, *J. Inorg. Nucl. Chem.*, 1981, **43**, 1849.
13. J. H. Espenson and S. G. Wolenuk, *Inorg. Chem.*, 1972, **11**, 2035.
14. A. R. Butler, C. Glidewell, A. R. Hyde and J. McGinnis, *Inorg. Chem.*, 1985, **24**, 2931.
15. A. D. James and R. S. Murray, *J. Chem. Soc., Dalton*, 1976, 1182.
16. D. H. McCartney and A. McAuley, *Inorg. Chem.*, 1979, **18**, 2091.
17. G. Davies and A. R. Garafolo, *Inorg. Chem.*, 1980, **19**, 3543.
18. H. E. Toma, A. A. Batista and H. B. Gray, *J. Am. Chem. Soc.*, 1982, **104**, 7509.
19. A. R. Butler, C. Glidewell, A. S. McIntosh, D. Reed and I. H. Sadler, *Inorg. Chem.*, 1986, **25**, 970.
20. D. H. McDaniel and C. R. Smoot, *J. Phys. Chem.*, 1956, **60**, 966.
21. M. Hojatti, A. J. Kresge and W. H. Wang, *J. Am. Chem. Soc.*, 1987, **109**, 4023.

CHAPTER 4

THE REACTION OF THE NITROPRUSSIDE ION

WITH PENTANE-2,4-DIONE (HACAC) IN

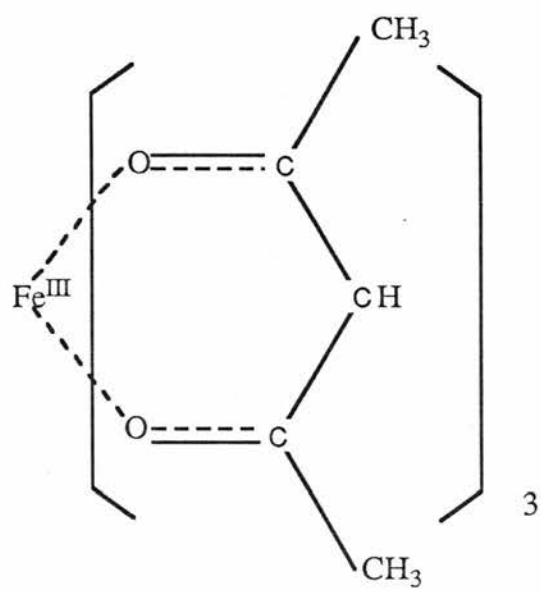
ALKALINE SOLUTION



#### 4.1 INTRODUCTION

Carbanions are known<sup>1</sup> to occur in biological systems and the reactions of the nitroprusside ion (NP) with several carbanions were considered as a continuation of investigations of clinically significant reactions of NP.<sup>2</sup> The reaction of NP with ethyl cyanoacetate in alkaline solution (Chapter 3) is a typical example of these reactions; NP undergoes nucleophilic attack at the nitrosyl nitrogen to form a deep red adduct (1). Rapid fading of the reaction solution from red to yellow is a manifestation of adduct decomposition and for the reaction of NP with the ethyl cyanoacetate carbanion the products were shown to be the oxime ethyl isonitrosocyanoacetate and (yellow) aquapentacyanoferrate(II),  $[\text{Fe}^{\text{II}}(\text{CN})_5\text{H}_2\text{O}]^{3-}$ , or its polymeric derivatives.

Pentane -2,4-dione [(2), referred to as acetylacetone] is a carbon acid of low  $\text{pK}_a$  (8.87)<sup>3</sup> and was of interest as a model for the reactions of NP with physiologically occurring carbanions. The reaction of NP with acetylacetone (Hacac) in alkaline solution has been cited<sup>4</sup> as an example of nucleophilic attack at the NP nitrosyl ligand and there is indirect evidence of formation of the oxime 3-hydroxyiminopentane-2,4-dione [(3), referred to as isonitrosoacetylacetone]. However, it was found in this study that although NP and Hacac in alkaline solution reacted to give the characteristic deep red adduct, the associated colour persisted instead of fading immediately to yellow as observed for reactions of NP with other carbanions. The oxime isonitrosoacetylacetone (Hinaa)



(4)

could not be isolated or identified but a red precipitate was recovered from NP and acetylacetone reaction solutions. The precipitate did not correspond to the adduct or any other cyanoferrate complex but to tris(pentane-2,4-dionato-0,0)iron(III) (4).

Although cyanoferrate complexes have very high formation constants<sup>5</sup> and NP, as a  $d^6$  low spin complex, is kinetically inert to ligand substitution, the formation of tris(pentane-2,4-dionato-0,0)iron(III) implies that under mild reaction conditions, as might be found *in vivo*, cyanide is apparently released from NP. The possibility of cyanide release from NP during its medical administration is of considerable concern and the mechanism of the reaction of NP and Hacac in alkaline solution was investigated with regard to the alleged toxicity of NP.

## 4.2 RESULTS

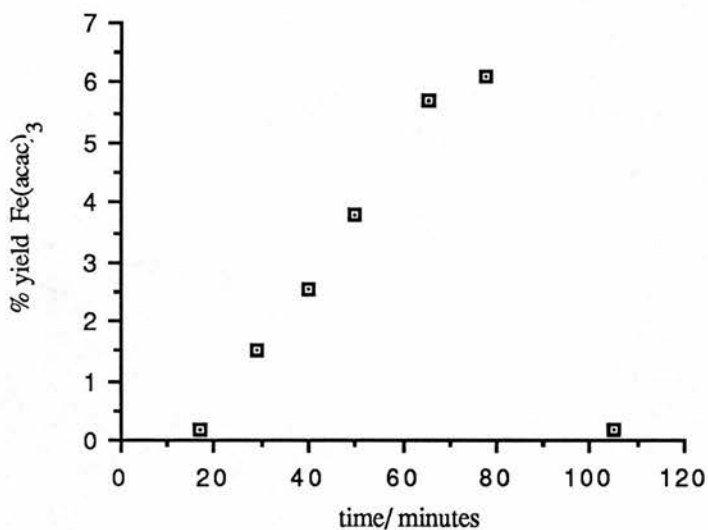
### 4.2.1 Attempted isolation of isonitrosoacetylacetone (Hinaa)

Isonitrosoacetylacetone (Hinaa) is readily prepared<sup>6</sup> by addition of sodium nitrite to a solution of acetylacetone (Hacac) in dilute HCl, and can be extracted in high yield from this solution with methylene chloride. In contrast to the ease with which the oxime ethyl isonitrosocynoacetate was extracted from alkaline solutions of NP and ethyl cyanoacetate (Chapter 3), repeated attempts, using a variety of conditions, to isolate Hinaa from alkaline solutions of Hacac and NP in the same way were unsuccessful although it was possible to extract tris(pentane-2,4-dionato-0,0)iron(III) and unreacted acetylacetone. Additionally, it was not possible to detect Hinaa in carbon-13 nmr, u.v., or mass spectra of reaction solutions.

### 4.2.2 Formation of tris(pentane-2,4-dionato-0,0)iron(III) (Fe(acac)<sub>3</sub>)

Tris(pentane-2,4-dionato-0,0)iron(III), Fe(acac)<sub>3</sub> was formed following reaction of various concentrations and proportions of NP, Hacac, and hydroxide. The formation of Fe(acac)<sub>3</sub> was recorded at room temperature, in light or complete darkness. In a series of solvent extractions, the amount of Fe(acac)<sub>3</sub> ( $\lambda_{\text{max}}$  440 nm) in aliquots of the reaction mixture withdrawn at set intervals was determined by extracting with methylene chloride and measuring the absorbance at 440 nm. In a typical experiment there was a

**Figure 1** : Plot of percentage yield  $\text{Fe}(\text{acac})_3$ <sup>a</sup> vs. time



a.  $[\text{nitroprusside}] = 0.095 \text{ M}$ ,  $[\text{acetylacetonate}] = 0.30 \text{ M}$

**Table 1** : yields of  $\text{Fe}(\text{acac})_3$  from nitroprusside and acetylacetonate reaction solutions

acac <sup>-</sup> : NP	%yield $\text{Fe}(\text{acac})_3$	time/minutes	[acac <sup>-</sup> ]/M	[NP]/M
50 : 1	5.7	16	1.0	0.02
50 : 1	9.5	50	1.0	0.02
6 : 1	15.5	120	0.5	0.05
5 : 1	0.14	300	0.1	0.02
4 : 1	8.2	80	0.1	0.02
3 : 1	4.83	47	0.50	0.15 (in $\text{N}_2$ )
3 : 1	8.2	60	0.50	0.15 (in $\text{N}_2$ )
3 : 1	4.82	47	0.50	0.15 (in air)
3 : 1	8.6	60	0.50	0.15 (in air)

slow increase in the amount of  $\text{Fe}(\text{acac})_3$  extracted as the reaction progressed followed by a sharp decrease in the amount of  $\text{Fe}(\text{acac})_3$  extracted (Figure 1). The apparent decrease in  $\text{Fe}(\text{acac})_3$  yield with time is consistent with the independently observed decomposition of  $\text{Fe}(\text{acac})_3$  in alkaline solution, complicating determinations of yield.

Yields of  $\text{Fe}(\text{acac})_3$ , either isolated as the solid or extracted with methylene chloride from a variety of Hacac and NP reaction solutions, as a function of time, are listed in Table 1. The time required for  $\text{Fe}(\text{acac})_3$  formation varied from twelve minutes to more than five hours, apparently depending on the initial reactant concentrations and the maximum yield was 15.5% with respect to NP as the limiting reagent.

Two identical solutions of NP and Hacac were made from freshly deoxygenated water and completely protected from light. Upon addition of identical aliquots of a thoroughly deoxygenated hydroxide solution, air was bubbled through one reaction mixture while nitrogen bubbled through the other at a rapid rate. The yields and formation times for  $\text{Fe}(\text{acac})_3$  precipitated from both of these solutions were identical (Table 1). Additionally,  $\text{Fe}(\text{acac})_3$  was collected from the reaction of solutions of NP (0.30 M), Hacac (0.40 M) and hydroxide (0.40 M) degassed separately and mixed by means of evacuated connecting glassware.

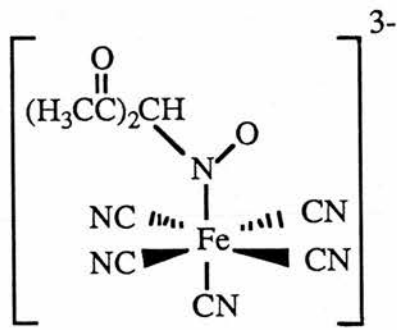
These two experiments establish that the formation of  $\text{Fe}(\text{acac})_3$  from NP and Hacac reaction solutions is independent of oxygen, as well as light. From the data of Table 1 it

can be concluded that  $\text{Fe}(\text{acac})_3$  is a minor but significant reaction product and is formed more rapidly and in higher yields from more concentrated NP and Hacac reaction solutions.

#### 4.2.3 Adduct isolation and characterisation

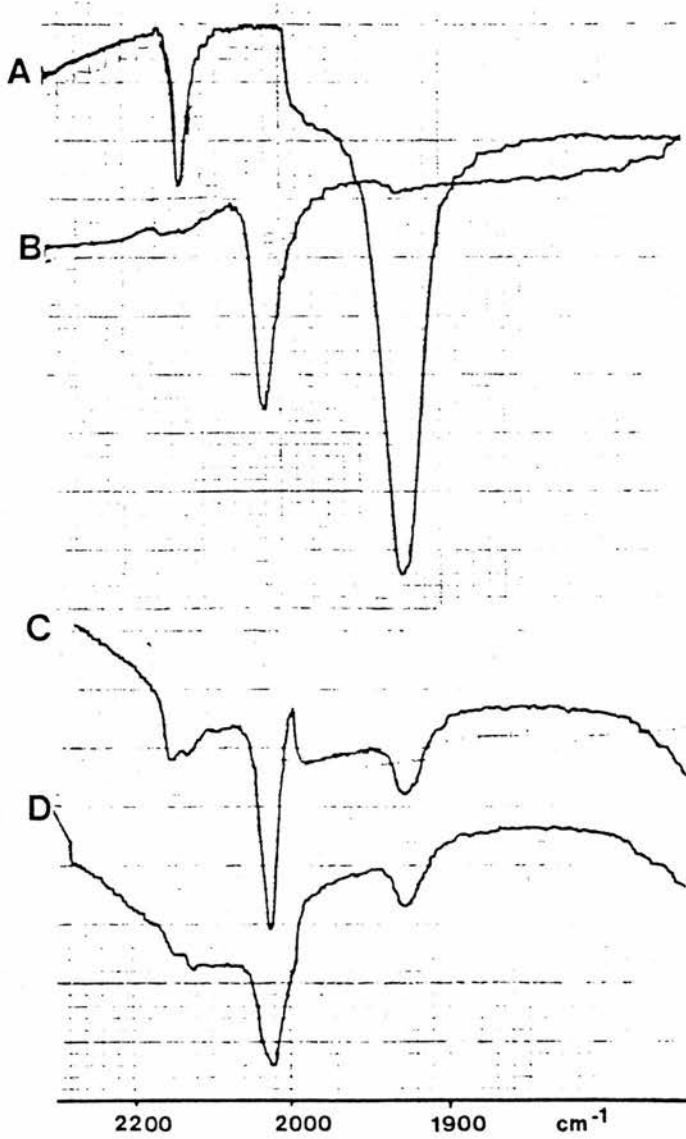
As discussed in Chapter 3, the reactions of NP with carbon acids in alkaline solution are characterised by an immediate red colouration ( $\lambda_{\text{max}}$  480 nm), due to adduct formation (1) which rapidly fades to yellow (within several minutes). Similarly, the reaction of NP and Hacac in alkaline solution results in a red colour ( $\lambda_{\text{max}}$  480 nm) but this colour does not fade. The isolation of the initially formed red species was attempted to determine if its structure were related to (1).

Addition of alkali to an alcoholic solution of NP and Hacac in an ice bath resulted in the rapid formation of a dark red oil which could be triturated to a red powder. The visible spectrum ( $\lambda_{\text{max}}$  480 nm) recorded after dissolving the powders in water, was similar to that of NP and Hacac reaction solutions immediately upon mixing, and the adducts of NP and other carbanions have similar spectra.<sup>7,8</sup> The carbon-13 nmr of these powders were poorly resolved but peaks recorded in the region 175 - 185 p.p.m. were characteristic of pentacyanoferrate(II) species.<sup>9</sup> The cyanide stretch at  $2040 \text{ cm}^{-1}$  observed in the infra-red spectra of these powders was also characteristic of cyanide bound to iron(II).<sup>10</sup> Although the powders obtained from several experiments did not analyse consistently or correspond to an adduct related



(5)

Figure 2 : Solution state infra-red spectra of nitroprusside and acetylacetonate solutions



to (1), spectral characteristics of these powers do support formation of a NP and acetylacetonate ( $\text{acac}^-$ ) adduct (5).

Alkaline or neutral solutions of the red powders and Hacac did not react rapidly or significantly to form  $\text{Fe}(\text{acac})_3$ ; the maximum yield obtained was 0.6% in two hours assuming the red powders consisted of only the proposed adduct. Flushing identical solutions with oxygen and nitrogen did not significantly alter the low rate of formation or yield of  $\text{Fe}(\text{acac})_3$ . Although the visible spectra of the red powders were identical to spectra recorded immediately after adding hydroxide to NP and Hacac solutions, the inconsistent analyses for the carbon:nitrogen ratio in addition to the difficulties encountered in obtaining carbon-13 nmr spectra of the red powders, suggest that other (non-reactive) cyano-ferrate complexes may have co-precipitated with the adducts.

#### 4.2.3.1 Infra-red spectroscopy of reaction solutions

In solution, the NP cyanide stretching bands occur in the region of  $2130\text{ cm}^{-1}$  and that of the NO ligand at  $1940\text{ cm}^{-1}$  (Figure 2A). These bands, and an additional cyanide stretching band, were apparent in a solution state infra-red spectrum recorded immediately after adding a hydroxide solution (1.5 M) to a solution of Hacac (1.5 M) and NP (0.5 M) (Figure 2D). After ten minutes both decrease of the NP cyanide stretching band at  $2130\text{ cm}^{-1}$  and increase of the stretching band at  $2020\text{ cm}^{-1}$  were apparent (Figure 2C). Within twenty minutes of mixing (Figure 2B), the cyanide stretching band at  $2020\text{ cm}^{-1}$  was the only feature of the indicated region. The poor resolution of the spectra preclude definite assignment but

the cyanide stretching frequency at  $2020\text{ cm}^{-1}$  is characteristic of cyanide bound to iron(II);<sup>10</sup> the cyanide stretching frequency of NP is in the region of the spectrum associated with cyanide attached to iron(III).<sup>11</sup>

It was unfortunately not possible, due to the low solubility of other carbon acids, to record the corresponding spectra for the reaction of NP with the ethyl cyanoacetate carbanion or any other carbanions for comparison with the NP and Hacac reaction solution spectra. Nevertheless, the solution state infra-red spectra of the NP and Hacac reaction solution indicate that at very high concentrations the conversion of NP to another cyanoferrate(II) species, corresponding to the adduct or perhaps to products, is completed rapidly.

#### 4.2.3.2 Rate of adduct formation

The spectral characteristics of the red powders detailed above suggest that the initial reaction of NP with  $\text{acac}^-$  is formation of an adduct (5) as observed for the reaction of NP with other carbanions. The initial absorbance upon reaction of NP with  $\text{acac}^-$  ( $\lambda_{\text{max}} 480\text{ nm}$ ) is characteristic of the adducts of NP and carbanions and the appearance of this absorbance can be followed by stopped-flow spectrophotometry.

Solutions of Hacac and NP were in one syringe and hydroxide solutions in the other, a sequence of mixing used in all investigations of this system as neither NP nor Hacac are stable in alkaline solutions. Earlier workers have established<sup>8</sup> that the carbanion is formed in a rapid pre-equilibrium, and the concentration of the carbanion  $\text{acac}^-$

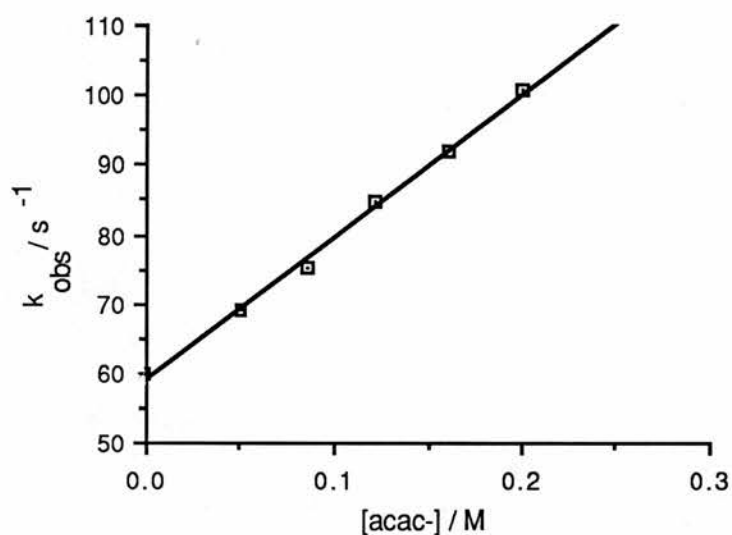
was determined directly from the hydroxide concentration. Hacac was always in excess, to maintain pseudo first-order conditions, and the concentration of  $\text{acac}^-$  was varied by changing the hydroxide solution concentrations. From the data displayed in Table 2, it can be seen that the observed rate constant,  $k_{\text{obs}}$ , varies with  $\text{acac}^-$  and a plot of  $k_{\text{obs}}$  against ( $\text{acac}^-$ ) is rectilinear (Figure 3). It is clear that under these conditions the rate-determining step of adduct formation is the reaction of the carbanion  $\text{acac}^-$  with NP (Scheme 1). The positive intercept indicates that adduct formation is an equilibrium process.

Although there is evidence for secondary ionisation of malononitrile upon reaction with NP,<sup>8</sup> the rate-determining step in the formation of the NP and ethylcyanoacetate adduct (Chapter 3) was also found to be the reaction of the carbanion with NP.

#### 4.2.3.3 Spectrophotometric studies of reaction solutions

For the reaction of NP with ethylcyanoacetate in alkaline solution, adduct decomposition was followed spectrophotometrically and found to be independent of hydroxide and carbanion concentrations (Chapter 3). Although NP and acetylacetone reaction solutions changed colour slightly - from deep red to a lighter red - the rapid fading to bright yellow associated<sup>7,12,13</sup> with rapid decomposition of the adducts of NP and other carbanions to an oxime and aquapentacyanoferrate(II) or its polymeric derivatives ( $\lambda_{\text{max}}$  400 nm)<sup>14</sup> was not observed for NP and Hacac reaction solutions. The kinetics of the change in absorbance at 480 nm of these

**Figure 3** : Plot of  $k_{\text{obs}}^{\text{a}}$  vs. concentration of acetylacetonate for the reaction of nitroprusside<sup>b</sup> with acetylacetonate<sup>c</sup> in alkaline solution at 25° C



- a. Adduct formation at 490 nm
- b. Initial concentration = 0.01 M
- c. Initial concentration = 1.0 M

**Table 2** : Kinetic data for the reaction of nitroprusside with acetylacetonate ( $\text{acac}^-$ ) at 25° C

$[\text{acac}^-] / \text{M}$	0.200	0.162	0.122	0.086	0.050
$k_{\text{obs}} / \text{s}^{-1}$	101 ± 1	90.6 ± 1	84.7 ± 2.0	75.2 ± 2.5	70.2 ± 1

**Table 3**

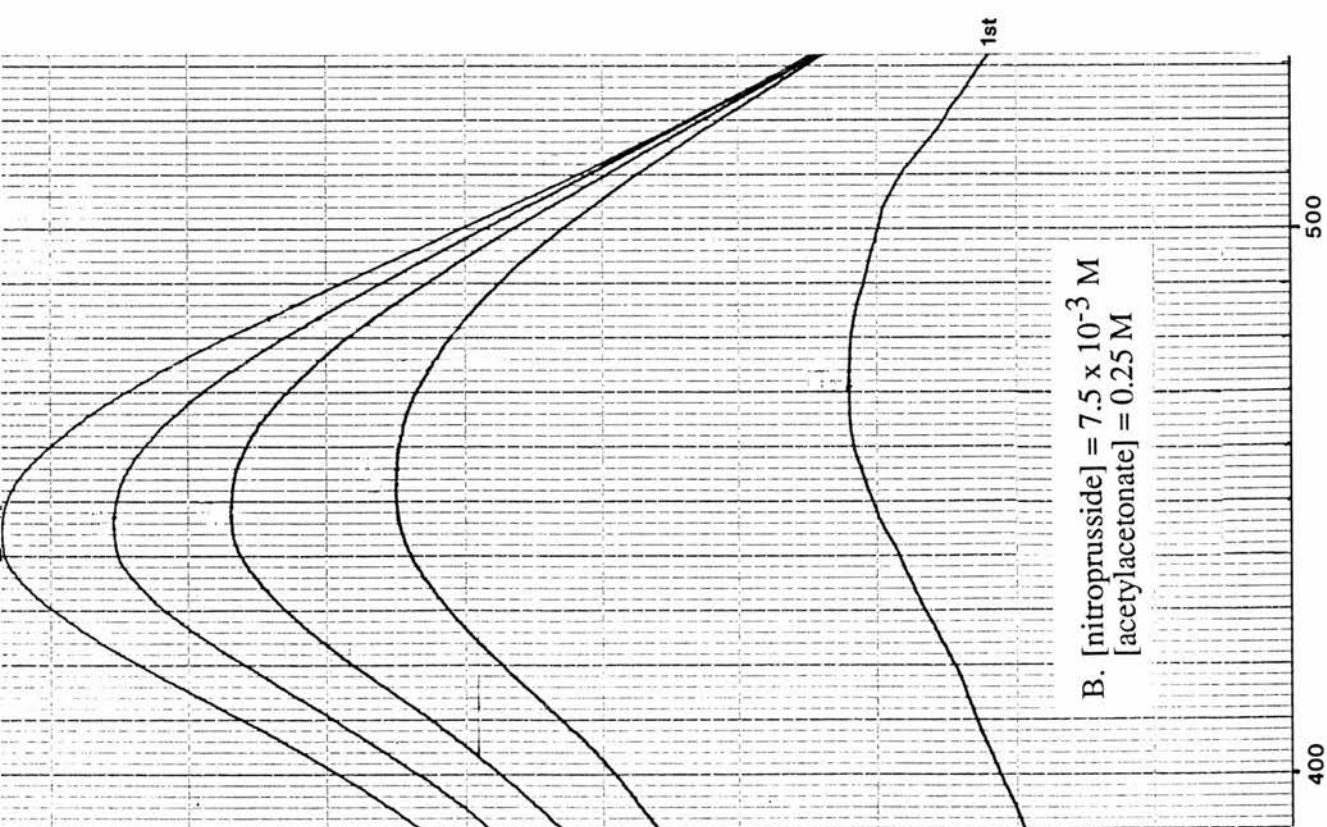
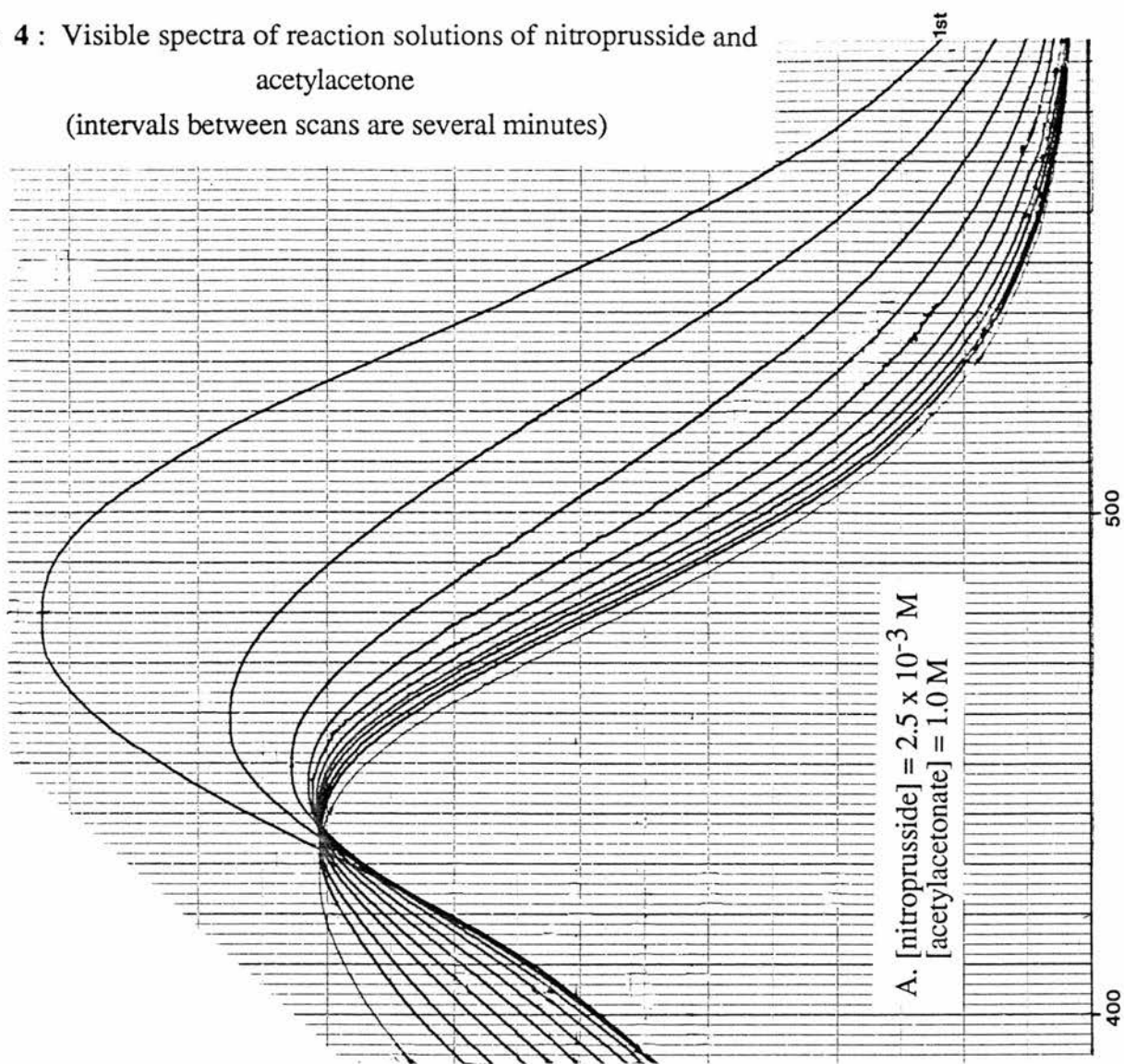
[acac-]/M	$10^3$ [NP]/M	Observations
1.0	2.5	Absorbance at 480nm decreases rapidly Maximum shifts slowly to 435nm
0.25	7.5	Initial maximum at 480nm. Absorption at 480nm slowly increases as maximum shifts to 450 nm
0.002	2.0	Initial maximum at 400 nm slowly increases. Maximum shifts to 430 nm while absorption at 480 nm slowly increases.

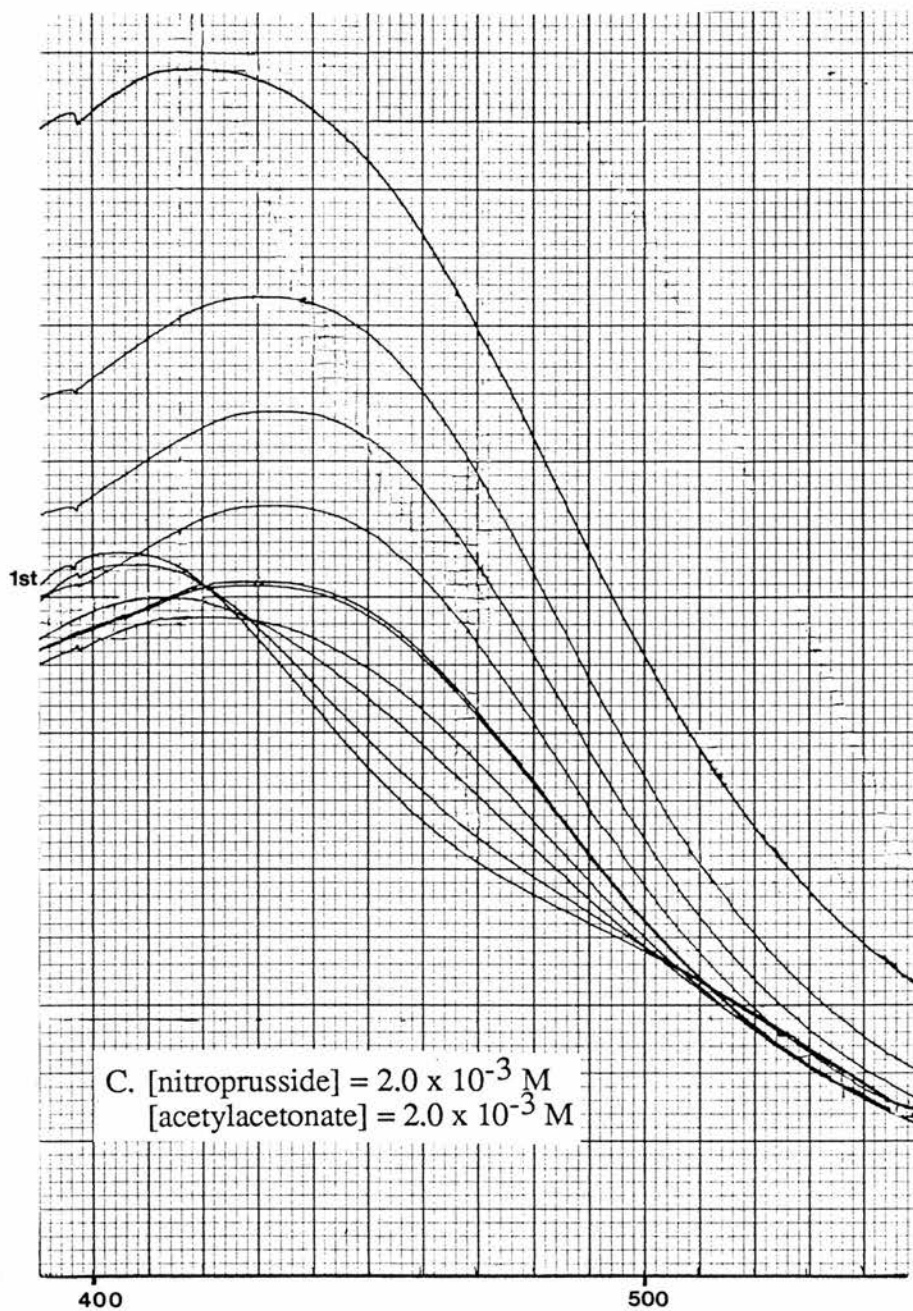
solutions were found to be complex.

In Figures 4A, 4B, and 4C it can be seen that the concentration of the carbanion  $\text{acac}^-$  considerably affects the absorbance attributed to the adduct at 480 nm (Table 3). At relatively high  $\text{acac}^-$  concentrations adduct formation was too rapid to be followed and Figure 4A illustrates the increase in absorbance at 480 nm and concomitant shift in the maximum to shorter wavelengths. In contrast, the reactions of dilute solutions proceeded slowly and Figures 4B and 4C record an *increase* in the absorbances at 480 nm as well as a gradual shift in the maxima to shorter wavelengths. Although the increasing absorbances in the region of 440 nm seen in Figures 4A, 4B and 4C are not inconsistent with the formation of  $\text{Fe}(\text{acac})_3$  ( $\lambda_{\text{max}}$  440 nm), calculation of the yield of  $\text{Fe}(\text{acac})_3$  from these data resulted in unrealistically high values indicating that other chromophoric species were present. The absorbance of the adduct ( $\lambda_{\text{max}}$  480 nm) is the only assignment that is unambiguous: the absorbance maxima of other cyanoferrate complexes including NP,<sup>11</sup>  $[\text{Fe}(\text{CN})_5\text{H}_2\text{O}]^{3-}$ ,<sup>14</sup>  $[\text{Fe}(\text{CN})_5\text{H}_2\text{O}]^{2-}$ ,<sup>15</sup>  $[\text{Fe}(\text{CN})_5\text{NO}_2]^{4-}$ ,<sup>7</sup>  $[\text{Fe}(\text{CN})_6]^{4-}$ ,<sup>16</sup> and  $[\text{Fe}(\text{CN})_6]^{3-}$ ,<sup>16</sup> overlap in the visible region.

By characterisation of both reaction solutions and the red solids isolated from them immediately after mixing, it seems clear that an adduct (5), related to (1), is the initial species formed upon reaction of NP and  $\text{acac}^-$ . The adduct represents nucleophilic attack of  $\text{acac}^-$  at the NP nitrosyl ligand, as observed for the reaction of NP with

**Figure 4 :** Visible spectra of reaction solutions of nitroprusside and acetylacetone  
(intervals between scans are several minutes)





other carbanions, but the NP and  $\text{acac}^-$  reaction solution did not fade in the usual manner to (yellow)  $[\text{Fe}(\text{CN})_5\text{H}_2\text{O}]^{3-}$  and its polymeric derivatives. The extraordinary conversion of NP to  $\text{Fe}(\text{acac})_3$  must therefore arise from further reaction of  $\text{acac}^-$  with the adduct, or products of adduct decomposition.

#### 4.2.4 Attempted detection of free cyanide or hydrogen cyanide in reaction solutions

The formation of  $\text{Fe}(\text{acac})_3$  from NP and Hacac reaction solutions allows for the possibility of cyanide release. Determination of free cyanide levels was important to safe experimentation as well as mechanistic consideration, with special regard to the medical administration of NP.

Free cyanide,  $\text{CN}^-$ , can be detected in alkaline solutions (e.g.  $\text{pH} > 10$ ; the  $\text{p}K_a$  of HCN is 9.21)<sup>17</sup> using a cyanide sensitive electrode. The electrode detection range is  $1 \times 10^{-2}$  M to  $5 \times 10^{-6}$  M; the calibration curve is not linear below  $5 \times 10^{-6}$  M due to the small but significant amount of cyanide ion contributed to the solution by the electrode membrane material.

The potential of the cyanide-sensitive electrode in a freshly mixed solution of NP ( $1.67 \times 10^{-3}$  M), Hacac ( $3.33 \times 10^{-2}$  M) and hydroxide ( $13.3 \times 10^{-2}$  M, to maintain the  $\text{pH} > 10$ ) was monitored over four hours. The potential remained below the reading corresponding to the lower detection limit. This limit represents less than 0.1% release of free cyanide from NP in this experiment. Solutions containing NP and a ten-fold excess of Hacac in a solution of  $\text{pH}$  greater than 10 were monitored for several

hours and the meter reading again remained below the minimum detection level.

The cyanide sensitive electrode was also used to test for any cyanide expelled as  $\text{HCN}_{(\text{gas})}$  from a solution of NP ( $2.6 \times 10^{-3}$  M), Hacac ( $1.2 \times 10^{-2}$  M) and hydroxide ( $1.2 \times 10^{-2}$  M) acidified some time after mixing. The solution was flushed with nitrogen at a rate of approximately 0.3 litre/minute for an hour and trapped in 1.0 M hydroxide solutions (150 ml). The electrode potentials of these solutions were always lower than the reading corresponding to the minimum detection limit, representing less than 0.5% conversion of the cyanide ligands of NP in this experiment to free cyanide.

Additionally, there was no evidence of HCN in the infra-red spectrum <sup>18a</sup> of the gas collected 45 minutes after addition of degassed solution of hydroxide (0.4 M), via evacuated connecting glassware, to a separately degassed solution of NP (0.3 M) and Hacac (0.4 M).

Using carbon-13 nmr and 90% carbon-13 labelled NP it was possible to monitor the fate of the cyanide ligands in a reaction solution of NP, Hacac and hydroxide to a high degree of sensitivity. Two spectra were recorded - one shortly after mixing and one several hours later (Table 4) - and no signal corresponding to undissociated hydrogen cyanide (recorded independently at 120 p.p.m. by addition of  $\text{Na}^{13}\text{CN}$  to a neutral solution) was apparent. Similarly no signal for HCN was detected in carbon-13 nmr spectra of reaction solutions recorded over fifteen hours (section 4.2.7). These

spectra will be discussed in further detail below.

In summary, no significant formation of  $\text{CN}^-$  or HCN could be detected by gas infra-red, carbon-13 nmr or with the use of a cyanide-sensitive electrode following reaction of NP with Hacac in alkaline solution.

#### 4.2.5 Isolation of NO

The infra-red spectrum of the gas collected 45 minutes after addition of a degassed solution of hydroxide (0.4 M) to a separately degassed solution of NP (0.3 M) and Hacac (0.3 M) was, as mentioned above, devoid of any bands for HCN, but the distinctive Q-branch <sup>18b</sup> for NO ( $1875 \text{ cm}^{-1}$ ) was observed. The solutions containing NP were protected from light at all times to avoid photolytic decomposition of NP, which also gives rise to NO. The gas collected in the gas infra-red cell was initially colourless but gradually turned yellow; the cell was under partial vacuum and air slowly leaking in reacted with NO (colourless) to form  $\text{NO}_2$  (yellow).

#### 4.2.6 Determination of the inorganic products of reaction

From consideration of the maximum yield of  $\text{Fe}(\text{acac})_3$  isolated (15.5%) it is clear that  $\text{Fe}(\text{acac})_3$ , although formed in significant amounts, is not a major product of the reaction of NP with  $\text{acac}^-$ . Failure to detect  $\text{CN}^-$  or HCN in NP and Hacac reaction solutions suggests that cyanoferrate complexes are also formed. However, isolation of cyanoferrate complexes from aqueous solution is difficult and as previously detailed, the absorbance maxima of cyanoferrate complexes and  $\text{Fe}(\text{acac})_3$  overlap in the visible region to such

**Table 4** : Carbon-13 nmr data for the reaction of 90% carbon-13 labelled nitroprusside<sup>a</sup> and acetylacetone<sup>b</sup> in alkaline solution

	Chemical shift/ppm	splitting	assignment	intensity
First spectrum <sup>c</sup>				
	132.2	multiplet	NP ( <sup>13</sup> CN <sub>ax</sub> )	<3
	134.4	doublet	NP ( <sup>13</sup> CN <sub>eq</sub> )	26
	176.7	multiplet	?	<3
	177.5	multiplet	?	<3
	177.9	doublet	?	20
	178.2	doublet	?	6
Second spectrum <sup>d</sup>				
	132.2	multiplet	NP ( <sup>13</sup> CN <sub>ax</sub> )	>0.2
	134.4	doublet	NP ( <sup>13</sup> CN <sub>eq</sub> )	2.5
	177.9	singlet	[Fe(CN) <sub>6</sub> ] <sup>4-</sup>	12

- a. Initial concentration  $7.4 \times 10^{-2}$  M  
b. Initial concentration  $10.0 \times 10^{-2}$  M  
c. Recorded shortly after mixing  
d. Recorded several hours after mixing

an extent that the only absorbance that can be assigned unambiguously is that of the NP and  $\text{acac}^-$  adducts.

Carbon-13 nmr is a more suitable technique for monitoring the NP and Hacac reaction solutions and high-field nmr experiments were conducted using 90% carbon-13 labelled NP. The statistical distribution of the  $^{13}\text{CN}$  ligands of 90% carbon-13 labelled NP was described in Chapter 3; a good approximation of the spectra of 90% carbon-13 labelled NP is a quintet for the axial ligand at 132.4 p.p.m. due to coupling with the four equatorial  $^{13}\text{CN}$  ligands, and a doublet of the equatorial  $^{13}\text{CN}$  ligands at 134.2 p.p.m. due to coupling with the one axial  $^{13}\text{CN}$  ligand.

The data for the first NP and  $\text{acac}^-$  reaction solution spectrum, recorded a short while after mixing, are displayed in Table 4. The distinctive doublet ( $^{13}\text{CN}_{\text{eq}}$  134.4 p.p.m.) and quintet ( $^{13}\text{CN}_{\text{ax}}$  132.2 p.p.m.) of NP dominates the spectrum (Figure 5) but in an expansion of the region 175 - 180 p.p.m. (Figure 6), at least two other sets of doublets and quintets, characteristic<sup>9</sup> of pentacyanoferrate(II) species, are apparent. Two pentacyanoferrate(II) species that are obviously possible reaction intermediates or products are nitropentacyanoferrate(II),  $[\text{Fe}(\text{CN})_5\text{NO}_2]^{4-}$ , and aquapentacyanoferrate(II),  $[\text{Fe}(\text{CN})_5\text{H}_2\text{O}]^{3-}$ . Nitropentacyanoferrate(II) is the product of the reaction of NP with hydroxide and is in equilibrium with aquapentacyanoferrate(II). Aquapentacyanoferrate(II) is the inorganic product proposed by earlier workers<sup>7,13</sup> for systems that yield the oxime as the organic product. In reaction solutions of 90% carbon-13

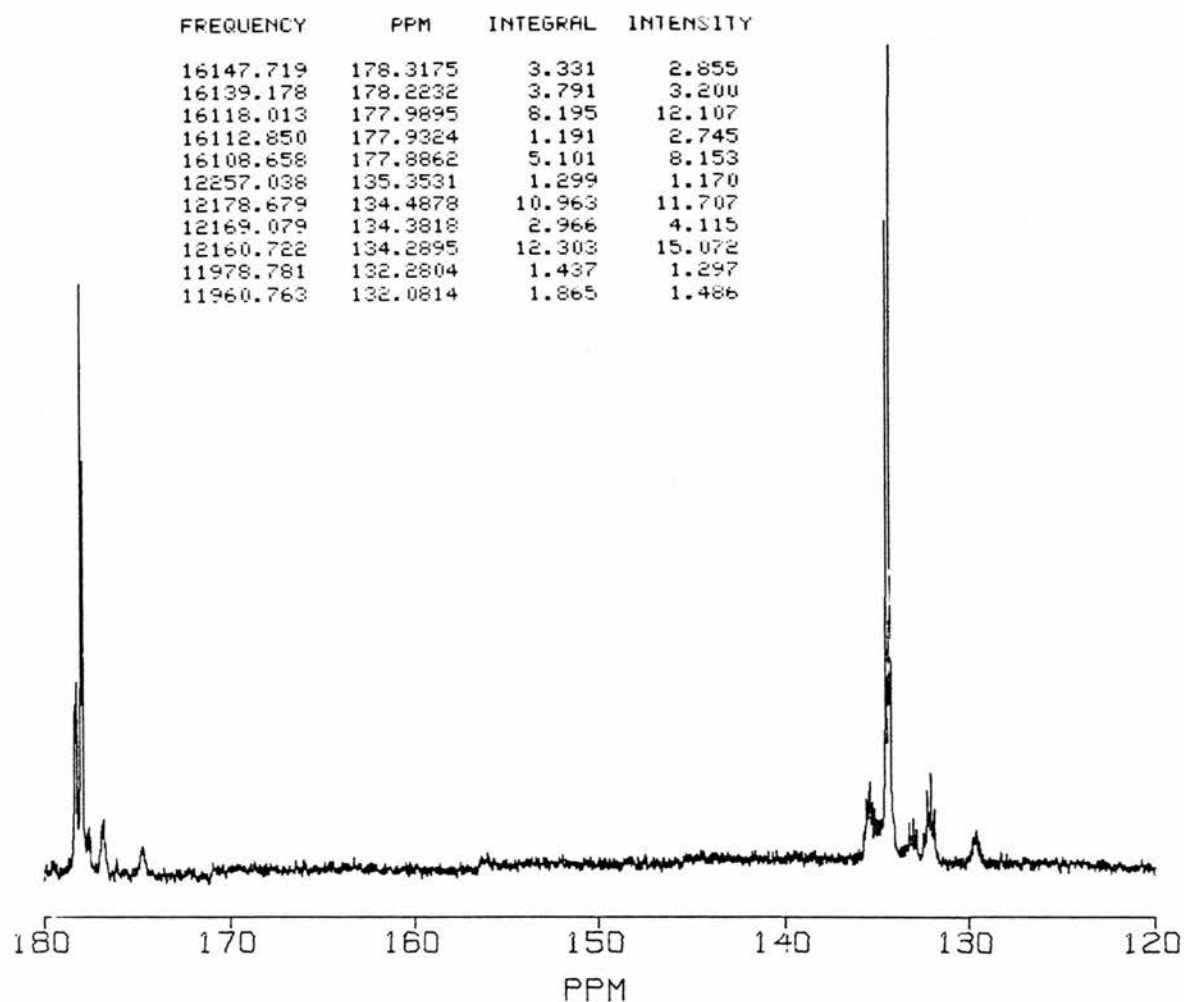


**Figure 5 :** Carbon-13 nmr spectrum of 90% carbon-13 labelled nitroprusside and acetylacetonate in alkaline solution, shortly after mixing

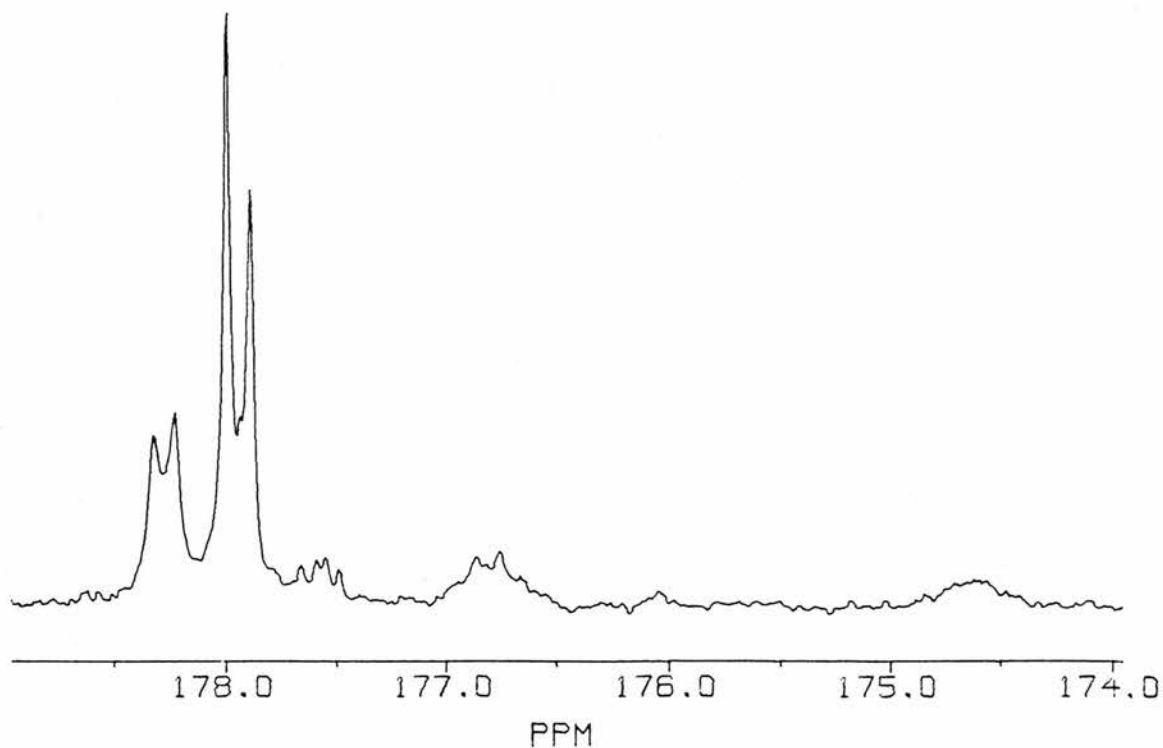
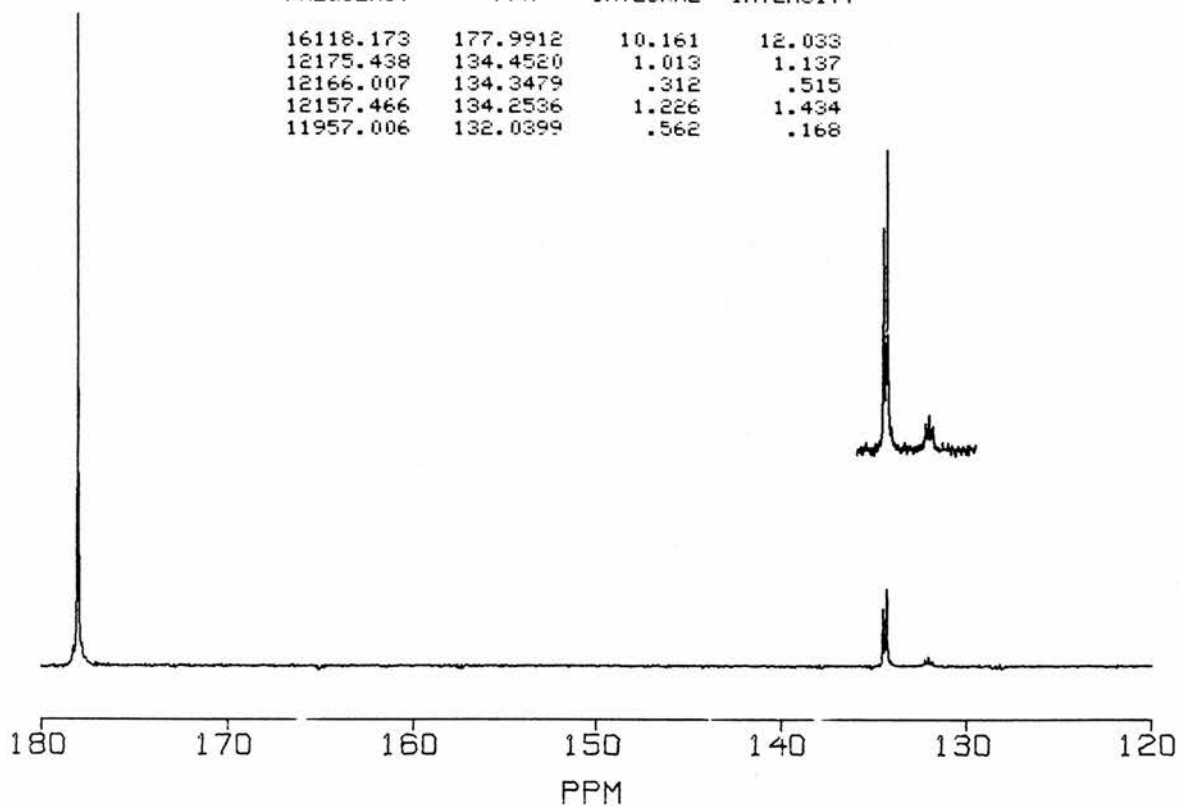


**Figure 6 :** Carbon-13 nmr spectrum of 90% carbon-13 labelled nitroprusside and acetylacetonate in alkaline solution, shortly after mixing and expanded in chemical shift region of pentacyanoferrate(II) complexes

Figure 7 : Carbon-13 nmr spectrum of 90% carbon-13 labelled nitroprusside and acetylacetonate in alkaline solution, several hours after mixing

FREQUENCY	PPM	INTEGRAL	INTENSITY
16118.173	177.9912	10.161	12.033
12175.438	134.4520	1.013	1.137
12166.007	134.3479	.312	.515
12157.466	134.2536	1.226	1.434
11957.006	132.0399	.562	.168

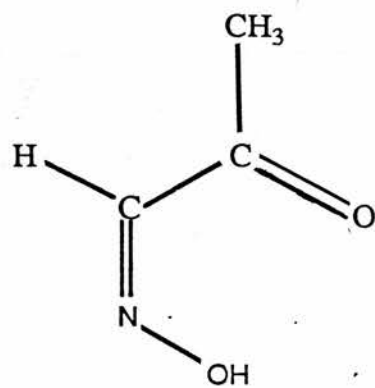


labelled NP and ethyl cyanoacetate (from which the oxime ethyl isonitrosocyanoacetate has been isolated) a signal at 175.4 p.p.m. was assigned to the equatorial cyanide ligands of aquapentacyanoferrate(II), ionised aquapentacyanoferrate(II) or its polymeric derivatives, collectively referred to as the aqua complex (Chapter 3).

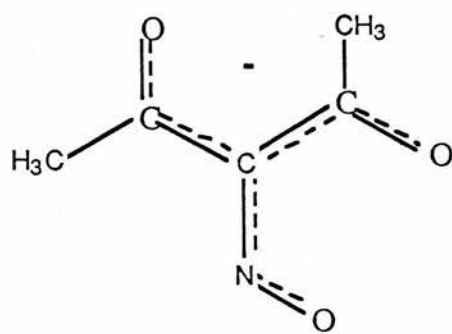
However, neither the chemical shifts nor the differences between the quintets and doublets for  $[\text{Fe}(\text{}^{13}\text{CN})_5\text{H}_2\text{O}]^{3-}$  ( ${}^{13}\text{CN}_{\text{ax}} 172.8$ ,  ${}^{13}\text{CN}_{\text{eq}} 177.2$ ,  $\Delta = 4.4$  p.p.m.)<sup>9</sup> or  $[\text{Fe}(\text{}^{13}\text{CN})_5\text{NO}_2]^{4-}$  ( ${}^{13}\text{CN}_{\text{ax}} 174.0$ ,  ${}^{13}\text{CN}_{\text{eq}} 176.7$ ,  $\Delta = 2.7$  p.p.m.)<sup>9</sup> or the aqua complex ( ${}^{13}\text{CN}_{\text{eq}} 175.4$  p.p.m.) occur in the first spectrum ( $\Delta = 1.5$ ,  $1.2$ ,  $0.7$ , or  $0.4$  p.p.m.). While a direct comparison of chemical shifts is not always possible for spectra recorded under different conditions, the difference in chemical shift between the quintet and associated doublet for a single pentacyanoferrate(II) species should remain constant.

In the second reaction solution spectrum, recorded several hours after mixing, only two products were apparent; the distinctive NP doublet and quintet, and a single peak at 177.9 p.p.m. This single resonance corresponds to hexacyanoferrate(II),  $[\text{Fe}(\text{}^{13}\text{CN})_6]^{4-}$ ; the chemical shift of the six equivalent cyanide ligands has been recorded previously<sup>19</sup> at 177.7 p.p.m. in aqueous buffer.

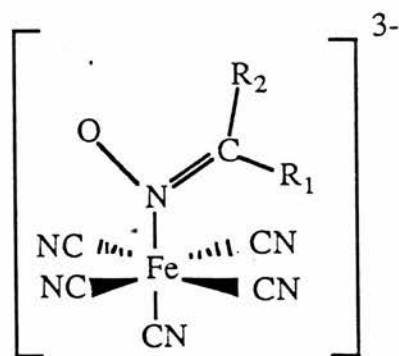
From these two reaction solution spectra it is apparent that neither aquapentacyanoferrate(II) nor nitropentacyanoferrate(II) are products of the reaction of NP and  $\text{acac}^-$  and as previously mentioned (section 4.2.4), no hydrogen cyanide (recorded independently at 120 p.p.m.) was apparent. As shown



(6)



(7)



(8)

in the second spectrum, hexacyanoferrate(II) and unreacted NP are the only diamagnetic products observed.  $\text{Fe}(\text{acac})_3$  is paramagnetic and thus not evident in these spectra.

#### 4.2.7 Determination of the organic products of reaction

The report of the reaction of NP with ethyl cyanoacetate in alkaline solution (Chapter 3) indicated that the oxime ethyl isonitrosocyanoacetate was the major organic product of reaction. The relatively low maximum yield of  $\text{Fe}(\text{acac})_3$  (15.5%) obtained suggests that a significant proportion of the initially formed NP and  $\text{acac}^-$  adduct hydrolyses in the established manner to an oxime. However, repeated failure to isolate Hinaa or any other organic soluble component (with the exception of unreacted Hacac and  $\text{Fe}(\text{acac})_3$ ) from NP and Hacac reaction solutions led to reconsideration of the original report<sup>4</sup> of Hinaa as a product of this reaction.

Cambi and colleagues<sup>4</sup> cite isolation of a hygroscopic red powder following addition of sodium methoxide to a methanolic solution of NP and Hacac cooled in an ice bath. They record satisfactory analyses of the red powders as the NP and  $\text{acac}^-$  adduct, corresponding to (5), and record isolation of a trace amount of the oxime isonitrosoacetone (6) from an alkaline solution of the adduct. They postulated that isonitrosoacetone was formed by decomposition of isonitrosoacetylacetone (Hinaa) in the alkaline conditions used to hydrolyse the adduct. By a similar method, more recent workers have isolated aliphatic oximes following the reaction of NP with cyclic ketones in alkaline solution.<sup>20</sup>

From solutions of the red powders described in Section

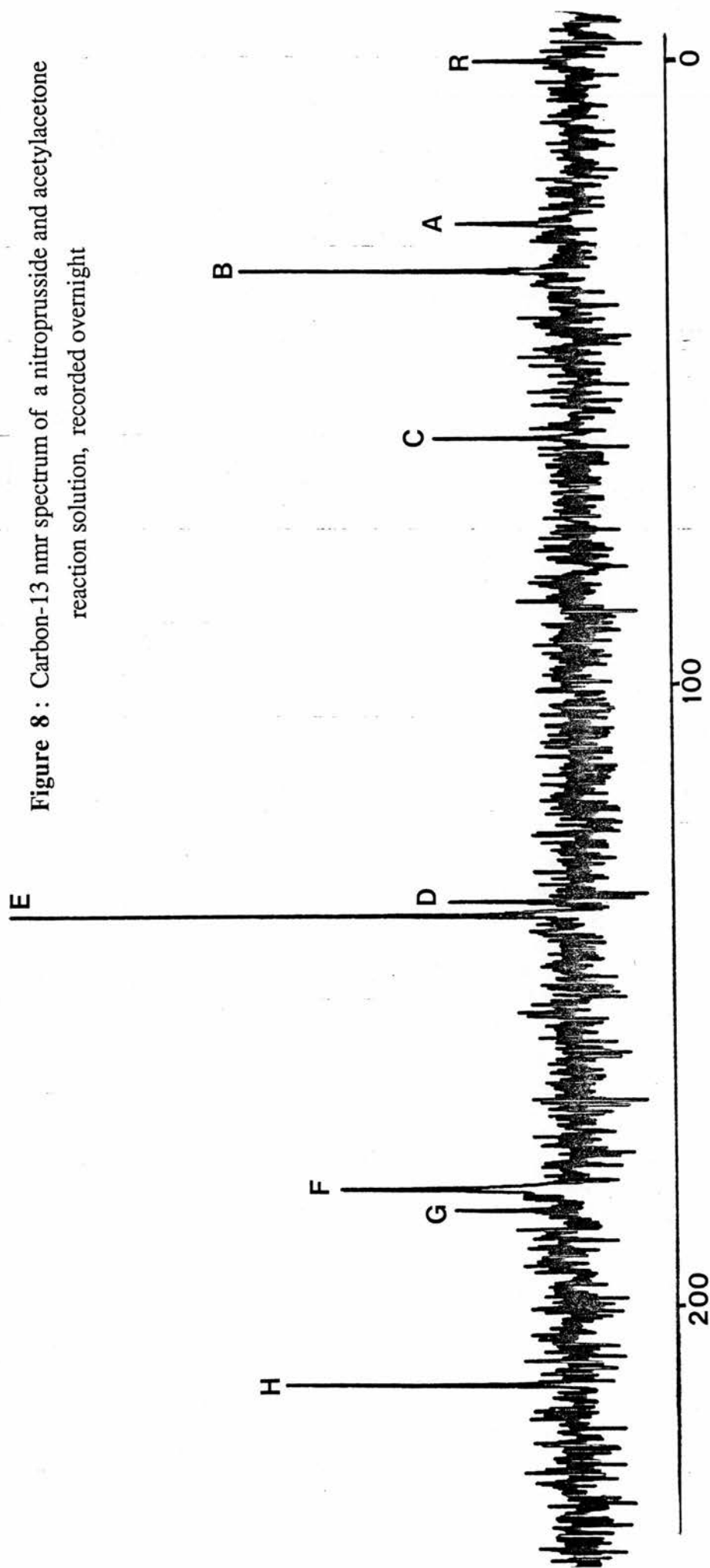
4.2.3 it was possible to isolate isonitrosoacetone (Ina) in very low yields. It was not possible to obtain Ina from NP and Hacac in alkaline solution directly; Ina is highly water soluble and can be isolated only by exhaustive extraction with methylene chloride which also extracts unreacted Hacac and  $\text{Fe}(\text{acac})_3$ , from which mixture Ina is difficult to detect and separate.

A series of low-field carbon-13 nmr experiments were conducted to identify the elusive organic reaction products (the high-field carbon-13 nmr experiments to determine the inorganic reaction products were confined to the region 100 - 200 p.p.m. and signals for the carbons at natural abundance were not observed). The experiments at low-field and natural abundance necessitated high concentrations and long accumulation times in which conditions the spectra were invariably noisy, due to precipitation of  $\text{Fe}(\text{acac})_3$ .

There were *no* signals corresponding to Hinaa or inaa<sup>-</sup> (7) in any of the carbon-13 nmr spectra of NP and acac<sup>-</sup> reaction solutions recorded but the other possible organic products of this reaction will be considered on the basis of the carbon-13 nmr spectra of Hacac (1), acac<sup>-</sup>, Hinaa (2), inaa<sup>-</sup> and isonitrosoacetone [(6), Ina] described in Chapter 2. The carbon-13 nmr reaction solution spectra reported below are representative of several repetitions of each experiment, for which similar results were obtained. It was not possible to discern any difference between initial and final <sup>1</sup>H nmr spectra of NP and acac<sup>-</sup> reaction solutions.

Although the oxime Ina has been isolated from alkaline

Figure 8 : Carbon-13 nmr spectrum of a nitroprusside and acetylacetonate reaction solution, recorded overnight



R = internal reference 3-(trimethylsilyl)propane sulphonic acid, sodium salt

A= 23.4 (acetate), B=30.9 (Hacac), C=57.5 (Hacac), D=132.4 ( $^{13}\text{C}_{\text{ax}}$  NP), E=134.4 ( $^{13}\text{C}_{\text{eq}}$  NP), F=177.9 ( $[\text{Fe}^{\text{II}}(\text{CN})_6]^{4-}$ ), G=181.1 (acetate), H=208.9 ppm (Hacac).

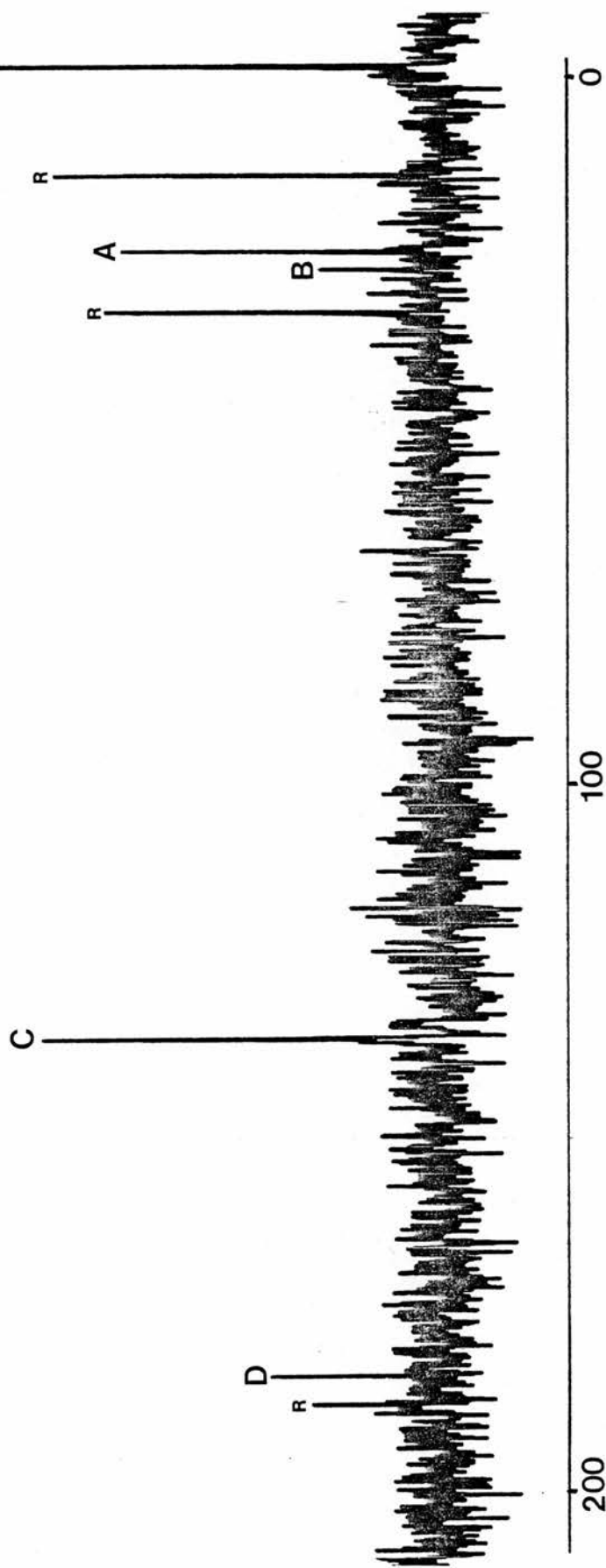
solutions of the precipitated NP and  $\text{acac}^-$  adduct, there were no signals for Ina in the NP and  $\text{acac}^-$  reaction solution spectrum (Figure 8). There were signals for acetate, which Cambi and colleagues postulated as the other product, in addition to Ina, of Hinaa hydrolysis. It was not possible to isolate acetate from the aqueous reaction solutions.

Ina was isolated from the reaction of NP with acetone in alkaline solution by extracting the reaction solution with methylene chloride. However, there were no signals corresponding to Ina in the carbon-13 nmr spectrum of this reaction solution recorded overnight.

Oximes, while prone to decomposition in acidic solution, are generally stable to alkaline hydrolysis<sup>21</sup> and it has been shown by separate carbon-13 nmr studies (Chapter 2) that Hinaa does not decompose in alkaline solution. A structure has been assigned to the (stable) anion  $\text{inaa}^-$  (7) and there was no evidence of formation of Ina even after many hours. However, although Ina has been isolated from reaction solutions of NP and Hacac or acetone, it seems clear from carbon-13 nmr spectra of these reaction solutions that the oxime Ina undergoes decomposition to undetected products during the long accumulation times (up to fifteen hours) required.

One explanation for the absence of Hinaa in reaction solution spectra was that Hinaa reacted with intermediate cyanoferrate complexes. The reaction of NP in alkaline solution with some oximes to yield adducts of the type (8) has been recorded in the literature.<sup>22,23</sup> It was not possible to detect reaction of Hinaa with aquapentacyanoferrate(II) or

**Figure 9 :** Carbon-13 nmr spectrum of a nitroprusside and isonitrosoacetylacetonone (Hinaa) reaction solution, recorded overnight



R = internal reference 3-(trimethylsilyl)propane sulphonic acid, sodium salt

A = 23.6 (acetate), B = 26.1 (Hinaa), C = 134.4 ( $^{13}\text{C}_{\text{N}_{\text{eq}}}$  NP), D = 181.1 ppm (acetate).

nitropentacyanoferrate(II), both products of the reaction of NP with hydroxide, but an apparent (red) adduct rapidly formed and faded upon addition of alkali to a solution of Hinaa and NP. A carbon-13 nmr spectrum of this reaction solution (Figure 9) contained signals for acetate and NP, as well as unreacted Hinaa. One interpretation of this result is that decomposition of the NP and  $\text{inaa}^-$  adduct occurs in a manner similar to that of the NP and  $\text{acac}^-$  adduct, that is to acetate and Ina (Ina will not be observed in the carbon-13 nmr spectrum for the reason detailed above).

It is clear that the reaction of  $\text{inaa}^-$  and NP originally considered as an explanation for repeatedly failing to recover or identify Hinaa from an alkaline solution of NP and Hacac is not a significant side reaction as the rapid formation and fading of the red colour associated with this reaction has not been observed for Hacac and NP reaction solutions. Additionally, a preparative scale experiment in which a known amount of Hinaa was added to an alkaline solution of NP and Hacac suggested no reaction with Hinaa occurred as all the added Hinaa was recovered upon extraction with methylene chloride.

There are several important observations to be made from the low-field carbon-13 nmr spectra reported above. It is not likely that failure to isolate or identify Hinaa or its anion  $\text{inaa}^-$  from NP and Hacac reaction solutions is due to side reactions with NP or other cyanoferrate complexes. Signals for acetate, but not for Hinaa or  $\text{inaa}^-$ , were apparent in reaction solution spectra of NP and  $\text{acac}^-$  and it is

known that  $\text{inaa}^-$  does not decompose to Ina or acetate in alkaline solution. However, Ina apparently decomposes to undetected products in the conditions required for recording carbon-13 nmr spectra of NP and Hacac or acetone reactions solutions, from which Ina has been isolated. Therefore, acetate and the oxime Ina, but not the oxime Hinaa, are products of decomposition of the NP and  $\text{acac}^-$  adduct.

#### 4.2.8 Reactions of acetylacetone with other cyanoferrate complexes

The reaction of Hacac and  $\text{acac}^-$  with what was designated as NP and  $\text{acac}^-$  adducts isolated from cold, alcoholic reaction mixtures did not lead to significant formation of  $\text{Fe}(\text{acac})_3$ . These materials had some characteristics associated with the adducts of NP and carbanions, in particular an absorbance maximum at 480 nm, although they did not analyse consistently or correspond to the adduct of NP and  $\text{acac}^-$  (5). The extinction coefficient of NP and carbanion adducts is very high and it is possible that the characteristic absorbance ( $\lambda_{\text{max}}$  480 nm) would still be discerned even if the isolated red powders were heavily contaminated with non-reactive products of reaction [e.g. hexacyanoferrate(II)]. Before accepting that the low reactivity of the isolated adducts was due to this contamination, the reactions of Hacac and  $\text{acac}^-$  with cyanoferrate complexes that could be expected from adduct decomposition or reaction of NP with hydroxide were investigated as routes for  $\text{Fe}(\text{acac})_3$  formation from NP and  $\text{acac}^-$ .

**Table 5 :** Yields of Fe(acac)<sub>3</sub> from the reactions of acetylacetone with cyanoferrate complexes

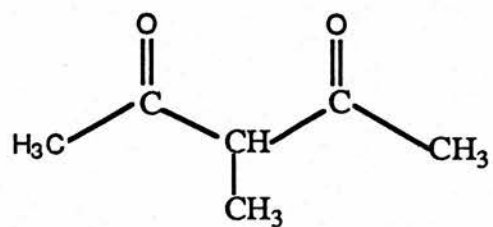
Complex	[complex]/M <sup>a</sup>	[acac-]/M	%yield Fe(acac) <sub>3</sub>	time/hours
[NP]	0.28	0.20	5.35	3 (in air)
[Fe <sup>II</sup> (CN) <sub>5</sub> H <sub>2</sub> O] <sup>3-</sup>	0.28	0.20	<1.0	3 (in air)
[Fe <sup>II</sup> (CN) <sub>5</sub> H <sub>2</sub> O] <sup>3-</sup>	0.28	0.20	<1.0	3 (in N <sub>2</sub> )
[Fe <sup>III</sup> (CN) <sub>5</sub> H <sub>2</sub> O] <sup>2-</sup>	0.28	0.20	<1.0	3 (in air)
[Fe <sup>III</sup> (CN) <sub>5</sub> H <sub>2</sub> O] <sup>2-</sup>	0.28	0.20	<1.0	3 (in N <sub>2</sub> )

a. Although [Fe<sup>II</sup>(CN)<sub>5</sub>H<sub>2</sub>O]<sup>3-</sup> and [Fe<sup>III</sup>(CN)<sub>5</sub>H<sub>2</sub>O]<sup>3-</sup> are subject to dimerisation in concentrated solutions this was not important in these experiments reproducing the conditions under which the formation of Fe(acac)<sub>3</sub> upon reaction of nitroprusside and acetylacetone was noted.

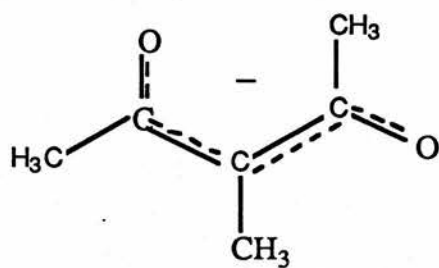
$\text{Fe}(\text{acac})_3$  formation was determined spectrophotometrically; aliquots of reaction solutions were extracted with methylene chloride at timed intervals and the concentration of  $\text{Fe}(\text{acac})_3$  in each aliquot was calculated from the extinction coefficient of  $\text{Fe}(\text{acac})_3$  determined in an independent experiment. The influence of air on these reactions was investigated by flushing identical deoxygenated solutions of the cyanoferrate complex and  $\text{Hacac}$  or  $\text{acac}^-$  with air or nitrogen and extracting aliquots of the solutions with methylene chloride at timed intervals. Apart from the extractions which were performed quickly in subdued lighting, the reactions of  $\text{Hacac}$  and  $\text{acac}^-$  with cyanoferrate complexes were investigated in complete darkness. There was no detectable reaction of  $\text{Hacac}$  or  $\text{acac}^-$  with nitropentacyanoferrate(II), hexacyanoferrate(II) or hexacyanoferrate(III), and the reactions with other pentacyanoferrate complexes (Table 5) yielded only marginal amounts of  $\text{Fe}(\text{acac})_3$ . The presence of air had no effect on these yields and from these experiments it was concluded that the only cyanoferrate complex which reacts with  $\text{acac}^-$  to form  $\text{Fe}(\text{acac})_3$ , apart from possibly the NP and  $\text{acac}^-$  adduct, is NP.

#### 4.2.9 Reaction of NP with 3-methyl-2,4-pentanedione in alkaline solution

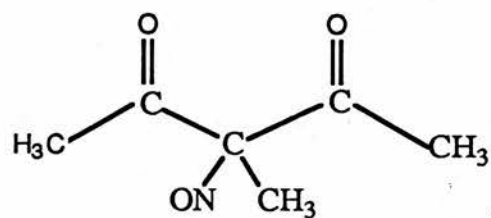
The reaction of NP with 3-methyl-2,4-pentanedione [ $\text{MHacac}$ , (9)] in alkaline solution proceeded in a manner exactly analogous to the reaction of NP with acetylacetone (2,4-pentanedione) in alkaline solution. The deep red colour of the alkaline NP and  $\text{MHacac}$  reaction solution, like that of NP and  $\text{acac}^-$ , did not fade rapidly as observed for the reaction of



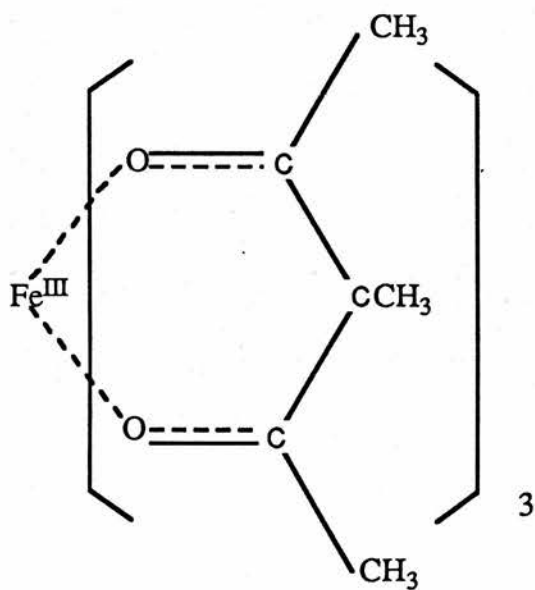
(9)



(10)



(11)



(12)

NP with all other carbanions studied. This red colour ( $\lambda_{\max}$  480 nm) is attributed to the adduct of NP and the carbanion  $\text{Macac}^-$  (10), presumably related to (5). It was not possible to characterise this adduct with any more success than that achieved with the adduct of NP and  $\text{acac}^-$ . The material that could be isolated from cold alcoholic reaction solutions of NP and MHacac was dark brown and hygroscopic and when re-dissolved had an absorbance ( $\lambda_{\max}$  480 nm) identical to that of a solution of NP and  $\text{Macac}^-$  immediately after mixing.

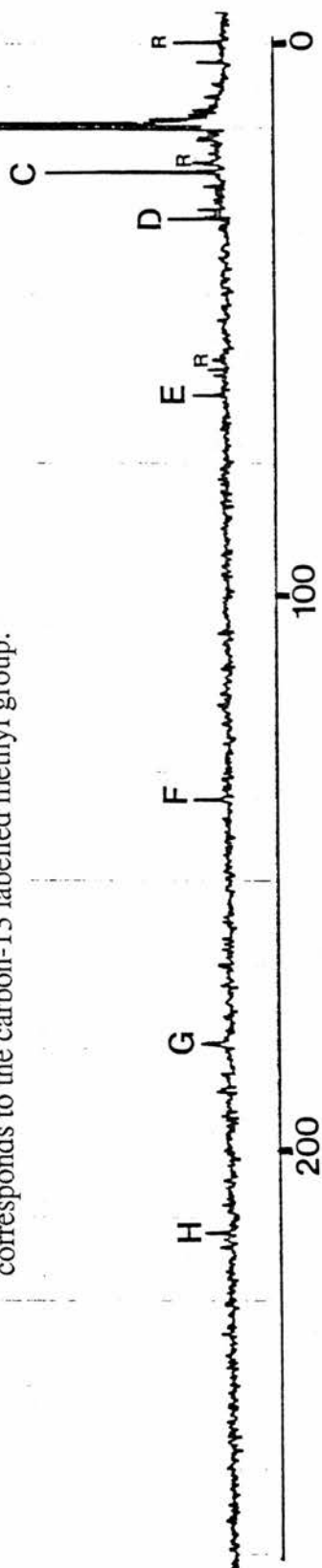
As for the acetylacetone reaction the interpretation of the visible spectra of NP and MHacac in alkaline solution was limited by the overlapping absorbances of the possible initial, intermediate and final cyanoferrate species. Kinetic studies of the rate of formation of the adduct were not possible on the stopped-flow spectrometer as the low water solubility of MHacac imposed concentrations too low for the sensitivity of the spectrophotometer unit. The product of reaction can not be the oxime of MHacac but the crystalline nitroso compound 3-methyl-3-nitrosopentane-2,4-dione (11) is readily prepared from an acidified solution of sodium nitrite and MHacac. 3-Methyl-3-nitrosopentane-2,4-dione is not soluble in neutral solutions but decomposes rapidly in alkaline media and could not be isolated from reaction solutions of NP and MHacac. The reaction of concentrated solutions of NP and  $\text{Macac}^-$  in complete darkness gave rise to the complex  $\text{Fe}^{\text{III}}(\text{Macac})_3$  (12) formed in a maximum 12% yield with respect to the limiting reagent NP. Use of a cyanide-sensitive electrode with reaction solutions of NP and  $\text{Macac}^-$ , as previously described

**Figure 10** : Carbon-13 nmr spectrum of nitroprusside and 3-methylpentane-2,4-dione (MHacac, 20 atom % carbon-13 in the 3-methyl position) in alkaline solution, recorded several hours after mixing

R = internal reference 3-(trimethylsilyl)propane sulphonic acid, sodium salt

A= 12.4 (?), B=13.2 (MHacac), C=21.0 (MHacac), D=29.3 (MHacac),  
 E=61.0 (MHacac), F=134.4 ( $^{13}\text{CN}_{\text{eq}}$  NP), G=178.0 ( $[\text{Fe}^{\text{II}}(\text{CN})_6]^{4-}$ ),  
 H=208.9 ppm (MHacac).

Peak A and two additional peaks at 57.4 and 28.5 ppm were apparent in a spectrum recorded several hours later ; the intensity of peak A indicates that it corresponds to the carbon-13 labelled methyl group.

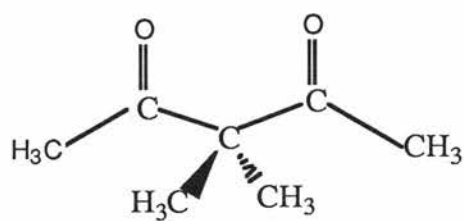


(Section 4.2.4) for the reaction of NP with  $\text{acac}^-$ , did not support release of cyanide from NP.

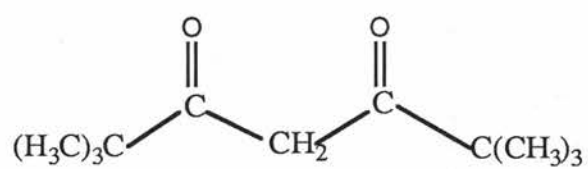
The carbon-13 nmr spectra of MHacac,  $\text{Macac}^-$ , and the nitroso compound of MHacac (11), at natural abundance and 20 atom.%  $^{13}\text{C}$  in the 3-methyl group, have been discussed in Chapter 2. In the carbon-13 spectrum of a  $\text{Macac}^-$  and NP reaction solution (not shown) the starting materials, as well as  $[\text{Fe}(\text{CN})_6]^{4-}$ , were apparent but several remaining signals did not correspond to the carbon-13 nmr spectrum of the nitroso compound recorded in  $\text{CDCl}_3$ .

Carbon-13 enriched MHacac was prepared by 3-methylation of Hacac with 20 atom %  $^{13}\text{C}$  methyl iodide in an attempt to characterise the organic reaction products and avoid the long acquisition periods required for carbon-13 nmr spectra of dilute solutions at natural abundance and low-field. In the reaction solution spectrum of NP and carbon-13 labelled MHacac in alkaline solution (Figure 10) there were the same number of peaks though not of the same chemical shift as recorded for an alkaline solution of the carbon-13 labelled nitroso compound (20 atom %  $^{13}\text{C}$  in the 3-methyl group) in DMSO. This is not direct evidence of the formation of the nitroso compound upon reaction of NP and  $\text{Macac}^-$  but the solvent difference for the two spectra could influence not only chemical shifts but the products of the nitroso compound decomposition.

It can be concluded that the reaction of NP with MHacac in alkaline solution proceeds in the same manner as reaction of NP with  $\text{acac}^-$ . The red colour associated with the adduct apparent immediately upon mixing persists instead of fading



(13)



(14)

rapidly to yellow and the kinetics of the change in the absorbance maximum of reacting solutions from 480 nm to shorter wavelengths were complex. The organic products of the reaction have not been identified but could include the nitroso compound (11).  $\text{Fe}^{\text{III}}(\text{Macac})_3$  has been isolated from solution in 12% maximum yield and formation of hexacyanoferrate(II) has been recorded by carbon-13 nmr.

#### 4.2.10 Reactions of NP with other 1,3-diketones

Addition of NP to an alkaline solution of 3,3-dimethylpentane-2,4-dione ((13), DMacac) resulted in the immediate formation of an intense red colour which rapidly faded to yellow. The rapid fading of what is assumed to be the adduct of NP and the carbanion of DMacac indicates that this reaction proceeds in a manner identical to the reaction of NP with carbon acids such as acetone and ethyl cyanoacetate, for which formation of **only** the corresponding oxime and aquapentacyanoferrate(II) has been recorded. (In contrast, the red colour associated with the adducts of NP and  $\text{acac}^-$  or  $\text{Macac}^-$  persisted and the complexes  $\text{Fe}(\text{acac})_3$  and  $\text{Fe}(\text{Macac})_3$  were isolated.) Aromatisation of the diketone ligand by loss of a proton at the 3 position, as for the complexes  $\text{Fe}(\text{acac})_3$  and  $\text{Fe}(\text{Macac})_3$ , is obviously not possible for DMacac.

There was no apparent adduct formation upon addition of NP to an alkaline solution of 2,2,6,6-tetramethylheptane-3,5-dione [(14), TMHacac]; the solution did turn bright yellow ( $\lambda_{\text{max}}$  400 nm), but this is attributed to the reaction of NP with hydroxide to form nitropentacyanoferrate(II).

TMHacac is an exceptionally bulky ligand and it has been observed<sup>8</sup> that nucleophilic attack at the nitrosyl of NP is subject to steric hindrance.

### 4.3 DISCUSSION

It has been shown in Chapter 3 that the reaction of NP with ethyl cyanoacetate in alkaline solution, typical of the reactions of NP with most carbanions, results in formation of the oxime ethyl isonitrosocyanoacetate and aquapentacyanoferrate(II). In this reaction NP is a source of  $\text{NO}^+$  in alkaline solution. However, the experiments detailed above indicate that nitrosation of the carbanion is not the only reaction that occurs when hydroxide is added to a solution of NP and Hacac or MHacac. For these two carbanionic systems the formation of  $\text{Fe}(\text{acac})_3$  or  $\text{Fe}(\text{Macac})_3$  has been recorded, a most surprising result in view of the exceptionally high formation constant of NP and its kinetic inertness as a low spin  $d^6$  iron(II) complex. The mild conditions in which these complexes are formed are not significantly different from the conditions that might be encountered *in vivo* and the mechanism of the reaction of NP with Hacac or MHacac in alkaline solution therefore has important implications for the use of NP as a hypotensive agent.

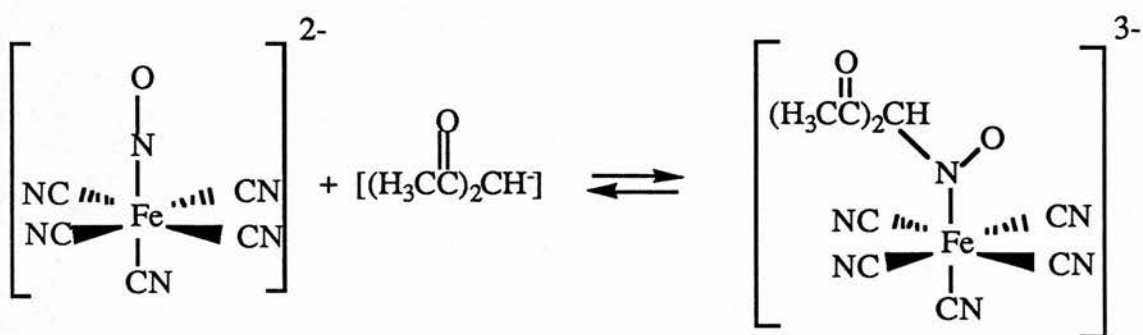
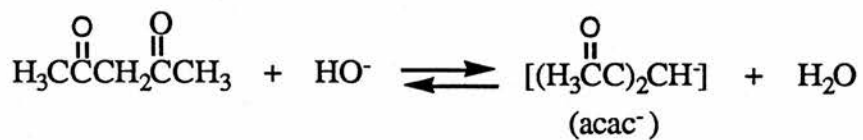
Two features of the conversion of NP to  $\text{Fe}(\text{acac})_3$ , iron oxidation and NO release, could arise from the photolytic decomposition of NP to the kinetically *labile* species aquapentacyanoferrate(III) and NO, but it has been repeatedly demonstrated that  $\text{Fe}(\text{acac})_3$  is formed in the absence of light. Additionally, oxidation of iron is not dependent upon the presence of oxygen and it has not been possible to obtain  $\text{Fe}(\text{acac})_3$  in significant yield from the reaction of Hacac or  $\text{acac}^-$  with any kinetically labile or inert cyanoferrate

complexes, with the exception of NP and possibly the isolated adduct.

Both iron oxidation and NO release in the absence of light and oxygen can be explained by metal to ligand charge transfer (MLCT); the charge distribution of NP is formally iron(II) and  $\text{NO}^+$  but transfer of an electron from iron to the nitrosyl ligand results in the distribution iron(III) and NO. The mechanism proposed for the conversion of NP to  $\text{Fe}(\text{acac})_3$  by metal to ligand charge transfer can not be proven directly but is the only mechanism that is consistent with the seventeen observations listed below.

1. The red colouration resulting from reactions of NP with  $\text{acac}^-$  or  $\text{Macac}^-$  and characteristic of the adducts of NP and carbanions did not fade rapidly, in contrast to all other carbanionic systems studied.
2. The materials precipitated from alcoholic solutions of NP and  $\text{acac}^-$  or  $\text{Macac}^-$  had infra-red and carbon-13 nmr spectra characteristic of pentacyanoferrate(II) species.
3. The oxime Hinaa could not be isolated or identified in reaction mixtures of NP and Hacac.
4. Acetate was apparent in carbon-13 nmr spectra of the reaction solution and the oxime Ina could be isolated from an alkaline solution of what was designated the NP and  $\text{acac}^-$  adduct.
5. Kinetic studies of the formation of the adduct of NP and  $\text{acac}^-$  suggest that secondary ionisation of the adduct does not occur.
6.  $\text{Fe}(\text{acac})_3$  or  $\text{Fe}(\text{Macac})_3$  were isolated from reaction solutions kept in the dark.
7.  $\text{Fe}(\text{acac})_3$  was formed in the same yield, at the same rate, in oxygenated and deoxygenated solutions.
8.  $\text{Fe}(\text{acac})_3$  was formed in maximum 15.5% yield with respect to NP as the limiting reagent.
9.  $\text{Fe}^{\text{III}}(\text{Macac})_3$  was formed in maximum 12.2% yield with respect to NP as the limiting reagent.

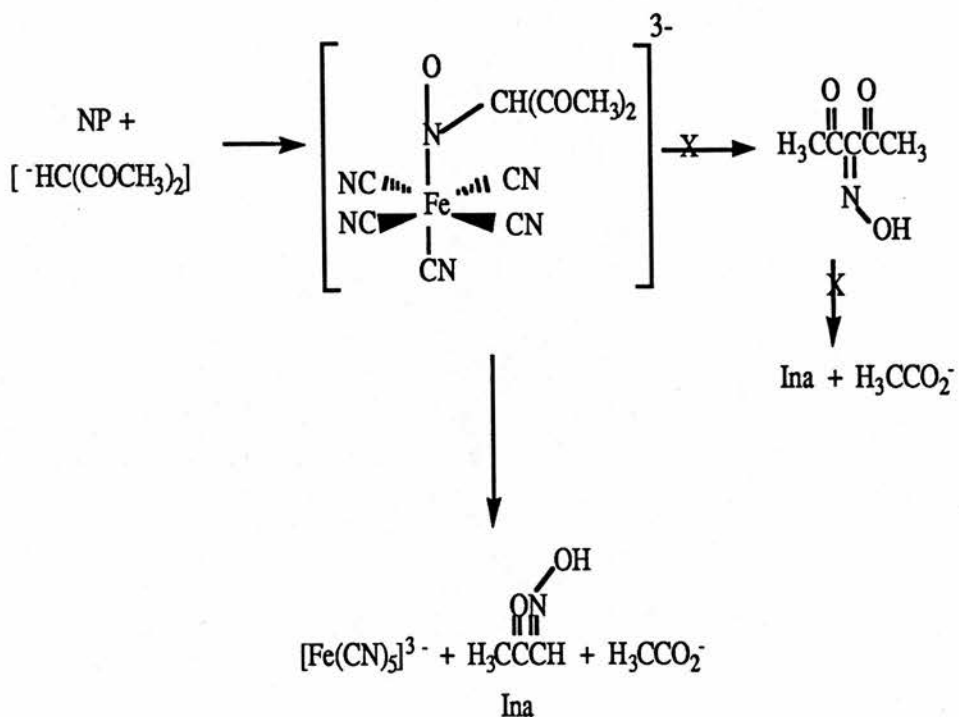
Scheme 1 : Formation of the adduct of nitroprusside and acetylacetonate



10. NP reacted with 3,3-dimethylpentane-2,4-dione to form a red adduct which very rapidly faded to yellow, but did not react with 2,2,6,6-tetramethylheptane-3,5-dione.
11. No free cyanide was detected in NP and Hacac or MHacac reaction solutions with a cyanide sensitive electrode and there were no signals for undissociated HCN in carbon-13 nmr spectra of a reaction solution of 90% carbon-13 enriched NP and Hacac. Similarly, there were no signals for HCN in carbon-13 nmr spectra of NP and Hacac or MHacac reaction solutions recorded overnight.
12. No HCN could be detected in the infra-red spectrum of the gas collected over a reaction solution of NP and Hacac.
13. Solution infra-red spectra recorded immediately after mixing concentrated solutions of NP and  $\text{acac}^-$  contained CN stretches characteristic of a pentacyanoferrate(II) species.
14. Transient pentacyanoferrate(II) species, which do not correspond to known complexes including  $[\text{Fe}(\text{CN})_5\text{H}_2\text{O}]^{3-}$  and  $[\text{Fe}(\text{CN})_5\text{NO}_2]^{4-}$ , were observed in the carbon-13 nmr spectrum of 90% carbon-13 NP and  $\text{acac}^-$ .
15. Neither Hacac nor  $\text{acac}^-$  reacted with any cyanoferrate complexes, other than NP and possibly the isolated adduct, to form  $\text{Fe}(\text{acac})_3$ .
16.  $[\text{Fe}(\text{CN})_6]^{4-}$  was detected in carbon-13 nmr spectra of NP and Hacac or MHacac reaction solutions.
17. NO was recovered following reaction of degassed solutions of NP with  $\text{acac}^-$  and identified by gas infra-red spectroscopy.

From the above evidence it seems clear that the adduct of NP and  $\text{acac}^-$  (5) is formed by nucleophilic attack of the carbanion  $\text{acac}^-$  at the NP nitrosyl ligand (Scheme 1): the red colour is characteristic of such adducts and the infra-red and carbon-13 nmr spectra obtained of the reaction solution immediately after mixing and the isolated adduct correspond to pentacyanoferrate(II) species. Kinetic studies using stopped-flow spectrometry establish that the rate of formation of the adduct ( $\lambda_{\text{max}}$  480 nm) is, in pseudo first-order

**Scheme 2 :** The decomposition of the adduct of nitroprusside and acetylacetonate to Ina and acetate

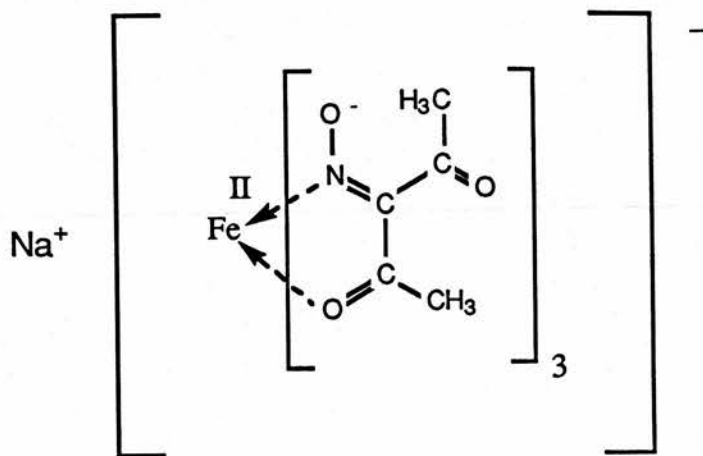


conditions, proportional to the carbanion concentration and follows the pre-equilibrium of Hacac and hydroxide. Further ionisation of the adduct is apparently not important: the reaction of NP with  $\text{Macac}^-$  yields  $\text{Fe}(\text{Macac})_3$ .

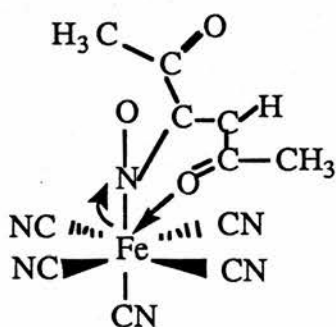
Once formed, it is clear the adduct of NP and  $\text{acac}^-$  does *not* react in the same way as adducts of NP and other carbanions. The rapid fading from red (480 nm) to yellow (400 nm) representing formation of an oxime and aquapentacyanoferrate(II) or its polymeric derivatives was not observed for NP and  $\text{acac}^-$  or  $\text{Macac}^-$  solutions. Instead, the persistent red colourations associated with adducts of NP and  $\text{acac}^-$  or  $\text{Macac}^-$  were evident as maxima in the region 450 - 480 nm (Figures 4A, 4B, 4C).

The oxime isonitrosoacetylacetone (Hinaa) is the product expected from hydrolysis of the NP and  $\text{acac}^-$  adduct by analogy with the reaction of NP with other carbanions but Hinaa has never been isolated following the reaction of NP with  $\text{acac}^-$ . However, with the method of Cambi,<sup>4</sup> the oxime isonitrosoacetone (Ina) has been isolated from an alkaline solution of the adduct precipitated from a cold, alcoholic solution of NP and  $\text{acac}^-$ . Low-field natural abundance spectra of NP and  $\text{acac}^-$  reaction solutions reveal that the adduct does hydrolyse, but acetate and Ina, not Hinaa, are the primary products. A scheme for the hydrolysis of the NP and  $\text{acac}^-$  adduct is shown in Scheme 2.

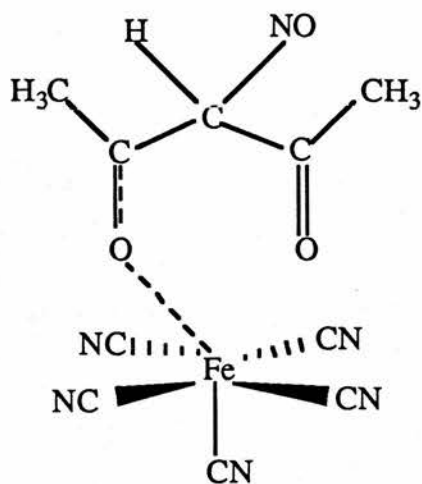
The adduct (5) can adopt a conformation similar to that of the complex (15) of iron(II) and the anion of Hinaa if the carbonyl oxygen approaches the iron centre (16). As



(15)



(16)

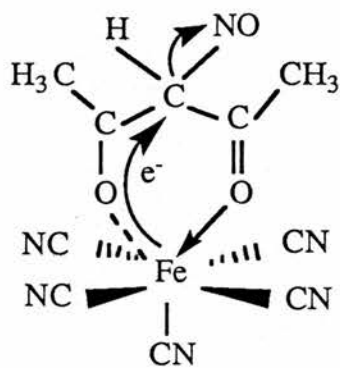


(17)

rearrangement proceeds an oxygen to iron bond can be formed at the expense of the iron to nitrogen bond (17).

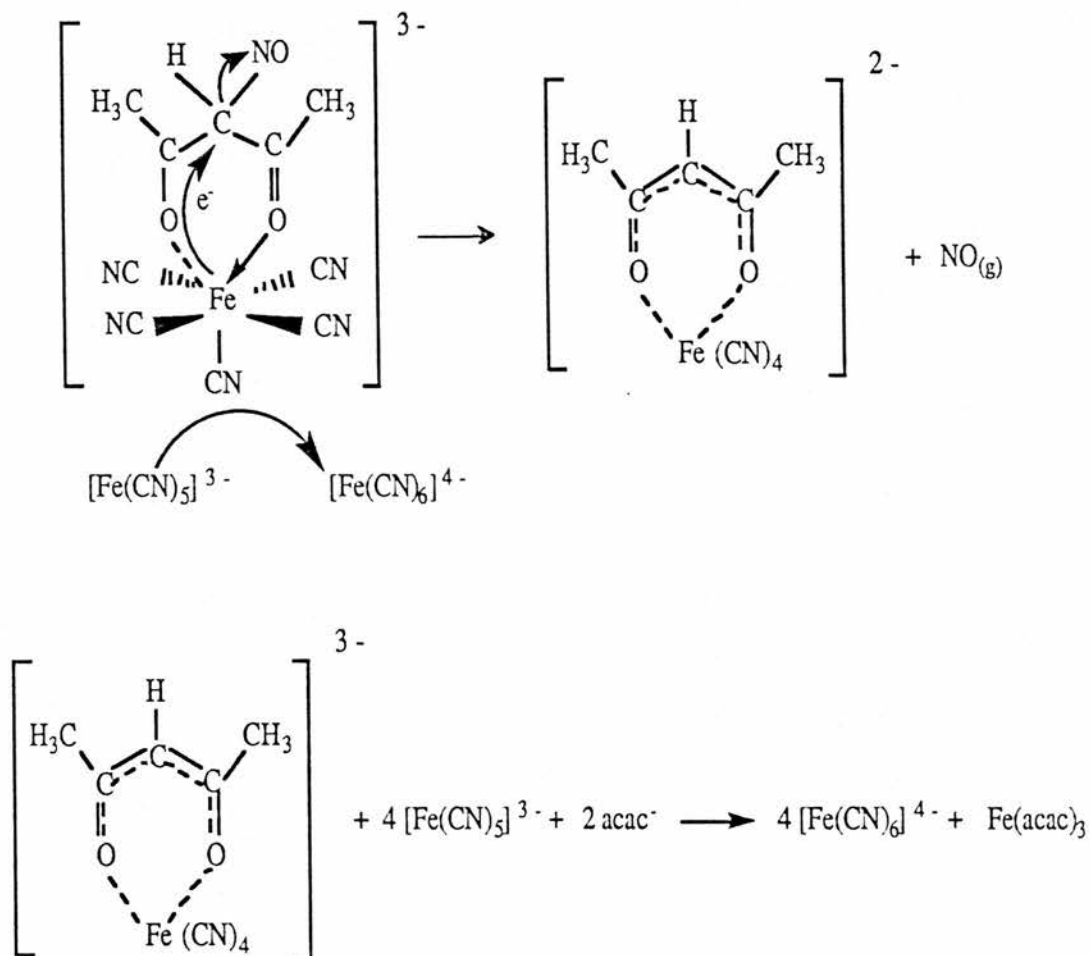
The persistence of the red colour of NP and Hacac or MHacac reaction solutions supports rearrangement of the initially formed adduct, in addition to hydrolysis. It seems likely that it is the adduct and species resulting from rearrangement that are responsible for the longevity of the red colour of the reaction solutions. The high-field carbon-13 nmr spectra recorded shortly after mixing 90% carbon-13 labelled NP and  $\text{acac}^-$  contained signals characteristic of pentacyanoferrate(II) species that were not present in a later spectrum and did not correspond to any isolable cyanoferrate complexes. These transient signals are consistent with rearrangement of the adduct to form a low spin  $d^6$  complex such as (17) which is kinetically inert and diamagnetic.

Both the nitrosyl ligand and iron, formally  $\text{NO}^+$  and  $\text{Fe}^{2+}$  in NP, can assume several oxidation states. If an electron were transferred from the iron atom to the nitrosyl moiety the resulting complex would contain iron(III) and NO. This process is termed metal to ligand charge transfer (MLCT) and in this way the oxidation of the kinetically inert  $d^6$  iron(II) adduct to a kinetically *labile*  $d^5$  iron(III) complex can be achieved independently of oxygen and light. The transfer of charge in such a manner is usually associated with photo-induced electronic excitation when the energy gap between the acceptor LUMO and donator HOMO is not large. The absorbance band for this excitation is in the visible region for NP and photodecomposition of NO results in the same



(18)

Scheme 3 : Metal to ligand charge transfer from adduct iron atom to nitrosyl ligand

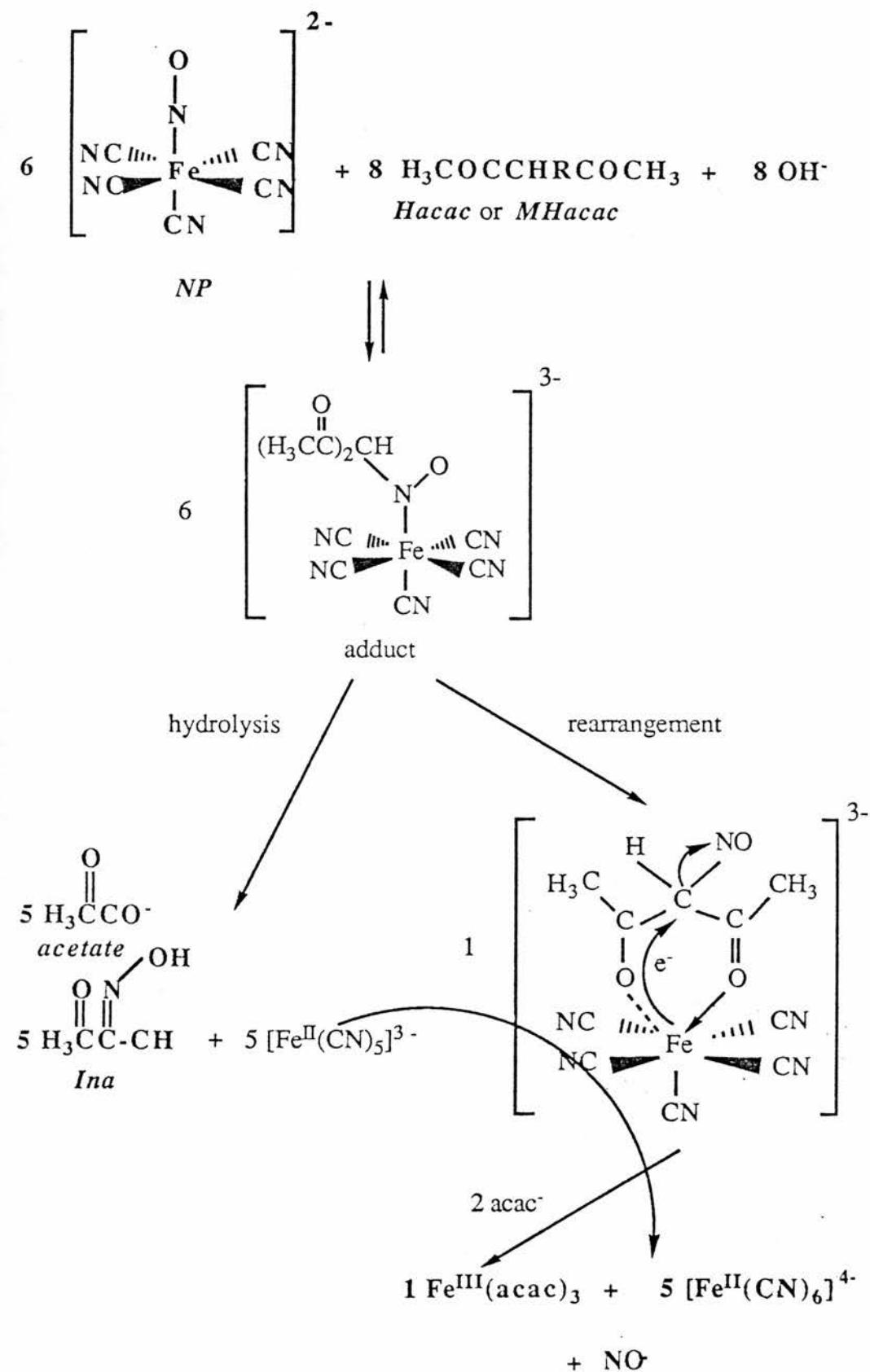


distribution of charge between iron and the nitrosyl ligand, that is  $\text{NO}^\bullet$  and  $[\text{Fe}^{\text{III}}(\text{CN})_5\text{H}_2\text{O}]^{2-}$ .<sup>24,25</sup> It has been shown that the formation of  $\text{Fe}(\text{acac})_3$  from alkaline solutions of NP and Hacac is independent of light and therefore the driving force for the transfer of charge from iron to the nitrosyl moiety must originate from the ensuing reactions of the rearranged adduct.

Iron(III) has a strong affinity for coordinating to oxygen and with the approach of the second carbonyl oxygen to the iron centre, aromatisation of the acetylacetonato ligand can be achieved by the loss of the nitrosyl moiety as  $\text{NO}$  (18). (Clearly, although aromatisation of the  $\text{acac}^-$  and  $\text{Macac}^-$  ligands can be achieved in this way, this reaction is not possible for 3,3-dimethylpentane-2,4-dione.) With the generation of the bidentate  $\text{acac}^-$  ligand the six-coordination of the now kinetically *labile* complex can be maintained by the transfer of a cyanide ligand to the pentacyanoferrate(II) species arising from the hydrolysis of the adduct (Scheme 3). No free cyanide has been detected in NP and Hacac or Macac reaction solutions using a range of techniques, but a variety of cyanide-bridged complexes are known, including  $[\text{Fe}_2(\text{CN})_{10}]^{4-}$ ,<sup>15</sup>  $[\text{Fe}_2(\text{CN})_{10}]^{6-}$ ,<sup>15</sup> and  $[\text{Fe}_2(\text{CN})_{11}]^{5-}$ ,<sup>26</sup> and it is likely that hexacyanoferrate(II) is formed not by direct release of free cyanide but by transfer of cyanide from the rearranged adduct to  $[\text{Fe}(\text{CN})_5]^{3-}$ .

Metal to ligand charge transfer of the initially formed adduct of NP and  $\text{acac}^-$  can be seen to promote the aromatisation of the  $\text{acac}^-$  ligand and the concomitant energetically

**Scheme 4** : Mechanism for the reaction of nitroprusside with acetylacetonate (or 3-methylpentane-2,4-dione, MHacac) in alkaline solution



favourable formation of  $\text{Fe}(\text{acac})_3$  and  $[\text{Fe}(\text{CN})_6]^{4-}$ . Additionally, an increase in entropy will accompany the loss of the nitrosyl ligand as  $\text{NO}_{(\text{gas})}$ . The optimum stoichiometry of this reaction should be eight Hacac (or MHacac) to six NP (Scheme 4) and the 15.5% experimental maximum yield of  $\text{Fe}(\text{acac})_3$  (or 12.2%  $\text{Fe}(\text{Macac})_3$ ) corresponds closely to the proposed conversion of one in six NP to  $\text{Fe}(\text{acac})_3$ , that is 16.6%.

The formation of the  $\text{Fe}(\text{acac})_3$  and  $\text{Fe}(\text{Macac})_3$  complexes from alkaline reaction solutions of NP and Hacac or MHacac in mild conditions was initially an alarming observation with particular regard to the toxicity of NP administered as a hypotensive agent. However, while the proposed mechanism (Scheme 4) includes effective loss of the five cyanide ligands from one in six NP it is consistent with *no* detectable production of *free* cyanide; the reaction represents formation of five hexacyanoferrate(II),  $[\text{Fe}^{\text{II}}(\text{CN})_6]^{4-}$ , by *transfer* of five cyanide ligands to five  $[\text{Fe}(\text{CN})_5]^{3-}$ . Therefore there is no net change in the number of cyanide ligands co-ordinated to iron.

Although the reaction of NP with  $\text{acac}^-$  or  $\text{Macac}^-$  results in release of  $\text{NO}$ , in contrast with carbanion nitrosation established in Chapter 3 for the reaction of NP with other carbanions, it is not likely that the proposed reaction mechanism could be reproduced in biological systems to effect hypotension through activation of the enzyme guanylate cyclase. It is the unique conformations available to the adducts of NP and  $\text{acac}^-$  or  $\text{Macac}^-$  that promote metal to

ligand charge transfer favoured by the increased entropy and high formation constants of the products. In this way, kinetically inert NP is converted by MLCT and the ensuing kinetically labile intermediates to hexacyanoferrate(II), another kinetically inert complex with a high formation constant that contributes to the driving force of this reaction and accounts for no detection of free cyanide.

#### 4.4 EXPERIMENTAL PROCEDURES

##### *Materials and instruments*

Acetylacetone (Laboratory grade) was redistilled prior to use, and solutions were made up and used on the same day. Sodium hydroxide solutions were prepared by dilution of concentrated volumetric solutions and, for kinetic experiments, were made up and used on the same day. Samples of 90% carbon-13 labelled sodium nitroprusside were prepared by Dr. J. McGinnis, as reported.<sup>9</sup> The preparations of isonitrosoacetylacetone, 3-methylpentane-2,4-dione, 3-methyl-3-nitropentane-2,4-dione and isonitrosoacetone have been described in Chapter 2. All other reagents, with the exceptions of those prepared as described below, were of AnalaR grade where available.

Solid sodium nitroprusside was stored in a dark cupboard. All solutions containing nitroprusside were protected from light with a complete covering of aluminium foil during storage and use.

Carbon-13 nmr spectra described as low-field experiments were recorded on a Varian CFT-20 instrument in the FT mode with a carbon resonance of 20 MHz in a field of 1.9 T. The number of scans for overnight spectra was typically 80,000 with a pulse width of 7  $\mu$  seconds and no pulse delay. The sodium salt of 3-(trimethylsilyl)propane sulphonate was used as an internal reference but all chemical shifts quoted refer to tetramethylsilane (TMS).

High-field carbon-13 nmr experiments were recorded on a Bruker WH-360 spectrometer of the SERC Regional NMR Service,

at the University of Edinburgh, in the FT mode at 25 °C with a carbon resonance of 90.56 MHz in a field of 8.5 T. The number of scans was typically 600 with a pulse width of 4  $\mu$  seconds and a delay time of 0.14 seconds. The reference was external TMS.

Proton nmr experiments were conducted on a Bruker WP-80 instrument in the FT mode. Uv/visible spectra were recorded on a Pye-Unicam SP8 100 spectrophotometer. Infra-red spectra were recorded on a Perkin Elmer 1420 spectrometer.

The rates of formation of the NP and carbanion adducts were determined by use of a Hi-Tech 3F-3L stopped-flow spectrophotometer and SF-40C control unit attached to a Data-Lab DL901 transient recorder and Farnell DTV12-14 oscilloscope; data acquisition and processing were conducted by an Apple II microcomputer using a Hi-Tech system kinetic package. Each reported rate constant represents the average of at least six runs giving similar results and a linear correlation plot established that all reactions were first order for the conditions used.

The cyanide sensitive and associated reference electrodes were supplied by Russell Electrodes, Auchtermuchty, and were calibrated with cyanide solutions made up from a stock solution of sodium cyanide in 0.2 M hydroxide.

Distilled water refluxed in an atmosphere of nitrogen for thirty minutes was used to make up solutions described as *deoxygenated*. Solutions described as *degassed* were subjected to at least three repetitions of a freeze-pump-thaw cycle on a vacuum line.

Details for the yield of  $\text{Fe}(\text{acac})_3$  from reaction solutions of acetylacetone and a range of cyanoferrate complexes in the presence and absence of air have been given. Experiments to detect  $\text{HCN}$ ,  $\text{CN}^-$  and  $\text{NO}$ , and to monitor the visible spectra of nitroprusside and acetylacetone reaction solutions also have been previously described.

### Methods

#### Preparation of $\text{Fe}(\text{acac})_3$

- A. Over a period of fifteen minutes a solution of acetylacetone (3.8 g, 0.038 mol) in ethanol (10 ml) was added to a stirring solution of ferric chloride hexahydrate (3.3 g, 0.012 mol) in water (25 ml). Upon addition of a solution of sodium acetate trihydrate (5.1 g, 0.037 mol) in water (15 ml), red crystals of  $\text{Fe}(\text{acac})_3$  precipitated and were isolated by filtration. M.p. 175 - 176 °C. Mass spectrum:  $m/z$  353 ( $\text{M}^+$ ), 254, 155, (successive loss of acac); 100 (Hacac).
- B. In a typical experiment, acetylacetone (2.9 g, 0.0243 mol) was added to sodium nitroprusside (1.45 g, 0.0049 mol) in water (50 ml). To this solution was added hydroxide (0.0293 mol) and a deep red colour was immediately apparent. The reaction mixture was left in a cupboard several hours and red crystals of  $\text{Fe}(\text{acac})_3$  were recovered by filtration. M.p. 175 - 176 °C, mixed m.p. with a genuine sample 175 - 176 °C. Mass spectrum:  $m/z$  353 ( $\text{M}^+$ ), 254, 155, (successive loss of acac); 100 (Hacac). Found C, 50.80%; H, 5.90%.  $\text{Fe}(\text{acac})_3$  requires C, 51.01%; H, 5.99%.

### Preparation of Fe(Macac)<sub>3</sub>

- A. Fe(Macac)<sub>3</sub> was prepared exactly as detailed above, with the substitution of 3-methylpentane-2,4-dione (4.3 g 0.038 mol) for acetylacetone. Red crystals of Fe(Macac)<sub>3</sub> were isolated by filtration. M.p. 142 - 145 °C. Mass spectrum:  $m/z$  395 ( $M^+$ ), 282, 169 (successive loss of Macac), 114 (MHacac).
- B. In a typical experiment 3-methylpentane-2,4-dione (3.42 g, 0.03 mol) was added to sodium nitroprusside (8.94 g, 0.03 mol) in water (50 ml). To this solution was added hydroxide (0.06 mol) and a deep red colour was immediately apparent. The reaction mixture was left in a cupboard several hours and red crystals of Fe(Macac)<sub>3</sub> were recovered by filtration. M.p. 143 - 145 °C, mixed m.p. with genuine sample 143 - 145 °C. Mass spectrum:  $m/z$  395 ( $M^+$ ), 282, 169 (successive loss of Macac), 114 (MHacac).

### Isolation of Isonitrosoacetone from solutions of nitroprusside and acetylacetonate adducts

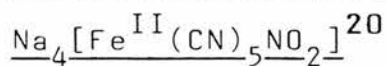
To a stirred ice-cold alcoholic solution of acetylacetone (25.0 g, 0.025 mol) and sodium nitroprusside (22.3 g, 0.075 mol) was added a solution of hydroxide (0.025 mol). A dark red oil was immediately apparent which upon trituration with ethanol yielded a dark red powder. The characterisation of such powders as the nitroprusside and acetylacetonate adducts was discussed in Section 4.2, and when dissolved in dilute hydroxide solution, decolourisation was apparent. A solution of decolourised adduct was exhaustively extracted

with methylene chloride. The organic fractions were combined, dried ( $\text{MgSO}_4$ ) and evaporation of the solvent yielded a trace amount of crystalline isonitrosoacetone, m.p. 57 - 59 °C, mixed m.p. with genuine sample 57 - 59 °C.  $\delta_{\text{H}}$  ( $\text{CDCl}_3$ ) 2.40 (s, 3H), 7.65 (s, 1H),  $\delta_{\text{C}}$  27.5, 151.5, 203.0 p.p.m.

Preparation of 3,3-dimethylpentane-2,4-dione (DMacac)<sup>27</sup>

To a stirred solution of 3-methyl-2-butanone (22.0 ml, 0.2 mol) and acetic anhydride (40 ml) was added boron trifluoride-diacetic acid complex (49 ml, 0.4 mol). After stirring overnight the mixture was added to an aqueous solution of sodium acetate (0.8 mol in 600 ml), then refluxed for three hours. When cool, the mixture was extracted with ether (3 x 200 ml). The ether extracts were combined, washed with a solution of sodium bicarbonate, and dried ( $\text{MgSO}_4$ ). The solvent was evaporated under reduced pressure and the residue was distilled. The fraction boiling at 130 - 140 °C was collected and redistilled, yielding 3,3-dimethylpentane-2,4-dione (8.34 g,  $6.5 \times 10^{-2}$  mol) in 33% yield. B.p. 136-140 °C/140 mmHg.  $\delta_{\text{H}}$  ( $\text{CDCl}_3$ ) 1.35 (s, 6H), 2.17 (s, 6H) p.p.m.

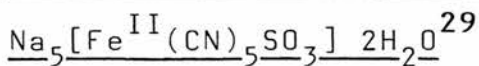
Preparation of sodium nitropentacyanoferrate(II)



To an aqueous solution of sodium nitroprusside (3.0 g, 0.01 mol) protected from light was added a solution of hydroxide (0.02 mol), yielding a bright yellow solution. After several hours ethanol was added to precipitate sodium nitropentacyanoferrate(II) as a yellow powder. Visible

absorbance maximum 400 nm. Infra-red:  $2050\text{ cm}^{-1}$ .

Preparation of sodium sulphitopentacyanoferrate(II)



To an aqueous solution of sodium nitroprusside (6.70 g, 0.022 mol) protected from light was added an alkaline solution of sodium sulphite heptahydrate (5.80 g, 0.023 mol), yielding a bright yellow red solution. After fifteen hours sodium sulphitopentacyanoferrate(II) was precipitated as a yellow powder by addition of methanol. Visible absorbance maximum 360 nm. Infra-red  $2060\text{ cm}^{-1}$ .

Formation of aquapentacyanoferrate(II) from sulphitopentacyanoferrate(II)<sup>14</sup>

The conversion of sulphitopentacyanoferrate(II) to aquapentacyanoferrate(II) was monitored by the change in the visible absorbance (360 nm) of a solution of the former to 440 nm, usually within thirty minutes. For experiments to determine the reactions of acetylacetone or its carbanion with cyanoferrate complexes, the concentration of aquapentacyanoferrate(II) was assumed to be the same as sulphitopentacyanoferrate(II). Although this assumption is not valid at high concentrations for which dimerisation of aquapentacyanoferrate(II) occurs, this was not important to experiments reproducing conditions at which  $\text{Fe}(\text{acac})_3$  was formed from the reaction of nitroprusside and acetylacetone.

Preparation of aquapentacyanoferrate(III)<sup>15</sup>

To a solution of sodium nitroprusside (6.0 g, 0.20 mol) protected from light was added sodium carbonate (2.33 g,

0.022 mol) and hydroxylamine hydrochloride (1.53 g, 0.022 mol). The solution was left in the dark for several hours after which ethanol was added, yielding a red yellow oil which was triturated to a light yellow powder,  $\text{Na}_6[\text{Fe}_2^{\text{II}}(\text{CN})_{10}]$ . The powder was redissolved in water and bromine (1 ml, 0.020 mol) was added, yielding a dark purple solution of  $[\text{Fe}_2^{\text{III}}(\text{CN})_{10}]^{4-}$  which was stirred for several hours in the dark. After this time ethanol was added to precipitate a dark blue oil and the mixture was left, protected from the light, in a cold room for fifteen hours. The oil was triturated with ethanol and the resulting blue precipitate,  $\text{Na}_4[\text{Fe}_2^{\text{III}}(\text{CN})_{10}]$ , was removed by filtration and redissolved in a solution of hydroxide (0.25 M), to hydrolyse  $[\text{Fe}_2^{\text{III}}(\text{CN})_{10}]^{4-}$  to  $[\text{Fe}^{\text{III}}(\text{CN})_5\text{OH}]^{3-}$ . After several hours the monomer was separated from the dimer by column chromatography (Sephadex G25);  $[\text{Fe}_2^{\text{III}}(\text{CN})_{10}]^{4-}$  passed through the column first and  $[\text{Fe}^{\text{III}}(\text{CN})_5\text{OH}]^{3-}$  was eluted with water. Ethanol was added to the solution of  $[\text{Fe}^{\text{III}}(\text{CN})_5\text{OH}]^{3-}$  to precipitate  $\text{Na}_3[\text{Fe}^{\text{III}}(\text{CN})_5\text{OH}]$  as a green powder, which could be converted to  $[\text{Fe}^{\text{III}}(\text{CN})_5\text{H}_2\text{O}]^{2-}$  by dissolution in water, visible absorbance maximum 400 nm.  $\text{Na}_3[\text{Fe}^{\text{III}}(\text{CN})_5\text{OH}]$  was stored in the dark and used within several days of preparation.

## REFERENCES

1. C. J. Suckling, *Chem. Soc. Reviews*, 1984, **13**, 97.
2. A. R. Butler, C. Glidewell, J. Reglinski, and A. Waddon, *J. Chem. Res. (S)*, 1984, 279.
3. J. P. Guthrie, *Can. J. Chem.*, 1979, **57**, 1177.
4. L. Cambi, *Atti Accad. Nazl. Lincei*, 1914, **23**, 812 (*Chem. Abstr.*, 1915, **9**, 452).
5. G. D. Watt, J. J. Christensen, and R. M. Izatt, *Inorg. Chem.*, 1965, **4**, 220.
6. L. Wolff, *Annalen*, 1902, **325**, 129.
7. J. H. Swinehart and W. G. Schmidt, *Inorg. Chem.*, 1967, **6**, 232.
8. A. R. Butler, C. Glidewell, V. Chaipanich, and J. McGinnis, *J. Chem. Soc., Perkin II*, 1986, 7.
9. A. R. Butler, C. Glidewell, A. R. Hyde, and J. McGinnis, *Inorg. Chem.*, 1985, **24**, 2931.
10. A. G. Sharpe, 'The Chemistry of the Cyano-complexes of the Transition Metals, Academic Press Inc., London, 1976, p.105.
11. J. H. Swinehart, *Coord. Chem. Rev.*, 1967, **2**, 385.
12. S. K. Wolfe and J. H. Swinehart, *Inorg. Chem.*, 1968, **7**, 1855.
13. K. W. Loach and T. A. Turney, *J. Inorg. Nucl. Chem.*, 1961, **18**, 179.
14. E. Borghi, M. A. Blesa, and P. J. Aymonino, *J. Inorg. Nucl. Chem.*, 1981, **43**, 1849.
15. J. E. Espenson and S. G. Wolenuk, *Inorg. Chem.*, 1972, **11**, 2034.

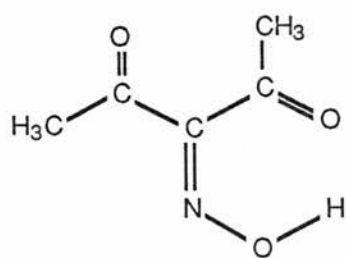
16. Ref. 10, p.106.
17. R. M. Izatt, J. J. Christensen, R. T. Pack, and R. Bench, *Inorg. Chem.*, 1962, **1**, 828.
- 18a. G. Herzberg 'Infrared and Raman Spectra of Polyatomic Molecules', D. van Nostrand, 1945, p. 279.
- 18b. G. Herzberg, 'Spectra of Diatomic Molecules', D. van Nostrand, 1950, p. 62.
19. A. R. Butler, C. Glidewell, A. S. McIntosh, D. Reed, and I. H. Sadler, *Inorg. Chem.*, 1986, **25**, 970.
20. T. Shono, H. Nii, K. Shinra, *Kogyo Kagaku Zsishi*, 1969, **72**, 1669. *Chem. Abstr.*, 1970, **72**, 21437.
21. S. Dayagi and Y. Degani in 'The Chemistry of the Carbon-Nitrogen Double Bond', (S. Patai, Ed.), John Wiley and Sons Ltd., 1970, pp. 61 - 148.
22. V. Hankonyi, N. Burger, and V. Karas-Gašparec, *Z. Phys. Chemie, Leipzig*, 1975, **256**, S.87.
23. N. Burger and V. Hankonyi, *Polyhedron*, 1986, **5**, 663.
24. S. K. Wolfe and J. H. Swinehart, *Inorg. Chem.*, 1975, **14**, 1049.
25. G. Stochel, R. van Eldik, and Z. Stasicka, *Inorg. Chem.*, 1986, **25**, 3663.
26. G. Emschwiller, *Compt. Rend.*, 1969, **268**, 692.
27. C. Mao, F. C. Frostick, E. H. Mann, R. M. Manyik, R. L. Wells, and C. R. Hauser, *J. Org. Chem.*, 1969, **34**, 1425.
28. Ref. 10, p. 136.
29. E. J. Baran and A. Müller, *Z. Anorg. Allgm. Chem.*, 1969, **368**, 144.

CHAPTER 5

COMPLEXATION OF IRON(II) WITH

3-HYDROXYIMINOPENTANE-2,4-DIONE

(HINAA)



(1)

## 5.1 INTRODUCTION

Brightly coloured complexes of transition metals and 3-hydroxyiminopentane-2,4-dione (1), also known as isonitrosoacetylacetone (Hinaa), have been known since the beginning of this century.<sup>1</sup> More recently,<sup>2-4</sup> oximes such as Hinaa have been used to extract metal ions from aqueous solution. In particular, the reaction of Hinaa with iron(II) in slightly alkaline solution to form a bright blue complex has been used as a quantitative analytical procedure for the determination of iron(II) in the presence of iron(III), with which Hinaa does not react.<sup>4</sup>

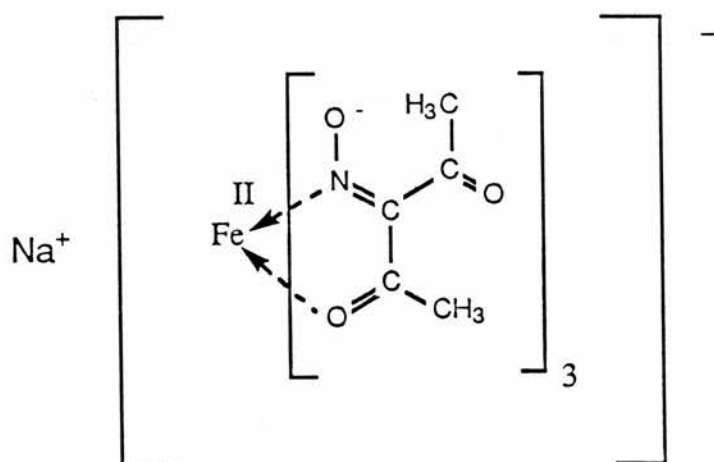
By analogy with the reactions of nitroprusside with ethyl cyanoacetate and other carbanions (Chapter 3), Hinaa is the product expected from the reaction of nitroprusside with acetylacetone in alkaline solution (Chapter 4). However, it was not possible to isolate Hinaa from nitroprusside and acetylacetone reaction solutions and thus the reactions of Hinaa with iron(II) and cyanoferrate complexes were investigated as possible routes through which Hinaa, if formed, was consumed. The reaction of Hinaa with NP is described in Chapter 4 but there was no discernible reaction of Hinaa with hexacyanoferrate(II) or hexacyanoferrate(III) and the characteristic intense blue species arising from reaction of Hinaa with iron(II) was not detected at any time in reaction solutions of acetylacetone and nitroprusside.

The structure of the blue iron(II)inaa<sup>-</sup> complex, elucidated by infra-red and nmr spectroscopy, bears an intriguing resemblance to intermediate species proposed (Chapter 4) for

the conversion of the acetylacetonate and NP adduct to  $\text{Fe}(\text{acac})_3$ . Kinetic studies of the rate of formation of the blue species indicate that the rate-determining step involves a third  $\text{inaa}^-$  ligand. An interesting historical coincidence arises; early this century Cambi and colleagues investigated the formation of oximes following reactions of NP with carbanions, as discussed in Chapters 3 and 4, as well as the reactions of various oximes with iron(II).<sup>5</sup>

**Table 1 :** Infra-red spectra of Hinaa,  $\text{Co}(\text{inaa})_3$ ,  $\text{Na}[\text{Fe}(\text{inaa})_3]$ , and  $\text{Pd}(\text{inaa})_2$

assignment	wave number/ $\text{cm}^{-1}$			
	Hinaa	$\text{Co}(\text{inaa})_3$	$\text{Na}[\text{Fe}(\text{inaa})_3]$	$\text{Pd}(\text{inaa})_2$
OH stretch	3160	-	-	-
C=O stretch (out of ring)	1715	1684	1665	1660, 1640
C=O stretch (in ring)	1645 1563	-	1650(shoulder)	
C=N stretch	1560	1530	1525	1513, 1510

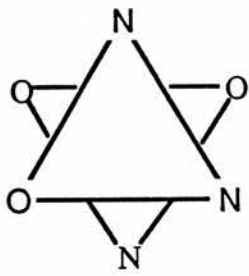


## 5.2 RESULTS AND DISCUSSION

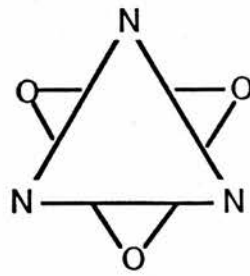
### 5.2.1 Characterisation of the iron(II)inaa<sup>-</sup> complex

There is some disagreement in the literature regarding the structure of the blue iron(II)inaa<sup>-</sup> complex. Several reports<sup>2-4</sup> have referred to the blue complex as Fe<sup>II</sup>(inaa)<sub>2</sub>, a neutral species consistent with its solubility in organic solvents but other workers<sup>6</sup> have described the species as Na[Fe<sup>II</sup>(inaa)<sub>3</sub>]. Elemental analysis (C, H, N) of the blue complex isolated from an alkaline solution of iron(II) and Hinaa confirms the latter formulation.

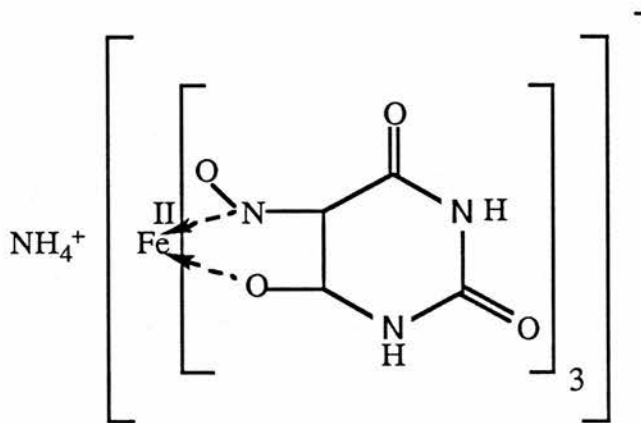
Although the crystal structure of the blue complex has not been determined, it is possible to make an assignment of its structure (2) by comparison of spectroscopic data with those of related complexes. An orange species is formed upon reaction of Hinaa with cobalt(II) which has been identified as the neutral octahedral complex Co<sup>III</sup>(inaa)<sub>3</sub>.<sup>7</sup> Infra-red spectra (Table 1) and proton nmr of Co(inaa)<sub>3</sub> have shown that inaa<sup>-</sup> is a bidentate ligand, bound to the metal through nitrogen and the oxygen of one carbonyl group.<sup>7</sup> Two neutral complexes have been isolated<sup>8,9</sup> following reaction of Hinaa with palladium(II) and analysis has revealed them to be of identical composition, Pd(inaa)<sub>2</sub>. Proton nmr and infra-red spectra of these two complexes indicate that there are two (*cis* and *trans*) isomers of Pd(inaa)<sub>2</sub> and the chelation of inaa<sup>-</sup> is the same as observed for Co(inaa)<sub>3</sub>. The crystal structure of bis(3-methylpyridine)-bis(pentane-2,3,4-trione-<sup>‡</sup>-3-oximato)iron(III) has revealed a similar five-membered chelate ring configuration of the inaa<sup>-</sup> ligand<sup>10</sup> and the <sup>‡</sup>or isonitrosoacetylacetone (Hinaa)



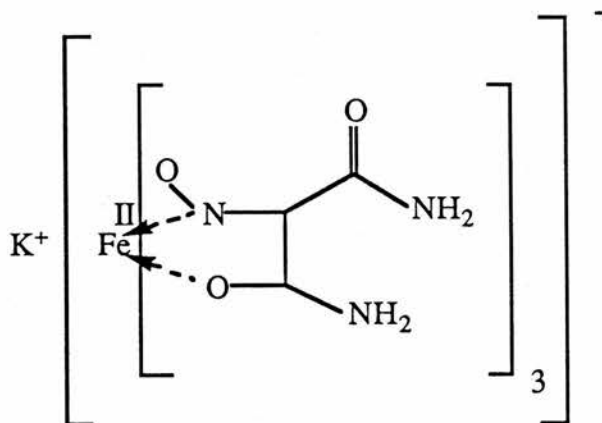
( 3 )



( 4 )



( 5 )



( 6 )

similarities of the infra-red spectra shown in Table 1 indicate that binding is the same in  $\text{Na}[\text{Fe}(\text{inaa})_3]$  as in  $\text{Co}(\text{inaa})_3$  and  $\text{Pd}(\text{inaa})_2$ .

The proton nmr spectrum of Hinaa in DMSO contains two methyl resonances, at 2.25 and 2.35 ppm, corresponding to (1) in which the methyl groups are not equivalent. Of the two possible isomers of  $[\text{Fe}(\text{inaa})_3]^-$ , mer (3) and fac (4), it is only for the fac isomer that the three  $\text{inaa}^-$  ligands are equivalent. The proton nmr spectrum of  $[\text{Fe}(\text{inaa})_3]^-$  in DMSO has only two methyl signals (2.50 and 2.10 ppm), with no evidence of splitting, consistent with formation of only the fac isomer of  $[\text{Fe}(\text{inaa})_3]^-$ . X-ray crystallography indicates this is also the preferred ligand disposition of the related salts ammonium tris(violurato)ferrate(II) hydrate (5)<sup>5</sup> and potassium tris(isonitrosomalamido)ferrate(II) hydrate (6).<sup>11</sup>

### 5.2.2 Kinetic studies of the formation of $\text{Fe}(\text{inaa})_3$

The conversion of  $[\text{Fe}(\text{H}_2\text{O})_6]^{2+}$  to  $[\text{Fe}(\text{inaa})_3]^-$  must occur in a step-wise manner and kinetic studies of the formation of  $[\text{Fe}(\text{inaa})_3]^-$  were conducted in order to determine the rate-determining step. The formation of  $[\text{Fe}(\text{inaa})_3]^-$  ( $\lambda_{\text{max}}$  600 nm) was followed by stopped-flow spectrophotometry and the concentration of Hinaa was always in excess to ensure pseudo first-order conditions. A solution of Hinaa and iron(II) was in one syringe and a solution of sodium hydroxide in the other. The concentration of  $\text{inaa}^-$  in each reaction solution could be calculated using the  $\text{pK}_a$  of Hinaa (7.4)<sup>12</sup> and the pH values of the reaction solutions could be kept constant by

**Figure 1** : Plot of  $1/k_{\text{obs}}$  vs.  $[\text{inaa}^-]^3$  for the reaction of Fe(II) and isonitrosoacetylacetone (Hinaa)

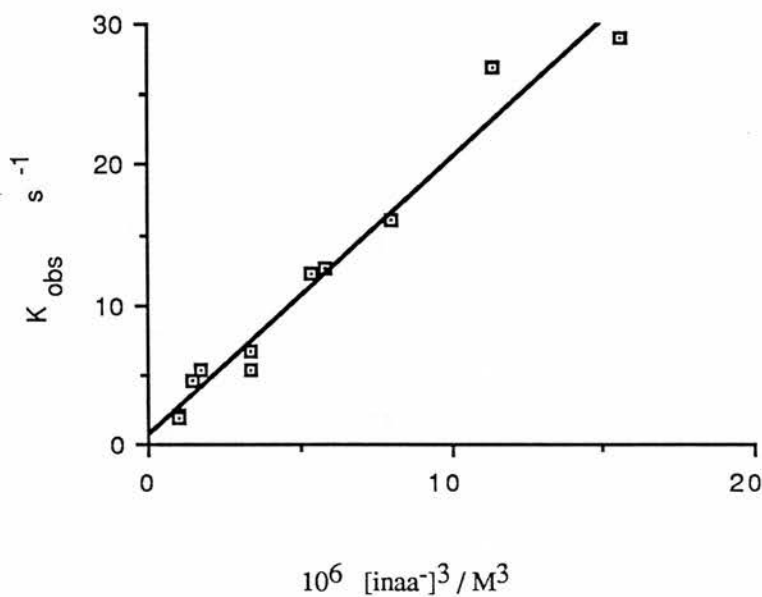


**Table 2** : Kinetic data<sup>a</sup> for the reaction of inaa- and Fe(II)<sup>b</sup> at 25° C

$10^2 [\text{inaa}^-] / \text{M}$	$10^6 [\text{inaa}^-]^3 / (\text{M})^3$	pH	$k_{\text{obs}} / \text{s}^{-1}$
25.0	15.60	7.40	$29.0 \pm 1$
22.5	11.40	7.14	$27.0 \pm 2.7$
20.0	8.80	7.40	$16.0 \pm 2.7$
18.0	5.83	7.58	$12.6 \pm 1.8$
17.5	5.36	7.14	$12.3 \pm 0.3$
15.0	3.38	7.40	$6.7 \pm 0.5$
15.0	3.38	7.14	$5.4 \pm 0.5$
12.0	1.73	7.40	$5.3 \pm 0.1$
11.2	1.42	7.14	$4.5 \pm 0.1$
10.0	1.00	7.40	$2.1 \pm 0.1$
10.0	1.00	6.80	$1.9 \pm 0.3$

a.  $I = 0.25 \text{ M}$

b.  $[\text{Fe}^{2+}] = 2.5 \times 10^{-4} \text{ M}$

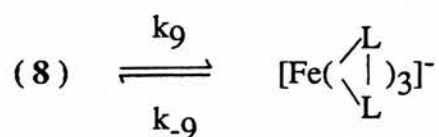
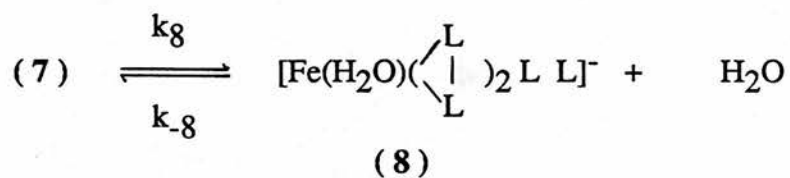
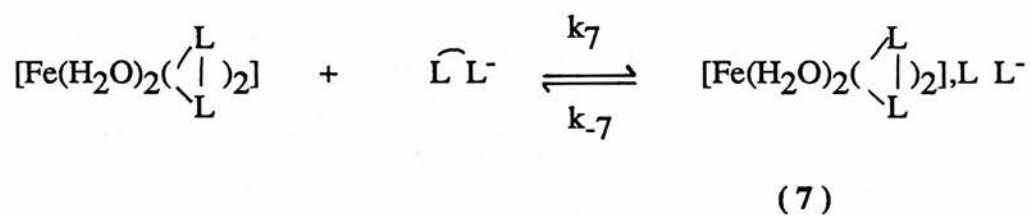
maintaining the proportions of Hinaa and hydroxide within a series of experiments.

The results, displayed in Table 2, show that there is no change of the first-order rate constant  $k_{\text{obs}}$  with pH over the range studied, but  $k_{\text{obs}}$  does change with the concentration of  $\text{inaa}^-$ . A plot of  $k_{\text{obs}}$  against  $[\text{inaa}^-]^3$  (Figure 1) is rectilinear with no intercept; the slow step in the formation of  $[\text{Fe}(\text{inaa})_3]^-$  must involve the third  $\text{inaa}^-$  ligand. Similar kinetics have been observed for the formation of  $\text{Fe}(\text{L})_3$  ( $\text{L} = 1,10\text{-phenanthroline}$  or  $2,2'\text{-bipyridyl}$ ) in acidic solution, attributed to a rapid pre-equilibrium of aquated iron(II) and two ligands preceding rate-determining association of the third ligand with the intermediate metal complex.<sup>13</sup>

Complex formation from a solution of hydrated metal ions and ligands proceeds by series of equilibria and for each step, loss of a water ligand precedes collapse of the ion pair outer sphere complex to an inner sphere complex and, for the formation of a chelated complex such as  $[\text{Fe}(\text{inaa})_3]^-$ , ring closure. These three possible rate-determining steps are illustrated in Scheme 1. It is not clear from the kinetic results which of these is rate-determining; the few kinetic studies of iron(II) complex formation have been limited to mono complexes or highly acidic conditions<sup>14,15</sup> by the rapid rate of iron(II) complexation reactions.

Formation of ion pairs (e.g. (7), Scheme 1) is largely determined by electrostatic forces and therefore unlikely to be rate-determining. Loss of the fifth  $\text{H}_2\text{O}$  ligand and

**Scheme 1 : Mechanism for the reaction of iron(II) with  
isonitrosoacetylacetonate in alkaline solution (inaa<sup>-</sup>)**



*low spin product*

$\widehat{\text{L}}\text{L}^-$  represents  $^-\text{ON}=\text{C}(\text{COCH}_3)_2$ , inaa<sup>-</sup>

formation of an inner sphere complex (e.g. (8), Scheme 1), should also be fast as the collapse of ion pairs to inner sphere complexes is commonly of the same order of magnitude as solvent exchange for labile species. The rate of solvent exchange of  $[\text{Fe}(\text{H}_2\text{O})_6]^{2+}$  is of the order  $10^6 \text{ s}^{-1}$  and complexes in which some water ligands have been replaced are generally subject to (inductive) labilisation.<sup>16,17</sup> Therefore, loss of the sixth water ligand and ring closure of  $\text{inaa}^-$  is likely to be the rate-determining step.

A notable feature of the formation of  $[\text{Fe}(\text{inaa})_3]^-$  is the change in spin state of the iron during reaction;  $[\text{Fe}(\text{H}_2\text{O})_6]^{2+}$  is a  $d^6$  high spin complex and therefore kinetically labile, but diamagnetic  $[\text{Fe}(\text{inaa})_3]^-$  is a low spin, kinetically inert complex. It is probable that change to a low spin, diamagnetic complex from high spin, paramagnetic iron(II) occurs upon association of the third  $\text{inaa}^-$  ligand;  $[\text{Fe}(\text{phen})_2(\text{H}_2\text{O})_2]^{2+}$  is known to be paramagnetic although  $[\text{Fe}(\text{phen})_3]^{2+}$  is diamagnetic.<sup>18</sup>

### 5.2.3 Attempted studies of related reactions

The reactions of Hinaa with palladium and cobalt were not suitable for stopped-flow kinetic studies due to low solubilities of the metal complexes. It was not possible to detect any complex formation upon addition of Hinaa to solutions of ruthenium, nickel, copper, manganese, or vanadate salts. Likewise, it was not possible to detect a reaction between iron(II) and the oxime 4-isonitroso-2,2,6,6-tetramethylheptane-3,5 dione in alkaline solution, probably for steric reasons.

### 5.3 EXPERIMENTAL SECTION

#### Materials and instruments

The preparation of isonitrosoacetylacetone (Hinaa) has been described in Chapter 2; solutions for kinetic studies were always made up and used on the same day. Sodium hydroxide solutions were prepared by dilution of concentrated volumetric solutions and, for kinetic experiments, were made up and used on the same day. All other materials were AnalaR, where available.

Proton nmr experiments were conducted on a Bruker WP-80 instrument in the FT mode. Uv/visible spectra were recorded on a Pye-Unicam SP8-100 spectrophotometer, infra-red spectra were recorded as nujol mulls on a Perkin Elmer 1420 spectrometer.

The rates of formation of  $[\text{Fe}(\text{inaa})_3]^{-\dagger}$  were determined by use of a Hi-Tech 3F-3L stopped-flow spectrophotometer and SF-40C control unit attached to a Data-Lab DL901 transient recorder and Farnell DTV12-14 oscilloscope; data acquisition and processing were conducted by an Apple II microcomputer using a Hi-Tech system kinetic package. The experiments were conducted at 25 °C and ionic strength ( $I = 0.25 \text{ M}$ ) was maintained with KCl. A linear correlation plot, part of the Hi-Tech kinetics program, established that all the reactions were first order for the conditions used. Each reported observed rate constant represents the average of at least six runs giving consistent results.

$\dagger (\lambda_{\text{max}} 600 \text{ nm})$

## Methods

### Preparation of Na[Fe(inaa)<sub>3</sub>]<sup>6</sup>

To a solution of FeCl<sub>2</sub> (10 mmol) and Hinaa (3.90 g, 30 mmol) in water (20 ml) was added anhydrous sodium acetate (2.46 g, 30 mmol). After heating at 40 - 50 °C under a nitrogen atmosphere for one hour, the resulting dark blue crystals were filtered and washed several times with ice-cold water. (Found: C, 38.81%; H, 3.84%; N, 8.88%. Na[Fe(inaa)<sub>3</sub>] requires C, 38.90%; H, 3.92%; N, 9.07%.)

### Preparation of 3-isonitroso-2,2,6,6-tetramethylheptane-3,5-dione<sup>19</sup>

A solution of 2,2,6,6-tetramethylheptane-3,5-dione (0.92 g, 4.5 mmol) in glacial acetic acid was flushed with nitrogen, and then NOCl for several minutes, until the solution was murky red. After further flushing with nitrogen the solution turned yellow and a white precipitate formed. Crystalline 4-nitroso-2,2,6,6-tetramethylheptane-3,5-dione was collected by filtration and washed with hexane. M.p. 125 - 126 °C (lit.<sup>19</sup> 125 - 126 °C), infra-red spectrum: 1728, 1712 cm<sup>-1</sup>. The nitroso compound (0.40 g, 1.7 mmol) was dissolved in ethanol (2 ml) and a solution of sodium hydroxide (2.2 ml, 2.2 mmol). After a short period of shaking and warming, the mixture was poured into acid and the resulting oil was extracted into methylene chloride. The organic fractions were combined, dried (MgSO<sub>4</sub>), and the solvent was evaporated under reduced pressure leaving a white powder, 4-isonitroso-2,2,6,6-tetramethylheptane-3,5-dione. M.p. 100 °C (lit.<sup>19</sup> 100 °C), infra-red spectrum: 1685, 1665 cm<sup>-1</sup>.

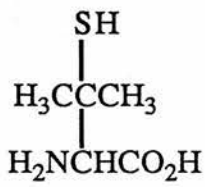
## REFERENCES

1. T. W. J. Taylor and E. K. Ewbank, *J. Chem. Soc.*, 1926, 218.
2. A. Mrozowski and T. Lipiec, *Acta Pol. Pharm.*, 1971, 28, 291.
3. J. Bernal Nievas and J. Aznarez Alduan, *Rev. Acad. Cienc. Exactus, Kis-Quim. Natur. Zaragoza*, 1971, 26, 381.
4. U. B. Talwar and B. C. Haldar, *J. Indian Chem. Soc.*, 1972, 49, 785.
5. C. L. Raston and A. H. White, *J. Chem. Soc. Dalton*, 1976, 1915 and references therein.
6. A. V. Ablov and V. N. Zubarev, *Russian J. Inorg. Chem.*, 1968, 13, 1563.
7. N. J. Patel and B. C. Haldar, *J. Inorg. Nucl. Chem.*, 1967, 29, 1037.
8. U. B. Talwar and B. C. Haldar, *J. Inorg. Nucl. Chem.*, 1970, 32, 213.
9. D. A. White, *J. Chem. Soc. A*, 1971, 233.
10. B. N. Figgis, C.L. Raston, R. P. Sharma, and A.H. White, *Austr. J. Chem.*, 1978, 31, 2431.
11. C. L. Raston and A. H. White, *J. Chem. Soc. Dalton*, 1977, 329.

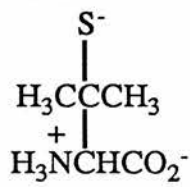
12. J. D. Aubort, R. F. Hudson, and R. C. Woodcock, *Tetrahedron Letters*, 1973, **24**, 2229.
13. H. Holyer, C. D. Hubbard, S. F. A. Kettle, and R. G. Wilkins, *Inorg. Chem.*, 1965, **4**, 929.
14. R. S. Bell and N. Sutin, *Inorg. Chem.*, 1962, **1**, 359.
15. J. H. Baxendale and P. George, *Trans. Faraday Soc.*, 1950, **46**, 736.
16. R. G. Pearson and P. C. Ellgen in "*Physical Chemistry: An Advanced Treatise*" (H. Eyring, Ed.) Academic Press, Inc., New York, Vol.VII, 1975, 218 - 298.
17. K. Kustin and J. Swinehart in "*Inorganic Reaction Mechanisms*" (J. O. Edwards, Ed.), J. Wiley & Sons, Inc., New York, 1970, 107 - 158.
18. H. Irving and D. H. Mellor, *J. Chem. Soc.*, 1962, 5222.
19. C. W. Shoppee and D. Stevenson, *J. Chem. Soc., Perkin I*, 1972, 3015.

## CHAPTER 6

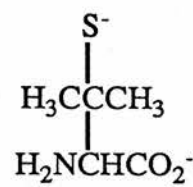
THE REACTION OF THE NITROPRUSSIDE ION  
WITH HYDROGEN SULPHIDE AND METHYL SULPHIDE IONS,  
GLUTATHIONE, CYSTEINE AND RELATED THIOLS  
IN ALKALINE SOLUTION



( 1 )

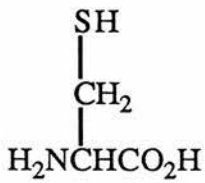


( 1A )

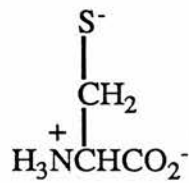


( 1B )

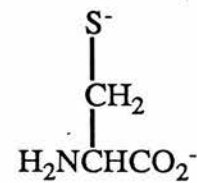
*Penicillamine*



( 2 )

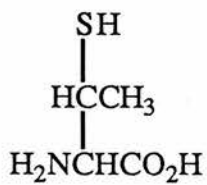


( 2A )

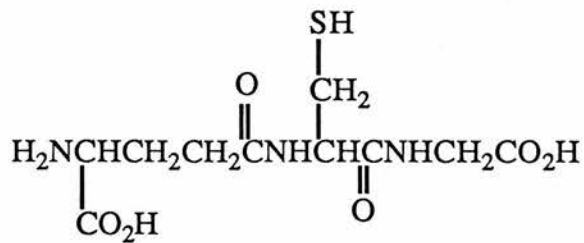


( 2B )

*Cysteine*



( 3 )



( 4 )

*β-Methylcysteine*

*Glutathione*

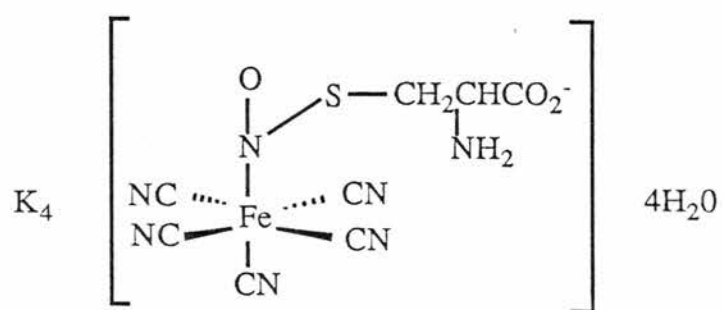
## 6.1 INTRODUCTION

The reactions of the nitroprusside ion (NP) with thiols in alkaline solution\* are characterised by immediate formation and subsequent slower fading of bright magenta species, the basis of simple but sensitive tests for cysteine and other thiols.<sup>1,2</sup> A number of investigations<sup>3-6</sup> have revealed features of the reaction of the nitroprusside ion (NP) with thiols but the final products have not always been identified. In particular, there is a lack of information concerning the inorganic product(s); cyanoferrate complexes are difficult to isolate from solution and have overlapping absorbances in the visible and ultra-violet regions.

The reaction of NP with thiols<sup>5</sup> is two orders of magnitude faster than reactions with amines<sup>7</sup> or carbanions (Chapter 3). Additionally, thiols are chemically the most reactive functional groups found within cells and there is evidence that thiols of guanylate cyclase, the enzyme through which NP and related agents act to reduce blood pressure, participate in enzyme activation.<sup>8-12</sup> The characterisation of the reactions of NP with a range of thiolates, including some occurring naturally, will be discussed with consideration of the hypotensive activity of NP.

The thiols penicillamine (1) and cysteine (2) were of interest as models of the reaction of NP with sterically hindered thiols, potentially important to the reaction of NP

\* It has been established that it is the ionised thiol, the thiolate anion, that reacts with NP but for convenience in discussing NP reactions and adducts, the less precise term thiol will be used interchangeably with thiolate.



( 5 )

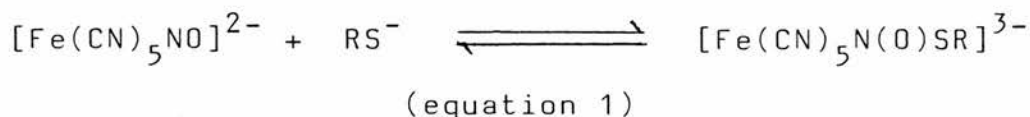
at enzyme active sites. Penicillamine is a metabolite of penicillin and has two methyl groups adjacent to the thiol function. It was possible to synthesise<sup>13</sup> the thiol  $\beta$ -methylcysteine (3), in which the thiol function is adjacent to one methyl group. The amino acid cysteine is the sole thiol-containing constituent of proteins and has been implicated in the catalytic function of a number of enzymes (to be discussed in Chapter 7).<sup>14</sup> The tripeptide glutathione (4), of which one residue is cysteine, is the most abundant intracellular non-protein thiol within the human body.<sup>15</sup> Compared to cysteine and related thiols, the hydrogen sulphide or methyl sulphide ions are poor models for enzymic thiols but the reaction of NP with a large excess of hydrogen sulphide or methyl sulphide ions yielded entirely unexpected products, the significance of which will be discussed below.

Despite the lack of information on the products of the reactions of NP with thiols, many features of these reactions have been studied and a brief survey of the work to date is presented below.

The bright magenta species formed upon reaction of NP with thiols in alkaline solution are presumed<sup>2-5</sup> to be adducts, similar to the previously described NP and carbanion adducts (Chapter 3), arising from nucleophilic attack of the thiol at the nitrosyl ligand. The structures of NP and thiolate adducts are thought to resemble that of the red violet complex (5) precipitated from the reaction of NP, cysteine, and potassium hydroxide in methanol.<sup>1</sup>

Johnson and Wilkins<sup>5</sup> have studied the kinetics of the

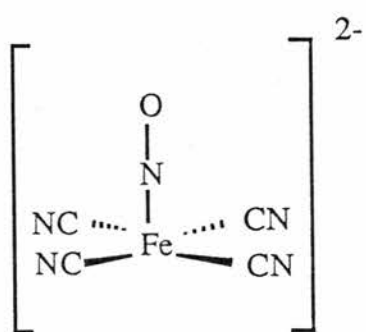
reactions of NP and a number of thiols with a stopped-flow/temperature-jump combination and report that the adduct formation reaction (equation 1) is second order in the forward direction and first order in the reverse direction.



For reactions of NP with mercaptoethanol, 1-pentanethiol, N-acetylcysteine, cysteine, 2-aminoethanethiol and glutathione, the adduct formation rate constants were found to be remarkably similar, ranging from  $1.4 \times 10^4$  to  $4.9 \times 10^4 \text{ M}^{-1} \text{ sec}^{-1}$ . A slightly lower adduct formation constant was recorded for penicillamine, which they considered to be associated with steric hindrance near the C-S<sup>-</sup> bond.

Decomposition of the NP and thiolate adduct is apparently a slow process in contrast to the rapid fading of the colour of NP and most carbanion reaction solutions, a manifestation of adduct hydrolysis to an oxime and aquapentacyanoferrate(II) (Chapter 3). The proportions of reactants, pH and the presence of oxygen have been shown to affect studies of NP and thiolate adduct decomposition.<sup>3-5</sup>

Mulvey and Waters<sup>3</sup> have recorded the formation of a paramagnetic species following reaction of NP with several thiols, including cysteine. This paramagnetic species is associated with the reduction of NP and the formulation has been reported<sup>3,16,17</sup> by a number of workers to be  $[\text{Fe}(\text{CN})_5\text{NO}]^{3-}$ . Blesa *et al*<sup>4</sup> put forward a complex scheme for the reaction of NP and cysteine which includes regeneration of NP upon



(6)

oxidation of  $[\text{Fe}(\text{CN})_5\text{NO}]^{3-}$ .

A variety of products from the reactions of NP with thiols have been proposed; the disulphide of the thiol,<sup>4</sup> aquapentacyanoferrate(II) and its polymeric derivatives,<sup>3,5</sup> nitropentacyanoferrate(II),<sup>4</sup> as well as a variety of intermediate species.<sup>3-5</sup> With the exception of the disulphide of cysteine<sup>4</sup>, these products have been determined by spectrophotometry or epr spectroscopy; oxidation levels but not always exact formulae were assigned by these means.<sup>3</sup> With the additional use of carbon-13 nmr to monitor reaction solutions containing thiols and 90% carbon-13 labelled NP it is possible in this study to reassess the wide range of intermediates and products reported in the literature and put forward a comprehensive scheme for the reaction of NP with a wide range of thiols in alkaline solution which includes the paramagnetic intermediate  $[\text{Fe}(\text{CN})_4\text{NO}]^{3-}$  and the diamagnetic product  $[\text{Fe}(\text{CN})_6]^{4-}$ .

#### Identification of the primary product of nitroprusside reduction

As the reduction of nitroprusside will feature strongly in this Chapter, and Chapters 7 and 8, it is important to report recent and as yet unpublished work by Glidewell and Johnson<sup>18</sup> which elucidates the formula of the primary nitroprusside reaction product. The formulation  $[\text{Fe}(\text{CN})_5\text{NO}]^{3-}$  has been adopted<sup>3,16,17</sup> but an epr spectrum of 90% carbon-13 labelled nitroprusside has revealed<sup>18</sup> conclusive evidence for the formulation  $[\text{Fe}(\text{CN})_4\text{NO}]^{2-}$  (6). A three-line signal, ( $g = 2.024$ ,  $A(^{14}\text{N}) = 15.2 \text{ G}$ ), from coupling of the unpaired electron to the nitrosyl ligand nitrogen, is apparent in epr

spectra of solutions of NP of normal isotopic composition after one-electron reduction. When carbon-13 enriched nitroprusside was reduced each component of the standard three-line signal was split into a 1:4:6:4:1 quintet; clearly the unpaired electron was coupled to the one  $^{14}\text{N}$  of the nitrosyl ligand and only four  $^{13}\text{C}$  nuclei (of four labelled cyanide ligands). Theoretical studies by Johnson and Glidewell indicate that the observed  $^{14}\text{N}$  hyperfine coupling is consistent only with a square pyramidal ion with an essentially linear Fe-N-O group. The epr parameters reported for what has been determined to be  $[\text{Fe}(\text{CN})_4\text{NO}]^{2-}$  are identical to those in the literature assigned to  $[\text{Fe}(\text{CN})_5\text{NO}]^{3-}$ .

**Table 1 :** Visible absorbance maxima of some nitroprusside and thiol adducts<sup>a</sup>

RS <sup>-</sup>	absorbance maximum/ nm
HS	570
MeS	522
cysteine	522
N-acetylcysteine	522
β -methylcysteine	521
N-acetyl- β -methylcysteine	520
homocysteine	520
penicillamine	525
N-acetylpenicillamine	526
glutathione	520

a.  $[\text{Fe}(\text{CN})_5\text{N}(\text{O})\text{SR}]^{3-}$

## 6.2 RESULTS

(The work of sections 6.2.1, 6.2.2, and 6.2.3 C was done in collaboration with Ian Johnson, at the University of St. Andrews.)

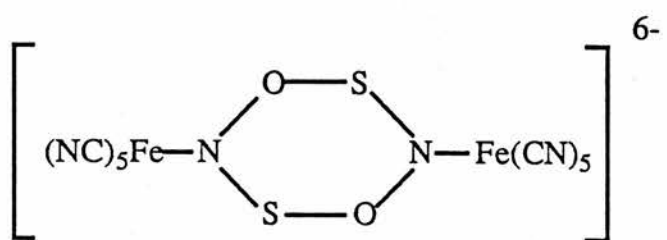
### 6.2.1 Reactions of nitroprusside with hydrogen sulphide and methyl sulphide ions

#### A. Adduct formation from nitroprusside and equimolar hydrogen sulphide or methyl sulphide ions

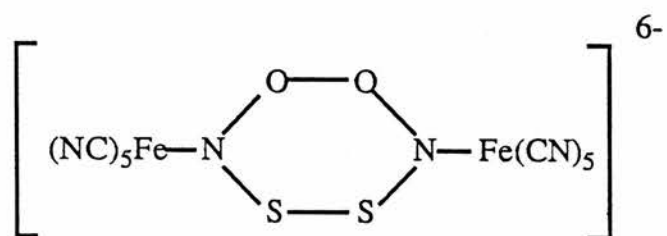
The absorbance maxima of the adducts of NP and  $\text{HS}^-$ ,  $\text{MeS}^-$  and a number of other thiols are listed in Table 1 and with the exception of the adduct of NP and  $\text{HS}^-$ , all the absorbance maxima fall within the range 520 - 526 nm. Although it is not clear why the visible spectrum of the NP and  $\text{HS}^-$  adduct ( $\lambda_{\text{max}}$  570 nm) is different, secondary ionisation of this adduct, not possible for any of the other NP and thiol adducts, cannot be disregarded. There is evidence that the NP and  $\text{HS}^-$  adduct exists as a dimer (7),<sup>19</sup> not the monomer corresponding to (5) as postulated by some workers.<sup>6</sup> The adduct of NP and  $\text{MeS}^-$ , on the basis of the similarity of its absorbance maxima with those of other NP and thiolate anion adducts, is assumed to resemble (5).

#### B. Intermediate species of the reaction of nitroprusside with equimolar hydrogen sulphide or methyl sulphide ions

Aliquots of a degassed solution of NP were added to closely equimolar solid NaSH or NaSMe and epr spectra of the resulting solutions were recorded. The characteristic three-line epr signal (Figure 1) attributed<sup>18</sup> to  $[\text{Fe}(\text{CN})_4\text{NO}]^{2-}$  and associated



or



(7)

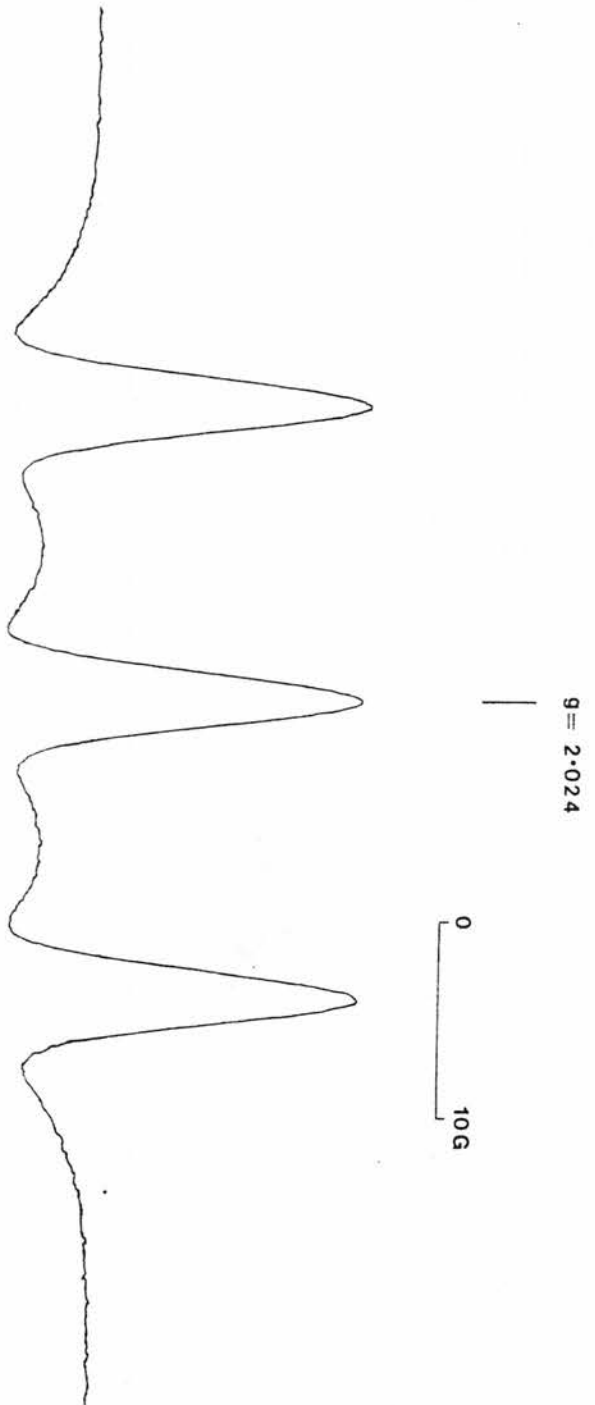
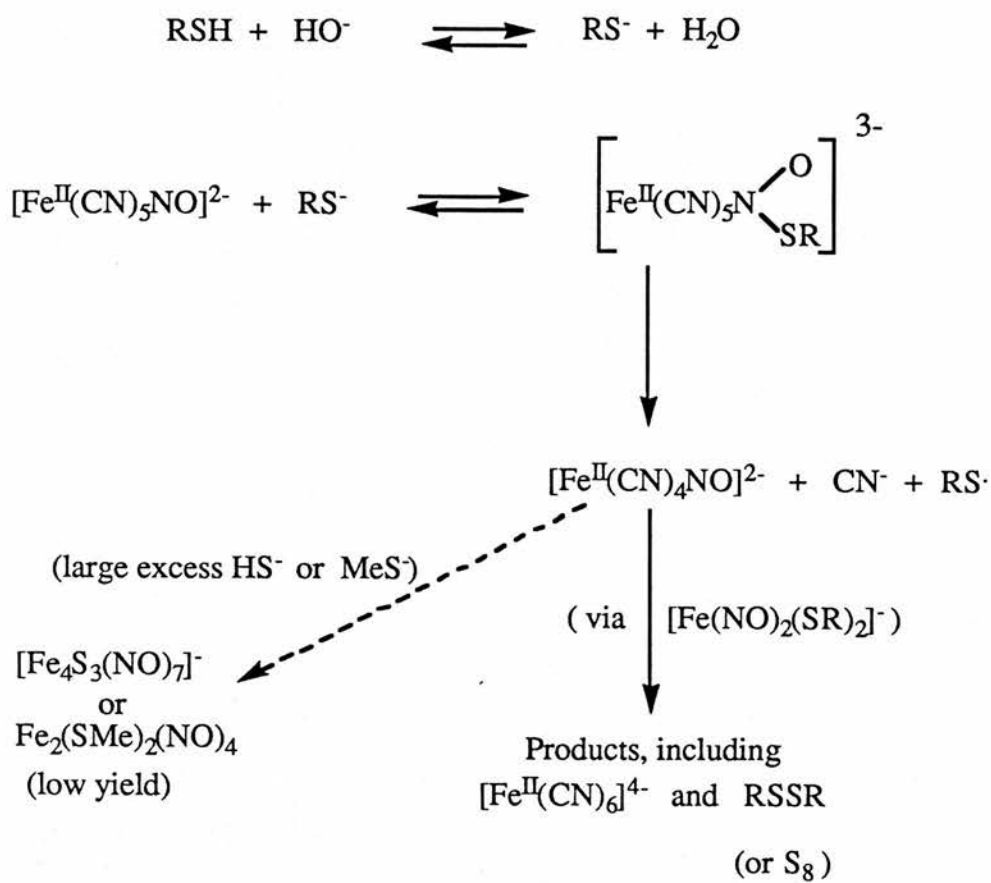


**Figure 1 :** The epr spectrum of [Fe(CN)<sub>4</sub>NO]<sup>2-</sup>

**Scheme 1:** Mechanism for the reaction of nitroprusside with hydrogen sulphide and methyl sulphide ions



with the reduction of NP, was apparent shortly after mixing both reaction solutions. The epr spectrum of the NP and HS<sup>-</sup> solution recorded 30 minutes after mixing contained a weak signal identical to that of [Fe(NO)<sub>2</sub>(SH)<sub>2</sub>]<sup>-</sup>, recorded independently. The significance of this species will be discussed below.

C. Products of the reaction of nitroprusside with equimolar hydrogen sulphide or methyl sulphide ions

In carbon-13 nmr spectra of the equimolar reaction solutions of NP and HS<sup>-</sup> or MeS<sup>-</sup>, the only signals apparent were single peaks at 177.9 p.p.m., which were assigned to hexacyanoferrate(II) on the basis of previously recorded spectra.<sup>20</sup> There is no evidence of unreacted NP (<sup>13</sup>CN<sub>eq</sub> 134.4, <sup>13</sup>CN<sub>ax</sub> 132.4 p.p.m.)<sup>21</sup> or hydrogen cyanide (recorded independently at 120 p.p.m.) in either spectrum. Elemental sulphur was isolated from the NP and HS<sup>-</sup> reaction solution and identified by mass spectrometry. Dimethyl disulphide (MeSSMe) is a volatile liquid and immiscible with water; there was no methyl signal in the NP and MeS<sup>-</sup> reaction solution nmr spectrum but an oily yellow layer was evident above the aqueous portion of the sample.

The above evidence substantiates a mechanism (Scheme 1), discussed in full later, for reduction of NP by equimolar HS<sup>-</sup> or MeS<sup>-</sup> leading to formation of [Fe(CN)<sub>6</sub>]<sup>4-</sup> via an adduct and [Fe(CN)<sub>4</sub>NO]<sup>3-</sup>.

6.2.2 The reactions of nitroprusside with an excess of hydrogen sulphide or methyl sulphide ion

The reaction of NP with an excess of HS<sup>-</sup> or MeS<sup>-</sup> gave

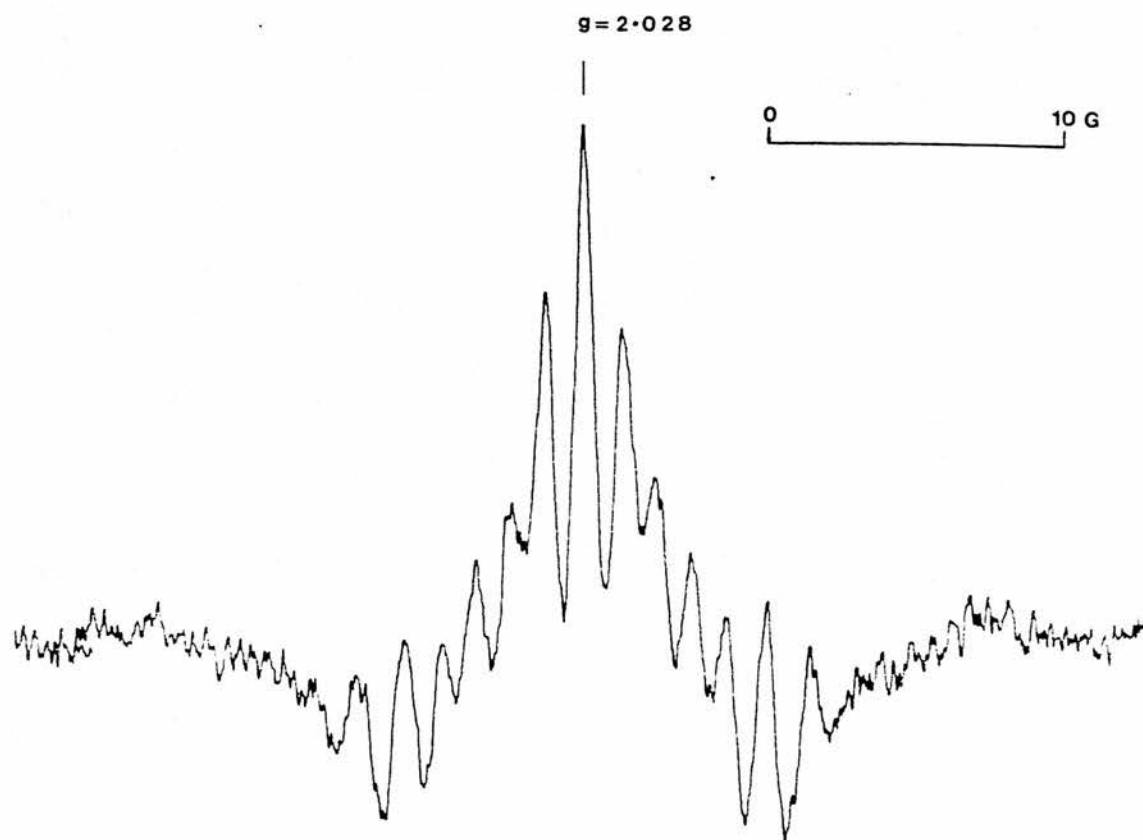


**Figure 2 :** The epr spectrum of  $[\text{Fe}(\text{NO})_2(\text{SMe})_2]^-$  from the reaction of nitroprusside with an excess of  $\text{MeS}^-$

rise to the distinctive vivid magenta associated with NP and thiolate anion adducts. However, one readily observable distinction between the reaction of NP with equimolar  $\text{HS}^-$  or  $\text{MeS}^-$  and the reaction of NP with an excess of  $\text{HS}^-$  or  $\text{MeS}^-$  was the increased rates of fading of the adducts for the latter reactions. From kinetic studies of the reaction of NP with an excess of  $\text{HS}^-$  Rock and Swinehart<sup>6</sup> have suggested that the adduct  $[\text{Fe}(\text{CN})_5\text{N}(\text{O})\text{SH}]^{3-}$  is converted to  $[\text{Fe}(\text{CN})_5\text{NOS}]^{4-}$  which decomposes to aquapentacyanoferrate(II) and  $[(\text{H}_2\text{O})\text{Fe}(\text{CN})_4\text{NOS}]^{3-}$ . In similar reaction conditions it was not possible to detect these cyanoferrate complexes; however, iron-sulphur complexes were isolated from solution, as discussed below.

The distinctive three-line signal of  $[\text{Fe}(\text{CN})_4\text{NO}]^{2-}$ , observed for the reaction of NP with equimolar  $\text{HS}^-$  or  $\text{MeS}^-$ , was also seen in epr spectra recorded shortly after mixing aliquots of degassed NP solutions with an excess of solid NaSMe or of NaSH. After many hours the signals of  $[\text{Fe}(\text{CN})_4\text{NO}]^{2-}$  from the reaction of NP with an excess of  $\text{HS}^-$  or  $\text{MeS}^-$  were completely replaced by signals for another species.

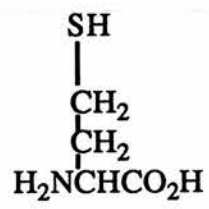
The new signal of the NP and  $\text{HS}^-$  reaction solution spectrum was identical to previously recorded spectra of  $[\text{Fe}(\text{NO})_2(\text{SH})_2]^-$ , also seen as a weak signal in the reaction of equimolar NP and  $\text{HS}^-$ . Similarly, the new signal of the NP and  $\text{MeS}^-$  reaction solution spectrum (Figure 2) was identical to previously recorded spectra of  $[\text{Fe}(\text{NO})_2(\text{SMe})_2]^-$ . The epr spectrum of  $[\text{Fe}(\text{NO})_2(\text{SR})_2]^-$  consists of a quintet,

due to coupling with the two  $^{14}\text{N}$  nuclei. The signal is split further by the magnetic coupling of the protons bonded to the C-S carbon of the alkyl R group, resulting in a more complicated signal as seen for  $[\text{Fe}(\text{NO})_2(\text{SMe})_2]^-$  (Figure 2). The significance of the formation of  $[\text{Fe}(\text{NO})_2(\text{SH})_2]^-$  and  $[\text{Fe}(\text{NO})_2(\text{SMe})_2]^-$  will be discussed later.

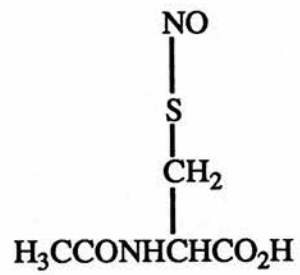
Preparative scale experiments were conducted with an approximately twenty fold excess of  $\text{HS}^-$  or  $\text{MeS}^-$  to NP and the organic soluble species were extracted after 15 hours of stirring under nitrogen. From the  $\text{HS}^-$  and NP reaction solution Roussin's black salt  $\text{Na}[\text{Fe}_4\text{S}_3(\text{NO})_7]$  was isolated in 26% yield with respect to NO. In a similar experiment, the methyl ester of Roussin's red salt  $[\text{Fe}_2(\text{SMe})_2(\text{NO})_4]$  was isolated in 7.2% yield with respect to NO from a solution of NP and excess  $\text{MeS}^-$ , leaving a small amount of Prussian Blue ( $\text{Fe}^{\text{III}}_4[\text{Fe}^{\text{II}}(\text{CN})_6]_3$ ) in the aqueous layer.

Roussin's black salt and the methyl ester of Roussin's red salt are commonly prepared from iron(II) salts, sodium sulphide and sodium nitrite, and by carbonyl-nitrosyl exchange of iron-sulphur carbonyl complexes.<sup>22,23</sup> The unlikely conversion of NP to Roussin's black salt was recorded by Roussin when he first prepared the salt last century and this procedure was recently reinvestigated by Glidewell and McGinnis.<sup>24</sup> It was found that Roussin's black salt could be isolated in 78% yield based on NO after boiling a solution of NP through which  $\text{H}_2\text{S}$  had been bubbled.

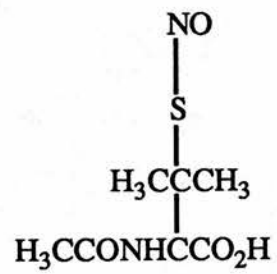
Although the conversion of NP to Roussin's black salt under the severe conditions of Roussin's original experiment



( 8 )



( 9 )



( 10 )

is remote from the conditions of medical administration of NP, the above evidence of conversion of NP to the methyl ester of Roussin's red salt, in addition to Roussin's black salt, by incubation with excess  $\text{MeS}^-$ , or  $\text{HS}^-$ , at room temperature represents the release of cyanide from NP in mild conditions. However, it will be shown in succeeding discussions that these reactions are exceptional and do not represent reactions of NP with thiols expected to occur in physiological conditions.

### 6.2.3 Reaction of nitroprusside with cysteine, penicillamine and related thiols

In contrast to the reactions of NP with all other thiols studied, including homocysteine (8), cysteine (2), N-acetylcysteine and  $\beta$ -methylcysteine (3), detectable formation of the magenta adduct of NP and penicillamine (1) or N-acetylpenicillamine required what seem to be excessively basic conditions. Additionally, it has not been possible to detect any recycling of the adducts of NP and penicillamine or N-acetylpenicillamine upon introduction of air into the reaction solutions. A similar result was recorded for the reaction of NP with the sterically hindered thiol  $\text{HSC}(\text{CH}_2\text{CH}_3)_3$ .\*

Another divergence in the reactivity of penicillamine and cysteine has been recorded upon incubation with glyceroltrinitrate (a hypotensive agent with similar action to NP) in the presence of guanylate cyclase.<sup>25</sup> Cysteine and several other thiols enhanced degradation (measured as NO release)

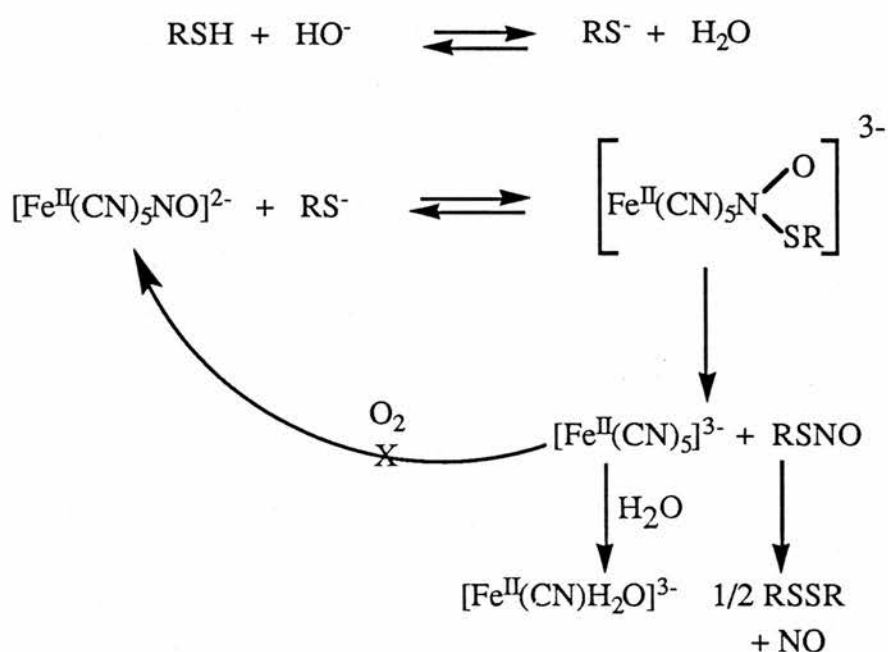
\* Kindly supplied by Sir Derek Barton

of glyceroltrinitrate in the presence of guanylate cyclase but penicillamine had no effect. However, Schröder *et al*<sup>25</sup> found little correlation of enzyme stimulation with trinitro-glycerol degradation, which they interpreted to represent formation of variably active S-nitrosothiols.

One explanation of the apparent anomaly in the reactivity of penicillamine towards NP is that a different mechanism than previously proposed (Scheme 1) is in operation. In a study of vascular smooth muscle relaxation by NP and related agents, Ignarro and co-workers<sup>10</sup> have reported that NP reacts with cysteine *via* production of the thionitrite of cysteine in ice cold, near neutral conditions (in which the stability of cysteine thionitrite is enhanced).<sup>26</sup> The intermediacy of S-nitrosothiols is of particular relevance to studies of the origin of the hypotensive action of nitroprusside; it is the nitrosyl moiety of NP that is thought<sup>12</sup> responsible for its physiological activity and several studies have shown that hypotension can be induced by thionitrites of N-acetylcysteine (9) and to a lesser degree, N-acetylpenicillamine (10).<sup>10,11,25,27,28</sup>

The thionitrite of N-acetylpenicillamine is known<sup>29</sup> to be unusually stable compared to the reactive thionitrite of N-acetylcysteine which decomposes rapidly in aqueous solution, and the formation of thionitrites following reaction of NP and thiols was consequently considered as a possible source of the apparently anomalous reactivity of N-acetylpenicillamine with NP. The exceptional stability of the thionitrite of N-acetylpenicillamine, as opposed to the reactivity of

**Scheme 2** : Mechanism for the reaction of nitroprusside with (N-acetyl)penicillamine including thionitrite formation<sup>a</sup>



- a. Adduct decomposition to a relatively stable thionitrite such as that of (N-acetyl)penicillamine, as shown in this scheme, is one possible explanation for no observation of the recycling reaction for reaction solutions of nitroprusside and (N-acetyl)penicillamine.

the thionitrite of N-acetylcysteine could account for failure to regenerate the adduct of NP and NAP reaction solution as in Scheme 2. Formation of thionitrites is not inconsistent with the reported isolation of disulphides following reaction of NP and some thiols; thionitrites decompose to disulphides with release of NO.<sup>26</sup> Moreover, the formation of thionitrites following reaction of NP and thiols suggests a parallel with the reaction of NP with most carbanions in which the nitrosyl ligand of NP is incorporated into the oxime of the carbon acid.

A. Consideration of the  $pK_a$  values for N-acetylcysteine, N-acetyl- $\beta$ -methylcysteine, N-acetylpenicillamine and glutathione

Above mention of what seemed to be excessively basic conditions for detectable formation of the NP and penicillamine or N-acetylpenicillamine adduct refers to the following observations. Whereas NP reacted noticeably with equimolar N-acetylcysteine at a pH of 7.6 it was not possible to discern reaction below pH 10 with N-acetylpenicillamine at the same concentration. In a temperature-jump study<sup>5</sup> of the formation of the adducts of NP and various thiolate anions poor relaxation effects for the NP and penicillamine system limited experiments to pH 11.2, in contrast to accurate results for N-acetylcysteine at pH 7.9 and cysteine at pH 8.75. As it has been established<sup>5</sup> that it is only the  $RS^-$  form of thiols that react with NP in these conditions, consideration of the  $pK_a$  values of cysteine and penicillamine is worthwhile.

**Table 2:** Some literature pKa values for cysteine, penicillamine, N-acetylcysteine and N-acetylpenicillamine

Cysteine	penicillamine	NAC	NAP	conditions	reference
8.15±.05	7.90±.05	9.52±.05	9.90±.05	I=0.3, 25°	a
8.65 <sup>1</sup> 9.95 <sup>2</sup>				I=0.15, 25°	b
8.20				I=0.1, 20°	c
8.38 <sup>1</sup> 9.74 <sup>2</sup>	8.05 <sup>3</sup> 9.70 <sup>4</sup>		10.19	I=0.3, 25°	d
		9.76±.02		I=0.1	e
8.54 <sup>1</sup> 10.21 <sup>2</sup>				I=0.08, 25°	f
	8.17 <sup>3</sup> 10.33 <sup>4</sup>			I=0.1, 20°	g
		9.3		I=0.4, 25°	h

1. (2A) 2. (2B) 3. (1A) 4. (1B)

NAC = N-acetylcysteine

NAP = N-acetylpenicillamine

a. Ref. 30

b. NC Li, RA Manning, J. Am. Chem. Soc., 1955, **77**, 5225.

c. JP Danehy, CJ Noel, J. Am. Chem. Soc., 1960, **82**, 2511.

d. Ref. 31

e. Ref. 32

f. E Coates, CG Marsden, B Rigg, Trans. Fara. Soc., 1969, **65**, 3032.

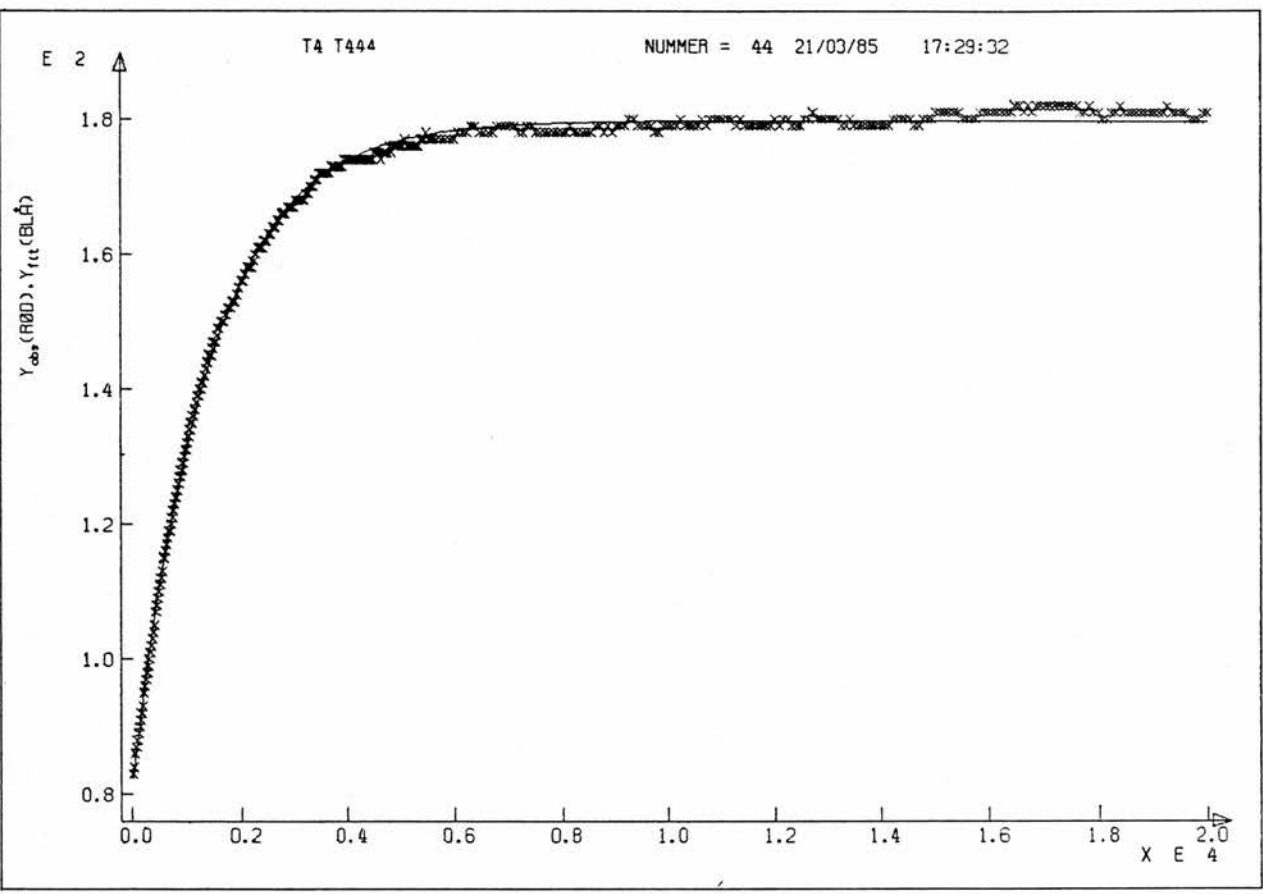
g. DA Doornbos, MT Feitsma, Pharm. Weekbl., 1967, **102**, 587.  
(Chem. Abstr. 1968, **68**, 63246j).

h. Ref. 5

A survey of literature cysteine and penicillamine  $pK_a$  values (Table 2) reveals significant variation in the values for each thiol:  $pK_a$  determination of amino-thiols is complicated by deprotonation of the thiol and ammonium groups over similar pH ranges. The literature  $pK_a$  values for the N-acetylated derivatives of penicillamine and cysteine, for which  $pK_a$  determination is simplified, are also listed in Table 2; the two N-acetylpenicillamine values (9.90,<sup>30</sup> 10.19<sup>31</sup>) are 0.4  $pK_a$  units apart but are both higher than the three listed values for N-acetylcysteine (9.52,<sup>30</sup> 9.76,<sup>32</sup> 9.3<sup>5</sup>). On the basis of these values it is concluded that the pH required to ionise the thiol group of N-acetylpenicillamine (NAP) is slightly higher than that required for ionisation of the thiol group of N-acetylcysteine (NAC). The difference in  $pK_a$  can be understood in terms of the enhanced electron density at the thiol function of NAP contributed by the adjacent methyl groups that will slightly destabilise the corresponding thiolate anion relative to that of NAC.

The thiol  $pK_a$  of glutathione (GSH) has been recorded<sup>30</sup> as 8.56, and from the reactivity of  $\beta$ -methylcysteine and its N-acetylated derivative (NAZ) with NP there is no reason to suspect the thiol  $pK_a$  value of NAZ does not fall within the range considered for NAC and NAP. The  $pK_a$  of homocysteine has been determined to be 8.66 at 25 °C (I = 0.3 M).<sup>31</sup>

**Figure 3 :** Plot of change in absorbance vs. time (milliseconds) for the reaction of nitroprusside with homocysteine, superimposed on a first-order curve



B. Reactions of nitroprusside with several thiols including N-acetylcysteine and N-acetylpenicillamine in the presence of air

Temperature-jump kinetic studies

(The work of this section was conducted with the assistance of Dr. P. Sorensen during a visit to the Technical University of Denmark.)

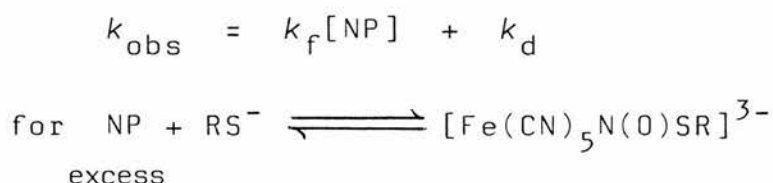
The observed rate constants for the formation of the adducts of NP and N-acetylcysteine, homocysteine (8), penicillamine and N-acetylpenicillamine were determined by the temperature-jump technique, a means of studying reactions too fast for stopped-flow spectroscopy or other methods for which rate measurements are limited by mixing times. With the temperature-jump technique it is not the initial rapidly established equilibrium that is studied but the return to equilibrium following the perturbing effect of an increase in temperature.

For the kinetic studies, concentrations of NP were in excess and the temperature jump was made immediately upon mixing, before subsequent fading reactions disrupted the equilibrium. In these conditions the reactions were shown to be first-order (Figure 3) although the accuracy of the results was restricted by the limited life of the adduct. It was found that the observed first order rate constant  $k_{obs}$  could be determined for the adducts of NP and N-acetylcysteine and homocysteine at a pH of 10.5, but a pH of 11.2 was required to make the same determination for the adducts of NP and penicillamine or N-acetylpenicillamine.

**Table 3 :** Some values of  $k_{\text{obs}}$  for the reaction of nitroprusside with N-acetylpenicillamine, penicillamine and homocysteine

thiol	[nitroprusside]/mM	$10^{-3} k_{\text{obs}}/\text{s}^{-1}$
N-acetylpenicillamine	100	4.3
	80	3.9
	60	3.6
penicillamine	80	5.1
	40	4.5
homocysteine	100	3.8
	80	4.2
	40	4.6

The observed rate constants for the reaction of NP with the studied thiols were found to be remarkably similar (Table 3) considering the accuracy of the results and plots of the observed rate constants against the concentration of NP were shallow, with large intercepts. This restricted further treatment of the kinetic data but does suggest that the back reaction contributes significantly to the equilibrium between the adduct and reactants (equation 2). The results obtained from these experiments are in agreement with

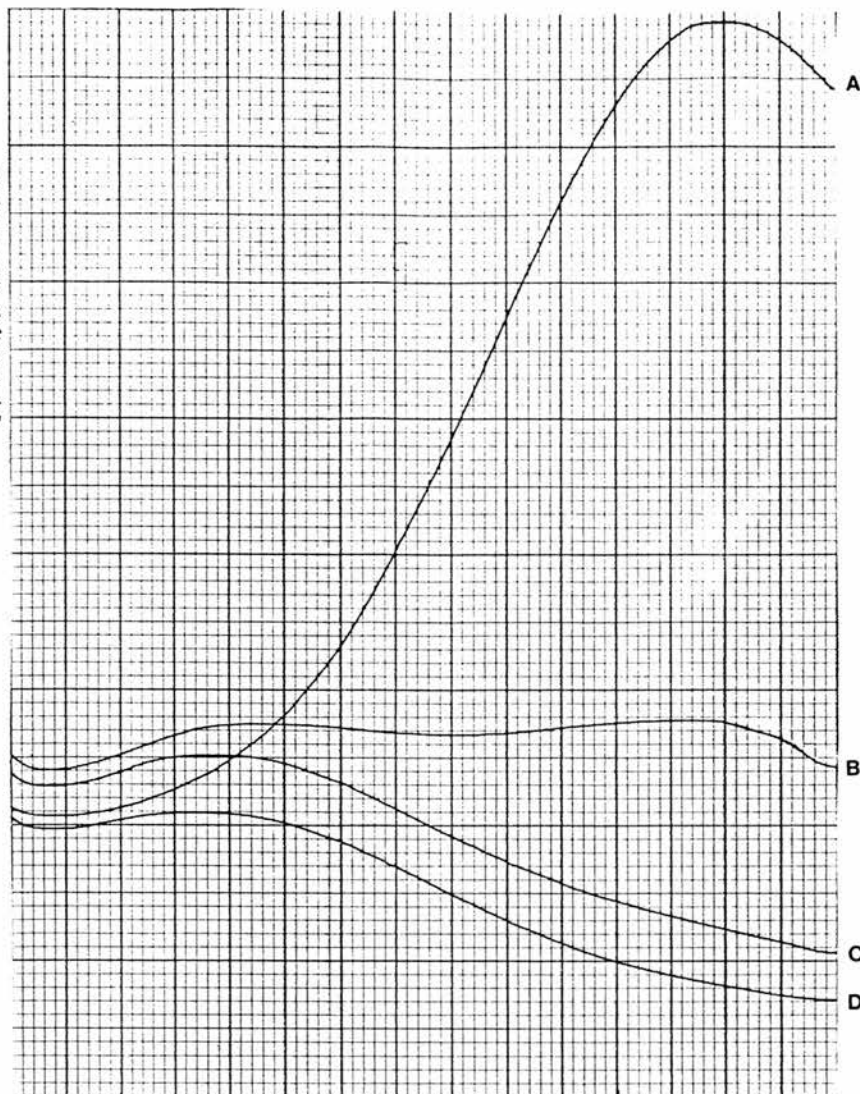


(equation 2)

the more extensive studies with a stopped-flow/temperature-jump combination by Johnson and Wilkins<sup>5</sup> who report a narrow range of rate constants for the formation of the adducts of NP and N-acetylcysteine, cysteine, glutathione and mercaptoethanol. They were additionally able to discern a slightly lower rate of formation for the NP and penicillamine adduct.

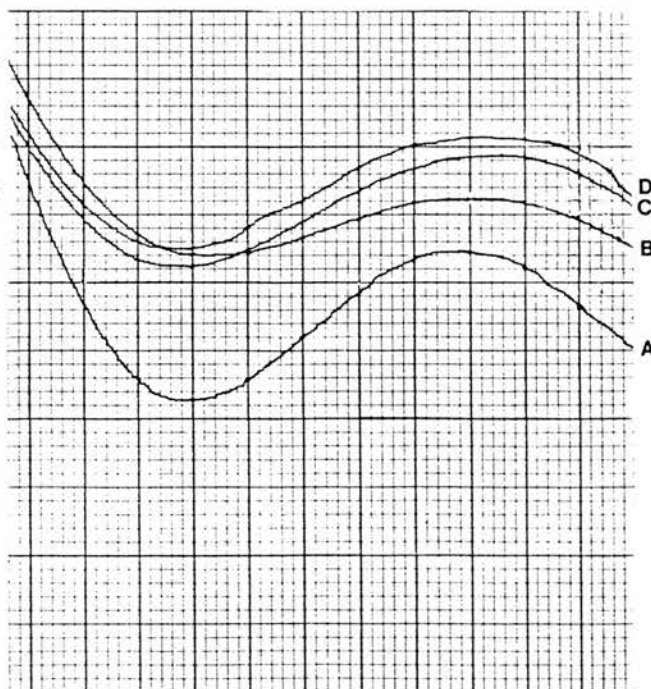
Albumin (from bovine serum) is known to bind both cations and anions thereby reducing the efficacy of some therapeutic agents infused into the blood stream. There was no significant change in the rate of NP and thiolate anion adduct formation upon addition of albumin (up to 0.4 mM) to some solutions, consistent with studies showing only weak binding of NP to albumin,<sup>33</sup> which may contribute to the high potency of NP as a hypotensive agent. Similarly, the observed rate

**Figure 4 :** Fading of buffered (pH 10.45) reaction solution of nitroprusside (0.05 M) and N-acetylcysteine (0.05 M) in the presence of air (spectra were recorded after 15-fold dilution of reaction solutions at timed intervals, absorbance setting 2.0 )



- A. immediately after mixing,  
T=0
- B. T=2 minutes
- C. T=4 minutes
- D. T=16 minutes

**Figure 5 :** Fading of buffered (pH 10.45) reaction solution of nitroprusside (0.05 M) and N-acetylpenicillamine (0.05 M) in the presence of air (spectra were recorded after 15-fold dilution of reaction solutions at timed intervals, absorbance setting 0.2 )



- A. immediately after mixing,  
T=0
- B. T=2 minutes
- C. T=4 minutes
- D. T=8 minutes

constant for the reaction of NP with several thiols was apparently unaffected by addition of DMSO (up to 0.5 M), a co-ordinating solvent.

#### Fading reactions

While measurements of the rate of formation of NP and thiol adducts require relaxation methods, the rate of fading can be monitored on a recording spectrophotometer. The fading reactions of NP and (equimolar) N-acetylcysteine (NAC) or N-acetylpenicillamine (NAP) in buffered solutions (pH 10.45) are shown in Figures 4 and 5, respectively. For the NAP reaction solution the absorbance due to the adduct increased within the first five minutes after mixing and faded slowly thereafter. In contrast, in exactly the same conditions the absorbance of the NAC adduct was ten times more intense and began to fade immediately after mixing. It is clear that the fading reaction of NAC is far more rapid than that of NAP and it also appears that at a pH of 10.45, the NAC reaction proceeds to a far greater extent than that of NAP, judging by the relative intensities of the absorbances due to the adducts (assuming similar extinction coefficients).

Small scale experiments under the same conditions indicated that the magenta colour associated with the NAC adduct could be regenerated at a noticeably diminished intensity upon introduction of air into the system but this recycling reaction could not be demonstrated for the NAP system.

The thionitrites of both NAC and NAP have distinctive spectra in the visual region<sup>26</sup> but there is no evidence of

these species in either Figures 5 or 6, or in a separate study of NAC and NAP reaction solutions (not shown). This result does not necessarily conflict with the results obtained by Ignarro *et al*;<sup>10</sup> although the only method used to identify the thionitrite was the absorbance at 550 nm, their work was conducted at lower pH and temperature at which thionitrites are more stable.<sup>26</sup>

#### Carbon-13 nmr spectra

Carbon-13 spectra of equimolar 90% carbon-13 labelled SNP and N-acetylcysteine (NAC) or N-acetylpenicillamine (NAP) in phosphate buffer, pH 11.2, were recorded at high field at designated time intervals (Figures 6a-e and 7a-d respectively). The only signals apparent in these spectra recorded within five minutes of mixing to six hours after mixing, were those of unreacted NP ( $^{13}\text{C}_{\text{eq}}$  134.4 p.p.m.) and hexacyanoferrate(II). It is significant that there were no signals for  $[\text{Fe}^{\text{II}}(\text{CN})_5\text{NO}_2]^{4-}$ ,  $[\text{Fe}^{\text{II}}(\text{CN})_5\text{H}_2\text{O}]^{3-}$ , the adduct  $[\text{Fe}^{\text{II}}(\text{CN})_5\text{N}(\text{O})\text{SR}]^{4-}$  or hydrogen cyanide apparent in any of these spectra.

The magenta colour of the NAC and NAP solutions had faded noticeably one hour after mixing, although the NAC solution was originally, and for several hours remained, more intensely coloured than the NAP solution. At this time both solutions were shaken vigorously to introduce air and the light magenta of the NAC solution intensified, though to a hue considerably less intense than seen originally. There was no apparent change in the colour of the NAP solution. The signal to noise ratio of the spectrum recorded within five minutes of shaking the NAC solution (Figure 6c) was significantly greater than

**Figure 6 :** Carbon-13 nmr spectra of a reaction solution of 90% carbon-13 labelled nitroprusside and N-acetylcysteine in the presence of air

spectrum (e)

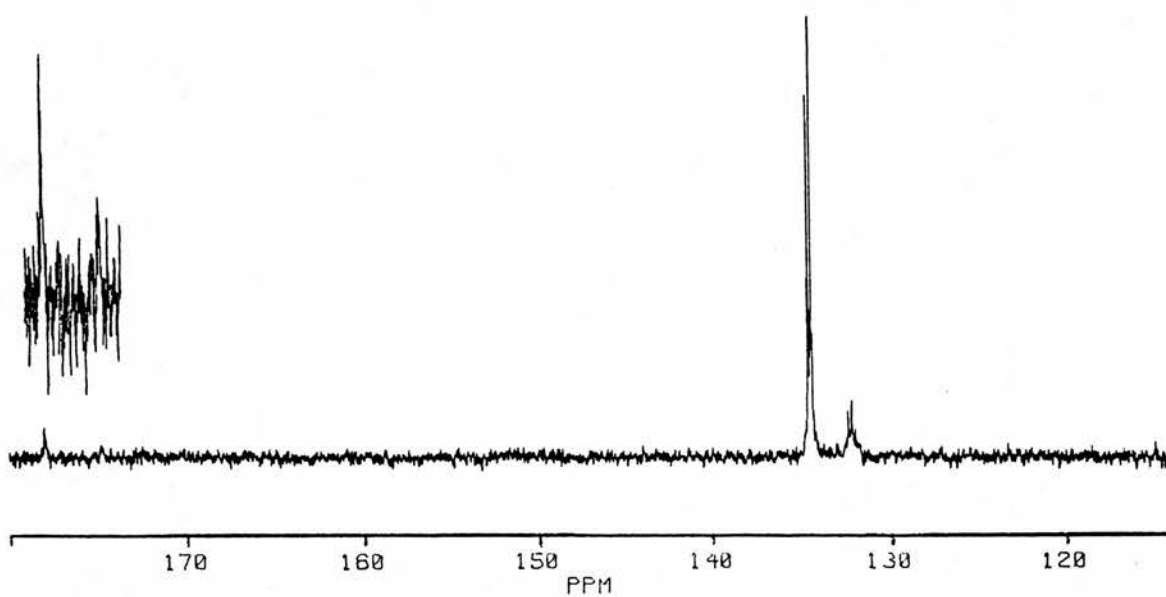


Figure 6 : Carbon-13 nmr spectra of a reaction solution of 90% carbon-13 labelled nitroprusside and N-acetylcysteine in the presence of air

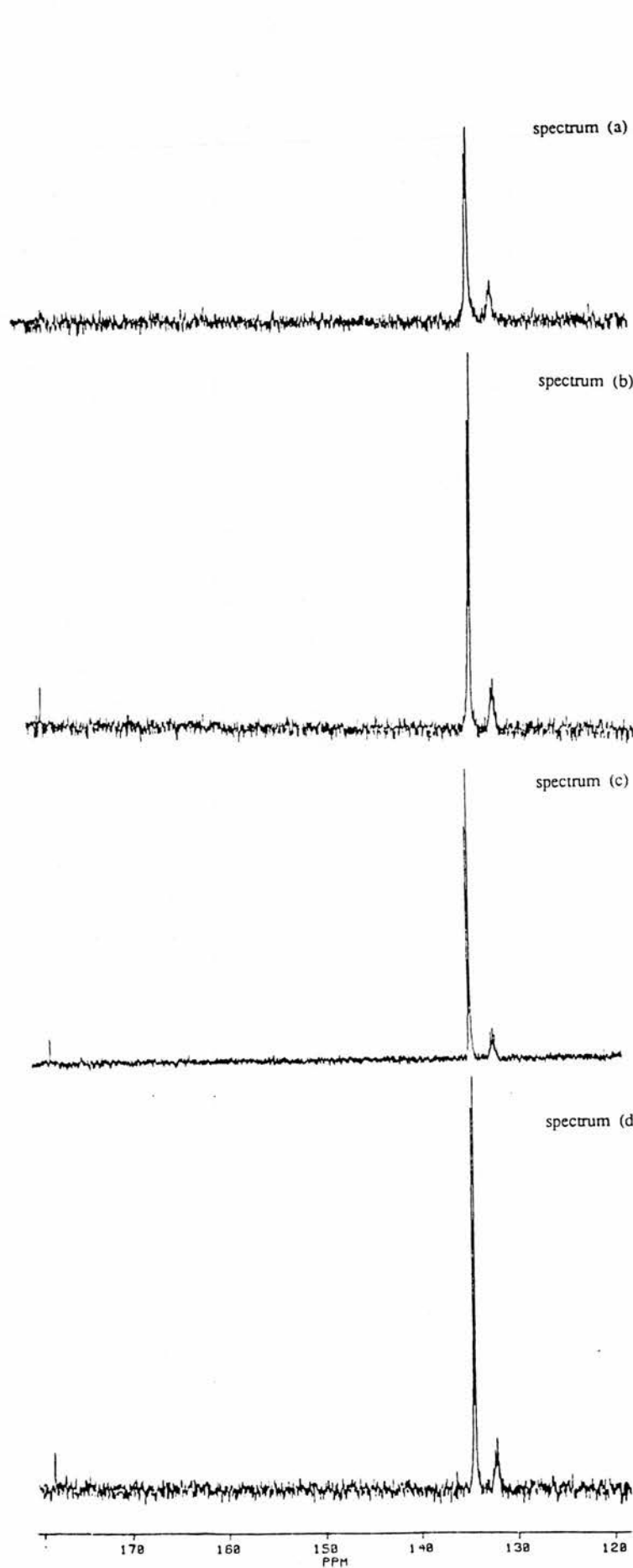
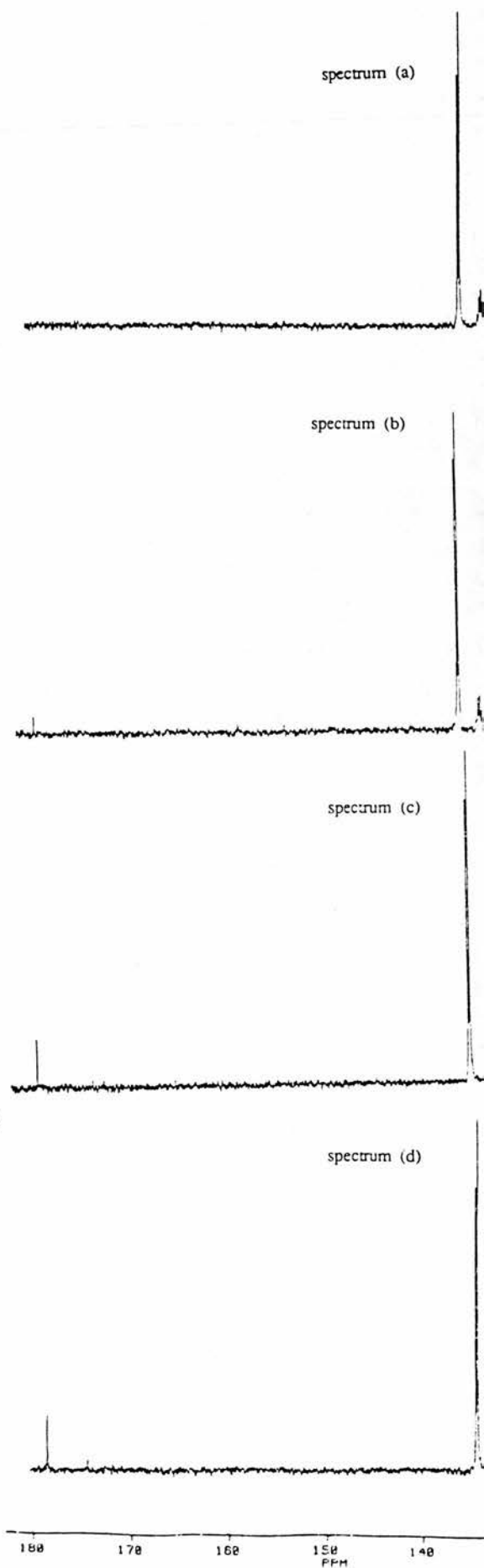


Figure 7 : Carbon-13 nmr spectra of a reaction solution of 90% carbon-13 labelled nitroprusside and N-acetylpenicillamin in the presence of air



for the previous two NAC spectra (Figures 6a and 6b) which were rather noisy compared to the corresponding NAP solutions (Figures 7a and 7b). However, the signal to noise ratio of the NAC spectrum recorded four hours after mixing (Figure 6d) was again significantly lower than for the corresponding NAP spectrum (Figure 7c). In the final NAC spectrum (Figure 6e) recorded six hours after mixing, the signal to noise ratio was similar to the corresponding NAP spectrum (Figure 7d).

For the spectra recorded up to four hours after mixing, (Figures 6a-c, 7a and 7b) the signal for hexacyanoferrate(II) was more intense for the NAC solutions than for the corresponding NAP solutions. However, spectra recorded after this time (Figures 6d, 6e, 7c and 7d) indicated the opposite.

To summarise, there are several significant differences in the reaction solution spectra of NP and NAC or NAP (Figures 6a-e and 7a-d respectively). The signal to noise ratios of NAC solutions were lower than for the corresponding NAP solutions, except many hours after mixing (Figure 6e) and shortly after saturating the solution with air (Figure 6c). The signal of hexacyanoferrate(II) was greater in the spectra of NAC reaction solutions up to 4 hours after mixing, after which time there was more hexacyanoferrate(II) apparent in the spectra of NAP reaction solutions. The significance of these observations will be discussed later.

#### Spin-echo proton nmr experiments

(These experiments were conducted by Dr. John Reglinski at the University of Strathclyde, Glasgow.)

In a series of spin-echo  $^1\text{H}$  nmr experiments, glutathione

was titrated against NP in aerobic conditions and the reaction stoichiometries NP : glutathione were found to range from 1:2 to 1:3. This result demonstrates that NP can act as a catalyst for oxidation of thiols in the presence of air. The application of the spin-echo nmr technique to the study of the reaction of NP with intracellular glutathione of intact erythrocytes will be discussed in Chapter 7.

C. Reactions of nitroprusside with several thiols, including N-acetylcysteine and N-acetylpenicillamine in the absence of air

EPR Spectra

The epr spectra of N-acetylcysteine (NAC), N-acetyl- $\beta$ -methylcysteine (NAZ), or N-acetylpenicillamine (NAP) and approximately equimolar NP in phosphate buffer (pH 11.2) were recorded after mixing the separately degassed solutions. After 45 minutes, the characteristic three-line signal of  $[\text{Fe}(\text{CN})_4\text{NO}]^{2-}$  (Figure 1) could be discerned in all three reaction solution spectra. The relative intensities of the signals were of approximately the same order of magnitude initially but slowly *increased* over a period of several hours. The time dependence of the  $[\text{Fe}(\text{CN})_4\text{NO}]^{2-}$  signal, which has been observed to *decrease* in intensity within several hours of formation by dithionite reduction, suggests that the longevity of the signal for the NP and thiol reaction solutions results from slow decomposition of the NP and thiol adduct. The epr spectrum of glutathione and NP, in which the signal for  $[\text{Fe}(\text{CN})_4\text{NO}]^{3-}$  was also apparent, was recorded in a separate series of experiments at pH 7.6.

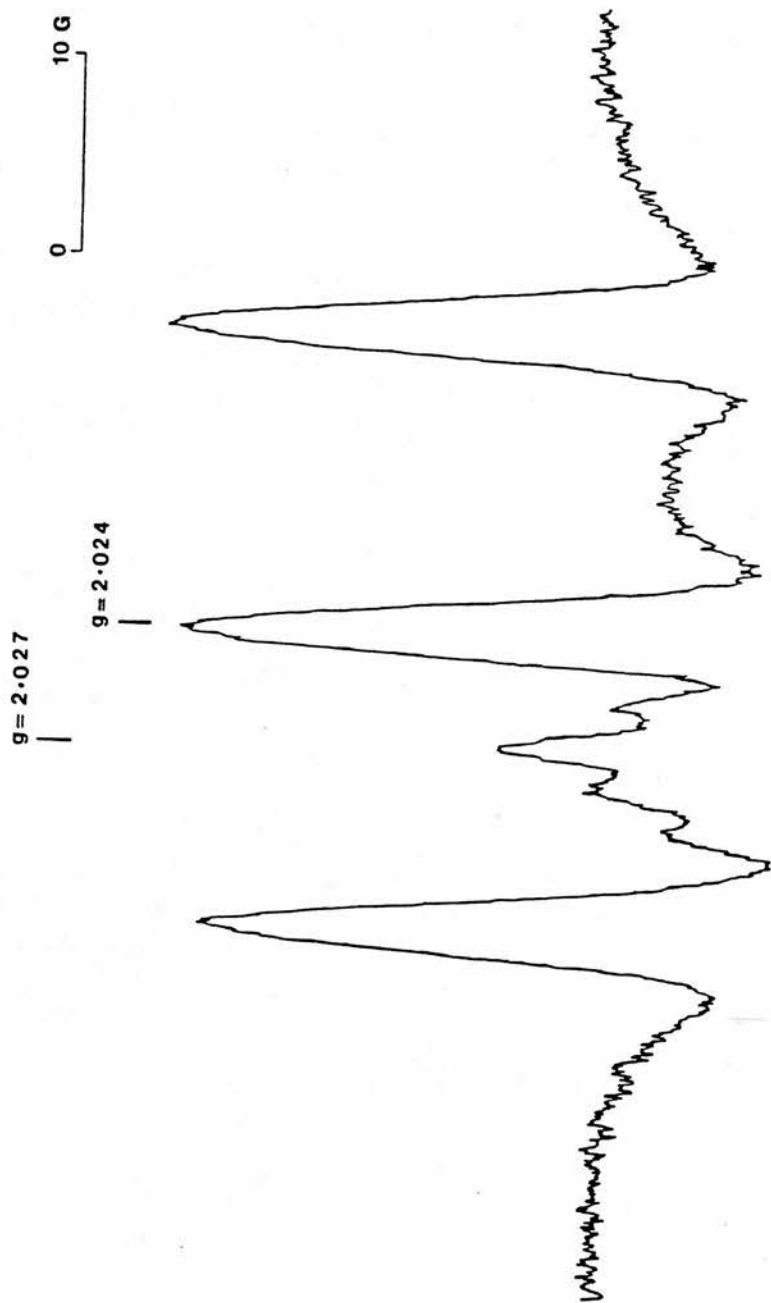


**Figure 8 :** The epr spectrum of  $[\text{Fe}(\text{CN})_4\text{NO}]^{2-}$  and  $[\text{Fe}(\text{NO})_2(\text{SR})_2]^-$  ( $\text{R} = \text{N-acetylcysteine, N-acetyl-}\beta\text{-methylcysteine, and N-acetylpenicillamine}$ ) from reaction of nitroprusside with equimolar thiol

**Table 4 :** Epr data for  $[\text{Fe}(\text{NO})_2(\text{SR})_2]^-$

$\text{RS}^-$	$g^{\text{a}}$	$g^{\text{b}}$
HS	2.028	2.027
MeS	2.028	2.027
PHCH <sub>2</sub> S	2.027	-
N-acetylcysteine		2.027
N-acetyl- $\beta$ -methylcysteine		2.027
N-acetylpenicillamine		2.027

a. Reference 23

b. This study

In the spectra of the NAC, NAZ, and NAP reaction solutions recorded after several hours, additional weak signals were observed within the three-line signals for  $[\text{Fe}(\text{CN})_4\text{NO}]^{2-}$  (Figure 8). Similar signals observed following the reaction of NP with  $\text{HS}^-$  and  $\text{MeS}^-$  corresponded to signals for  $[\text{Fe}(\text{SR})_2(\text{NO})_2]^-$  ( $\text{R} = \text{H}, \text{Me}$ ), recorded independently. Although the analogous species  $[\text{Fe}(\text{SR})_2(\text{NO})_2]^-$  ( $\text{R} = \text{NAC}, \text{NAZ}, \text{NAP}$ ) have apparently not been observed before, the epr parameters, apart from proton coupling which has not been resolved in these spectra, should be similar (Table 4) to  $[\text{Fe}(\text{SR})_2(\text{NO})_2]^-$  ( $\text{R} = \text{H}, \text{Me}$ ).

From these spectra it is clear that NAC, NAZ, and NAP all react with NP at pH 11.2 to form  $[\text{Fe}(\text{CN})_4\text{NO}]^{2-}$ . Furthermore, weak signals assigned to the species  $[\text{Fe}(\text{SR})_2(\text{NO})_2]^-$  ( $\text{R} = \text{NAC}, \text{NAZ}, \text{NAP}$ ) were apparent in epr spectra of all three reaction solutions several hours after mixing. The significance of these results will be discussed below.

#### Carbon-13 nmr spectra

Carbon-13 nmr of solutions of equimolar NP and glutathione, cysteine, N-acetylcysteine (NAC),  $\beta$ -methylcysteine, penicillamine or N-acetylpenicillamine (NAP) were recorded at low field immediately after mixing the separately degassed solutions by means of evacuated connecting glassware. The spectrum recorded several hours after mixing exactly equimolar NP and glutathione (pH  $\sim 7$ ) indicated complete conversion to hexacyanoferrate(II) ( $[\text{Fe}(\text{CN})_6]^{4-}$ ) and the disulphide of glutathione. Similarly, complete conversion to hexacyanoferrate(II) and the disulphide was apparent in the spectrum

recorded several hours after mixing NP with exactly equimolar  $\beta$ -methylcysteine or NAC at a pH of approximately 10.

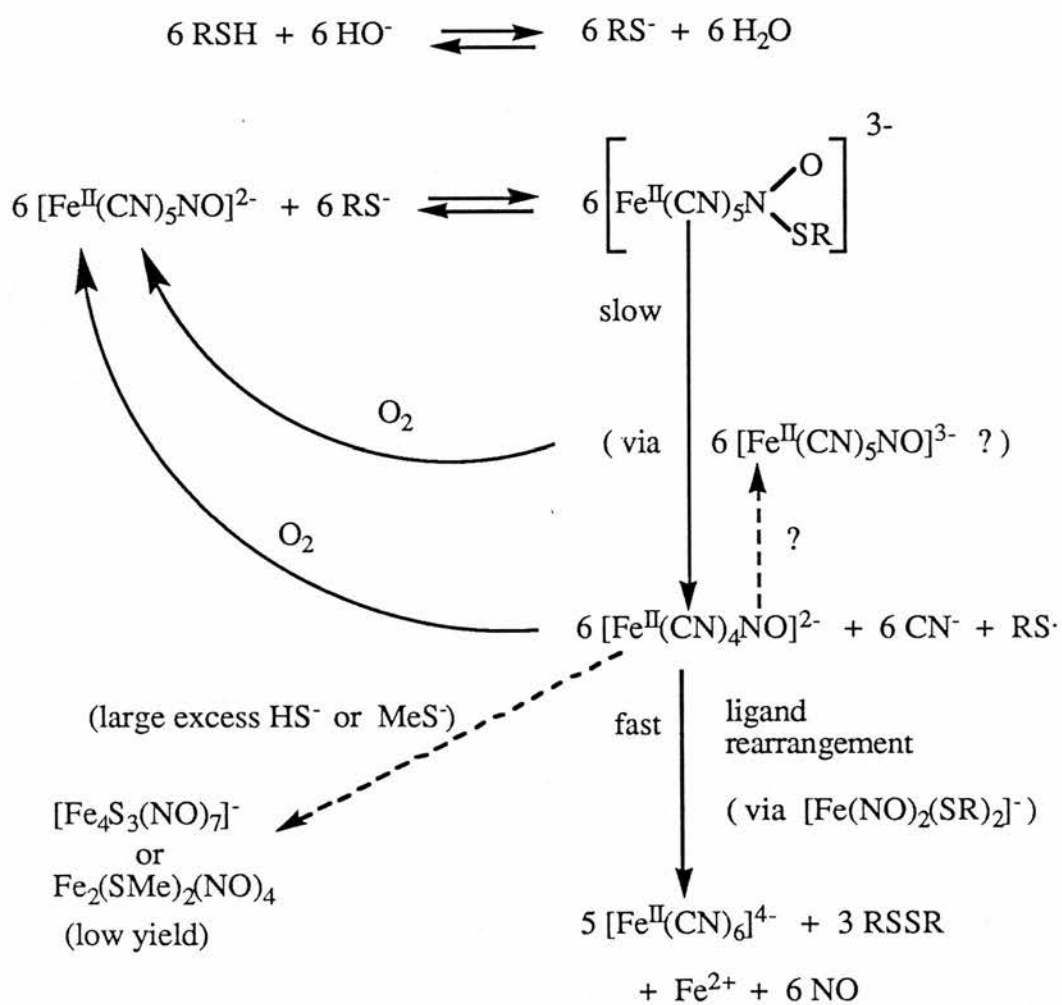
In contrast, there was no detectable conversion of NP and equimolar NAP to  $[\text{Fe}^{\text{II}}(\text{CN})_6]^{4-}$  and N-acetylpenicillamine disulphide at pH 10; the only signals in the spectrum corresponded to NP and NAP. The spectrum of a solution of NP and equimolar penicillamine, pH approximately 11, showed incomplete conversion to  $[\text{Fe}^{\text{II}}(\text{CN})_6]^{4-}$  and penicillamine disulphide; signals for unreacted penicillamine and NP were also apparent. Complete conversion to  $[\text{Fe}^{\text{II}}(\text{CN})_6]^{4-}$  and N-acetylpenicillamine disulphide was apparent in the spectrum of a solution of equimolar NP and NAP at a pH of greater than 11.

It is apparent from the above experiments that the only (diamagnetic) products of reactions of NP with NAC,  $\beta$ -methylcysteine, penicillamine or NAP were hexacyanoferrate(II) and the corresponding disulphide. The higher pH required to observe complete conversion of NP and the thiol to hexacyanoferrate(II) and the corresponding disulphide is the only difference observed between the reactions of NAC,  $\beta$ -methylcysteine and the sterically hindered thiols penicillamine and NAP. Significantly, there was no evidence of the formation of the thionitrite of NAP in the spectra of NP and NAP reaction solutions. By analogy with the NAC thionitrite, for which the chemical shift of the C-S carbon is distinctive,<sup>34</sup> the NAP thionitrite is expected to have a distinctive carbon-13 nmr spectrum. The thionitrite of NAC was not apparent in reaction solution spectra of NP and NAC, but it is known that decomposition to the disulphide is rapid at elevated pH.<sup>20</sup>

Infra-red spectra

Following the same procedure used to obtain the carbon-13 nmr spectrum of NP and thiols in the absence of air, equimolar buffered (pH ~7) solutions of NP and glutathione were degassed separately and then mixed *via* evacuated connecting glassware. As the colour due to the adduct faded, evolution of gas from the reaction solution was noted. The gas was collected in an evacuated gas infra-red cell and the spectrum recorded immediately after contained the characteristic absorption of NO (Q branch at  $1875\text{ cm}^{-1}$ )<sup>35a</sup> and no trace of HCN.<sup>35b</sup>

**Scheme 3** : Mechanism for the reaction of nitroprusside with thiols, including (N-acetyl)cysteine and (N-acetyl)penicillamine, in alkaline solution



### 6.3 DISCUSSION

A comprehensive mechanism for the reaction of equimolar NP with N-acetylcysteine and related thiols, including penicillamine and N-acetylpenicillamine of apparently anomalous reactivity, in buffered solution is proposed (Scheme 3). This scheme accounts for the observations summarised below and, in general, is not inconsistent with previously proposed,<sup>3-5</sup> but incomplete, schemes for the reactions of NP with thiols.

#### Adduct formation

Intense magenta species are rapidly formed upon reaction of NP with thiols and the reaction of NP with the thiolate anions of this study, but not  $\text{HS}^-$ , for which secondary ionisation is possible, led to similar species (Table 1). Consequently, the structure of these species is presumed to be similar to that of the NP and cysteine adduct (5), regardless of the nature of group R.

Temperature-jump kinetic studies showed that the observed rate constants for the formation of the adducts of NP and N-acetylcysteine, homocysteine, penicillamine and N-acetylpenicillamine fall within a remarkably narrow range, even in the presence of albumin (0.4 mM) or DMSO (0.5 M). These results are consistent with a more extensive investigation by Johnson and Wilkins<sup>5</sup> who additionally note that the rate formation constant for the NP and penicillamine adduct is slightly lower than for the values for some other NP and thiol adducts. Johnson and Wilkins suggest that the

steric hindrance of the two methyl groups adjacent to the C-S<sup>-</sup> bond of penicillamine is a factor in the deceleration of the formation rate constant.

#### Formation of the paramagnetic species $[\text{Fe}(\text{CN})_4\text{NO}]^{2-}$

The characteristic three line signal of  $[\text{Fe}(\text{CN})_4\text{NO}]^{2-}$  was seen in the epr spectra recorded following reaction of NP with HS<sup>-</sup> and other thiols of this study, including N-acetylcysteine, N-acetyl- $\beta$ -methylcysteine and N-acetylpenicillamine. The formation of  $[\text{Fe}(\text{CN})_4\text{NO}]^{2-}$  is associated with reduction of NP; the same species has been recorded following electrolytic reduction of NP as well as reduction by dithionite and sodium borohydride.<sup>3</sup>  $[\text{Fe}(\text{CN})_4\text{NO}]^{2-}$  also represents the conversion of NP to a kinetically labile cyanoferrate complex of which the appearance of signals for  $[\text{Fe}(\text{NO})_2(\text{SR})_2]^-$  (R = H, Me, NAC, NAZ, and NAP) is one manifestation. The formation of  $[\text{Fe}(\text{NO})_2(\text{SR})_2]^-$  (R = H, Me, NAC, NAZ, and NAP) is consistent with the conversion of  $[\text{Fe}(\text{CN})_4\text{NO}]^{2-}$  to  $[\text{Fe}(\text{CN})_6]^{4-}$ , discussed in further detail below.

#### Recycling reaction

The magenta colour characteristic of the adducts of NP and thiols can be regenerated, though only to a limited extent, by addition of air to faded reaction solutions of NP and mercaptoethanol, cysteine, N-acetylcysteine, 2-methylcysteine, N-acetyl- $\beta$ -methylcysteine, or glutathione. This observation is termed the 'recycling' reaction and is attributed to oxidation of the products of adduct

decomposition to NP, which reacts with further thiol to form more (magenta) adduct. This recycling reaction has never been observed for the sterically hindered thiols penicillamine, N-acetylpenicillamine, and  $\text{HSC}(\text{CH}_2\text{CH}_3)_3$ .

From the available evidence it is not possible to discern which (if not both) of the oxidation pathways illustrated in Scheme 3 operate. Oxidation of  $[\text{Fe}(\text{CN})_4\text{NO}]^{2-}$  would give rise to  $[\text{Fe}(\text{CN})_4\text{NO}]^-$  which could rapidly recombine with  $\text{CN}^-$  to form NP, a process favoured by the very high formation constant of cyanoferrate complexes such as NP.<sup>36</sup> Alternatively, although there was no indication of formation of the paramagnetic species  $[\text{Fe}(\text{CN})_5\text{NO}]^{3-}$  in epr spectra recorded after reduction of 90% carbon-13 labelled NP,<sup>18</sup> it is possible that this species is at a very low steady state concentration. Oxidation of  $[\text{Fe}(\text{CN})_5\text{NO}]^{3-}$  would yield NP directly.

In the presence of air, the recycling reaction is significant; nitroprusside to glutathione reaction stoichiometries of 1:2 and 1:3 were obtained by proton nmr titration in the presence of air. Similarly, one mole of NP has been reported<sup>5</sup> to react with up to ten moles of cysteine by repeated addition of cysteine to NP in mildly alkaline solution. In these conditions, NP is a catalyst for the oxidation of thiols.

#### Formation of hexacyanoferrate(II), $[\text{Fe}(\text{CN})_6]^{4-}$

Carbon-13 nmr spectra of reaction solutions of NP and  $\text{HS}^-$ ,  $\text{MeS}^-$ , cysteine, N-acetylcysteine (NAC),  $\beta$ -methylcysteine, penicillamine, N-acetylpenicillamine (NAP) and GSH in air or nitrogen saturated atmospheres, revealed hexacyanoferrate(II)

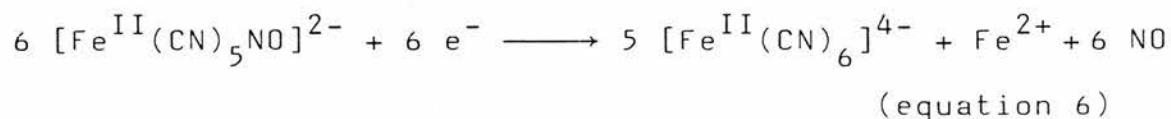
as the only diamagnetic product. There were no signals for the adducts, nitropentacyanoferrate(II), aquapentacyanoferrate(II) or hydrogen cyanide apparent in any of these spectra.

Hexacyanoferrate(II) has also been recorded as the sole cyanoferrate complex in a carbon-13 nmr spectrum of a reaction solution of 90% carbon-13 labelled NP (one equivalent) and the reducing agent dithionite (one half equivalent).<sup>37</sup>

Equations 3 - 5 outline the conversion of kinetically inert NP to kinetically inert hexacyanoferrate(II) via ligand rearrangement of kinetically labile  $[\text{Fe}(\text{CN})_4\text{NO}]^{2-}$ . No signal for hydrogen cyanide was apparent in the spectrum of carbon-13



net reaction :



labelled NP and dithionite or in any of the spectra of NP and thiol reaction solutions; this important observation can be rationalised by assuming equation 5 is the fastest step in the reaction, a reasonable supposition considering the extremely high formation constant of hexacyanoferrate(II).<sup>36</sup>

### Formation of $[\text{Fe}(\text{NO})_2(\text{SR})_2]^-$

The formation of the paramagnetic species  $[\text{Fe}(\text{NO})_2(\text{SR})_2]^-$  is not inconsistent with conversion of NP to hexacyanoferrate by reduction and ligand rearrangement. As shown in equation 6, ligand rearrangement of 6  $[\text{Fe}(\text{CN})_4]^{3-}$  and 6  $\text{CN}^-$  to 5  $[\text{Fe}(\text{CN})_6]^{4-}$  leaves one uncoordinated iron, which in the presence of thiols and NO can form a complex such as  $[\text{Fe}(\text{NO})_2(\text{SR})_2]^-$  (SR = SH, SMe, NAC, NAZ, NAP have been observed). Although Mulvey and Waters<sup>3</sup> report similar signals in the epr spectra of NP and thiols such as PhSH which they interpret to represent  $[\text{Fe}(\text{CN})_5\text{NH}_2\text{OH}]^{3-}$ , the similarity of these signals to independently recorded spectra of  $[\text{Fe}(\text{SR})_2(\text{NO})_2]^-$  favours the latter designation.

In the epr spectra of reaction solutions of NP and equimolar  $\text{HS}^-$ ,  $\text{MeS}^-$ , NAC, NAZ, and NAP, the signal for  $[\text{Fe}(\text{NO})_2(\text{SR})_2]^-$  was weak (Figure 8), which is consistent with the above explanation. However, in the epr spectra of reaction solutions of NP and an excess of  $\text{HS}^-$  or  $\text{MeS}^-$ , complete conversion of the signal for  $[\text{Fe}(\text{CN})_4\text{NO}]^{2-}$  to that for  $[\text{Fe}(\text{NO})_2(\text{SR})_2]^-$  was observed after many hours. It was shown on a preparative scale that the iron-sulphur clusters Roussin's black salt and the methyl ester of Roussin's red salt were formed and the species  $[\text{Fe}(\text{NO})_2(\text{SR})_2]^-$  (R = H, Me) are intermediates in these processes.<sup>38</sup>

### Reaction of NP with excess $\text{HS}^-$ and $\text{MeS}^-$

Thiol reduction of NP to  $[\text{Fe}(\text{CN})_4\text{NO}]^{2-}$  transforms kinetically inert NP to a kinetically labile species; complete conversion of the signal for  $[\text{Fe}(\text{CN})_4\text{NO}]^{2-}$  to

$\text{Fe}(\text{NO})_2(\text{SR})_2$  ( $\text{R} = \text{H}, \text{Me}$ ) observed in the epr spectrum of NP and an excess of the reactive nucleophiles  $\text{HS}^-$  or  $\text{MeS}^-$  is a clear manifestation of this phenomenon.

Although formation of Roussin's black salt and the methyl ester of Roussin's red salt from NP and  $\text{HS}^-$  and  $\text{MeS}^-$ , respectively, indicates that in some conditions the cyanide ligands are released from NP, these conditions are far from being physiologically significant. Both  $\text{H}_2\text{S}$  and  $\text{MeSH}$  are present in trace amounts in the body from either the metabolic activities of gut micro-organisms or from some foods, but neither are of consequence with regard to the hypotensive activity of NP infused into the blood stream. The low yield of Roussin's black salt and even lower yield of the methyl ester of the red salt indicate that reaction of excess thiols with NP is a highly inefficient method of preparing iron-sulphur clusters. It is doubtful, on this basis, that the corresponding iron-sulphur clusters of cysteine and related thiols could be formed in detectable quantities, if at all.

Comparison of the reactions of (N-acetyl)cysteine and (N-acetyl)penicillamine

The visible spectra of freshly mixed NP and N-acetylpenicillamine (NAP) reaction solutions of high pH ( $\lambda_{\text{max}}$  525 nm) resemble those of NP and N-acetylcysteine (NAC) reaction solutions ( $\lambda_{\text{max}}$  522 nm) and therefore it is reasonable to presume that the adduct of NP and NAP is of the same structure as that of NP and NAC (e.g.(5)). Spectrophotometric studies of adduct decomposition (Figures 4 and 5) indicate that for reaction solutions of identical concentrations, the NP and

NAC adduct was formed in much higher proportions and faded more rapidly than the NP and NAP adduct. Epr spectra indicated that the adducts of NP and NAP or NAC decomposed similarly to give  $[\text{Fe}(\text{CN})_4\text{NO}]^{2-}$  and a slight amount of  $[\text{Fe}(\text{NO})_2(\text{SR})_2]^-$  (R = NAP, NAC). The only signals in the carbon-13 nmr of the oxygen-free reaction solutions of NAP and NP at pH 10 were those of the starting materials (in contrast with complete reaction of NP and NAC at this pH) but above pH 11 conversion to the disulphide of NAP and hexacyanoferrate(II) was complete. The reaction stoichiometry was, in the absence of air, 1:1 for NP and NAP or NAC.

The carbon-13 nmr spectra of NP and equimolar NAP or NAC recorded in the presence of air (Figures 6a-e and 7a-d) indicated that, for the first four hours of reaction, there was greater formation of hexacyanoferrate(II) in the NP and NAC reaction solution, consistent with other observations that the NP and NAC reaction proceeded faster and to a greater extent than that of NP and NAP. For the same reason, the signal to noise ratios for the NP and NAC reaction solution spectra were noticeably lower than those for the NP and NAP reaction solution spectra; transient improvement in the ratio upon saturating the NP and NAC solution with air, indicates that the paramagnetic species  $[\text{Fe}(\text{CN})_4\text{NO}]^{2-}$  was disrupting the spectral resolution. (As the reaction of NP and NAC proceeds to a greater extent than that of NP and NAP,  $[\text{Fe}(\text{CN})_4\text{NO}]^{2-}$  would have been more abundant in the NP and NAC reaction solution.)

Although the solutions were initially equimolar in thiol

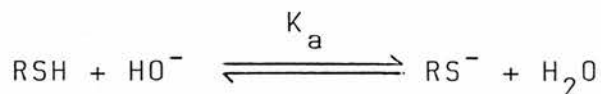
and NP, the high proportion of unreacted NP, even after many hours suggests that NP catalysed thiol oxidation. From the improved signal to noise ratio of the final NP and NAC reaction solution spectrum, it can be inferred that adduct decomposition to  $[\text{Fe}(\text{CN})_4\text{NO}]^{2-}$  had diminished and thus the majority, if not all, of the thiol had been consumed at this time. The apparently diminished hexacyanoferrate(II) formation in NAC reaction solutions after four hours can be explained by oxidation of hexacyanoferrate(II) to hexacyanoferrate(III)\*, in the absence of a more readily oxidised species such as  $[\text{Fe}(\text{CN})_4\text{NO}]^{2-}$ .

The above experiments indicate that the products (hexacyanoferrate(II) and disulphide) and intermediates (adduct,  $[\text{Fe}(\text{CN})_4\text{NO}]^{2-}$  and  $[\text{Fe}(\text{SR})_2(\text{NO})_2]$ ) of the reaction of NP with NAP or NAC are the same at elevated pH and room temperature, regardless of the observed variations in the reaction rates. These results are *not* consistent with Scheme 2 for which thionitrites are reaction intermediates (although in ice cold solutions at near neutral pH this may represent an alternative pathway).<sup>10</sup> Additionally, there was no evidence of the thionitrite of NAP in carbon-13 nmr spectra or spectrophotometric studies of NP and NAP reaction solutions despite the exceptional stability of this species.<sup>29</sup> Likewise, the thionitrite of NAC was not detected in NP and NAC reaction solutions. Therefore, differential stability of the NAC and

\* Separate experiments<sup>20</sup> have shown that the paramagnetism of aquapentacyanoferrate(III) does not perturb the spectra of diamagnetic cyanoferrate complexes. The same is likely to be true with hexacyanoferrate(III), for which no carbon-13 nmr signal could be detected.

NAP thionitrites is not a factor in the differential reactivities of NAC and NAP with NP.

Several features of the reactions of NP with thiols are important to explanation of the apparent anomalous reactivity of penicillamine and N-acetylpenicillamine; in particular the equilibrium between the thiolate anion, NP and adduct, expressed in the following equations. Additionally, it is



$$[\text{RS}^-] = K_a [\text{RSH}][\text{HO}^-] \quad (\text{equation 7})$$

$$[\text{adduct}] = K_1 [\text{RS}^-][\text{NP}] \quad (\text{equation 8})$$

important to note that for systems in which the recycling reaction could be observed, solutions of the regenerated adduct were always much less intense than initial reaction solutions.

From equations 7 and 8 it is apparent that the concentration of the adduct is proportional to the concentration of the thiolate anion, in turn proportional to the hydroxide concentration. From evaluation of the literature values listed in Table 2 it was concluded that the  $pK_a$  of NAP is higher than that of NAC and it has been shown<sup>5</sup> that the rate of formation of the NP and penicillamine adduct is slightly lower than the same values for adducts of NP and several other thiols, including cysteine and NAC. Consequently, the equilibrium is more towards the reactants for the reaction of NP with NAP than with NAC, and at a given pH more NAC is ionised than NAP.

Therefore as a higher concentration of ionised NAP than NAC is necessary for comparable adduct formation, what have seemed to be excessively basic conditions are required for detectable reaction (magenta adduct formation) of NP with NAP. The intensity of the regenerated adduct of NP and NAC was always much less than that of the initially formed adduct, reflecting the decreased concentration of one or more reactants, and it is therefore not surprising that regeneration of the adduct of NP and NAP, for which initial formation is much less favoured than the adduct of NP and NAC, could not be detected.

Of the other sterically hindered thiols considered,  $\text{HSC}(\text{CH}_2\text{CH}_3)_3$  exhibited similar behaviour to N-acetylpenicillamine (no adduct regeneration) but it is interesting that (N-acetyl)  $\beta$ -methylcysteine, with *one* methyl group adjacent to the thiol function, reacted much more like N-acetylcysteine than N-acetylpenicillamine. (Complete conversion of  $\beta$ -methylcysteine to the disulphide and hexacyanoferrate(II) was evident in carbon-13 nmr spectra recorded at  $\text{pH} < 11$  and the adduct could be regenerated.) For (N-acetyl)penicillamine, the two methyl groups contribute steric hindrance and electron density, respectively disfavoured adduct formation and destabilising the thiolate anion, to the extent that apparently anomalous reactivity towards NP was observed. Having shown that the reaction of NP with sterically hindered thiols occurs in the same manner as with unhindered thiols, the reactions of NP with the potentially hindered thiol groups of enzyme active sites can be considered (Chapter 7).

#### 6.4 CONCLUDING REMARKS

The mechanism proposed for the conversion of NP to hexacyanoferrate(II) in the presence of thiols (Scheme 3) is consistent with all observations made for the reactions of NP with equimolar  $\text{HS}^-$ ,  $\text{MeS}^-$ , cysteine, N-acetylcysteine,  $\beta$ -methylcysteine, N-acetyl- $\beta$ -methylcysteine, and glutathione as well as the sterically hindered thiols penicillamine and N-acetylpenicillamine in buffered solutions. In the presence of excess  $\text{HS}^-$  and  $\text{MeS}^-$  nitroprusside was converted in low yield to Roussin's black salt and the methyl ester of Roussin's red salt, respectively, but although these reactions reveal the kinetic lability of  $[\text{Fe}(\text{CN})_4\text{NO}]^{2-}$ , it is important to emphasise that the conditions under which they occurred represent a significant departure from conditions in biological systems. The long reaction time required for even a low yield of the methyl ester of Roussin's red salt demonstrates that the conversion of NP to iron sulphur clusters is not a rapid or efficient process. There is little expectation that, with the much less nucleophilic thiolate anions encountered biologically, this minor reaction is significant to the medical administration of NP.

Furthermore, it has been shown that upon reaction of NP with equimolar thiols including  $\text{HS}^-$  and  $\text{MeS}^-$ , the only reaction products are  $[\text{Fe}(\text{CN})_6]^{4-}$  and the disulphide; it is noteworthy that at no time under these conditions has hydrogen cyanide been detected. Therefore, in conditions that reasonably approximate those found physiologically, the reduction of kinetically inert NP to kinetically labile

$[\text{Fe}(\text{CN})_4\text{NO}]^{2-}$  by a wide range of thiols does not result in release of free cyanide but rapid ligand rearrangement to  $[\text{Fe}(\text{CN})_6]^{4-}$ , another kinetically inert complex. The observed release of NO, but *not* cyanide, following thiol reduction of NP may be relevant to the *in vivo* reactions of NP infused into the bloodstream to lower blood pressure.

## 6.5 EXPERIMENTAL

### Materials and Instruments

Glutathione, homocysteine, cysteine, penicillamine, N-acetylcysteine and N-acetylpenicillamine were obtained from Sigma and used without further purification.  $\text{HSC}(\text{CH}_2\text{CH}_3)_3$  was kindly supplied by Sir Derek Barton. Samples of carbon-13 labelled sodium nitroprusside were prepared by Dr. J. McGinnis as previously reported.<sup>21</sup> Buffer solutions were made with Borax,  $\text{KH}_2\text{PO}_4$  or  $\text{Na}_2\text{HPO}_4 \cdot 2\text{H}_2\text{O}$ , as appropriate. Solutions of sodium hydroxide were made from concentrated volumetric solutions. All other reagents, with the exceptions of those prepared as described below, were of AnalaR grade where available.

Solid sodium nitroprusside was stored in a dark cupboard. All solutions containing nitroprusside were protected from light with a complete covering of aluminium foil during storage and use.

Carbon-13 nmr experiments in the presence of air were recorded on a Bruker 360 spectrometer (of the S.E.R.C. Regional NMR Service at the University of Edinburgh) in the FT mode at 25 °C with a carbon resonance of 90.56 MHz in a field of 8.5 T. The number of scans was typically 350 with a pulse width of 4.0  $\mu$  seconds and a delay time of 0.14 seconds. The reference was external TMS.

Most carbon-13 nmr experiments in the absence of air were recorded on a Varian CFT-20 in the FT mode at room temperature with a carbon resonance of 20 MHz in a field of 1.9 T. For these experiments the number of scans was usually

20,000 with a pulse width of 7  $\mu$  seconds and no pulse delay. When the spectra were recorded on a Bruker AM 300 instrument in the FT mode at room temperature, the carbon resonance was 75 MHz in a field of 7.04 T. The number of scans was 1000 with a pulse width of 2.0  $\mu$  seconds and a delay of 3.0 seconds. For both instruments the reference was internal sodium 3-(trimethylsilyl)propanesulphonate but all chemical shifts quoted refer to TMS. Air was removed from the solutions of equimolar NP and thiol in buffer prior to mixing by degassing on a vacuum line.

Temperature-jump experiments were conducted on the instrument at the Technical University of Denmark. The concentration of nitroprusside was in excess (typically 40 - 100 mM) and the concentrations of the thiols were typically 1 mM for homocysteine and 5 mM for penicillamine or N-acetylpenicillamine. Borax or phosphate buffers were used, as appropriate, and solutions of thiol in buffer (pH 10.5 for homocysteine and pH 11.2 for penicillamine or N-acetylpenicillamine) were flushed with  $N_2$  to minimise thiol oxidation and were used within one hour of mixing. NP and thiol solutions were preincubated at 20 °C prior to reaction and the ionic strength was maintained ( $I = 0.2$  M) with NaCl. The rate constants were calculated from the application of the Kedzy-Swinbourne\* method to plots of absorbance vs time generated by a plotter connected, via an oscilloscope, to the temperature-jump instrument. The rate constants in Table 3 represent the average of several values of first or second

\* Correlation coefficients were better than 0.999

jumps of a solution of NP and thiol immediately (usually thirty seconds) after mixing. The accuracy of the results was limited by the short life of the adduct and decomposition of the thiol solutions in alkaline conditions.

The epr experiments were conducted by Ian Johnson in a quartz capillary at room temperature using a Bruker ER 200D spectrometer. Di-t-butyl-nitroxide was used as the standard for the measurement of the line positions. Solutions of NP or thiol in buffer (I = 0.1 M) were degassed separately, typical concentrations upon mixing were  $5 \times 10^{-3}$  M.

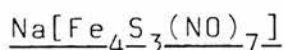
Spin-echo experiments were conducted by John Reglinski at the University of Strathclyde on a Bruker 250 MHz instrument in the FT mode at 20 °C. A 90- $\tau$ -180- $\tau$  pulse sequence ( $\tau = 40$  ms) was used and the data from 2000 complete pulse sequences were accumulated for each Fourier transform.

Ultraviolet and visible spectra were obtained on a Pye Unicam SP8 100 spectrophotometer. Infra-red spectra were obtained as Nujol mulls on a Perkin-Elmer 1420 instrument. Proton nmr were recorded on a Bruker WP-80 instrument.

### Methods

Conversion of nitroprusside to Roussin's black salt and the methyl ester of the red salt was conducted in collaboration with Ian Johnson

#### Conversion of nitroprusside to Roussin's black salt,



Sodium nitroprusside (1.12 g, 3.76 mmol) and NaSH (3.07 g, 54.8 mmol) were dissolved in phosphate buffer (140 ml,

I = 1.0 M, pH = 7.5) under  $N_2$  and stirred for fifteen hours. The mixture was evaporated to dryness under reduced pressure and a green residue was obtained. This was extracted with nitrogen-flushed acetone (4 x 50 ml) and the combined extracts were filtered through Hyflo-supercel. The solvent was evaporated under reduced pressure to yield  $Na[Fe_4S_3(NO)_7]$  (78.5 mg, 0.142 mol) in 26% yield with respect to NO. Uv/vis (MeOH) 460, 350, 415, 260 nm (all shoulders). The portion of the residue not soluble in acetone contained elemental sulphur (identified by mass spectrometry) and iron sulphides.

Conversion of nitroprusside to the methyl ester of Roussin's red salt,  $Fe_2(SMe)_2(NO)_4$

Sodium nitroprusside (1.82 g, 6.11 mmol) and NaSMe (3.21 g, 117 mmol) were dissolved in phosphate buffer (150 ml, I = 1.0 M, pH = 7.5) under  $N_2$ . Methylene chloride (30 ml) was added shortly after mixing nitroprusside and NaSMe and the mixture was stirred under  $N_2$  for fifteen hours. The orange methylene chloride layer was separated and the aqueous layer was neutralised to pH 7 before extracting with methylene chloride (4 x 50 ml). The orange organic fractions were combined, dried for fifteen minutes ( $MgSO_4$ ) and the solvent was evaporated under reduced pressure. The resulting crude  $Fe_2(SMe)_2(NO)_4$  was purified on an alumina column yielding pure  $Fe_2(SMe)_2(NO)_4$  (36 mg, 0.11 mol) in 7.2% yield with respect to NO. Mass spectrum;  $m/z$  326 ( $M^+$ ) 296, 266, 236, 206, 191, 176 (sequential loss of 4 NO and 2  $CH_3$ ). Infra-red 1778, 1752  $cm^{-1}$  (NO stretches).

### Preparation of the thionitrite of N-acetylcysteine (9)

To a stirred ice-cold solution of N-acetylcysteine (0.20 g,  $1.24 \times 10^{-3}$  mol) in methanol (2 ml) and 1 M HCl (1.33 mol) was added  $\text{NaNO}_2$  (0.092 g,  $1.33 \times 10^{-3}$  mol) in  $\text{H}_2\text{O}$  (1 ml). The mixture immediately became bright red and was extracted with methylene chloride. The extracts were combined, washed with  $\text{NaHCO}_3$ , then dried ( $\text{MgSO}_4$ ). Upon evaporation of the solvent under reduced pressure red needles of N-acetyl-S-nitrosocysteine were obtained (0.153 g) in 64% yield. Visible absorbance maximum ( $\text{H}_2\text{O}$ ) 553, 519 (shoulder), 550 nm.<sup>26</sup> This thionitrite was very unstable in the presence of air.

### Preparation of the thionitrite of N-acetylpenicillamine (10)<sup>29</sup>

To a stirred ice-cold solution of N-acetylpenicillamine (0.956 g,  $5 \times 10^{-3}$  mol) in methanol (13 ml), 1 M HCl (6.4 mol) and concentrated  $\text{H}_2\text{SO}_4$  (0.64 ml) was slowly added  $\text{NaNO}_2$  (0.690 g,  $1.0 \times 10^{-2}$  mol). After fifteen minutes green crystals of the thionitrite of N-acetylpenicillamine, with a red cast, were filtered from the solution in 64% yield (0.451 g,  $2.05 \times 10^{-3}$  mol). Visible absorbance maximum ( $\text{H}_2\text{O}$ ) 590 nm.<sup>26</sup>  $\delta_{\text{H}}$  (DMSO) 1.89 (s, 3H), 1.96 (3H), 1.98 (s, 3H).

### Synthesis of N-acetyl- $\beta$ -methylcysteine

#### 1. Condensation of hippuric acid and acetaldehyde<sup>39</sup>

Acetaldehyde (158 ml) was added to hippuric acid (56.47 g, 0.315 mol) and sodium acetate (25.99 g, 0.317 mol) in acetic anhydride (158 ml). The mixture developed a chalky appearance upon refluxing for three hours. Upon cooling, a

precipitate formed, was filtered and washed with ice cold water. Addition of ice cold water to the filtrate precipitated more product, similarly filtered and washed. The white precipitate (44.1 g, 0.236 mol) was identified as Benzoyl- $\alpha$ -aminocrotonic acid azlactone (BACA) and was obtained in 75% yield.  $\delta_{\text{H}}$  ( $\text{CDCl}_3$ ) 2.2 (d, 3H), 6.8 (q, 1H), 7.6 - 8.1 (m, 5H) p.p.m.

## 2. Addition of benzyl mercaptan to BACA

Benzyl mercaptan (25 ml, 0.213 mol) was added to sodium (10.61 g, 0.46 mol) dissolved in methanol (212 ml). This mixture was kept stirring at 5 - 10 °C while BACA (39.7 g, 0.212 mol) in toluene (212 ml) was slowly added. After addition was complete the bath was removed and the mixture was left stirring overnight. The next morning the mixture was acidified (HCl) to Congo Red and the solvent was evaporated under reduced pressure. The resulting yellow syrup was dissolved in glacial acetic acid (500 ml) and refluxed for one hour. After cooling, the mixture was stored in a cold room overnight. A beige precipitate was apparent the next morning and was washed with acetic acid, then water, yielding 21.0 g benzoyl- $\alpha$ -amino- $\beta$ -benzylthio-n-butyric acid (abbreviated benzoyl derivative).  $\delta_{\text{H}}$  ( $\text{CDCl}_3$ ) 1.3 (d, 3H), 3.8 (s, 2H), 5.0 (dxd, 1H), 7.3 (m, 10H) p.p.m. Mass spectrum  $m/z$  300 ( $\text{M}^+$ ), 285 ( $\text{M}^+ - \text{CO}_2\text{H}$ ), 238 ( $\text{M}^+ - \text{H}_2\text{CC}_6\text{H}_5$ ), 207 ( $\text{M}^+ - \text{SCH}_2\text{C}_6\text{H}_5$ ).

### 3. Hydrolysis of benzoyl derivative

The benzoyl derivative (21.0 g,  $6.38 \times 10^{-2}$  mol) was suspended in 85% formic acid (325 ml), concentrated HCl (325 ml) and water (325 ml) and refluxed for four hours; at this time not all the solid had dissolved. The solvent was evaporated under reduced pressure and the remaining beige residue was extracted with hot 60/80 petroleum ether (2 x 260 ml) then hot water (2 x 260 ml), leaving unreacted benzoyl derivative which was removed by filtration. The filtrate was neutralised with  $\text{NH}_4\text{OH}$ , concentrated to 65 ml and left to cool overnight. Crystalline  $\alpha$ -amino- $\beta$ -benzylthio- $n$ -butyric acid (abbreviated amino acid) was collected by filtration in 74% yield (10.95 g,  $4.83 \times 10^{-2}$  mol).  $\delta_{\text{H}}$ ( $\text{CDCl}_3$ ) 1.3 (d, 3H), 2.1 (s, 2H), 3.4 (m, 1H), 3.7 (s, 2H), 5.0 (dxd, 1H), 7.3 (m, 5H) p.p.m. Mass spectrum:  $m/z$  180 ( $\text{M}^+ - \text{CO}_2\text{H}$ ), 151 ( $\text{M}^+ - \text{H}_2\text{NCHCO}_2\text{H}$ ), 124 ( $\text{SCH}_2\text{C}_6\text{H}_5$ ).

### 4. Reduction of amino acid

Amino acid (2.0 g,  $8.9 \times 10^{-3}$  mol) was dissolved in liquid ammonia (55 ml) to which sodium (0.83 g,  $3.6 \times 10^{-2}$  mol) had been added in small lumps until a permanent blue colour was observed. Ammonium chloride was added very carefully in small portions until the blue colour disappeared after which point an additional portion (0.93 g,  $1.74 \times 10^{-2}$  mol) was added. After evaporation of the solvent ammonia, ether (33 ml) and concentrated HCl (0.67 ml) were added to the solid material which was broken up and warmed gently. The mixture was decanted and the residue was extracted further with ether (2 x 33 ml) and then slightly acidic warm ethanol (3 x 13 ml).

The ethanol layers were combined and evaporated to dryness under reduced pressure, leaving a residue which was dissolved in ethanol (10.7 ml) and ether (107 ml). After cooling overnight, the crystalline hydrochloride of  $\alpha$ -amino- $\beta$ -thiol-butyrac acid (called  $\beta$ -methylcysteine (3)) was collected in 85% yield (0.31 g,  $7.56 \times 10^{-3}$  mol) by filtration. Positive test with nitroprusside (magenta colour upon addition of alkali to solution of product and NP).  $\delta_{\text{H}}$   $\text{CDCl}_3$ , 1.4 (d, 3H), 3.7 (m, 1H), 4.0 (d, 1H) p.p.m. Mass spectrum:  $m/z$  90 ( $\text{M}^+ - \text{CO}_2\text{H}$ ), 75 ( $\text{M}^+ - \text{H}_3\text{CC}(\text{H})\text{SH}$ ).

#### 5. N-acetylation of $\beta$ -methylcysteine<sup>40</sup>

The hydrochloride of  $\beta$ -methylcysteine (0.385 g,  $2.2 \times 10^{-3}$  mol) was dissolved in 91% aqueous THF (0.96 ml) under an atmosphere of  $\text{N}_2$ . While stirring the mixture, sodium acetate trihydrate (0.640 g,  $4.44 \times 10^{-3}$  mol) was added. After twenty minutes the solution was cooled to 3 - 6 °C and acetic anhydride (0.202 ml,  $2.75 \times 10^{-3}$  mol) was added slowly. After addition, the bath was removed and the mixture continued to be stirred, under a nitrogen atmosphere, for twenty hours. The solution was then refluxed for four hours after which time one drop of concentrated HCl was added. Upon cooling to 5 - 10 °C a white precipitate was formed which was removed by filtration. The filtrate was concentrated, precipitating N-acetyl- $\beta$ -methylcysteine (NAZ, 0.122 g,  $6.87 \times 10^{-4}$  mol) in 31% yield. A positive test for the thiol reaction of NP was obtained.

## REFERENCES

1. G. Scaglierini, *Atti V. Congr. Nazl. Chim. Pura Appl.*, Rome 1935, Pt. 1, 546 (1936); *Chem. Abstr.*, 1937, **31**, 3407).
2. J. H. Swinehart, *Coord. Chem. Rev.*, 1967, **2**, 385.
3. D. Mulvey and W. A. Waters, *J. Chem. Soc., Dalton*, 1975, 951.
4. P. J. Morando, E. B. Borghi, L. M. de Schteingart, and M. A. Blesa, *J. Chem. Soc., Dalton*, 1981, 435
5. M. D. Johnson and R. G. Wilkins, *Inorg. Chem.*, 1984, **23**, 231.
6. P. A. Rock and J. H. Swinehart, *Inorg. Chem.*, 1966, **5**, 1078.
7. A. R. Butler, C. Glidewell, J. Reglinski, and A. Waddon, *J. Chem. Res. (S)*, 1984, 279.
8. V. A. W. Kreye and R. Gross in "Antihypertensive Agents", (F. Gross, Ed.), Springer Verlag, Berlin, 1977, 418 - 430.
9. E. H. Ohlstein, K. S. Wood, and L. J. Ignarro, *Arch. Biochem. Biophys.*, 1982, **218**, 1987.
10. L. J. Ignarro, H. Lipton, J. C. Edwards, W. H. Baricos, A. L. Hyman, P. J. Kadowitz, and C. A. Gruetter, *J. Pharm. Exp. Therap.*, 1981, **218**, 739.
11. L. J. Ignarro, B. K. Barry, D. Y. Gruetter, J. C. Edwards, E. H. Ohlstein, C. A. Gruetter, and W. H. Baricos, *Biochem. Biophys. Res. Comm.*, 1980, **94**, 93.
12. F. Murad, J. A. Lewicki, H. J. Brandwein, C. K. Mittal, and S. A. Waldmon in "Advances in Cyclic Nucleotide

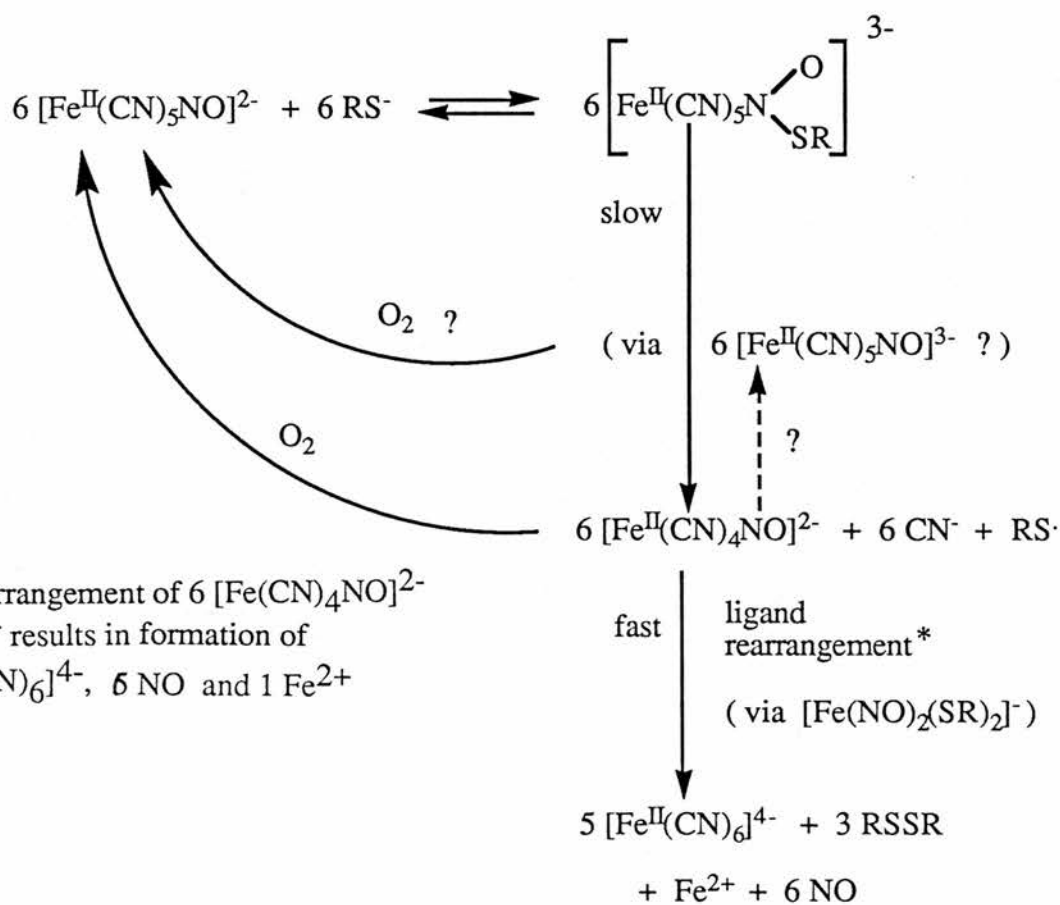
- Research" (J. E. Dumont, P. Greenyard and G. A. Robinson, Eds.), Raven Press, New York, 1981, Vol. XIV, 229 - 239.
13. H. E. Carter, C. M. Stevens, and L. F. Ney, *J. Biol. Chem.*, 1941, **139**, 247.
  14. P. C. Jocelyn, "Biochemistry of the SH Group", Academic Press Inc., London, 1972, p.3.
  15. Ref. 14, p.10.
  16. F. R. DeRubertis, P. A. Graven, and D. W. Pratt, *Biochem. Biophys. Res. Comm.*, 1978, **83**, 158.
  17. P. A. C. McNeil, J. B. Roynor, and M. C. R. Symons, *J. Chem. Soc.*, 1965, 410.
  18. C. Glidewell and I. Johnson, *Inorg. Chim. Acta*, in press.
  19. E. J. Baran, and A. Muller, *Angew. Chem. (Int. Ed.)*, 1969, **8**, 898.
  20. A. R. Butler, C. Glidewell, A. S. McIntosh, D. Reed, and I. H. Sadler, *Inorg. Chem.*, 1986, **25**, 970.
  21. A. R. Butler, C. Glidewell, A. Hyde, and J. McGinnis, *Inorg. Chem.*, 1985, **24**, 2931,
  22. J. McGinnis, Ph.D. Thesis, University of St. Andrews, 1983.
  23. A. R. Hyde, Ph.D. Thesis, University of St. Andrews, 1984.
  24. C. Glidewell and J. McGinnis, *Inorg. Chim. Acta*, 1982, **64**, L171.
  25. H. Schröder, W. Noack, and R. Müller, *J. Mol. Cell Cardiol.*, 1985, **17**, 931.
  26. W. A. Pryor, D. F. Church, C. K. Govindan, and G. Grank, *J. Org. Chem.*, 1982, **47**, 159.
  27. L. J. Ignarro, J. N. Degnan, W. H. Baricos, P. J. Kadowitz, and M. S. Wolin, *Biochim. Biophys. Acta*, 1982, **718**, 49.

28. L. J. Ignarro and C. A. Gruetter, *Biochim. Biophys. Acta*, 1980, **631**, 221.
29. L. Field, R. V. Dilts, R. Ravichandran, P. G. Lenhart, and G. E. Carnahan, *J. Chem. Soc., Chem. Comm.*, 1978, 249.
30. M. Friedman, J. F. Calvin, and J. S. Wall, *J. Am. Chem. Soc.*, 1965, **87**, 3672.
31. R. S. Reid and D. Rabenstein, *Can. J. Chem.*, 1981, **59**, 1505.
32. J. Inczedy and J. Marothy, *Acta Chim. Acad. Sci. Hung.*, 1975, **86**, 1; *Chem. Abstr.*, 1975, **83**, 121819w.
33. A. S. Roberts McIntosh, Ph.D. Thesis, University of St. Andrews, 1986.
34. J. P. Gouesnard, *J. Chem. Soc., Perkin I*, 1986, 1901.
35. (a) G. Herzberg, "Infra-red and Raman spectra of Polyatomic Molecules", D. van Nostrand, 1945, p. 279.  
(b) G. Herzberg, "Spectra of Diatomic Molecules", D. van Nostrand, 1950, p. 62.
36. J. J. Christensen and R. M. Izatt, "Handbook of Metal-Ligand Heats", Marcel Dekker Inc., New York, 1970, p.66
37. Ian Johnson, unpublished results.
38. L. J. Ignarro and C. A. Gruetter, *Biochim. Biophys. Acta*, 1980, **631**, 221.
39. H. E. Carter, P. Handler, and D. B. Melville, *J. Biol. Chem.*, 1939, **129**, 359.
40. T. A. Martin, C. W. Waller, U. S. Patent 3,184,505, May 18th, 1965; *Chem. Abstr.*, 1965, **63**, 7107e.

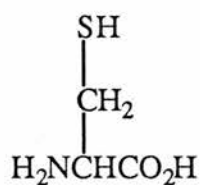
CHAPTER 7

THE REACTIONS OF THE NITROPRUSSIDE ION WITH  
INTACT ERYTHROCYTES AND THE ENZYMES PAPAIN  
AND GLYCERALDEHYDE-3-PHOSPHATE DEHYDROGENASE

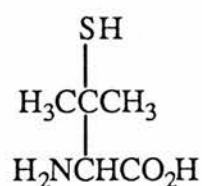
**Scheme 1** : Mechanism for the reaction of nitroprusside with equimolar thiols in alkaline solution



ligand rearrangement of  $6 [\text{Fe}(\text{CN})_4\text{NO}]^{2-}$  and  $6 \text{CN}^-$  results in formation of  $5 [\text{Fe}^{\text{II}}(\text{CN})_6]^{4-}$ ,  $6 \text{NO}$  and  $1 \text{Fe}^{2+}$



(1)



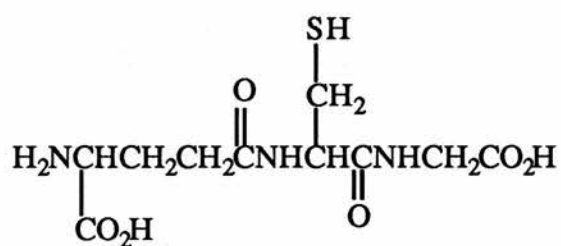
(2)

## 7.1 INTRODUCTION

The reactions of the nitroprusside ion (NP) with a range of thiols were reported in Chapter 6 with particular regard to their relevance to the hypotensive activity of NP; previous workers<sup>1-6</sup> have suggested that the activity of NP may arise from interaction with thiol groups at the active site of the enzyme guanylate cyclase. It was shown that the reactions of NP, in buffered solution, with equimolar NaSH, NaSMe, cysteine, N-acetylcysteine,  $\beta$ -methyl cysteine, penicillamine, N-acetylpenicillamine, and glutathione (GSH) occur by a common mechanism (Scheme 1). In all of these reactions the products are the disulphide and hexacyanoferrate(II),  $[\text{Fe}(\text{CN})_6]^{4-}$ , formed by ligand rearrangement of the paramagnetic species  $[\text{Fe}(\text{CN})_4\text{NO}]^{2-}$ .

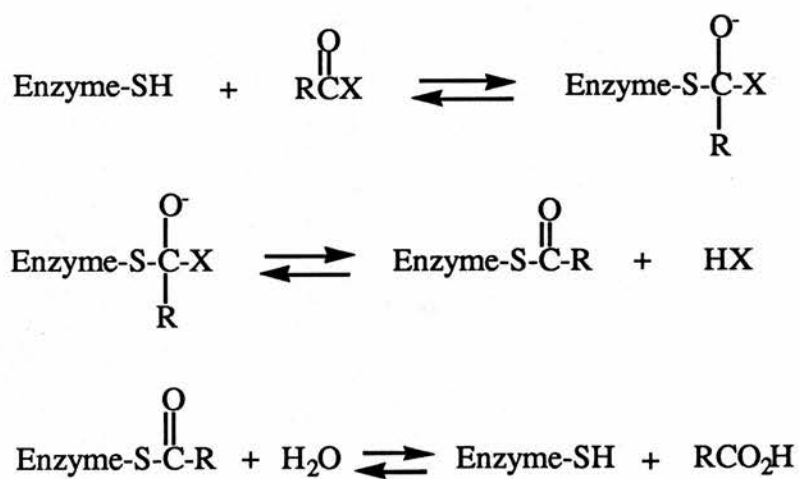
In particular, the reactions of NP with cysteine (1), as well as the sterically hindered thiol penicillamine (2), are consistent with Scheme 1; the high  $\text{p}K_a$  of penicillamine and comparatively low rate of formation of the NP and penicillamine adduct contribute to apparently anomalous reactivity of penicillamine with NP, in contrast to that of cysteine and other thiols, which initially suggested that the reaction of NP with hindered thiols proceeded by a different mechanism.

Cysteine residues are believed<sup>7</sup> to be the sole source of thiols in protein sequences and the reactions of NP with hindered thiols such as penicillamine were considered as models for the reaction of NP with less accessible thiol groups at enzyme active sites. With the similarity of the reactions of NP with sterically hindered and unhindered thiols



(3)

Scheme 2 : Catalytic mechanism of papain



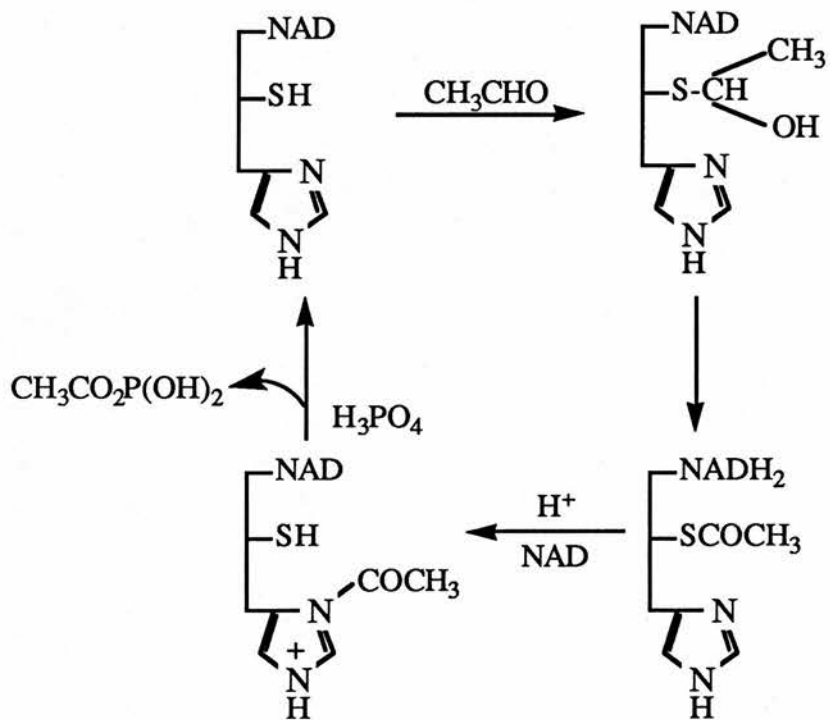
in mind, carbon-13 nmr, epr, visible spectroscopy and inhibition studies of the reactions of nitroprusside with two enzymes known to contain cysteine groups at the active site were conducted to assess the validity of Scheme 1 for enzymic thiols.

The enzyme papain (EC 3.4.4.10) is a well known example of a group of plant proteinases with catalytic thiol groups.<sup>8,9</sup> Papain, obtained from papaya latex, is a simple protein of 212 amino acid residues forming one peptide chain (Photograph 1). The active site cysteine (cys-25) is the only thiol residue of papain and the reactive intermediate is thought to be a thiol-acyl enzyme: enzyme-S-C(=O)-R (Scheme 2). The reactivity of cysteine-25 of papain towards cyanate has been shown to be 3000 times greater than that of free cysteine.<sup>10</sup> Crystallographic studies of papain have revealed the proximity of cys-25 to histidine (his-159) and aspartic acid (asp-158) residues, both thought to contribute to papain catalysis over a wide range of pH.<sup>11,12</sup>

Glyceraldehyde-3-phosphate dehydrogenase (GAPDH, EC 1.2.1.12) is the enzyme that catalyses the oxidation and phosphorylation of D-glyceraldehyde-3-phosphate (G-3P) to 1,3-diphosphoglycerate (DPGA) important to carbohydrate metabolism and is another well known example of an enzyme with an essential thiol at the active site. The structure of GAPDH, found in a wide range of animal and plant tissues, has been determined and consists of a tetramer of four identical subunits (two subunits are shown in Photograph 2).

Acetaldehyde has been used as a substrate for GAPDH and

**Scheme 3 :** Catalytic mechanism of glyceraldehyde-3-phosphate dehydrogenase (GAPDH)



the thiol group is implicated in the mechanism (Scheme 3) by labelling studies upon identification of a peptide with carbon-14 labelled thioester after incubation of carbon-14 labelled acetaldehyde with GAPDH.<sup>13</sup> The essential thiol (cys-149) is, by virtue of a helical configuration, close to the non-reactive thiol of the active site (cys-153). A histidine residue (his-176), also considered to be important to the catalytic mechanism of GAPDH, lies within hydrogen-bonding distance of the essential thiol.

The cysteine content of GAPDH varies from one to five for each of four subunits but it is the essential thiol (cys-149) that is the most reactive. The other thiol of the active site (cys-153), while not generally reactive,<sup>14</sup> can be induced to form a disulphide bond with cys-149 thereby permanently inactivating the enzyme, possibly due to irreversible conformation changes.

There are many reports<sup>15-22</sup> in the medical literature citing cyanide release upon infusion of NP; both tissue thiol groups<sup>16,17,21</sup> and red blood cells (erythrocytes)<sup>22,23</sup> have been implicated in NP decomposition. These reports of cyanide release from NP are not consistent with the high formation constant of cyanoferrate complexes or the *in vitro* reactions of NP with amines,<sup>24</sup> carbanions (Chapters 3 and 4) or thiols (Chapter 6) investigated thus far and there is strong evidence<sup>25,26</sup> that the analytical procedure (discussed in Chapter 1) commonly employed for quantification of free cyanide in tissue samples is subject to false readings when kinetically labile cyanoferrate complexes are present, as

from photodecomposition or metabolism of NP. In particular, if the *in vivo* reaction of NP with thiols parallels the reduction of NP by cysteine and related thiols investigated in Chapter 6, then the kinetically labile paramagnetic species  $[\text{Fe}(\text{CN})_4\text{NO}]^{2-}$  will be formed. It was shown that  $[\text{Fe}(\text{CN})_4\text{NO}]^{2-}$  undergoes ligand rearrangement to hexacyanoferrate(II) and release of cyanide has never been detected in these reaction solutions by carbon-13 nmr spectroscopy.

Despite the evidence suggesting that cyanide release from NP does not occur in physiological conditions, the complexity of biological systems can not be disregarded. Nmr spectroscopy is an ideal technique for study of biological systems; it is non-invasive, non-destructive and unambiguous assignment of the products can often be made. Butler *et al*<sup>27</sup> have used carbon-13 nmr to investigate the reaction of 90% carbon-13 labelled NP in whole blood. No significant change in the spectrum of NP was detected immediately after addition of NP to blood or after a long period of incubation; at the concentrations used 1% decomposition of NP to cyanide could have been detected.

By far the majority of the thiol groups in blood are attributed to the intracellular components haemoglobin and glutathione; the erythrocyte membrane contains less than 5% of the tritratable thiol groups, plasma contains no non-protein thiols and the very low protein thiol concentrations are due to the proteins serum albumin and the immunoglobulins.<sup>28</sup> Separate investigations<sup>29,30</sup> indicate that NP does not react with the thiol groups of (bovine) serum albumin and thiol

groups are apparently not involved in the reaction of NP with haemoglobin<sup>30</sup> (to be discussed in Chapter 8).

Transport experiments with carbon-14 labelled NP and intact erythrocytes indicate that NP can cross the red cell membrane and reactions with the intracellular thiol glutathione could thus be important to its medical administration. Preliminary resonance Raman experiments showed that NP affected thiol levels of lysed erythrocytes but a more diagnostic technique was required to follow the reaction and assess the applicability of Scheme 1, developed for the reaction of NP and thiols in simple buffered solutions.

Protons are ubiquitous in biological systems and although potentially a sensitive probe of reactions within cells, the large number of protons in different environments contributes to a complex and undecipherable spectrum. Simplification of the proton nmr spectrum of erythrocytes can be achieved with a multiple-pulse spin-echo technique which largely eliminates interfering resonances from protons on proteins. The sequence of pulses and delays selects resonances observed on the basis of spin-spin relaxation times so that intracellular small molecules such as glycine, alanine, creatine, lactate, ergothionine and glutathione dominate the resulting spectrum.<sup>31</sup> An important feature of the spin-echo experiments to be discussed is that the viability of the cells could be monitored by the changes in the lactate levels. If NP is transported across the cell membrane to react with intracellular glutathione, then keeping the cells alive is important to the results of the experiments.

Glutathione is implicated in oxidative processes and free radical scavenging, and the spin-echo technique has been used to study features of erythrocyte metabolism, including glutathione-diglutathione status.<sup>32,33</sup>



## 7.2 RESULTS and DISCUSSION

### 7.2.1 Spin-echo proton nmr of NP incubated with intact erythrocytes

The work in this section was conducted by Dr. J. Reglinski at the University of Strathclyde.

The pulse delays of the spin-echo pulse sequence for proton nmr can be altered to affect the phases of the monitored resonances. In particular, the resonance of the cysteinyl  $\beta$ -methylene residue ( $g_2$ ) (Figure 1) of glutathione changes upon oxidation to the disulphide diglutathione (GSSG). If  $\tau = 60$  ms,  $g_2$  has negative phase for GSH and positive phase for GSSG, but if  $\tau = 40$  ms,  $g_2$  for GSSG is at a null point in its phase modulation cycle and thus the GSSG resonance will not be observed.<sup>34</sup>

In initial experiments with freshly obtained red blood cells and  $\tau = 60$  ms, the concentration of NP was 3.35 mM, compared to an estimated intracellular glutathione concentration of 2.76 mM.<sup>34</sup> The spectra were not well resolved, possibly due to the presence of paramagnetic species, but oxidation of GSH to GSSG was apparent in the spectra recorded within the two hours after mixing (Figure 2). Spectra recorded after this time showed signs of cell death.

The experiments were repeated, but with a lower dose of NP (0.67 mM) and a delay of  $\tau = 40$  ms to highlight the conversion of GSH to GSSG in the freshly obtained red blood cells. The spectra were recorded at 30 minute intervals for the first 150 minutes (Figure 3) and changes in the relative abundance of GSH were determined by the changes in the  $g_2$

**Figure 2 :** Spin-echo proton nmr spectra ( $T_2 = 60$  ms) of the erythrocyte upon incubation with nitroprusside shortly after mixing (A), and after two hours (B)

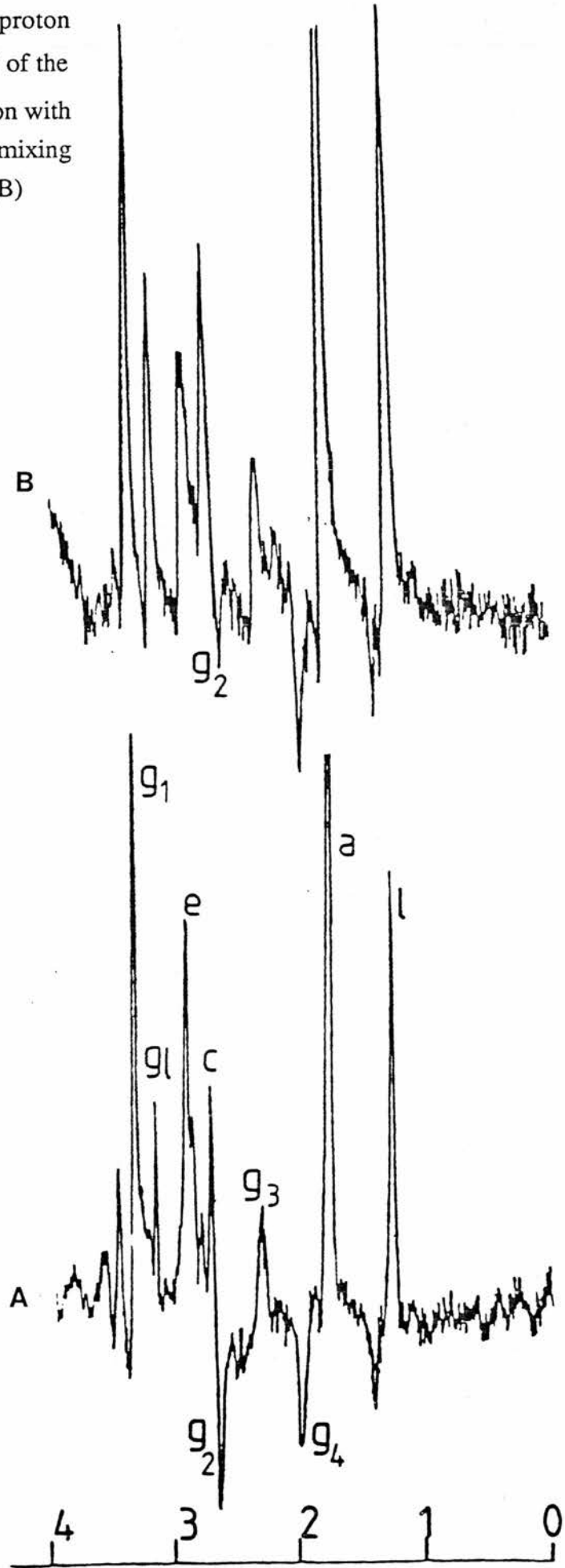


**Figure 3 :** Spin-echo proton nmr spectra ( $T_2 = 40$  ms) of the erythrocyte upon incubation with nitroprusside recorded at thirty minute time intervals until 150 minutes after mixing, at which time an additional dose of nitroprusside was added

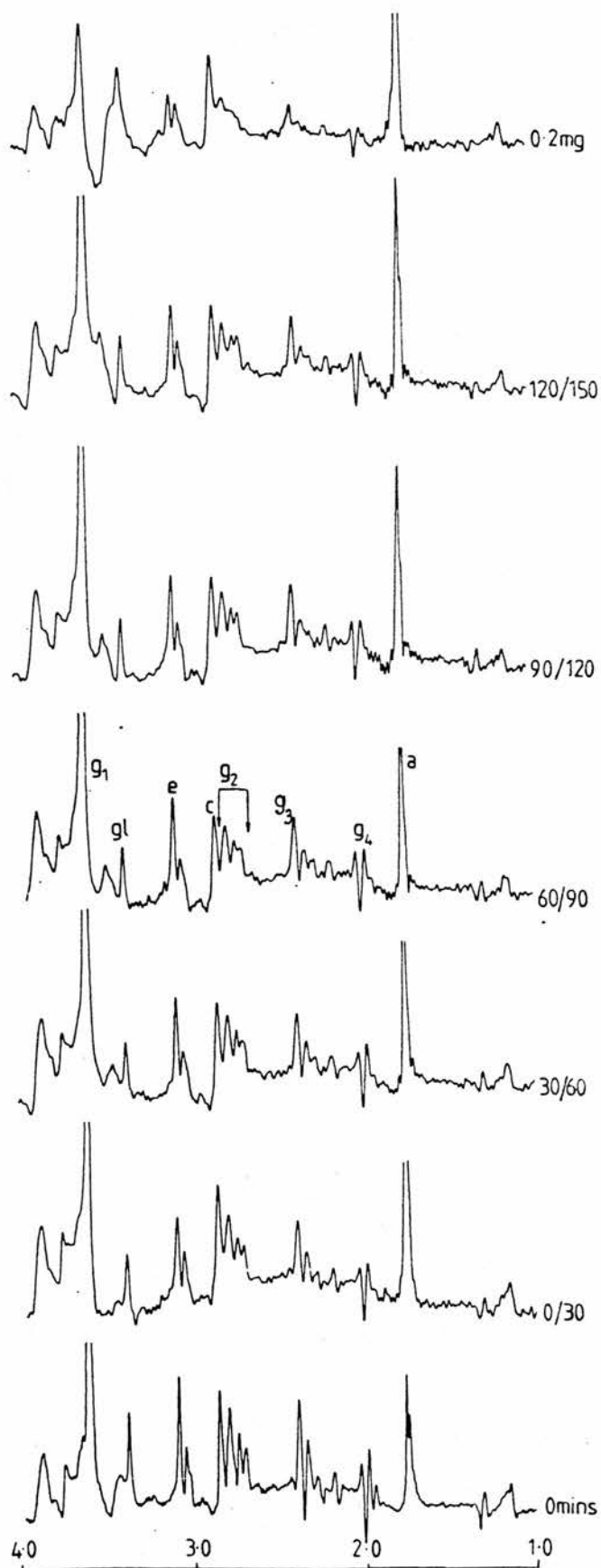
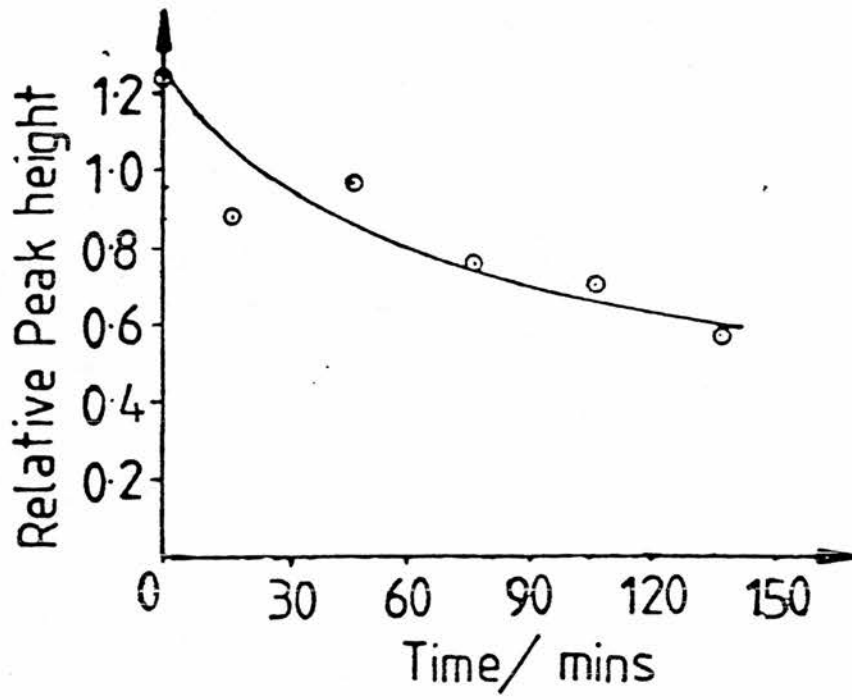


Figure 4 : Plot of relative peak heights of glutathione  $g_2$  signal  
(referenced against  $g_3$  signal) vs. time



resonance, referenced to the  $g_3$  resonance of glutathione (representing both GSH and GSSG). The plot of GSH levels against time (Figure 4) indicates increasing oxidation of intracellular GSH to GSSG during the incubation period. Approximately 150 minutes after addition of NP, the GSH concentration had decreased to one half of the original level.

After 150 minutes the dose of NP was increased to 1.33 mM and rapid depletion of reduced GSH was apparent. Additionally, ergothionine levels were lowered; the role of ergothionine in erythrocyte metabolism is not fully understood but similar depletion of cell ergothionine levels has been reported to be indicative of oxidative stress upon incubation of erythrocytes with dimethylarsonic acid.<sup>35</sup>

The cell response to the second addition of NP suggests that this dose (1.33 mM NP) is close to the defence capacity of the red cell, representing a reaction stoichiometry of approximately 1 NP : 2 GSH if the GSH concentration in red cells is 2.76 mM.<sup>34</sup>

After increasing the NP dose to 1.33 mM, spectral sensitivity was noticeably reduced. This observation can be attributed to formation of paramagnetic cyanoferrate complexes *within*\* the erythrocytes; studies in buffered solution (Chapter 6) have shown that NP reacts with GSH to form GSSG and  $[\text{Fe}^{\text{II}}(\text{CN})_6]^{4-}$  via the paramagnetic species  $[\text{Fe}(\text{CN})_4\text{NO}]^{2-}$ . Similarly, carbon-13 nmr spectra of alkaline

\* Paramagnetic species in the *extra* cellular space will not affect the resolution of spin-echo spectra of *intra* cellular molecules.

NP and N-acetylcysteine reaction solutions in the presence of air were subject to decreased signal to noise ratios, presumably arising from formation of  $[\text{Fe}(\text{CN})_4\text{NO}]^{2-}$ .

### 7.2.2 Transport of nitroprusside across erythrocyte membranes

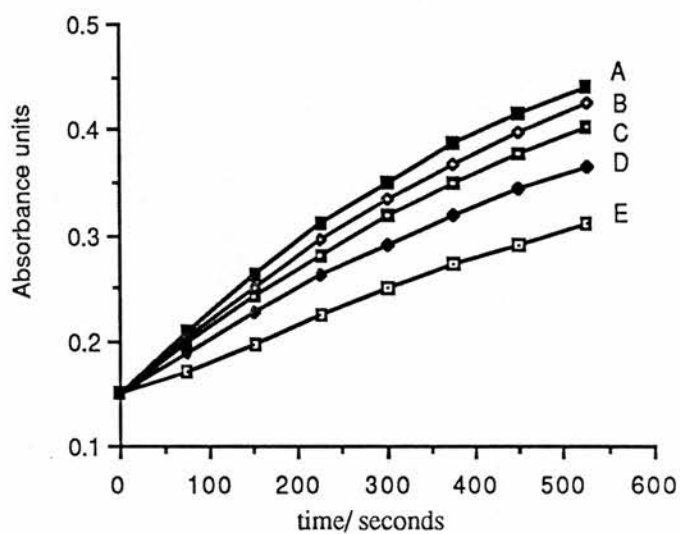
(The experiments in this section were conducted in the Department of Biochemistry, University of St. Andrews, with the assistance of Dr. I. Hunter and Mr. J. Hunter.)

Carbon-14 labelled nitroprusside was incubated at 37 °C with freshly obtained erythrocytes suspended in isotonic buffer. After 20 minutes, an aliquot of solution was removed and the erythrocytes were isolated by several careful washings with a vast excess of an ice cold isotonic NP solution. The intracellular fraction released upon lysing the cells contained 0.6% of the total activity of the aliquot. After 3 hours, 3.0% of the total activity of an aliquot treated in the same manner was detected in the intracellular fraction. Although there is apparently no transport of hexacyanoferrate(III) across the erythrocyte membrane,<sup>36</sup> the above experiments indicate that NP does cross the erythrocyte membrane.

### 7.2.3 Kinetic studies of the inhibition of the catalytic activity of papain by nitroprusside

Papain activity at pH 7.5 was determined by monitoring the hydrolysis of N-benzoyl-L-arginine ethyl ester (BAEE), according to an established procedure.<sup>37</sup> The inhibition of papain by cyanate, a known<sup>10</sup> inhibitor, was recorded but at

**Figure 5** : Plot of absorbance due to BAEE<sup>a</sup> vs. time for the inhibition<sup>b</sup> of papain<sup>c</sup>



a.  $[BAEE] = 1.24 \times 10^{-3} \text{ M}$

b.	$10^3$ [inhibitor] / M	plot	incubation/ minutes
	0.0 (control)	A	0
	0.15 (NP)	B	18
	3.0 (MeNO <sub>2</sub> )	B	17
	3.0 (NO <sub>2</sub> <sup>-</sup> )	C	23
	3.0 (NP)	D	0
	3.0 (NP)	E	21

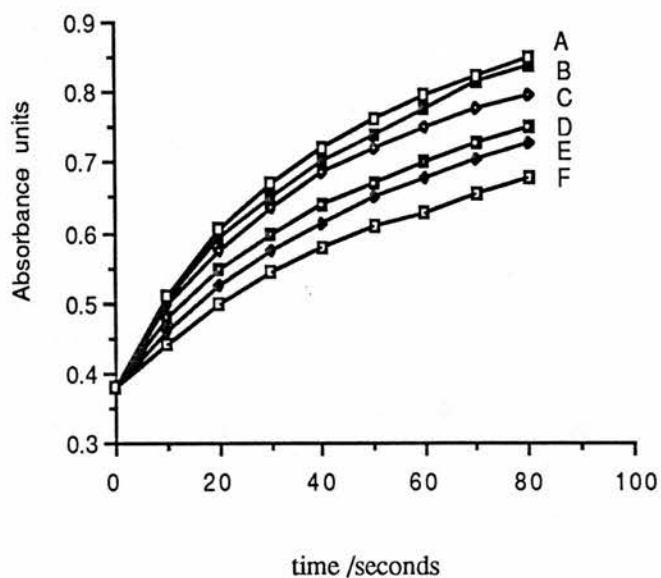
c.  $[papain] = 5.36 \times 10^{-6} \text{ M}$

similar concentrations nitroprusside inhibited papain only marginally and after long incubation times. At higher proportions of nitroprusside to papain (e.g. 560 : 1, figure 5), nitroprusside was found to inhibit papain. Additionally, nitroprusside inhibited papain at concentrations for which there was no detectable inhibition by comparable solutions of nitrite or nitromethane. It is interesting that the greater papain inhibition by nitroprusside than nitromethane and nitrite parallels the order of efficacy of these compounds as hypotensive agents, thought to effect hypotension through reactions with guanylate cyclase thiol groups.<sup>38,39</sup>

The inhibition of papain by thiol-blocking reagents has been studied and papain inactivation by the substrate  $p\text{-MeC}_6\text{H}_4\text{SO}_2\text{NHCH}_2\text{COCH}_2\text{Cl}$  has been shown to arise from alkylation of the thiol residue.<sup>9</sup> Selenosulphates ( $\text{RSeSO}_3^-$ ), reactive towards cysteine but non-reactive towards histidine, reversibly inhibited the papain catalysed hydrolysis of BAEE.<sup>40</sup> Thiol inhibition by selenosulphates is further supported by the absence of trypsin inhibition, an enzyme of similar function but with a serine residue as the catalytic centre instead of cysteine.<sup>40</sup>

Nitroprusside reacts rapidly with thiols,<sup>29</sup> more slowly with amines,<sup>24</sup> and not to any detectable extent with carboxyl groups. On this basis it seems reasonable to assume that the observed inhibition of papain by nitroprusside is due to reaction with cysteine-25, not the other residues occurring in the active site. Additionally, NP did not detectably inhibit trypsin catalysed hydrolysis of BAEE even at high proportions of NP to enzyme (e.g. 1000 : 1).

**Figure 6 :** Plot of absorbance due to  $\text{NAD}^+$  **a** vs. time for the inhibition **b** of GAPDH<sup>c</sup>



a.  $[\text{NAD}^+] = 1.50 \times 10^{-3} \text{ M}$

b.	$10^3$ [inhibitor]/ M	plot	incubation/ minutes
	0	A	0
	3.3 (NP)	A	20
	16.6 ( $\text{EtNO}_2$ )	B	17
	16.6 ( $\text{NO}_2^-$ )	C	16
	16.6 (NP)	D	1
	8.3 (NP)	E	14
	16.6 (NP)	F	16

c.  $[\text{GAPDH}] = 2.79 \times 10^{-7} \text{ M}$

#### 7.2.4 Molecular modelling of nitroprusside and papain

It is apparent from a representation of papain (Photograph 1) that cysteine-25 is not imbedded within the protein structure. The accessibility of cysteine-25 to nitroprusside can be better assessed in Photograph 3 showing NP in the same scale as a window of all the atoms within  $10 \text{ \AA}$  (in  $\pm x$ ,  $\pm y$ ,  $\pm z$  directions) of the cysteine-25 sulphur atom. Photograph 4 shows NP at the same scale as the residues known<sup>41</sup> to border the active site. These models demonstrate that there is no steric impediment to the reaction of NP with cysteine-25 of papain.

#### 7.2.5 Kinetic studies of the inhibition of the catalytic activity of GAPDH by nitroprusside

Glyceraldehyde-3-phosphate dehydrogenase (GAPDH), unlike papain, did not require activation and reactions of NP with GAPDH were thus suitable for epr and carbon-13 nmr experiments requiring more concentrated solutions as well as inhibition studies. The activity of GAPDH was determined by monitoring the increase in absorbance at 340 nm due to the reduction of NAD, a standard procedure.<sup>42</sup> It was found that a fifteen to twenty minute incubation of the enzyme solution with NP prior to initiation of the reaction by addition of the substrate glyceraldehyde-3-phosphate resulted in significant inhibition of enzyme activity at pH 7.5 (Figure 6).

Inhibition of GAPDH by other compounds that react with thiol groups has been reported in the literature and inhibition has been assumed to arise from interaction with the essential thiol group of the active site. GAPDH and other thiol-containing

enzymes are known<sup>43</sup> to be sensitive to certain platinum complexes. Nitroglycerin, a hypotensive agent thought to have the same mode of action as NP, reportedly reacts with thiols in alkaline conditions and inhibits GAPDH,<sup>42</sup> for which inhibition by nitrate has also been recorded.<sup>44</sup>

The activity of GAPDH decreased with NP dose (Figure 6) and comparison of GAPDH inhibition by NP and by the known inhibitor nitrate suggests that NP is a much more effective inhibitor at the same concentrations (not shown). Moreover, NP seems to be a more effective inhibitor of GAPDH than the related hypotensive agents, nitroethane or nitrite (Figure 6).

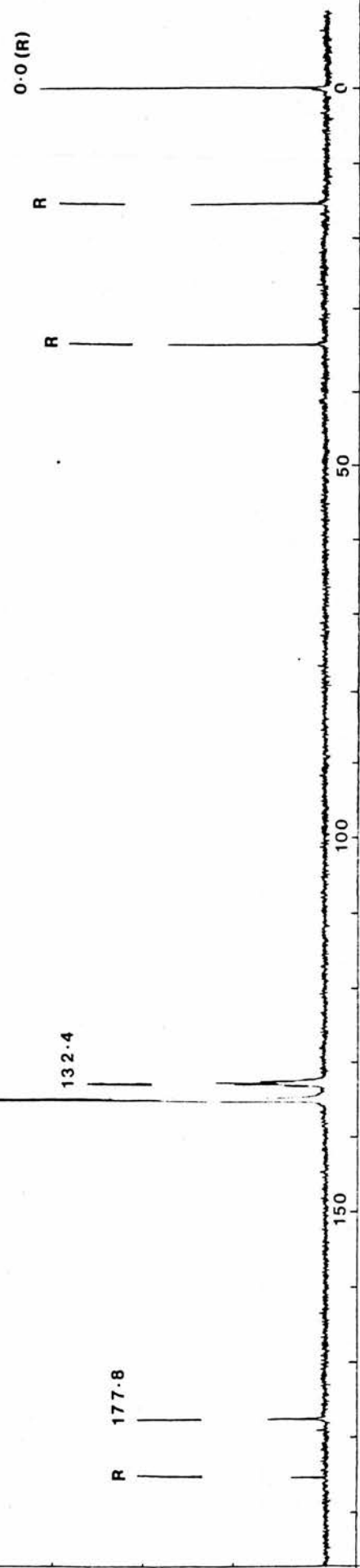
#### 7.2.6 Molecular modelling of nitroprusside and GAPDH

In a representation of two of the four GAPDH subunits (Photograph 2) the essential thiol (cysteine-149) of each subunit is located towards the centre of the enzyme (middle of Photograph 2), and as such are not imbedded within the protein structure. The accessibility of the active site to nitroprusside can be better assessed in Photograph 5 showing NP in the same scale as a window of all the atoms within 10 Å (in  $\pm x$ ,  $\pm y$ ,  $\pm z$  directions) of the cysteine-149 sulphur atom. The unreactive thiol cysteine-153 can also be discerned, close to cysteine-149, but clearly remote from the active site. In Photograph 6, NP is shown at the same scale as the residues known<sup>14</sup> to border the active site. These photographs demonstrate that there is no steric impediment to the reaction of NP with cysteine-149 of GAPDH.

BRUNNE

PCJULLS.M01  
DATE 25.2.87  
SF 25.469  
SY 112.0  
G1 6800.000  
G2 8298  
G3 8268  
G4 16518.513  
H2OFF 1.134  
F1 2.0  
F2 1.500  
F3 0.885  
F4 0.440  
F5 0.416  
F6 0.334  
FM 25.000  
D2 5600.000  
D1 16H CFD  
LB 2.000  
GB 0.0  
CY 55.00  
CF 0.0  
F1 200.560F  
F2 10.250F  
M2/CM 454.142  
PPH/CM 6.016  
SR -1419.40

Figure 7: Carbon-13 nmr spectrum of a reaction solution of glyceraldehyde-3-phosphate dehydrogenase (GAPDH) and an excess of 90% carbon-13 labelled nitroprusside



R=Reference:  
Na [3-(trimethylsilyl)propionate]

### 7.2.7 Epr and carbon-13 nmr studies of the reaction of nitroprusside with GAPDH

(The experiments in this section were conducted in collaboration with Ian Johnson at the University of St. Andrews.)

The epr spectra of a degassed solution of NP (0.5 M) added to solid GAPDH (12 mg,  $3.2 \times 10^{-4}$  M) in phosphate buffer (pH 7.4, I = 0.1) were recorded over one day. No signal was observed upon mixing but after two hours a strong three line signal was recorded and at this time it was noticed that the solution, originally clear, had become turbid. After five hours the signal intensity was unchanged. The three line signal observed was identical to that observed on previous occasions following the reduction of NP with thiols (Chapter 6) and corresponds to the species  $[\text{Fe}(\text{CN})_4\text{NO}]^{2-}$ .<sup>45</sup>

Similarly, no signal other than nitroprusside was observed in the carbon-13 nmr spectrum of a nitrogen-saturated solution of 90% carbon-13 labelled NP and GAPDH shortly after mixing. Within several hours turbidity was apparent and in the spectrum (Figure 7) recorded after filtering and storing the solution under a nitrogen atmosphere and in complete darkness for several weeks, a singlet at 177.8 corresponding to hexacyanoferrate(II),  $[\text{Fe}(\text{CN})_6]^{4-}$ ,<sup>46</sup> was apparent in addition to a signal for unreacted NP.

### 7.3 DISCUSSION

The reactions of nitroprusside with a range of thiols were investigated in Chapter 6 and it was shown that the reactions, in buffered solution, occur by a common mechanism (Scheme 1). In all of these reactions the products were the disulphide and hexacyanoferrate(II), formed by ligand rearrangement of the paramagnetic species  $[\text{Fe}(\text{CN})_4\text{NO}]^{2-}$ . In the absence of oxygen the reactions proceeded to completion with a 1 : 1 stoichiometry but in the presence of air, NP acted as a catalyst for thiol oxidation by recycling of  $[\text{Fe}(\text{CN})_4\text{NO}]^{3-}$  to NP (Scheme 1).

There is little doubt that the reaction of NP with GSH to form GSSG and hexacyanoferrate(II) proceeds by exactly the same mechanism within erythrocytes as in aqueous solution. The reduced spin-echo spectral sensitivity indicated that the paramagnetic species  $[\text{Fe}(\text{CN})_4\text{NO}]^{3-}$  was present *within* the cells, and the apparent reaction stoichiometry of 1 NP : 2 GSH, the same as observed for the reaction of NP with GSH in buffer (Chapter 6), reflects the presence of oxygen. This evidence indicates a substantial proportion of the nitroprusside ions cross the red cell membrane at this concentration.

The apparently low transport rate of NP into red blood cells<sup>25</sup> determined by the experiments with carbon-14 labelled NP can be rationalised by consideration of the toxic effects of NP on cells. The initial concentration of carbon-14 labelled NP in the transport experiments was 9.4 mM, significantly higher than 3.3 mM for which signs of cell

death were observed in the initial spin-echo spectra ( $\tau = 60$  ms). As the transport of NP is likely to be affected by cell viability, high doses of NP will reduce the proportion of ions transported.

The inhibition of papain and GAPDH by NP indicates that NP reacts with the active site cysteine residues of each enzyme, both well documented as enzymes containing essential thiol groups. Molecular modelling studies of papain and GAPDH indicate that there is no steric impediment to reaction of NP at either active site. There is evidence that the mechanism for the reaction of NP with cysteine residues of enzyme active sites is the same as the reaction of NP with cysteine in buffered solution and with intracellular glutathione (Scheme 1). The paramagnetic intermediate  $[\text{Fe}(\text{CN})_4\text{NO}]^{3-}$  and diamagnetic product hexacyanoferrate(II) were recorded in epr and nmr spectra, respectively, of NP and GAPDH reaction solutions. The turbidity observed several hours after adding a solution of NP to GAPDH suggests denaturation of the enzyme giving rise to a change in enzyme solubility. It is likely that this arises from formation of a disulphide; presumably from reaction of the essential thiol with adjacent cysteine-153 which has been associated with irreversible conformational changes in the enzyme.<sup>9</sup> With regard to the steric requirements of the enzyme it is not surprising that no signal for  $[\text{Fe}(\text{NO})_2(\text{SR})_2]^-$  (observed for SR = SH, SMe, cysteine, N-acetylcysteine, N-acetyl- $\beta$ -methylcysteine, N-acetylpenicillamine (Chapter 6)) was detected upon reaction with NP.

The origin of the apparent time dependence of both papain and GAPDH inhibition by nitroprusside (Figures 5 and 6) can be explained in two ways. While the reaction of nitroprusside with isolated thiols is extremely rapid, the rate of reaction with enzyme thiols may be susceptible to the steric requirements and accessibility of the active site. A slightly decelerated formation of the adduct of NP and (sterically hindered) penicillamine was recorded,<sup>29</sup> in comparison with the rates of formation of other NP and thiolate adducts.

However, if presuming reasonably rapid NP and enzyme adduct formation by analogy with other thiols, it seems more likely that the increase in degree of inhibition with incubation time may reflect not the rate of adduct formation but instead the rate of adduct *decomposition*. It is known that adduct formation is an equilibrium process and therefore subject to competition with the substrate for the active site, but the duration and unchanged intensity of the epr signal of  $[\text{Fe}(\text{CN})_4(\text{NO})]^{3-}$ , established in separate experiments to be a relatively short-lived species, indicates that irreversible decomposition of the adduct, *via*  $[\text{Fe}(\text{CN})_4\text{NO}]^{2-}$ , to hexacyanoferrate(II) and the corresponding disulphide is slow. Consequently, if it is the oxidation of the thiol function to the disulphide and not adduct formation itself that inhibits enzyme activity, then the longer the reaction of NP and enzyme thiol proceeds in the absence of substrate the greater will be the degree of inhibition observed.

The results presented above indicate that the reactions of NP with intracellular glutathione and the thiol containing

enzymes papain and GAPDH are consistent with Scheme 1, proposed in Chapter 6 for the reaction of NP with thiols in physiologically relevant conditions. With regard to the medical use of NP it is important to note that at no time has the release of free cyanide been detected following the reaction of NP with thiols in accordance with this scheme. It is interesting that NP is significantly more reactive towards enzymic thiols, e.g. a more effective inhibitor of both papain and GAPDH, than nitrite, nitromethane or nitroethane, also known hypotensive agents. The superiority of NP to these agents as an inhibitor of thiol-containing enzymes parallels the order of efficacy of these compounds as hypotensive agents. Additionally, the reaction of NP with thiols results in NO release, albeit rather slow. These observations are consistent with reports implicating thiols in the modulation of the activity of guanylate cyclase, the enzyme through which NO-releasing agents are thought to act.

## 7.4 EXPERIMENTAL

### *Materials and instruments*

Glutathione, papain (types III and IV), BAEE, dithiothreitol, trypsin (type IX, porcine pancreas), GAPDH (rabbit muscle),  $\text{NAD}^+$ , and  $\text{Na}_2\text{HAsO}_4$  were obtained from Sigma and used without further purification. Samples of carbon-14 labelled sodium nitroprusside were prepared by Dr. Alexis Roberts McIntosh<sup>30</sup>. DL-glyceraldehyde-3-phosphate was prepared from the monobarium salt of DL-glyceraldehyde-3-phosphate, diethylacetal, according to the standard procedure described by the suppliers (Sigma). All other reagents, with the exceptions of those prepared as described below, were of AnalaR grade where available.

Solid sodium nitroprusside was stored in a dark cupboard. All solutions containing nitroprusside were protected from light with a complete covering of aluminium foil during storage and use.

Spin-echo experiments were conducted by John Reglinski at the University of Strathclyde on a Bruker 250 MHz instrument in the FT mode at 20 °C. A 90- $\tau$  - 180- $\tau$  pulse sequence ( $\tau$  = either 40 ms or 60 ms) was used and the data from 2000 complete pulse sequences were accumulated for each Fourier transform.

Carbon-13 nmr experiments were recorded on a Bruker AM 300 spectrometer in the FT mode at 25 °C with a carbon resonance of 75 MHz in a field of 7.04 T. The number of scans was 31,000 with a pulse width of 2.0  $\mu$  seconds and a delay time of 1.5 seconds. The reference was the sodium salt of

3-(trimethylsilyl)propanesulphonate but all chemical shifts quoted refer to TMS.

The epr experiments were conducted by Ian Johnson in a quartz capillary at room temperature using a Bruker ER 200D spectrometer. Di-*t*-butyl-nitroxide was used as the standard for the measurement of the line positions.

Radioactive counting was conducted on an EMI NE LSC-2 liquid scintillation counter. The solutions for counting were made up with a pseudocumene scintillation cocktail (NE 265 from EMI). Enzyme assays were conducted with a thermostatically controlled Pye Unicam SP8 100 spectrophotometer.

All atomic parameters and structural data for molecular modelling were obtained from the Daresbury Laboratory Chemical Databank Service, a service of the S.E.R.C. The program Chem-X, developed and distributed by Chemical Design Ltd., Oxford, was used to display and manipulate structures in conjunction with a Tektronics 4107 colour terminal linked to a VAX 11/785 computer.

## *Methods*

### Preparation of erythrocyte samples for spin-echo nmr

(The erythrocyte samples were prepared by Dr. J. Reglinski at the University of Strathclyde.)

The erythrocytes were obtained from venous blood collected in heparinised tubes. The blood was centrifuged at 3000 rpm for 5 minutes at 4 °C and after the plasma was drawn off the packed cells were washed two times with isotonic  $^2\text{H}_2\text{O}$  saline (0.154 M in NaCl). Packed erythrocytes

(0.4 ml) were placed in a 5 mm nmr tube with acetate (0.1 ml, 1.0 mg/ml) as internal reference (1.764 p.p.m. with respect to TMS). The assignments of the resonances due to GSH, GSSG, ergothioneine, glycine, creatine and lactate follow those of previous studies.<sup>31-34</sup>

#### Erythrocyte transport experiments

(Erythrocyte transport experiments were conducted at the Department of Biochemistry, University of St. Andrews, with the assistance of Dr. I. Hunter and Mr. J. Hunter.)

The erythrocytes were obtained from fresh venous blood collected in heparinised tubes. The blood was centrifuged at 1800 rpm for 5 minutes at 4 °C and after the plasma was drawn off the packed cells were washed two times with isotonic phosphate buffer. The cells (9.0 ml) were then resuspended in isotonic buffer (9.0 ml). An aliquot (0.90 ml) of a solution of carbon-14 labelled sodium nitroprusside (0.0500 g, 0.167 mmol, 10.20  $\mu\text{C}_i$ ) in isotonic phosphate buffer (1.00 ml) was added to most of the cell solution (16.0 ml) and the resulting solution was gently shaken in the dark at 37 °C. After 30 minutes of incubation an aliquot (0.40 ml) of the erythrocyte and NP solution was removed and cold isotonic NP solution (25.0 ml) was added. The solution was centrifuged at 1800 rpm for 10 minutes at 4 °C. The washing was carefully removed and stored in the dark. Three additional washes were conducted following the same procedure. After the final wash the packed cells were lysed and deproteinated with a solution of trifluoroacetic acid; the total volume was 6.0 ml. This solution was centrifuged as before and the supernatant was

collected. The pellet was washed two additional times; total volumes 16.2 ml. The above procedures were repeated for an aliquot removed after a three hour incubation period.

The activity of each supernatant and washing was counted by addition of an aliquot of sample (typically 1.00 ml) to the liquid scintillation cocktail (final volume 10 ml). It had previously been established that there was no significant quenching of the measured activity at the concentrations of NP used in these experiments. When counting the activities of the washings and supernatants, it was possible to account for all the activity of the sample.

#### Papain assay

Papain activity at 30 °C was determined after activation following an established procedure.<sup>37</sup> In a standard experiment, papain was eluted from a sephadex column (G25) with phosphate buffer (pH 7.5, I = 0.1, containing 10 mM EDTA) following activation of papain (2.5 mg, 60 units) in buffer (0.4 ml) with dithiothreitol (2.4 mg) at room temperature for one hour. The concentration of this enzyme 'stock' solution was determined from the absorbance at 278 nm. Temperature-equilibrated enzyme stock solution (1.0 ml,  $1.34 \times 10^{-5}$  M) was added to water or an inhibitor solution (1.0 ml) and left to incubate. The reaction was initiated by addition of temperature-equilibrated BAEE (0.5 ml,  $6.2 \times 10^{-3}$  M) and the change in absorbance at 263 nm, read against a BAEE reference ( $1.24 \times 10^{-3}$  M), was recorded.

#### Trypsin assay

Trypsin activity at 30 °C was determined by a standard

procedure.<sup>47</sup> NP (up to  $2.7 \times 10^{-4}$  M) was incubated with trypsin ( $2.8 \times 10^{-7}$  M) at 21 °C for twenty minutes in phosphate buffer (pH 7.5, I = 0.1, containing 10 mM EDTA). BAEE ( $1 \times 10^{-3}$  M) was added to initiate the reaction, and BAEE hydrolysis was followed as detailed above for the papain assay.

#### Preparation of DL-glyceraldehyde-3-phosphate solution

DL-Glyceraldehyde-3-phosphate, diethylacetal, monobarium salt (100 mg) was added to Dowex-50 hydrogen form resin (1.5 g) in water (6.0 ml). The mixture, in a test tube, was immersed in boiling water for three minutes and shaken intermittently. The mixture was then chilled quickly by transferring the tube to an ice bath, and after several minutes was centrifuged. The supernatant fluid was decanted and the resin was resuspended in water (2 ml). The washing procedure was repeated several times to completely extract free DL-glyceraldehyde-3-phosphoric acid (200  $\mu$  moles) in the supernatant fluid.

#### GAPDH assay

The activity of GAPDH at 30 °C was determined by monitoring the change in absorbance at 340 nm, due to the reduction of NAD.<sup>42-44</sup> An enzyme 'stock' solution was prepared with GAPDH (105 units,  $8.77 \times 10^{-9}$  mol), NAD (35.8 mg,  $4.8 \times 10^{-5}$  mol) and  $\text{Na}_2\text{HAsO}_4$  (4.8 ml, 1.0 M solution) in phosphate buffer (pH 7.32, I = 0.1, containing 10 mM EDTA), total volume 24.8 ml. For each experiment water or a solution of the inhibitor (0.2 ml) was added to temperature-equilibrated

enzyme 'stock' solution (1.9 ml) and following incubation the reaction was initiated by the addition of temperature-equilibrated glyceraldehyde-3-phosphate solution (0.3 ml, 2 mM).

## REFERENCES

1. E. H. Ohlstein, K. S. Wood, and L. J. Ignarro, *Arch. Biochem. Biophys.*, 1982, **218**, 187.
2. L. J. Ignarro, B. K. Barry, D. Y. Gruetter, E. H. Ohlstein, C. A. Gruetter, P. J. Kadowitz, and W. H. Baricos, *Biochim. Biophys. Acta*, 1981, **673**, 394.
3. L. J. Ignarro, P. J. Kadowitz, and W. H. Baricos, *Arch. Biochem. Biophys.*, 1981, **208**, 75.
4. H. J. Brandwein, J. A. Lewicki, and F. Murad, *J. Biol. Chem.*, 1981, **256**, 2958.
5. L. J. Ignarro and C. A. Gruetter, *Biochim. Biophys. Acta*, 1980, **631**, 221.
6. J. C. Edwards, B. K. Barry, D. Y. Gruetter, E. H. Ohlstein, W. H. Baricos, and L. J. Ignarro, *Biochem. Pharm.*, 1981, **30**, 2531.
7. P. C. Jocelyn, 'Biochemistry of the SH Group', Academic Press Inc., London, 1972, p.3.
8. G. Lowe, *Tetrahedron*, 1976, **32**, 291 and references therein.
9. A. N. Glazer and E. L. Smith in 'The Enzymes', 3rd Edn., (P. Boyer, Ed.) Academic Press Inc., London, 1971, Vol. III, pp. 502-546 and references therein.
10. L. A. AE. Sluyterman, *Biochim. Biophys. Acta*, 1967, **135**, 439.
11. K. G. D. Allen, J. A. Stewart, P. E. Johnson and D. E. Wettlaufer, *Eur. J. Biochem.*, 1978, **87**, 575.
12. S. D. Lewis, F. A. Johnson, A. K. Ohno, and J. A. Shafer, *J. Biol. Chem.*, 1978, **253**, 5080.
13. Ref. 7, p.204.

14. J. I. Harris and M. Waters in 'The Enzymes', 3rd Edn., (P. D. Boyer, Ed.), Academic Press Inc., London, 1976, Vol. XIII, pp. 1 - 50.
15. W. P. Arnold, D. E. Longnecker, and R. M. Epstein, *Anaesthesiology*, 1984, **61**, 254.
16. V. Schulz, *Clin. Pharmacokinetics*, 1984, **9**, 239.
17. T. Pasch, V. Schulz, and G. Hoppelhäuser, *J. Cardiovasc. Pharm.*, 1983, **5**, 77.
18. J. R. Krapez, C. J. Vesey, L. Adams, and P. V. Cole, *Brit. J. Anaesth.*, 1981, **53**, 793.
19. C. J. Vesey, P. J. Simpson, L. Adams, and P. V. Cole, *Brit. J. Anaesth.*, 1979, **51**, 89.
20. H. E. Spiegel and V. Kucera, *Clin. Chem.*, 1977, **23**, 2329.
21. F. L. Rodkey and H. A. Collison, *Clin. Chem.*, 1977, **23**, 1969.
22. R. P. Smith and H. Kruszyna, *J. Pharm. Exp. Therap.*, 1974, **191**, 557.
23. C. J. Vesey, J. R. Krapez, and P. V. Cole, *J. Pharm. Pharmacol.*, 1980, **32**, 256.
24. A. R. Butler, C. Glidewell, J. Reglinski and A. Waddon, *J. Chem. Res. (S)*, 1984, 279.
25. W. I. K. Bisset, M. G. Burdon, A. R. Butler, C. Glidewell, and J. Reglinski, *J. Chem. Res. (M)*, 1981, 3501.
26. W. I. K. Bisset, A. R. Butler, C. Glidewell, and J. Reglinski, *Br. J. Anaesth.*, 1981, **53**, 1015.
27. A. R. Butler, C. Glidewell, J. McGinnis and W. I. K. Bisset, *Clin. Chem.*, 1987, **33**, 490.
28. Ref. 7, pp. 240 - 257.

29. M. D. Johnson and R. G. Wilkins, *Inorg. Chem.*, 1984, **23**, 231.
30. A. S. Roberts McIntosh, Ph.D. Thesis, University of St. Andrews, 1986.
31. D. L. Rabenstein and A. A. Isab, *FEBS Lett.*, 1980, **121**, 61.
32. F. F. Brown, I. D. Campbell, P. W. Kuchel, and D. L. Rabenstein, *FEBS Lett.*, 1977, **82**, 12
33. C. N. N. McKay, D. H. Brown, J. Reglinski, W. E. Smith, H. A. Capell, and R. D. Sturrock, *Biochim. Biophys. Acta*, 1986, **888**, 30.
34. D. L. Rabenstein, D. W. Brown, and C. J. McNeil, *Analy. Chem.*, 1985, **57**, 2294.
35. J. R. Reglinski and W. E. Smith, private communication.
36. R. K. Mishra and H. Passow, *J. Membrane Biol.*, 1969, **1**, 214.
37. J. R. Whitaker and M. L. Bender, *J. Am. Chem. Soc.*, 1965, **87**, 2728.
38. H. Schröder, E. Noack, and R. Müller, *J. Mol. Cell. Cardiol.*, 1985, **17**, 931.
39. L. J. Ignarro, H. Lipton, J. C. Edwards, W. H. Baricos, A. L. Hyman, P. J. Kadowitz and C. A. Gruetter, *J. Pharm. Exp. Therap.*, 1981, **218**, 739.
40. A. R. Scarf, E. R. Cole, and P. T. Southwell-Keely, *Biochem. J.*, 1982, **201**, 305.
41. J. Drenth, J. N. Jansonius, R. Koekoek, and B. G. Wolthers, in 'Advances in Protein Chemistry', (C. B. Anfinsen, J. T. Edsall, and F. M. Richards, eds.) Academic Press Inc., 1971, vol. 25, 103 - 105.

42. B. Jakschik and P. Needleham, *Biochem. Biophys. Res. Comm.*, 1973, **53**, 539.
43. J. L. Aull, R. L. Allen, A. R. Bapat, H. H. Daron, M. E. Friedman, and J. F. Wilson, *Biochim. Biophys. Acta*, 1979, **571**, 352.
44. A. Orsi and W. W. Cleland, *Biochemistry*, 1972, **11**, 102.
45. C. Glidewell and I. L. Johnson, *Inorg. Chim. Acta*, in press.
46. A. R. Butler, C. Glidewell, A. S. McIntosh, D. Reed, and I. H. Sadler, *Inorg. Chem.*, 1986, **25**, 970.
47. G. W. Schwert and Y. Takenaka, *Biochim. Biophys. Acta*, 1955, **16**, 570.

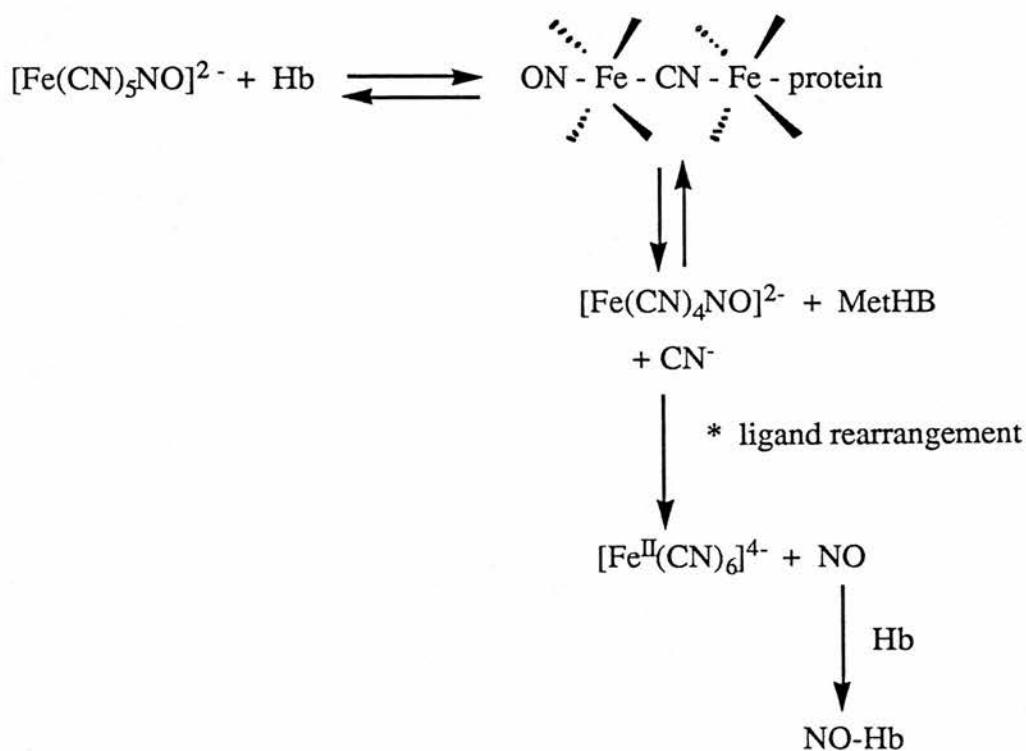
C H A P T E R    8

THE REACTIONS OF THE NITROPRUSSIDE ION

WITH THE HAEM ENZYMES CATALASE AND

LACTOPEROXIDASE

**Scheme 1** : Mechanism for the reaction of nitroprusside with haemoglobin  
 (Hb, MetHb and NOHb represent deoxy-, met-, and nitrosyl haemoglobins,  
 respectively)



\* ligand rearrangement of 6  $[\text{Fe}(\text{CN})_4\text{NO}]^{2-}$  and 6  $\text{CN}^-$  results in formation of 5  $[\text{Fe}^{\text{II}}(\text{CN})_6]^{4-}$ , 6 NO and 1  $\text{Fe}^{2+}$

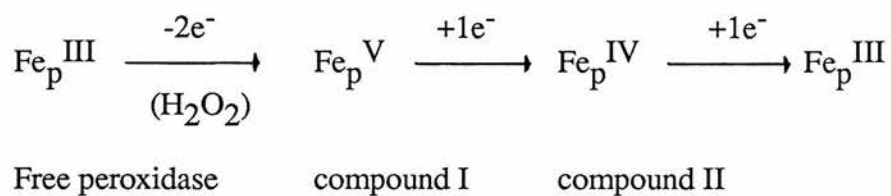
## 8.1 INTRODUCTION

The reactions of the nitroprusside ion (NP) with several nucleophiles have been considered as models for the reactions by which NP acts to effect hypotension. Thiols are one of the most reactive functional groups of the human body<sup>1</sup> and the reaction of NP with thiols is extremely rapid, suggesting a parallel with the rapid onset of the hypotensive action of NP upon infusion into the bloodstream. However, if it is the release of NO, not nitrosation of a functional group, that is the source of the hypotensive activity of NP then the NP and thiol system has some shortcomings as a model for the *in vivo* reaction of NP. The equilibrium between the NP and thiolate anion adduct and component thiol and NP is dominated by the back reaction and the release of NO occurs after decomposition of this adduct, a slow process (Chapter 6).

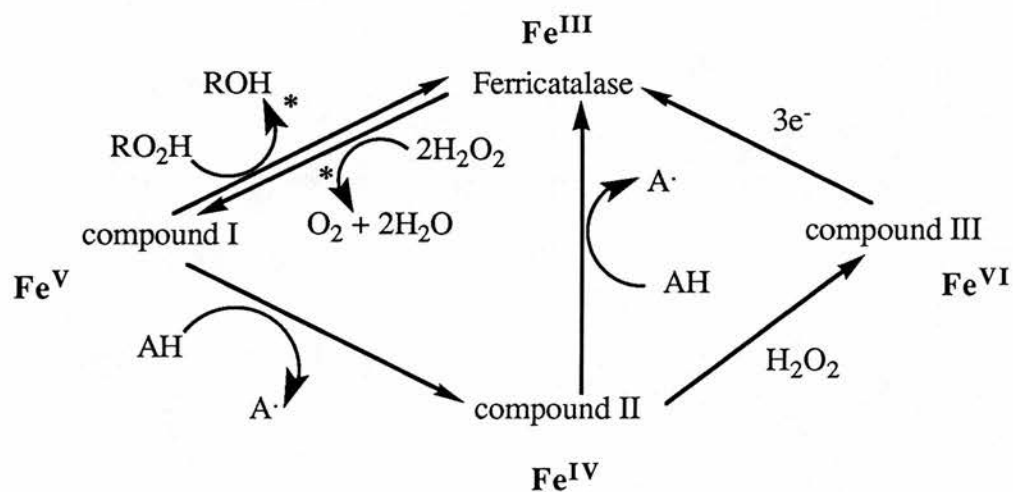
The reaction of NP with the intracellular thiol glutathione (GSH) in intact erythrocytes was investigated by spin-echo proton nmr (Chapter 7). There is evidence<sup>2-6</sup> that NP reacts with haemoglobin, the other major thiol-containing component of erythrocytes, but it was not possible to assess this reaction by spin-echo proton nmr. Recent investigations<sup>7</sup> of the reaction of NP with haemoglobin using carbon-13 nmr and epr spectroscopy support a mechanism involving reduction of NP by the **haem** group to yield the kinetically labile species  $[\text{Fe}(\text{CN})_4\text{NO}]^{2-}$  which undergoes ligand rearrangement to form hexacyanoferrate(II) (Scheme 1).

Transport and spin-echo nmr studies (Chapter 6) indicate that NP crosses the red cell membrane slowly, so it is not

**Scheme 2 : Reactions of lactoperoxidase**



**Scheme 3 : Catalytic reactions of catalase**



Compounds I, II, and III are enzyme peroxide derivatives, with the formal oxidation states indicated (\* denotes dominant reactions)

likely that the reaction of NP with haemoglobin contributes to the hypotensive activity of NP. However, there is evidence that guanylate cyclase, the enzyme through which NP and related NO-containing hypotensive agents mediate blood pressure, is activated by these agents only in the presence of a haem group.<sup>4,5,8</sup> It is known<sup>5,9,10</sup> that guanylate cyclase can be purified to homogeneity in a form containing a prosthetic haem and thus the reactions of NP with two readily available haem enzymes were investigated.

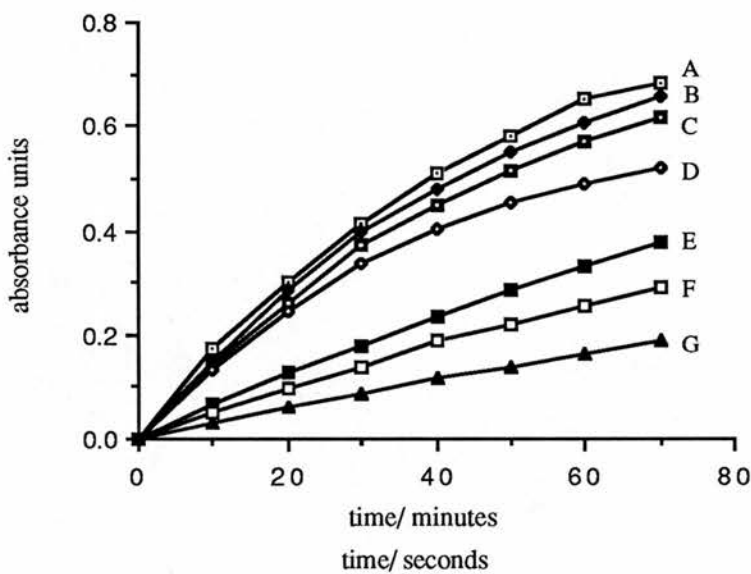
Peroxidase (EC 1.11.17, Donor: Hydrogen peroxide oxidoreductase) is a haem-bearing enzyme found in a variety of animal and plant tissues; the source used for this study was cow's milk, e.g. lactoperoxidase. The general reaction (Scheme 2) catalysed by the iron(III) haem group involves two-electron oxidation of the haem iron and decomposition of  $H_2O_2$  to water and  $O_2$ .<sup>11</sup> The standard assay for lactoperoxidase is the catalysed oxidation of pyrogallol to purpurogallin by  $H_2O_2$ , monitored by the increase in absorbance at 425 nm due to purpurogallin formation.<sup>12</sup>

The structure of lactoperoxidase has not been determined but the haem environment is thought to be similar to that of horseradish peroxidase.<sup>13</sup> The lactoperoxidase haem iron is in a crevice of the protein molecule and its sixth coordination site is vacant or occupied by a loosely associated water ligand. Lactoperoxidase inhibition by cyanide,  $HS^-$  and  $F^-$  is attributed to attachment of these ions at the sixth coordination site of the haem iron.<sup>14</sup> Lactoperoxidase has sixteen cysteine residues, thought to form eight disulphide bridges.<sup>15</sup>

The haem-bearing enzyme catalase (EC 1.11.16 hydrogen peroxide: hydrogen peroxide oxidoreductase) is present in nearly all aerobically respiring organisms and protects cells from the toxic effects of  $\text{H}_2\text{O}_2$  by catalysing its decomposition (Scheme 3). Catalase can oxidise a variety of compounds, such as ethanol, in the presence of  $\text{H}_2\text{O}_2$ .<sup>16</sup>

The structure of catalase has been determined and consists of four identical subunits. The sixth co-ordination site of the haem is vacant but the accessibility of the haem, in a crevice in the protein molecule, is limited by a channel 30 Å long and 15 Å wide.<sup>17</sup> The haem group of one catalase subunit is shown in Photograph 7.

**Figure 1** : Plot of absorbance due to purpurogallin<sup>a</sup> formation vs. time for the inhibition<sup>b</sup> of lactoperoxidase<sup>c</sup>



a. initial concentration of pyrogallol =  $2.72 \times 10^{-3}$  M

b. $10^3$ [inhibitor] / M	plot	incubation/ minutes
0.0 (Control)	A	0
7.6 ( $[\text{Fe}^{\text{II}}(\text{CN})_6]^{4-}$ )	B	0
7.6 ( $[\text{Fe}^{\text{II}}(\text{CN})_6]^{4-}$ )	C	30
76.0 ( $[\text{Fe}^{\text{II}}(\text{CN})_6]^{4-}$ )	D	0
1.5 (NP)	E	0
7.6 (NP)	F	0 and 30
76.0 (NP)	G	0

c. [lactoperoxidase] =  $1.23 \times 10^{-8}$  M

## 8.2 RESULTS

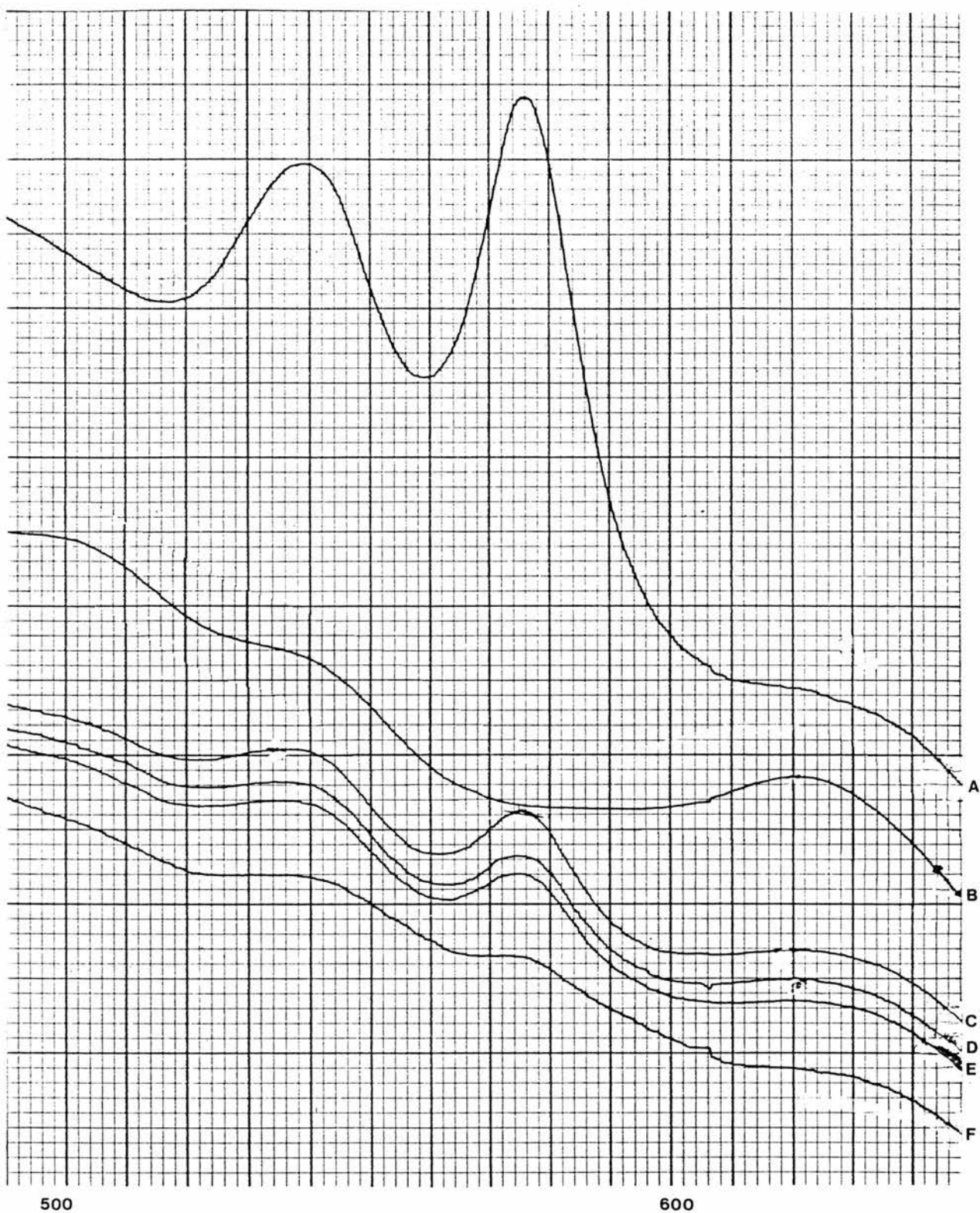
### 8.2.1 Inhibition of lactoperoxidase activity

Lactoperoxidase activity was measured in the presence of several cyanoferrate complexes. Addition of NP to enzyme solutions, followed by initiation of the reaction with  $H_2O_2$  and pyrogallol, markedly decelerated purpurogallin formation compared with the control (Figure 1). In a similar experiment, but with hexacyanoferrate(II) instead of NP, there was only a small depression of the rate of purpurogallin formation. At much higher concentrations of hexacyanoferrate(II) lactoperoxidase inhibition was more significant (Figure 1). It was not possible to determine the effect of hexacyanoferrate(III) on lactoperoxidase activity as independent observations established that this complex oxidises pyrogallol directly. In Figure 1 it is also apparent that there was no significant increase in the inhibition of lactoperoxidase by NP with incubation periods of up to thirty minutes.

### 8.2.2 Visible spectra of lactoperoxidase and cyanoferrate complexes

It was not possible to discern any change in the visible spectrum of lactoperoxidase upon incubation of NP, hexacyanoferrate(II), or hexacyanoferrate(III). However, small changes could have escaped detection as a result of the small amounts of enzyme available; the very low concentrations ( $3.05 \times 10^{-6}$  M) necessitated using the most sensitive spectrophotometer settings.

Figure 2



- |                                                                                                                           |                                |
|---------------------------------------------------------------------------------------------------------------------------|--------------------------------|
| A. genuine sample of NO-catalase                                                                                          | B. catalase                    |
| C. spectrum of nitroprusside ( $5.87 \times 10^{-3}$ M) and catalase ( $3.57 \times 10^{-5}$ M) five minutes after mixing | D. twenty minutes after mixing |
| E. thirty minutes after mixing                                                                                            | F. three hours after mixing    |

### 8.2.3 Attempted inhibition of catalase activity

It was not possible to detect any decrease in the activity of catalase upon incubation with NP or hexacyanoferrate(II) by following the rate of disappearance of  $H_2O_2$  ( $\lambda_{max}$  240 nm) added to an enzyme solution. The concentrations of these potential inhibitors were limited by overlap with the u.v. absorbance of  $H_2O_2$  and it is possible that at higher concentrations NP, if not hexacyanoferrate(II), inhibits catalase activity.

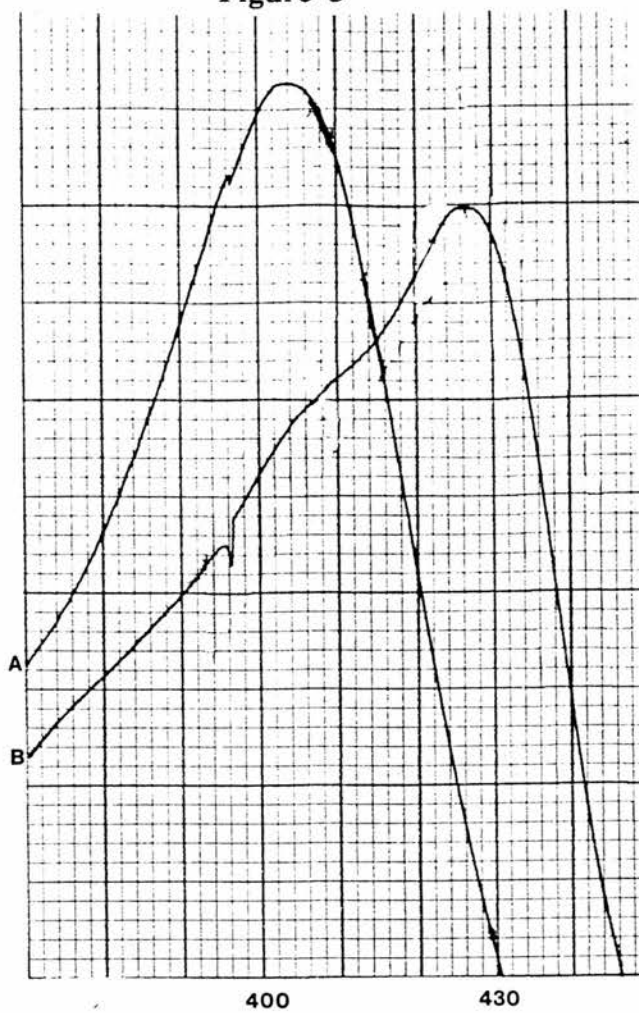
### 8.2.4 Visible spectra of catalase and cyanoferrate complexes

A 160-fold excess of NP was added to a solution of catalase (both solutions were made up with a phosphate buffer, pH 7.5) and the visible spectrum was recorded immediately. The resulting spectra (Figure 2) corresponded closely to both a spectrum of a genuine sample of the nitrosyl catalase complex (NO-catalase) prepared from catalase and NO (Figure 2) and literature values for the absorbance maxima of NO-catalase.<sup>18</sup> The absorbances due to NO-catalase decreased rapidly although the characteristic maxima could still be discerned three hours after mixing. This experiment was repeated with a 40-fold excess of NP and similar observations were made (Figure 3). It was not possible to discern any change in the visible spectra of catalase incubated with hexacyanoferrate(II) or hexacyanoferrate(III).

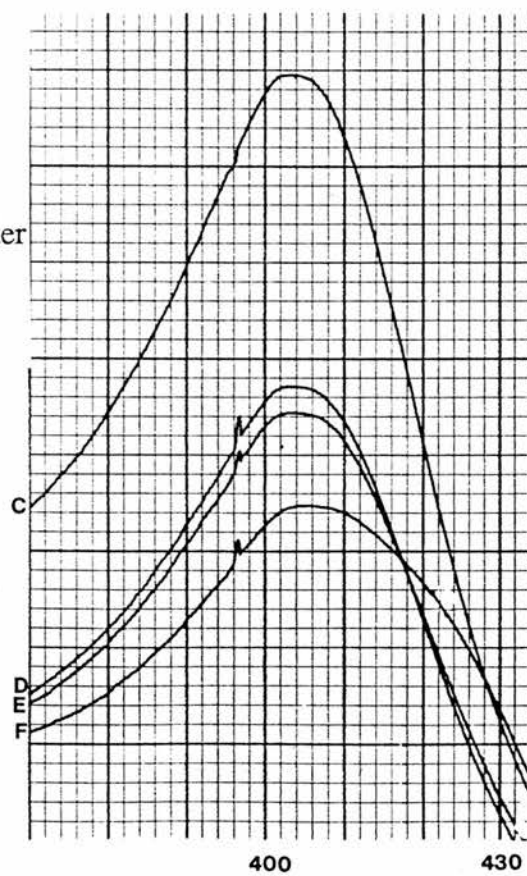
### 8.2.5 Epr spectra of catalase and nitroprusside

Epr spectra of a solution of degassed NP (in 200-fold excess) added to solid catalase were recorded at room

Figure 3



- A and C. catalase
- B. NO-catalase
- D. spectrum of nitroprusside ( $1.76 \times 10^{-3}$  M) and catalase ( $4.36 \times 10^{-5}$  M) five minutes after mixing
- E. twenty minutes after mixing
- F. three hours after mixing

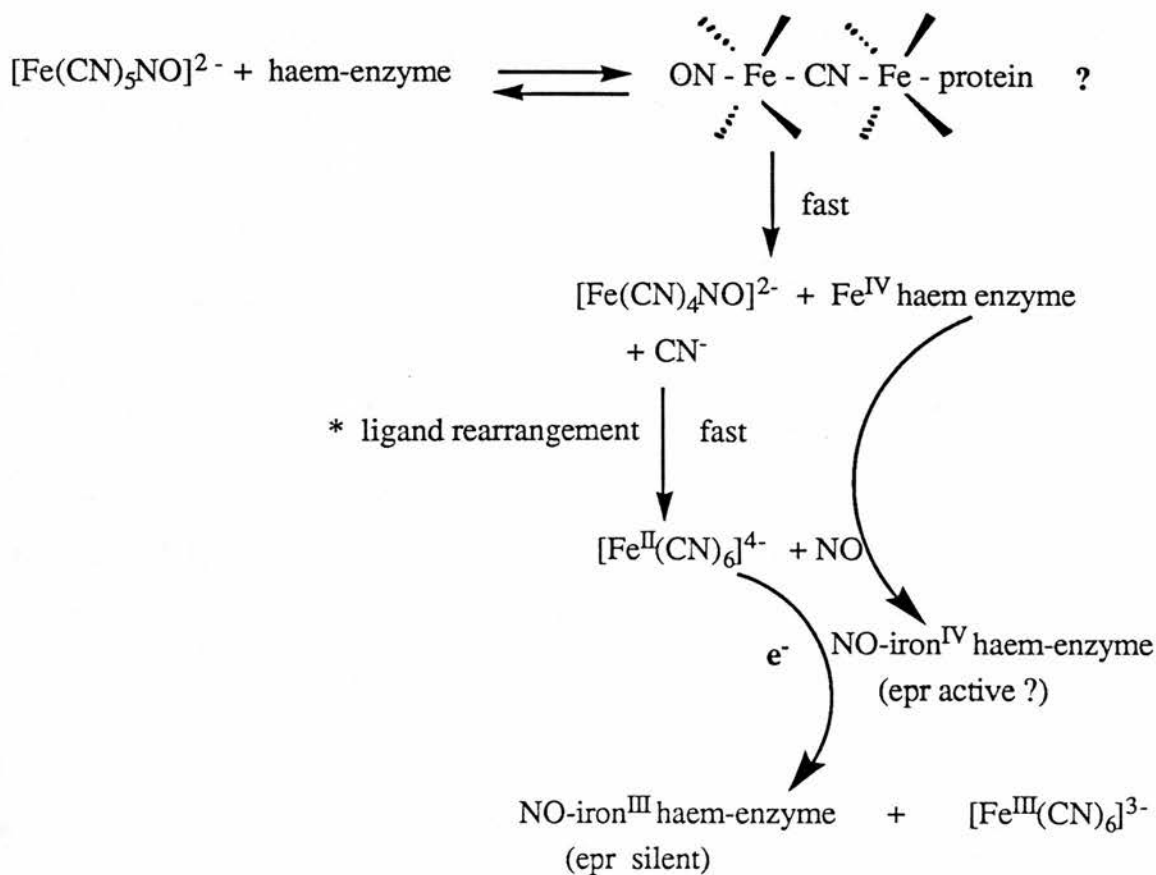


temperature and after cooling to 120 K. The spectra recorded immediately after mixing, at room temperature, contained a weak three line signal, identical to the signals for  $[\text{Fe}(\text{CN})_4\text{NO}]^{2-}$  described in Chapters 6 and 7 following reduction of NP. There was no signal apparent for catalase itself or for NO-catalase at room temperature or after cooling the sample to 120 K. Upon warming the sample to room temperature the intensity of the three line signal was enhanced but the solution in the epr tube had become turbid, a manifestation of enzyme denaturation. It is known<sup>19</sup> that catalase (bovine liver) contains eight thiol groups embedded within its protein structure which could have become exposed and reacted with NP. A solution of NP and catalase at similar concentrations but left at room temperature did not become turbid within the same period and the signal for  $[\text{Fe}(\text{CN})_4\text{NO}]^{2-}$  remained weak.

#### 8.2.6 Carbon-13 nmr of catalase and nitroprusside

A carbon-13 nmr spectrum of a deoxygenated and buffered (pH 7.0) solution of 90% carbon-13 labelled NP ( $5.0 \times 10^{-3}$  M) added to solid catalase (0.0232 g,  $1 \times 10^{-4}$  M) was recorded several hours after mixing. The only signals that could be discerned were those for NP and several signals that were found in a spectrum of catalase alone and probably represent residual solvent. It was shown (Chapters 6 and 7) that the inorganic product of thiol reduction of NP is hexacyanoferrate(II) but there are several reasons, to be discussed later, for not discounting formation of hexacyanoferrate(II) following reaction of catalase and NP.

**Scheme 4 :** Mechanism for the reaction of nitroprusside with the iron(III) haem enzymes lactoperoxidase and catalase



\* ligand rearrangement of 6  $[\text{Fe}(\text{CN})_4\text{NO}]^{2-}$  and 6  $\text{CN}^-$  results in formation of 5  $[\text{Fe}^{\text{II}}(\text{CN})_6]^{4-}$ , 6 NO and 1  $\text{Fe}^{2+}$

### 8.3 DISCUSSION

A mechanism for the reaction of NP with lactoperoxidase and catalase (Scheme 4), related to the reaction of NP with haemoglobin (Scheme 1), can be established from the observations presented above.

As the structure of lactoperoxidase has not been determined it is not certain that inhibition of enzyme activity (Figure 1) by direct interaction of NP with the haem moiety to form a complex analogous to the nitroprusside-haemoglobin complex of Scheme 1 is possible. Although the sixth co-ordination site of the haem iron is vacant and cyanide,  $\text{HS}^-$  and  $\text{F}^-$  inhibit lactoperoxidase by attachment at this site,<sup>14</sup> it is not unprecedented that electron transfer from haem iron to substrate NP can be effected without such a direct interaction. Electron transfer to the haem of cytochrome c does not occur directly but *via* the amino acids of the contiguous protein structure.<sup>20</sup> Bound oxygen of oxyhaemoglobin, effectively acting as a bridging peroxo ligand, promotes electron transfer between the haem group and  $[\text{Fe}^{\text{II}}(\text{CN})_5\text{H}_2\text{O}]^{3-}$ .<sup>21</sup>

One important feature of lactoperoxidase inhibition is that there is no apparent increase in the degree of inhibition upon incubation; in Figure 1 the inhibition by NP (7.6 mM) is effectively the same at one minute and thirty minutes after addition to the enzyme solution. In contrast the inhibition of the thiol-containing enzymes papain and glyceraldehyde-3-phosphate dehydrogenase (Chapter 7) was markedly enhanced by twenty minute incubation periods. These results

suggest that inhibition of lactoperoxidase is not due to slow reaction with enzyme thiols but to rapid oxidation of the haem moiety and concomitant reduction of NP.

Although the haem group of catalase is buried in a pocket well below the surface of the enzyme, the channel to the haem is 15 Å wide<sup>17</sup> and thus large enough to accommodate the nitroprusside ion (5.82 Å by 6.12 Å).<sup>22</sup> Reaction of NP and catalase to form NO-catalase was indicated in visible spectra recorded shortly after mixing. The formation of NO-catalase in these reaction solutions is attributed to release of NO upon decomposition of  $[\text{Fe}(\text{CN})_4\text{NO}]^{2-}$ , from reduction of NP. Both  $[\text{Fe}(\text{CN})_4\text{NO}]^{2-}$  and NO-catalase are short-lived species in the presence of air and thus the reaction of NP and decomposition of  $[\text{Fe}(\text{CN})_4\text{NO}]^{2-}$  must occur immediately after mixing NP and catalase.

The epr spectra of a solution of degassed NP added to solid catalase recorded at room temperature and 120 K immediately after mixing contained signals for  $[\text{Fe}(\text{CN})_4\text{NO}]^{2-}$ . The rapid **decrease** in the intensity of the  $[\text{Fe}(\text{CN})_4\text{NO}]^{2-}$  signal, contrasts to the **increase** in intensity of the same signal observed in spectra of NP and thiols reaction solutions.

The failure to observe signals for NO-catalase in the above epr spectra<sup>\*</sup> or a signal for hexacyanoferrate(II) in the carbon-13 nmr spectrum<sup>\*</sup> of NP and catalase is not necessarily due to low concentrations and is rationalised by Scheme 4.

The observed epr signal for  $[\text{Fe}(\text{CN})_4\text{NO}]^{2-}$  must represent reduction of NP. The appearance of this signal and lactoperoxidase inhibition were uncharacteristically rapid for the

\* recorded in the absence of air.

reaction of NP with thiols, indicating that fast electron transfer from haem to NP must be involved in some way.

Whereas decomposition of NO-catalase is rapid in air, nitrosyl haems are relatively stable in air-free solutions.<sup>18</sup> Although the nitrosyl compound of iron(IV) catalase should be epr active, the analogous compound of iron(III) catalase is epr silent due to electron delocalisation.<sup>18</sup> The absence of an epr signal for catalase itself can be explained by complete oxidation of catalase by NP (in excess) and the primary product of NP reduction is  $[\text{Fe}(\text{CN})_4\text{NO}]^{2-}$  which has been shown to lead to hexacyanoferrate(II). In the presence of oxidised catalase or NO-catalase hexacyanoferrate(II) is susceptible to oxidation. The final products of electron transfer are hexacyanoferrate(III), which cannot be detected by carbon-13 nmr, and the nitrosyl complex of iron(III) catalase, an epr silent species. The evidence for this scheme is incomplete and further investigation of the reactions of NP and iron(III) haem enzymes is required to substantiate this mechanism. Nevertheless, electron transfer is known<sup>20</sup> to occur between hexacyanoferrate(II) and the haem group of ferricytochrome c, and hexacyanoferrate(II) slightly inhibited lactoperoxidase activity (Figure 1).

Scheme 4 is not inconsistent with reports<sup>4,5,8-10</sup> that the expression of guanylate cyclase activity by NP and related agents requires the presence of a haem group, either added separately or as a prosthetic haem of the enzyme. Nitrosyl haems, including NO-haemoglobin and NO-catalase, or mixtures of haems and nitroprusside and a reducing agent are

potent activators of guanylate cyclase.<sup>4,5,8-10</sup>

There are two important features of Scheme 4 with implications for the hypotensive activity of NP. The rapid reaction of NP with haems to release NO is a good model for the near instantaneous onset of hypotension with NP infusion. The reaction of NP with haems proceeds through formation of the kinetically *labile* intermediate  $[\text{Fe}(\text{CN})_4\text{NO}]^{2-}$  and thus reports<sup>2,3,6</sup> of free cyanide release upon reaction with haemoglobin and blood fractions can be attributed to false readings for cyanide from the carrier-gas technique in the presence of labile cyanoferrate complexes.<sup>24,25</sup> No cyanide was detected by carbon-13 nmr upon reduction of NP by thiols which led to the same intermediate species; ligand rearrangement to form the kinetically *inert* product hexacyanoferrate(II) must be very fast.

## 8.4 EXPERIMENTAL

### *Materials and instruments*

Catalase (bovine liver, thymol-free purified powder) and lactoperoxidase (bovine milk, lyophilised powder) were obtained from Sigma and used without further purification. Samples of carbon-13 labelled sodium nitroprusside were prepared by Dr. J. McGinnis, as previously reported. All other reagents, with the exceptions of those prepared as described below, were of AnalaR grade where available.

Solid sodium nitroprusside was stored in a dark cupboard. All solutions containing nitroprusside were protected from light with a complete covering of aluminium foil during storage and use.

Carbon-13 nmr spectra were recorded on a Bruker AM 300 spectrometer in the FT mode at 25 °C with a carbon resonance of 75 MHz in a field of 7.04 T. The number of scans was typically 3700 with a pulse width of 2.0  $\mu$  seconds and a delay time of 1.5 seconds. The reference was the sodium salt of 3-(trimethylsilyl)propanesulphonate but all chemical shifts quoted refer to TMS.

The epr experiments were conducted by Ian Johnson in a quartz capillary at room temperature using a Bruker ER 200D spectrometer. Di-t-butyl-nitroxide was used as the standard for the measurement of the line positions. Enzyme assays were conducted with a thermostatically controlled Pye Unicam SP8 100 spectrophotometer.

Atomic parameters and structural data for molecular modelling of catalase were obtained from the Daresbury

Laboratory Chemical Databank Service, a service of the S.E.R.C. The program Chem-X, developed and distributed by Chemical Design Ltd., Oxford, was used to display and manipulate structures in conjunction with a Tektronics 4107 colour terminal linked to a VAX 11/785 computer.

## *Methods*

### Lactoperoxidase assay

The activity of lactoperoxidase at 18 °C was determined by following purpurogallin formation at 425 nm. An enzyme solution was prepared with lactoperoxidase (0.26 units/ml,  $4.07 \times 10^{-8}$  M) in phosphate buffer (pH 7.0, I = 0.067 M). For each experiment [temperature-equilibrated] buffer or inhibitor (0.5 ml) was added to the temperature-equilibrated enzyme solution (1.0 ml) and buffer (1.0 ml). The reaction was initiated by addition of  $\text{H}_2\text{O}_2$  (0.5 ml,  $4.00 \times 10^{-3}$  M) and pyrogallol (0.3 ml,  $3.00 \times 10^{-2}$  M).

### Catalase assay

The activity of catalase at 30 °C was determined by following the decrease in the absorbance of  $\text{H}_2\text{O}_2$  at 245 nm. An enzyme solution was prepared with catalase (50 units/ml,  $1.96 \times 10^{-8}$  M) in phosphate buffer (pH 7.0, I = 0.067 M). The catalysed decomposition of  $\text{H}_2\text{O}_2$  was initiated by addition of  $\text{H}_2\text{O}_2$  (2.9 ml,  $1.96 \times 10^{-2}$  M) to the enzyme solution (0.1 ml) and buffer or inhibitor (0.1 ml, maximum concentration  $2.0 \times 10^{-3}$  M, e.g.  $6.67 \times 10^{-5}$  M overall).

Preparation of NO-catalase<sup>26</sup>

A buffered solution of catalase ( $3.57 \times 10^{-5}$  M) was deoxygenated and chilled in an ice-bath. NO was bubbled through the solution briefly, followed by N<sub>2</sub>. The visible spectrum of the resulting solution of NO-catalase was recorded immediately. Visible absorbance maxima (H<sub>2</sub>O) 576, 539, 427 nm.

## REFERENCES

1. P. C. Jocelyn "Biochemistry of the SH Group", Academic Press, Inc., London, 1972, p.3
2. R. P. Smith and H.Kruszyna, *J. Pharm. Exp. Therap.*, 1974, **191**, 557.
3. H. E. Spiegel and V.Kucera, *Clin. Chem.*, 1977, **23**, 2329.
4. F. R. DeRubertis, P. A. Craven, and D. W. Pratt, *Biochem. Biophys. Res. Comm.*, 1978, **83**, 158.
5. P. A. Craven and F. R. DeRubertis, *Biochim. Biophys. Acta*, 1983, **745**, 310.
6. C. J. Vesey, J. R. Krapez, and P. V. Cole, *J. Pharm. Pharmacol.*, 1980, **32**, 256.
7. A. R. Butler, C. Glidewell, I. Johnson, and A. S. Roberts McIntosh, unpublished results.
8. I. J. Ignarro, J.B. Adams, P. M. Horwitz, and K. S. Wood, *J. Biol. Chem.*, 1986, **261**, 4997.
9. L. J. Ignarro, J. N. Degnan, W. H. Baricos, P. J. Kadowitz, and M. S. Wolin, *Biochim. Biophys. Acta*, 1982, **718**, 49.
10. E. H. Ohlstein, K. S. Wood, and L. J. Ignarro, *Arch. Biochem. Biophys.*, 1972, **218**, 187.
11. B. C. Saunders, A. G. Holmes-Siedle, and B. P. Stark, Peroxidase, Butterworth & Co., Ltd., London, 1964, pp.8-9.
12. S. M. Siegel and P. Frost, *J. Am. Chem. Soc.*, 1960, **82**, 2773.
13. Y. Shiro and I. Morishima, *Biochemistry*, 1986, **25**, 5844.
14. Ref. 11, page 102.
15. M. Morrison, W. A. Rombants, and W. A. Schroeder, in

- "Hemes and Hemoproteins" (B. Chance, R. W. Estabrook, and T. Yonetani, Eds.), Academic Press, Inc., London, 1966, p. 345.
16. G. R. Schonbaum and B. Chance in "The Enzymes", Vol. XIII, 3rd Edition (P. Boyer, Ed.), Academic Press, Inc., London, 1976, pp. 363 - 408.
  17. M. R. N. Murthy, T. J. Reid, A. Sicignano, N. Tanaka, and M. G. Rossman, *J. Mol. Biol.* 1981, **152**, 465.
  18. T. Yonetani, H. Yamamoto, J. E. Erman, J. S. Leigh, and G. H. Reed, *J. Biol. Chem.*, 1972, **247**, 2447.
  19. A. Pihl, R. Lange, and A. Evang, *Acta Chim. Scand.*, 1961, **15**, 1271.
  20. M. Dixon and E. C. Webb, "Enzymes" (3rd Edition), Longman Group Ltd., London, 1979, p. 498.
  21. S. Kawanishi and W. S. Canghey, *J. Biol. Chem.*, 1985, **260**, 4622.
  22. J. H. Swinehart, *Coord Chem. Rev.*, 1967, **2**, 385.
  23. G. P. Hess, K. G. Brandt, P. E. Parks, and G. Czerlinski in "Hemes and Hemoproteins" (B. Chance, R. W. Estabrook, and T. Yonetani, Eds.), Academic Press, Inc., London, 1966, p. 548.
  24. W. I. K. Bisset, M. G. Burdon, A. R. Butler, C. Glidewell, and J. Reglinski, *J. Chem. Res. (M)*, 1981, 3501.
  25. W. I. K. Bisset, A. R. Butler, C. Glidewell, and J. Reglinski, *Br. J. Anaesth.*, 1981, **53**, 1015.
  26. P. A. Craven, F. R. DeRubertis, and P. W. Pratt, *J. Biol. Chem.*, 1979, **254**, 8213.

A P P E N D I X    1

## P U B L I C A T I O N S

- i. The pentacyanonitrosylferrate ion. Part IV. Reaction with the carbanions of pentane-2,4-dione and 3-methylpentane-2,4-dione.  
A. R. Butler, A. M. Calsy, and C. Glidewell,  
*J. Organomet. Chem.*, in press.
- ii. The pentacyanonitrosylferrate ion. Part III. Reaction with the carbanion of ethyl cyanoacetate.  
A. R. Butler, A. M. Calsy, and C. Glidewell,  
*J. Chem. Soc., Perkin II*, submitted.
- iii. Changes in glutathione in intact erythrocytes during incubation with sodium nitroprusside as detected by  $^1\text{H}$  spin echo nmr spectroscopy: oxidation of glutathione by nitroprusside.  
A. R. Butler, A. M. Calsy, C. Glidewell, I. L. Johnson, J. Reglinski, and W. E. Smith, in preparation.
- iv. Complexation of iron(II) with 3-hydroxyiminopentane-2,4-dione (Hinaa).  
A. R. Butler, A. M. Calsy, and C. Glidewell,  
in preparation.

A P P E N D I X 2

P H O T O G R A P H S